THE UNIVERSITY OF ALBERTA

THE PYROCLASTIC ROCKS OF THE CROWSNEST FORMATION, ALBERTA

by

ROBIN N. ADAIR

A THESIS

SUBMITTED TO THE FACULTY OF GRADUATE STUDIES AND RESEARCH

IN PARTIAL FULFILMENT OF THE REQUIREMENTS FOR THE DEGREE

OF MASTER OF SCIENCE

DEPARTMENT OF GEOLOGY

EDMONTON, ALBERTA

SPRING, 1986

Permission has been granted to the National Library of Canada to microfilm this thesis and to lend or sell copies of the film.

The author (copyright owner) has reserved other publication rights, and neither the thesis nor extensive extracts from it may be printed or otherwise reproduced without his/her written permission.

L'autorisation a été accordée à la Bibliothèque nationale du Canada de microfilmer cette thèse et de prêter ou de vendre des exemplaires du film.

L'auteur (titulaire du droit d'auteur) se réserve les autres droits de publication; ni la thèse ni de longs extraits de celle-ci ne doivent être imprimés ou autrement reproduits sans son autorisation écrite.

ISBN 0-315-30258-5

THE UNIVERSITY OF ALBERTA

RELEASE FORM

NAME OF AUTHOR ROBIN N. ADAIR

TITLE OF THESIS THE PYROCLASTIC ROCKS OF THE CROWSNEST FORMATION, ALBERTA

DEGREE FOR WHICH THESIS WAS PRESENTED MASTER OF SCIENCE

YEAR THIS DEGREE GRANTED SPRING, 1986

Permission is hereby granted to THE UNIVERSITY OF ALBERTA LIBRARY to reproduce single copies of this thesis and to lend or sell such copies for private, scholarly or scientific research purposes only.

The author reserves other publication rights, and neither the thesis nor extensive extracts from it may be printed or otherwise reproduced without the author's written permission.

(SIGNED) Robin N. Adair

PERMANENT ADDRESS:

1309 Calbarne Cres. S.W.
Calgary, Alberta
Canada

DATED March 11 1986

THE UNIVERSITY OF ALBERTA

FACULTY OF GRADUATE STUDIES AND RESEARCH

The undersigned certify that they have read, and recommend to the Faculty of Graduate Studies and Research, for acceptance, a thesis entitled THE PYROCLASTIC ROCKS OF THE CROWSNEST FORMATION, ALBERTA submitted by ROBIN N. ADAIR in partial fulfilment of the requirements for the degree of MASTER OF SCIENCE.

R A Burwash
.....

Supervisor

F. J. Longstaffe
.....

R. H. Steele
.....

G. M. Cumming
.....

J. Lambert
.....

Date February 27, 1986.

DEDICATION

I would like to dedicate this work to five individuals who played a critical role in seeing it through to completion:

To Ron Burwash and Charlie Stelck who provided much needed moral support and showed genuine enthusiasm in the conquest of the Crowsnest Formation.

To my mother and aunt, Helen and Kay Leskiw, who gave me my start in geology at about the age of six.

Finally, to my father, Robert Adair, for the sometimes over-zealous encouragement of this *"late blooming scholar"*.

To all, my thanks.

ABSTRACT

The Crowsnest Formation in southwestern Alberta is composed of a differentiated suite of extrusive alkaline volcanics dominated by pyroclastic rocks. A relatively complete 400m section through the formation was exposed in 1981 west of Coleman, Alberta. This new section is herein proposed as the type section for the Crowsnest Formation. The deposits of this newly proposed type section are divided into a recessive, 124m lower and a resistant, 276m upper member.

Mineralogically, the lower and upper members differ somewhat. The lower member is composed of phenocrysts, cognate and juvenile rock fragments and finer matrix constituents, including pronounced alteration phases. The phenocryst phase is dominated by sanidine, melanite, aegrine - augite and, to a lesser extent, analcime, andesine and sphene. The distribution of the denser minerals, notably garnets and Fe-Ti oxides, define many bedding structures as a result of pronounced density-stratification. Cognate and juvenile rock fragments are found in all but the finest beds. Many exhibit a trachytic flow texture, reflecting their origin as lavas or viscous plugs. In many instances, rock fragments and crystals exhibit plastic deformation, sutured boundaries and baked/ resorbed margins indicating high emplacement temperatures and subsequent welding.

The matrix of the lower member is composed of finer rock fragments, small crystals and crystal fragments and a pronounced alteration assemblage. This alteration assemblage is dominated by both clay minerals (illite, illite/smectite) and calcite. Kaolinite and chlorite are also found. Zeolites are rare.

In the upper member, the phenocryst phase is less well developed except in the abundant cognate and juvenile rock fragments. Many phenocrysts, notably sanidine and analcime, have suffered recrystallization to chert-like adularia + sericite + epidote masses and pseudomorphs. Analcime as a discrete phenocryst was not observed. Garnets are relatively rare compared to the lower member.

The matrix of most upper beds is composed dominantly of a finely-crystalline, chert-like assemblage listed above. Also found were illite (10Å minerals), chlorite, biotite, apatite, hematite, titanomagmetite, ilmenite and pyrite.

Geochemical analyses of pyroclastic rocks and lava flows (in the latter case data taken from Pearce, 1967 and Ferguson and Edgar, 1978) classify the deposits of the Crowsnest

Formation as tristanites of the potassic alkaline basalt series. Blairmorites, however, classify as benmorites of the sodic series. The occurrence of carbonate (Fe-calcite) as a major component of bombs within the formation suggest the presence of a carbonatite phase. Geochemical comparison with known carbonatites does not favor a truly carbonatite phase; however, recrystallization under igneous conditions is indicated.

The deposits of the lower member are composed of interstratified pyroclastics of four kinds: pyroclastic flows (massive), surges (both cross and density-stratified), air-falls (including bombs) and lahars. The presence of both massive and cross-stratified flow deposits suggests emplacement by both massive and turbulent pyroclastic flows respectively. Many of these deposits had been previously identified as volcanogenic sediments by Pearce (1967) and Ricketts (1982). Comparison with modern pyroclastic deposits suggest a strictly pyroclastic origin and proximity to their source.

Resistant, thickly bedded pyroclastic breccias carrying charred plant remains comprise the upper member. The clasts of the breccias are dominated by cognate and juvenile types, ranging up to 3 meters in size. Textural evidence suggests that the deposits are essentially lavas which had incorpoated high concentrations of clasts during dome building eruptions.

Despite the absence of an exposed vent or vents, the sequence and style of Crowsnest eruptions can be interpreted from the nature of the deposits. Volcanism occurred on a broad flood plane which flanked the east side of the rising Cordillera during Upper Albian time. Early eruptions were violent and gas-charged, producing vertical eruption columns and subsequently the air-fall and ignimbrite deposits of the lower member. Such eruptions also produced deposits to the east in the Alberta basin, notably within the Viking Formation. Effusives occurred during the waning stages of these eruptions. Composite cones were probably produced by these early, gas-charged eruptions.

During the mature stages of Crowsnest volcanism, gas-poor, dome-building eruptions produced the thick pyroclastic breccias of the upper member. The deposits form a thick cap over the lower member in the vicinity of Coleman. Volcanism came to an end towards the close of Albian time and was followed by a trangression of the Cenomanain - Turonian sea in the area.

ACKNOWLEDGMENTS

I would like to acknowledge the following contributions to this study:

The Ewasiuk family for providing shelter and company.

Glenn and Kathy Karlen who gave up their time in the production of the computer generated diagrams of Chapter 3.

Dr. Fred Longstaffe and Diane Carid for help with, and use of the XRD lab (supported by NSERC grants to Dr. Longstaffe)

Dr. Ron Burwash and Dr. Charlie Stelck for providing entertainment and enlightenment on trips to Coleman.

Scott Reed for the excellent polishing job done on numerous samples.

Mr. A. McGregor for covering some of the production costs.

Kay Leskiw, Ian Piwek and David Adair for providing company on trips to Coleman.

Table of Contents

Chapter — Page

DEDICATION iv

ABSTRACT v

ACKNOWLEDGMENTS vii

List of Tables xii

List of Figures xiii

List of Plates xv

List of Abbreviations xvi

I. INTRODUCTION 1

A. Purpose and Methods 1

B. Location and Geological Setting 2

C. Previous Work 5

II. MINERALOGY 7

A. Phenocryst Phases 7

Sanidine 11

Garnet 13

Aegirine - Augite 14

Analcime 17

Plagioclase 18

Accessory Minerals 21

B. Rock Fragments 22

C. Matrix 24

Original Material: Glassy and Aphanitic Components 25

Clay Minerals 26

Carbonate 41

Feldspar Aggregate 47

Zeolites and Trace Minerals 48

D. Textures 48

Plastic Deformation Structures 48

Suture Boundaries 49

Baked Margins 52

E. Summary 52
III. GEOCHEMISTRY 54
A. Igneous spectrum 58
B. Whole Rock Classification 60
Total Alkalies versus Silica 61
An - Ab - Or Plot 61
Normative Color Index versus Normative Plagioclase Index 64
C. Minor Element Geochemistry 64
Zr/TiO_2 versus Nb/Y 68
SiO_2 versus Nb/Y 68
SiO_2 versus Zr/TiO_2 68
D. Bomb Geochemistry 68
E. Discussion 74
IV. CLASSIFICATION AND NOMENCLATURE 75
A. Pyroclastic Components 75
B. Eruptive Origins of Pyroclastic Rocks 77
Convective Columns and Gravitational Column Collapse 80
Boiling Over 82
Dome Collapse 82
Inclined Blast 83
C. Flow Mechanics 83
D. Pyroclastic Deposits 86
Ignimbrites 86
The Base Surge 92
Air-Fall Deposits 93
Lahars 94
E. Summarized Classification 95
V. DEPOSITS 97
A. Pyroclastic Flow Deposits: Ignimbrites 97
Agglomerates 97
Pyroclastic Breccias 98

Ash Flow Deposits 102
Surges 105
B. Air-Fall Deposits 120
Pink beds: Crystal Lapilli Tuffs 121
Green beds: Coarse Crystal Ashes 122
Purple beds: Crystal tuffs 123
Bomb Agglomerates 123
Clay beds: Bentonite 126
C. Lahar Deposits 127
D. Primary Flows and Intrusives 127
E. Volcanogenic Sediments 128
Discussion 128
VI. STRATIGRAPHY 130
A. Detailed Stratigraphy of the Proposed Type Section 130
Lower Member 130
Upper Member 137
B. Local Stratigraphy 138
C. Age and Correlation 140
D. Interpretive Stratigraphy 145
VII. HISTORY OF THE CROWSNEST FORMATION 148
A. Early Eruptions 149
Eruptive Model for Lower Crowsnest 150
Vent and Deposit Morphology 154
B. Late Eruptions 157
Eruption Model for the upper Crowsnest 157
Vent and Deposit Morphology 160
Discussion 162
C. Geological History of the Crowsnest Formation 162
Pre-Crowsnest: Early Upper Albian 162
Crowsnest time: Middle Upper Albian 165
Post Crowsnest: Cenomanian-Turonian Time 169

VIII. BIBLIOGRAPHY 170
IX. APPENDIX A 179
A. PROPOSED TYPE SECTION STRATIGRAPHIC COLUMN 180
X. Appendix B 193
A. Analytical Methods 194
Outcrop and Hand Specimen Descriptions 194
Thin Section Descriptions 194
Scanning Electron Microscopy 194
X-Ray Diffraction 194

List of Tables

Table 2.1 Mineralogical compositions 8

Table 2.2 Clay mineral abundances in the <2μm size fraction 29

Table 2.3 Clay mineral abundances in the <2μm, 2 - 5μm and 5 - 20μm size fractions for sample wch- 32 28

Table 2.4 Illite/Smectite compositional determinations 31

Table 3.1 Major and trace element XRF data 55

Table 3.2 Accuracy of McMaster XRF determinations 56

Table 3.3 Trace element-bearing minerals of the Crowsnest formation and their densities 67

Table 3.4 Bomb geochemistry compared with carbonatites 73

Table 4.1 Summarized classification of pyroclastic deposits 96

Table B1 Appendix B. Mixed-layer clay X-ray diffraction data 196

List of Figures

Figure 1.1 Location map and regional geological setting of the Crowsnest Formation. 3

Figure 1.2 Detailed geological setting of the Crowsnest Formation in the vicinity of the proposed type section. 4

Figure 2.1 X-Ray diffractograms of calcium-glycolated samples from the lower member for the <2μm size fraction (Co Kα). 27

Figure 2.2 Illite/smectite compositions using the $(001)_{10}/(002)_{17}$ and the $(002)_{10}/(003)_{17}$ deffractions 32

Figure 2.3 Illite/smectite compositions using the $(002)_{10}/(003)_{17}$ and the $(003)_{10}/(005)_{17}$ diffractions 33

Figure 2.4 Ordering of the illite/smectite using % smectite versus the $(001)_{10}/(001)_{17}$ diffraction 34

Figure 2.5 X-Ray diffractograms of calcium- glycolated samples from the upper member for the <2μm size fraction (Co Kα). 40

Figure 2.6 Occurrences of the major phases of the Crowsnest Formation. 53

Figure 3.1 Total alkalies versus $K_2O/Na_2O + K_2O$, and the "Igneous Spectrum" 59

Figure 3.2 Total alkalies versus silica 62

Figure 3.3 An - Ab' - Or ternary plot. 63

Figure 3.4 Normative color versus normative plag index. 65

Figure 3.5 $Zr/TiO_2 \times 10^4$ versus Nb/Y 69

Figure 3.6 SiO_2 versus Nb/Y. 70

Figure 3.7 SiO_2 versus Zr/TiO_2. 71

Figure 4.1 Classification of pyroclastic rock components. 76

Figure 4.2 Eruptive origins of pyroclastic rocks 79

Figure 4.3 Schematic diagrams of a fully convective column and a collapsing column. 81

Figure 4.4 Mechanisms of pyroclastic flow. 85

Figure 4.5 Flow transformations. 85

Figure 4.6 Standard ignimbrite depositional models 90

Figure 4.7 Deposit from a block and ash flow. 90

Figure 5.1 Detailed sketch of a density-stratified surge deposit, after Plates 5.4a and 5.5. ... 113

Figure 5.2 Detailed sketch of parallel-beds, erosional dune shapes and true dunes. 118

Figure 6.1 K/Ar ages for the Crowsnest Formation and a bentonite from the Viking Formation..... 143
Figure 6.2 Stratigraphic cross-section through southern Alberta. 147
Figure 7.1 Eruption models for the lower member of the Crowsnest Formation. 151
Figure 7.2 Probable vent morphology during early Crowsnest eruptions..... 156
Figure 7.3 Eruption models for the upper member of the Crowsnest Formation. 158
Figure 7.4 Probable vent morphology during late Crowsnest eruptions. 161
Figure 7.5 Eruptive evolution of the Crowsnest Formation. 163
Figure 7.6 Albian - Turonian paleogeography..... 164
Figure 7.7 Early Crownsnest paleogeography..... 166
Figure 7.8 Late Crowsnest paleogeography. 167
Figure 7.9 Post Crowsnest paleogeogrphy..... 168

List of Plates

Plate 2.1 Thin section photomicrographs of phenocryst phase minerals. 16

Plate 2.2 Thin section photomicrographs of phenocryst phase minerals and rock fragments. .. 20

Plate 2.3 SEM micrographs of phenocryst and matrix phase mineralogy. 37

Plate 2.4 SEM micrographs of matrix phase mineralogy. 39

Plate 2.5 SEM micrographs of matrix phase mineralogy. 43

Plate 2.6 Thin section photomicrographs of matrix phase mineralogy. 46

Plate 2.7 Thin section photomicrographs and photographs of various pyroclastic textures. 51

Plate 5.1 Photographs of cut and polished agglomerate and pyroclastic breccia specimens. .. 100

Plate 5.2 Photographs of surge and agglomerate - surge deposits in outcrop. 107

Plate 5.3 Photographs of cut and polished surge specimens. 109

Plate 5.4 Photographs comparing surge deposits from the Crowsnest Formation and those of proximal pyroclastic flows at Mount St. Helens. 112

Plate 5.5 Detailed photographs of cut and polished surge specimens 117

Plate 5.6 Photographs of cut and polished air-fall and conglomerate specimens. Also included is a photograph of Crowsnest bombs. 125

Plate 6.1 Photographs of the lower and upper members in outcrop at the proposed type section. 132

List of Abbreviations

Mineralogy

Cl = Clay

I = Illite

Chl = Chlorite

Ad = Adularia

I/S = Illite/Smectite

Fp = Sanidine

Gr = Garnet (melanite)

A = Aegirine-augite

Ca = Calcite

An = Analcime

Hb = Hornblende

Ep = Epidote

Ap = Aphanite/glass

Ox = Fe - Ti oxides

Pl = Plagioclase

Mg = Magnetite (titanomagnetite)

ch = chips (impact)

Cf = Crystal fragments

fg = Rock fragments

M = Matrix

SEM = Scanning Electron Microscope

EDA = Energy Dispersal Analysis

EDS = Energy Dispersal Spectrometry

1 μm = Micrometer (1 x 10^{-6} meters)

1 Å = Angstrom (1 x 10^{-10} meters)

Deposits

Ag = Agglomerate

Sg = Surge

Br = Pyroclastic breccia

Pb = Parallel beds.

Cs = Cross-stratification

Rs = Remobilization structures

Bm = Baked margins

Dc = Drop clasts

Ds = Deflation drape structures

T = Trachytic flow texture

I. INTRODUCTION

In 1981, a virtually complete section through the Crowsnest Formation was exposed along a relocated highway No. 3 west of Coleman, Alberta. This new exposure is herein proposed as the type section of the formation since no type section has previously been designated. A recessive lower member and resistant upper member are well defined at this exposure.

The deposits of the proposed type section are composed entirely of pyroclastic suites. Many similar deposits in other exposures of the formation were previously identified as volcanogenic sediments by Pearce (1967) and Ricketts (1982). The depositional characteristics of these deposts are compared to modern examples in order to determine an eruptive style and history for the Crowsnest Formation. To date, no study has investigated this aspect of the formation.

A. Purpose and Methods

The prime objective of this study is to determine a model for the genesis and deposition of the Middle Cretaceous Crowsnest Formation based upon the exposure of the critical section west of Coleman. Support sections were mapped immediately north and south of this section. Conclusions are based on the following lines of investigation:

Mineralogy. The mineralogical signature of the phenocryst, rock fragment and matrix phases are determined to provide insight into the compositional variation within beds, between beds and between each of the phases. The distribution of the phases in and between the lower and upper horizons are investigated to define the processes by which they were emplaced.

As alteration assemblages comprise a major part of many beds, the diagenetic mineral assemblages are investigated to define the conditions under which they were formed.

Geochemistry. Whole rock, major and trace element, compositions are used to classify the Crowsnest suite. Genetic assumptions are based upon the chemical signature and comparisons with chemical suites of igneous rocks of known origins. The degree of alteration is assessed by the amount of chemical variation between altered pyroclastic samples and those of both fresh, primary[1] Crowsnest suites and standard alkaline rocks.

---

[1]In this sense, the term "primary" is used for all igneous rocks (lavas, plugs, intrusives etc.) not of pyroclastic origin.

Volcanology. Perhaps the most important line of investigation is the identification and interpretation of the textures and depositional structures found in the beds of the formation. The fine line dividing truly sedimentary rocks from those of pyroclastic origin imparts a marked similarity between the structures although the medium which emplaced the deposits may be markedly different.

The type of pyroclastic deposit, determined from the preserved structures, provides insight into the eruption type, and origin of the deposit.

Stratigraphy. Stratigraphic relationships are discussed on two levels:

a. Detailed Stratigraphy. A detailed stratigraphic analysis characterizes the relationships between beds within the type section and subsequently with those of the support sections. As the lower beds (lower member) are highly recessive, the examination is confined to those sections with exposures of this horizon.

b. Regional. An analysis incorporating known studies on the middle and upper Cretaceous sequences of the area provides the regional stratigraphic relationships of the formation. The implications of having a volcanic horizon within this sequence will also be addressed.

The stratigraphic associations, both local and regional, provide evidence for the reconstruction of the paleogeography before, during and after Crowsnest time.

Mapping and sampling were carried out at the end of the summer of 1983 and periodically over 1984 and 1985. Attention was focussed on the lower member at the type section where it is best exposed.

One hundred and thirty-four samples were collected from the lower member at the type section and represent every type of bed observed. Less detailed, though representative sampling was conducted in the thick upper member and in some of the support sections.

B. Location and Geological Setting

The Crowsnest Formation crops out in a relatively small area in the extreme southwest corner of Alberta (Fig. 1.1). It is exposed in a series of en-echelon stacked, northerly trending thrust slices which have been emplaced along westerly dipping thrust faults (Fig. 1.2). The area was at one time overridden by Precambrian and Paleozoic sediments which were emplaced by the Lewis overthrust. Erosion has removed most of this cover in the vicinity of Coleman,

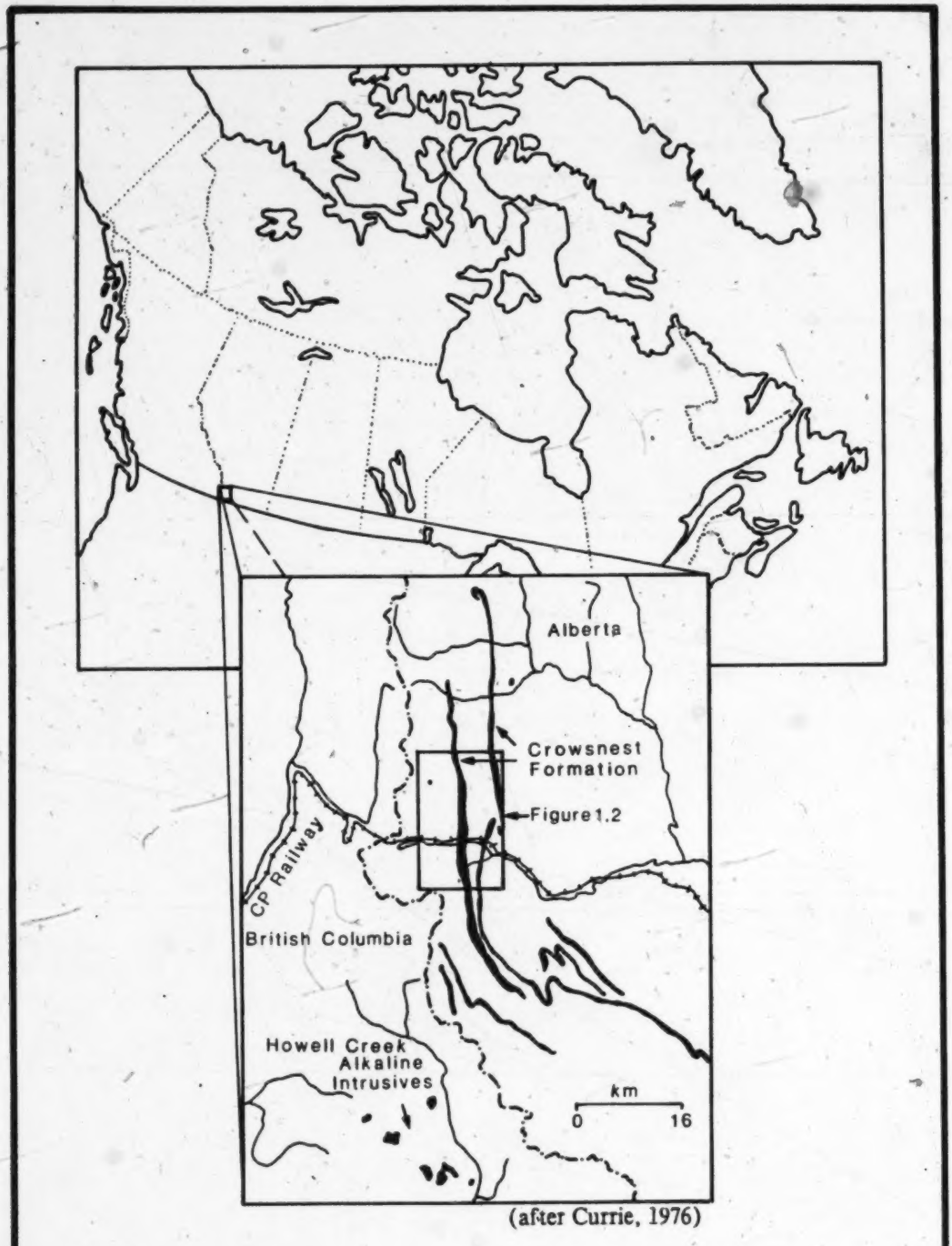

Figure 1.1 Location map and regional geological setting of the Crowsnest Formation.

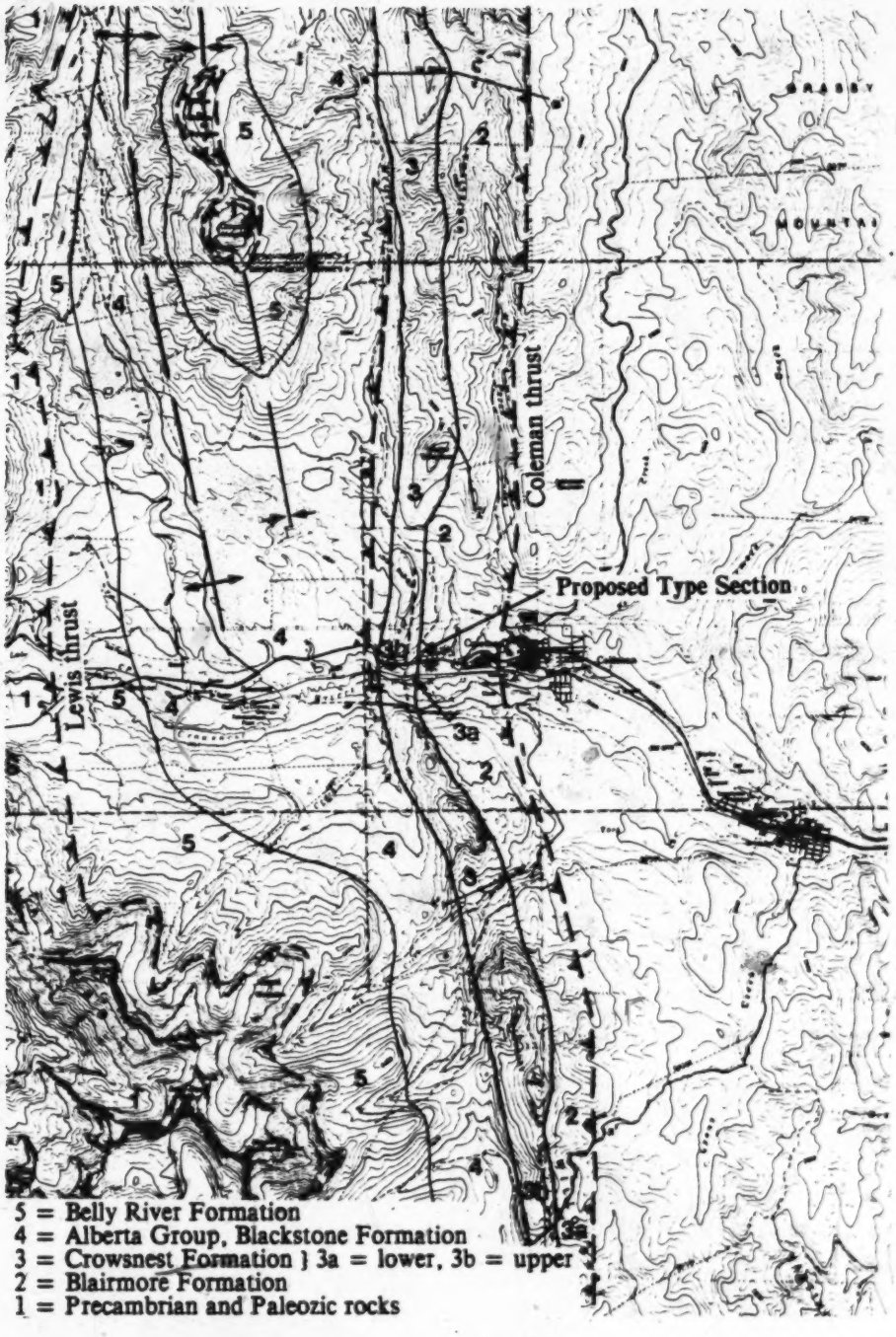
Coleman thrust
Lewis thrust
Proposed Type Section
5 = Belly River Formation
4 = Alberta Group, Blackstone Formation
3 = Crowsnest Formation } 3a = lower, 3b = upper
2 = Blairmore Formation
1 = Precambrian and Paleozic rocks

Figure 1.2 Detailed geological setting of the Crowsnest Formation in the vicinity of the proposed type section.
(Geological data from Price, 1962)

exposing the Mesozoic rocks below. To the west of the study area, these rocks still remain covered and expressions of the Lewis thrust are prominent (Fig. 1.2).

The best exposures of the Crowsnest Formation and the focus of this study are in the western-most major thrust slice emplaced by the Coleman thrust (Fig. 1.2). The thickest exposures are west of Coleman at the proposed type section and at Ma Butte (Fig. 1.2). Generally, the formation has a northerly strike and dips to the west. In the areas covered by this study, it strikes between 0 and 10 degrees north and dips to the west between 40 and 52 degrees.

The formation is underlain by the continental sediments of the Blairmore Formation (Glaister, 1958) and overlain by the marine shales of the Alberta Group, specifically the Blackstone Formation.

Generally, the dominantly pyroclastic sequences of the Crowsnest Formation occur as two distinct units, herein designated the lower and upper members. The lower member is a recessive sequence of thin to thickly bedded ash, tuff, lapilli tuff, and agglomerate. The upper member is a thick sequence of massive pyroclastic breccias and minor agglomerates. It is a prominent ridge former in the area and is known for the occurrence of blairmorite fragments.

C. Previous Work

The Crowsnest Formation was first reported by G.M. Dawson in 1885 and was subsequently remapped in 1912 by W.W. Leach. The first petrographic descriptions were given by C.W. Knight (1904) who coined the term "blairmorite" for rocks composed chiefly of analcite. MacKenzie (1914), described samples of blairmorite and proposed an igneous origin for the analcite. He further suggested that the Crowsnest was deposited in a shallow fresh water sea. Pirsson (1915) criticized these ideas, especially the igneous origin of the analcime. MacKenzie reiterated his ideas again in 1915. The crystal habits of the feldspars were investigated by Rutherford (1938). MacKenzie (1956) discussed the stratigraphy and mineralogy of the formation. Fresh sanidine phenocrysts were dated at 96 Ma by potassium argon methods in 1957 by Folinsbee *et al.*

Pearce (1967) produced a comprehensive doctoral thesis on the primary analcime-bearing rocks of the formation. He suggested that the parental magma was a hydrous alkaline trachyte and that the presence of analcime as a primary component was due to sodium

enrichment in a residual melt after sanidine, aegirine - augite and garnet were removed by fractionation. Carbonate-rich rocks were also identified and the possibility of carbonatite was suggested. Very brief attention was given to the pyroclastic rocks, however three vent locations were proposed at Ma Butte, Coleman and George Creek. Parts of the thesis were published in 1971.

The petrology of the analcime bearing-rocks of the formation was again investigated by Ferguson and Edgar in 1978. They substantiate the ideas of Pearce (1967, 1971) and give evidence that differentiation followed a sodic path. Further, they suggest that differentiation occurred at high pH_2O below 25 km and that partial melting of the crust below 35 km produced the trachytic magma.

Ricketts (1982) was the first to address the volcanology of the formation. He identified the occurrence of lahar deposits at locations south of the proposed type section. Beds containing ripples, planar cross-beds and parallel-laminae were identified as alluvial deposits and were suggested to be the result of short lived stream deposition.

Dingwell and Brearly (1985) have studied the mineral chemistry of the spectacularly zoned andradite garnets common in many beds of the formation and found them to be the titanium-bearing variety, melanite. Statistical models were proposed for elemental substitution in the garnets.

II. MINERALOGY

The mineralogy of the primary deposits of the Crowsnest Formation has been studied by Pearce (1967, 1970), Ferguson and Edgar (1978) and Dingwell and Brearly (1985). Most attention has been focused on the blairmorites due to their unique mineralogy. With the exposure of the section west of Coleman, a complete mineralogical assemblage of both the recessive lower member beds and the resistant upper member beds can be determined. Standard thin section, X-ray diffraction (XRD) and scanning electron microscopy (SEM) analyses are utilized to determine the mineralogy at sampling points through both the lower and upper members. A description of each technique and sample preparation procedures may be found in appendix B.

The phases of the Crowsnest Formation are divided into phenocryst, rock fragment and matrix categories. Table 2.1 lists the compositions of the phenocryst, matrix and rock fragment phases. Due to the large variety of rock fragments, only their abundances are considered. The samples are listed in stratigraphic order starting from the base of the lower member. Their location in the section may be found in foldouts A and B. The distribution and occurrence of any of these components is controlled by the type, intensity and source of the eruptions which produced the pyroclastic deposits, (see Chapters I & IV). Chapter V documents the pronounced density-stratification and component fractionation which has taken place.

Alteration assemblages are a pronounced feature of the pyroclastic deposits of the Crowsnest Formation and may comprise a substantial portion of the mineralogy. Generally, such assemblages are most concentrated in the matrix.

A. Phenocryst Phases

The Crowsnest suite has a distinctive phenocryst assemblage which is especially abundant in the crystal tuffs of the lower member and in cognate/juvenile fragments of the upper member. The lower member at the type section is notably composed of thin beds of crystal and lithic tuffs and lapilli tuffs. In many beds, individual crystals may be easily removed by hand due to the poorly consolidated nature of the matrix. It is clearly evident that alteration has occurred preferentially in the matrix and is most commonly in the form of clays and recrystallization assemblages which are discussed later. In the dense beds of the upper member, the phenocryst phase is less well developed; however, it is still an integral part of the deposits. Phenocrysts are well developed in the abundant rock fragments characteristic of the

TABLE 2.1 MINERAL PERCENTAGES DETERMINED BY POINT COUNTS

WCH #	PHENOCRYSTS									MATRIX							ROCK
	Gar	San	Pyx	Ana	Sph	Pla	Amp	op	tr	Cla	Cal	Aph	Chl	Bio	Fpa	tr	Frag
2	2.0	36.0	1.0	1.0	1.0	.8	tr	tr	-	29.0	-	tr	tr	-	tr	h	22.9
4	tr	32.0	2.3	-	.6	2	-	tr	-	29.0	2.6	-	tr	tr	-	-	31.5
5	2.0	42.3	6.6	-	2.0	.4	-	tr	z	-	5.2	40.5	-	-	-	-	tr
7	1.0	33.6	2.0	-	0.3	1.6	-	tr	-	14.2	-	27.4	-	-	-	H?	19.1
9	3.3	35.5	5.6	-	0.3	1.6	tr	tr	-	35.1	-	10.3	-	-	-	H?	8.3
14	2.0	27.6	6.6	tr	-	1.6	-	tr	-	7.6	52.6	2.0	-	-	-	-	tr
15	9.0	47.3	7.0	-	0.3	.6	0.3	tr	-	4.0	-	13.6	tr	-	-	-	17.9
16b	8.3	38.3	5.3	-	-	1.3	-	tr	-	3.1	tr	10.2	-	tr	-	A	33.5
16t	8.6	45.3	4.3	0.3	tr	1.6	-	tr	cz	4.0	tr	15.7	-	-	-	A,ap	20.2
20	5.0	18.3	1.3	18.6	0.3	-	-	tr	-	5.0	-	37.0	-	-	-	A	14.3
21	18.6	16.0	4.3	4.2	tr	1.7	-	tr	-	38.2	0.3	6.5	-	-	-	A	10.3
24	4.3	18.6	5.3	6.6	tr	-	tr	tr	-	6.0	-	13.3	-	-	10.0	A	35.6
30	3.6	21.6	2.0	1.3	tr	-	-	tr	cz	48.8	-	8.8	-	-	-	A	14.9
31b	9.0	37.0	4.0	4.6	-	-	0.6	tr	-	27.2	-	2.4	-	-	-	A	15.2
31t	8.0	33.6	3.3	3.0	tr	-	-	tr	e	24.3	-	1.0	-	-	3.2	A	23.6
32	12.0	40.6	5.3	-	-	-	-	tr	ap	36.6	-	2.0	-	-	tr	ap	2.6
33b	13.6	46.0	1.6	1.0	-	-	-	tr	-	27.0	-	3.6	-	-	-	A	7.2

TABLE 2.1 (Continued) MINERAL PERCENTAGES DETERMINED BY POINT COUNTS

WCH #	PHENOCRYSTS									MATRIX							ROCK
	Gar	San	Pyx	Ana	Sph	Pla	Amp	op	tr	Cla	Cal	Aph	Chl	Bio	Fpa	tr	Frag
33m	11.6	58.0	1.0	0.3	-	-	-	tr	-	9.0	2.6	2.8	-	-	6.0	A,ap	8.7
33t	11.0	52.6	4.3	1.3	-	-	-	tr	tr	9.6	tr	4.0	-	-	11.6	A	9.9
35	2.3	20.3	1.6	0.6	-	1.3	-	tr	-	37.0	-	-		-	2.2	-	34.7
40	6.6	37.3	9.6	tr	0.3	2.0	-	tr	-	4.3	3.6	20.7	-	-	3.2	A?	12.4
44	1.0	40.0	1.0	-	0.6	5.0	-	tr	e	44.0	-	4.0	-	-	-	e	4.4
47	4.0	26.0	6.0	-	1.3	0.3	-	tr	e,ap	18.3	-	6.7	-	tr	-	h,ap	36.8
52	2.6	25.6	-	-	1.0	tr	-	tr	ap	7.0	5.0	9.3	tr	-	18.7	h	30.0
53	0.6	16.6	3.6	-	.6	1.0	-	tr	ap	6.3	tr	28.0	-	-	-	h?	44.2
55	0.6	17.6	9.0	-	-	1.3	.3	tr	-	3.0	53.0	2.0	-	-	-	-	13.2
60	0.6	14.3	3.3	-	0.3	7.6	-	tr	-	13.2	-	34.7	-	-	-	z	26.0
61t	4.0	17.6	3.0	-	0.3	2.6	-	tr	-	20.0	-	45.0	-	-	-	-	7.5
67	0.3	13.3	5.0	-	tr	3.6	-	tr	-	12.3	55.0	-	-	-	-	ap	11.3
70	21.4	24.0	7.0	tr	0.3	1.6	-	tr	ap	4.2	-	68.0	-	-	6.0	A.e	43.3
71	6.0	32.0	3.3	.6	.3	tr	-	-	ap,e	tr	-	15.0	-	-	-	A,e	42.8
75	6.0	13.0	0.6	tr	0.6	tr	-	0.3	-	4.2	1.3	10.1	tr	-	tr	z	73.3
77	4.6	10.6	4.3	23.6	tr	-	-	tr	ap	27.6	-	8.0	tr	-	tr	A,e	20.6
78	6.6	30.3	2.0	tr	0.3	tr	-	tr	ap	tr	-	6.6	tr	-	-	A	53.6

TABLE 2.1 (CONTINUED) MINERAL PERCENTAGES DETERMINED BY POINT COUNTS

WCH #	PHENOCRYSTS									MATRIX							ROCK
	Gar	San	Pyx	Ana	Sph	Pla	Amp	op	tr	Cla	Cal	Aph	Chl	Bio	Fpa	tr	Frag
101B	.3	15.0	4.0	tr	tr	6.0	-	-	-	-	70.3	3.8	-	-	-	-	0.6
84	0.3	20.3	0.3	-	-	-	-	8.0	b	-	21.6	34.3	tr	tr	3.0	z,ap	12.0
85*	-	28.3	0.6	-	-	-	-	20.3	b	-	9.6	33.0	-	-	tr	-	8.8
87	6.0	34.0	tr	1.6	-	-	-	tr	b	5.0	1.3	20.0	-	-	-	-	31.6
88	.3	5.6	-	1.0	-	-	-	12.0	h,b	-	20.0	8.3	tr	0.3	tr	h,Z	52.6
90	-	7.6	0.6	-	-	-	-	0.6	b	-	7.6	20.6	5.0	-	5.0	h	52.6
93	-	tr	-	-	-	-	-	4.0	b	-	10.3	12.6	tr	tr	tr	b	73.3
94	-	4.6	-	-	-	-	-	2.0	b	-	3.0	31.0	tr	tr	4.0	sp	55.3
96	-	11.3	0.3	0.3	0.3	-	-	2.3	b	-	3.3	46.6	tr	tr	tr	sp	34.3
98	1.3	8.3	0.3	0.3	0.3	-	-	2.3	-	-	3.3	56.0	tr	tr	tr	sp,Z	30.0
99	-	-	-	-	-	-	-	tr	e	-	16.3	tr	42.3	-	tr	sp	26.6

Gar = Garnet, San = Sanidine, Pyx = Pyroxene (aegirine - augite), Ana = Analcime Sph = Sphene, Pla = Plagioclase (andesine), Amp = Amphibole, op = Opaques, tr = Trace minerals.

Cla = Clays, Cal = Calcite (Fe), Aph = Aphanitic debris, Chl = Chlorite Bio = Biotite, Fpa = Feldspar aggregate.

z = zoisite, Z = unidentified zeolite, cz = clinozoisite, e = epidote, ap = apatite

H = heulandite, A = analcime.

* = Sample is from a dyke which intrudes the upper member (see Foldout A).

upper member.

Sanidine

Sanidine is the most abundant mineral component of the Crowsnest rocks. In the lower member, it makes up from 10 to 60% of the phenocryst phase (Table 2.1). It is found in slightly lesser abundances, averaging around 20%[2] in the upper member.

In the lower member, sanidine is characteristically found as large euhedral to subhedral crystals up to four centimeters in length (Plate 2.1a). It is also readily observed as small, tabular laths in the matrix. In both cases, the crystals are commonly broken, fractured and slightly rounded, reflecting the nature of eruption and emplacement mechanisms. Carlsbad twinning is very common, especially in the larger crystals.

The pronounced zoning which is characteristic of sanidine may best be observed at right angles to the "a" crystallographic axis, as was noted by Pearce (1967) (Plate 2.1a). Resorption and continued growth cycles are apparent by the wavy and occasionally truncated patterns of some zones. It is not uncommon to observe twenty or more zones in large crystals. Ferguson and Edgar (1978) recognized an increase in sodium towards the outer edge of each zone, reflecting sodium enrichment in the residual melt. Upon subsequent crystallization of analcime, the trend was repeated as the melt returned to a more potassic composition (Ferguson and Edgar, 1978).

Inclusions may be observed in both the phenocryst and matrix sanidines, though many are inclusion free. Smaller matrix laths tend to contain few inclusions. Aegirine - augite, plagioclase, sphene, analcime and garnet may be found in order of decreasing abundance. The aegirine - augite, plagioclase and sphene generally occur as euhedral inclusions, often exhibiting well defined zonations. Garnets have less pronounced crystal forms. Inclusions are notably absent in some beds or horizons.

In the upper member, sanidine phenocrysts exhibit the same features as those in the lower member; however, they are often corroded and recrystallized.

Alteration

Alteration of sanidine occurs throughout both members. The intensity and type of alteration is, however, notably different between the two.

---

[2]Recrystallization of phenocryst phases, notably sanidine and analcime, has probably reduced their abundance.

The most common alteration in the lower member is the conversion of sanidine to clay minerals, calcite and, in some cases, epidote group minerals. Rims, zones and fractures may show preferential alteration. Illite/smectite, illite and kaolinite are common alteration products with the availabilty of K^+ and Al^{3+} from the sanidine. Scanning electron microscopy shows that crystals may or may not be corroded at the site of alteration (Plate 2.3a,b).

Calcite is occasionally found to rim crystals and fill fractures within the crystal. Crystals towards the top of the lower section may be completely replaced by calcite. Small rectangular to rhombohedral inclusions of calcite in sanidines are the pseudomorphic replacement of original aegirine - augite inclusions.

The red "albitization" described by Pearce (1967) was mostly found coating sanidines in primary, cognate clasts within the lower member. This seems to indicate that this alteration took place prior to deposition.

Increasingly towards the top of the lower member, and very commonly throughout the upper member, sanidine is seen to be recrystallized to the low temperature equivalent adularia. It occurs as a crystal aggregate strongly resembling chert (Plate 2.1b). The presence of adularia was determined by staining with sodium cobaltinitrite and by bulk X-ray diffraction. Zones and inclusions are rarely preserved. Epidote group minerals (zoisite and clinozoisite), sericite, apatite and rarely zeolites are associated with adularia in recrystallized feldspars. They are especially abundant in the upper member.

The alteration of the feldspars in the type section is represented by the following assemblages:

1. sanidine = albite (pink color, Pearce 1967) ± calcite ± clays
2. sanidine = clays (illite/smectite, illite, kaolinite) ± calcite ± zeolite (rare)
3. sanidine = adularia/sericite ± epidote group minerals ± calcite ± zeolite(rare)

The first two assemblages are primarily found in the lower member where the matrix and phenocrysts are most susceptible to devitrification. The third suite occurs in the upper part of the lower member and as the major alteration/recrystallization phase in the upper member. In the latter case, recrystallization to adularia shows little preference for the matrix, phenocryst or rock fragment phases. Slow cooling of an initially hot deposit is thought to have resulted in the recrystallization of sanidine to adularia and associated minerals.

Garnet

Black andradite garnets are an abundant accessory, if not major constituent of the lower member where they may reach abundances of 21% and generally average about 8% (Table 2.1). They occur in much lesser amounts in the upper section. Their distribution and concentration is largely controlled by strong density-stratification in many deposits. Aegirine - augite, sphene and magnetite are found in common association where this has has taken place (see chapter 5). Towards the top of the lower member, and throughout the upper member, andradite garnet, as a discrete phenocryst, is much less common, averaging less than one percent (Table 2.1).

Euhedral dodecahedrons which commonly show simple twinning are the major crystal form of the garnets (Plate 2.1c,d and Plate 2.3c). These forms are observed in both hand specimen and thin section. The crystals range in size from <0.1mm in the matrix to as large as 5mm in the phenocryst phase. In many cases, the crystals are fractured and broken.

The well zoned nature of these garnets (Plate 2.1d), termed melanites for their titanium content, has been studied by Pearce (1967, 1971) and Dingwell and Brearly (1985). Dingwell and Brearly showed that both normal and oscillatory zoning are present, rimming a resorbed core. Their findings showed the core to be enriched in Mn^{2+} and and Al^{3+}, while being depleted in Fe and Ti^{4+}. Further, the pronounced dark versus light zones rimming the core result from Ti^{4+} and Fe variations, with the darker zones being enriched in Fe, and Ti^{4+} relative to the lighter zones (Dingwell and Brearly, 1985).

The dark brown color and well defined zoning are characteristic of garnets in the lower member. Within the upper member, however, the garnets exhibit a bleached out brown color with very poorly developed zoning. This change seems roughly coincident with the decrease in abundance of garnets, perhaps resulting from changes in, or disruption of, favorable conditions in the magma chamber.

Inclusions within the garnets are very common (suggesting a later crystallizing phase), aegirine - augite, sphene and magnetite being the most abundant (Plate 2.1d). The former two commonly show euhedral crystal forms. Minor sanidine, andesine, apatite, and analcime also occur. Aegirine - augite often shares a common nucleation site with melanites and may totally encompass an entire garnet (Plate 2.1e).

Alteration

The melanites throughout much of the lower member are very fresh and show little or no alteration. Alteration of inclusions of aegirine - augite to calcite and sanidine to adularia were periodically found.

Towards the top of the lower member and throughout the upper member the color of the garnets becomes pale brown. Edges often show minor resorption, and develop a rim of a magnetite.

Aegirine - Augite

Aegirine - augite is the third most abundant mineral in the proposed type section averaging up to 5% in the lower member (Table 2.1). Much lower abundances are found in the upper section where it averages less than one percent. The crystals are most abundant towards the top of lower member and may be concentrated in certain beds where they reach abundances of up to 9% (Table 2.1).

Crystals are commonly euhedral, but are often broken, fractured or abraided at their corners. They are easily distinguished by their upper second order birefringence, cleavage and green pleochroism. Two types of zoning were identified (Plate 2.1f). The first is a marked core - rim zonation, with the core being augite, and the rim being aegirine. Pearce (1967) also identified the opposite. The second style, common in the upper beds of the lower unit, is a fine rhythmic zonation throughout the crystal (Plate 2.1f). Contacts between each zone are sharp, with no apparent resorption. Hourglass extinction patterns were found to overprint zoning styles in a number of crystals (Plate 2.1e). Ferguson and Edgar (1978) suggest that the differentiation trend of the melt to more sodic compositions is reflected in the zonations.

Pyroxenes are relatively free of inclusions, suggesting early crystallization. Subhedral garnets, analcime and Fe-oxide are occasionally found as inclusions. As mentioned, aegirine - augite often shares common nucleation sights with garnets.

It is of interest to note that clasts of fresh, primary aegirine aggregates are found occasionally in the upper section. These clasts have suffered little alteration aside from the rimming of the clast with Fe-Ti oxides. It is not known if such clasts are accidental or representative of the Crowsnest rocks. The latter is favored on the basis of the occurrence of aegirine - augite as a primary crystal component of the formation.

Plate 2.1

A. Photomicrograph of a rhythmically zoned sanidine phenocryst (**Fp**) supported by a matrix of clay minerals (**Cl**) and smaller fragments. Lower member, wch-56, field of view 1 x 1mm, X-polars.

B. Photomicrograph of a zoned sanidine phenocryst from an upper bed of the lower member showing alteration/recystallization to adularia aggregate (**Ad**) and clay minerals. Lower member, wch-65, field of view 1 x 1mm, X-polars.

C. Photomicrograph of euhedral, twinned melanite garnets separated from a green crystal ash. Lower member, wch-32, field of view 1cm x 1cm, X-polars.

D. Photomicrograph of an intensely zoned melanite phenocryst. Inclusions of sanidine and aegirine - augite are evident. The garnet is rimmed by a feldspathic coating. Lower member, field of view 2.7 x 2.7mm, X-polars.

E. Photomicrograph of an anhedral garnet (**Gr**) which has been completely surrounded by aegirine-augite (**A**). Lower member, wch-47, field of view 2.7 x 2.7mm, P-polars.

F. Photomicrograph of an intensely zoned aegirine-augite phenocryst showing sharply defined rhythmic zoning and hour-glass extinction. Lower member, wch-39, field of view 1 x 1mm, X-polars.

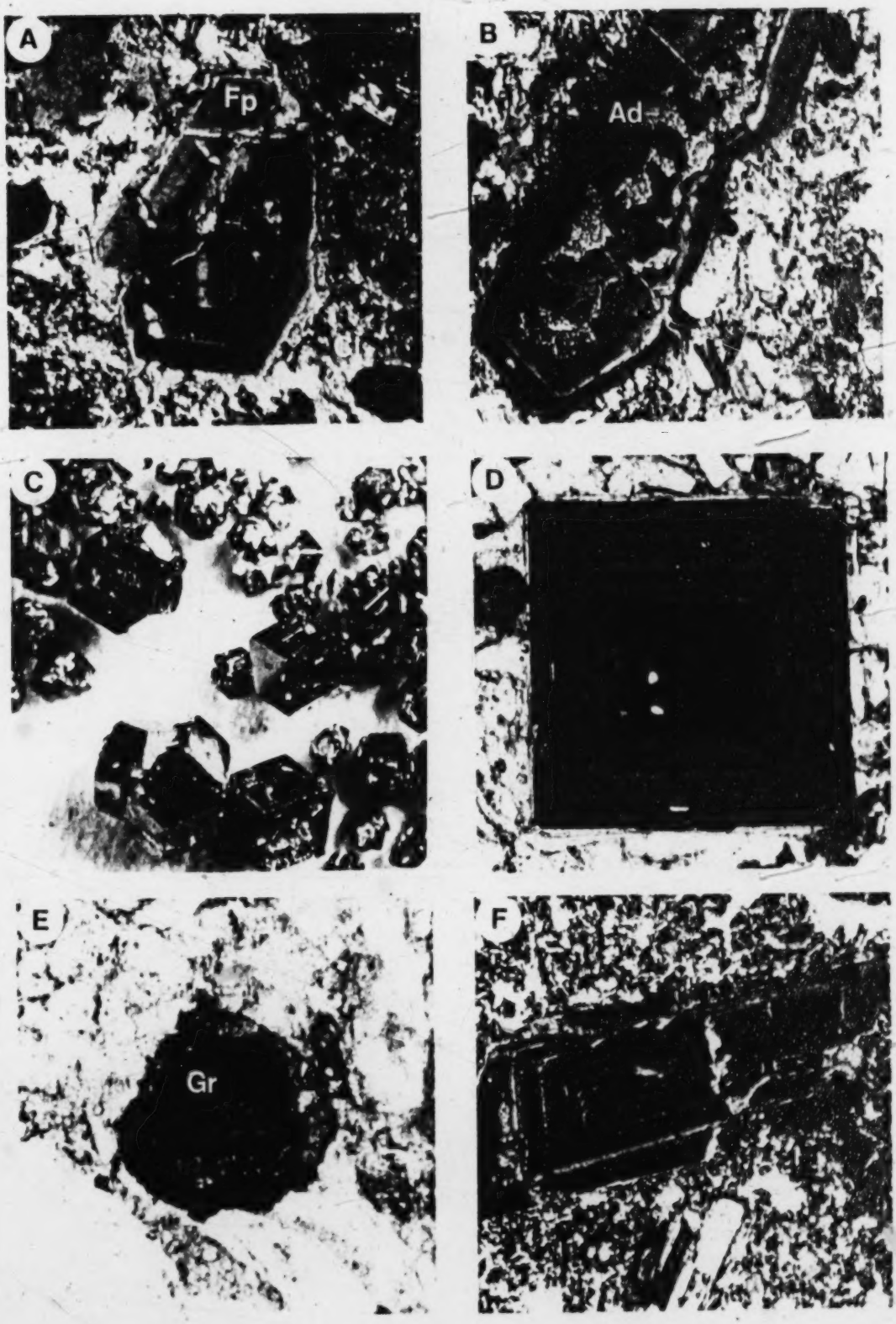
A
Fp
B
Ad
C
D
E
Gr
F

Alteration

Within the lower member two types of pyroxene alteration are observed. They are represented by the following assemblages:

1. Aegirine - augite = Fe calcite ± chlorite ± Fe-oxide
2. Aegirine - augite = amphibole (hornblende)/biotite ± calcite ± Fe-oxides.

In both cases the replacement may be pseudomorphic. Calcite replacement tends to preserve the original crystal shape, especially when it replaces euhedral inclusions in other minerals (Plate 2.2a).

The presence of pyroxene in the upper member is demonstrated by intensely corroded relict crystals. The original modal percentage cannot be determined. The two alteration assemblages common in the upper member are listed below.

1. Pyroxene = biotite = chlorite ± Fe-oxides,
2. Pyroxene = calcite ± Fe-oxides

It is possible that amphibole was an intermediate phase that was not recognized.

Analcime

Analcime, as discrete crystals, is most common in the crystal-rich beds of the lower member; however, it achieves greatest abundance in the upper member where it occurs as phenocrysts in cognate and juvenile blairmorite clasts. It does not survive as discrete phenocrysts in the upper member.

In the lower member, analcime averages around 2% but it may be totally absent from some beds (Table 2.1). Conversely, certain beds are notably rich in analcime, up to 24% (Table 2.1). Analcime is found as small microlites in the matrix (Plate 2.3d) and as larger phenocrysts up to .5cm. Large fragments suggest the presence crystals larger than 1 cm. The crystals are euhedral trapezohedrons (Pearce, 1967) which may or may not be rounded or broken.

In thin section, the analcimes of the type section have a characteristic yellow hue, apparently the result of minor replacement by hematite, which has been previously suggested by Pearce (1967) (Plate 2.2b). Of the three varieties identified by Pearce (1967), only the brown isotropic analcime was identified as a discrete phenocryst. The green and red anisotropic varieties were not observed except as components in blairmorite fragments.

Inclusions in analcime are rare if not totally absent.

Alteration

Analcime is best preserved as phenocrysts in the lower member. Preservation is enhanced in beds which have not undergone intense devitrification and retain their original matrix components. In intensely altered beds larger crystals have rounded edges and do not generally retain their euhedral nature. The low abundance of smaller crystals suggests that they have been completely converted to alteration products. Based upon textural and mineralogical associations, the alteration assemblage is as follows:

Analcime = clays (illite/smectite) ± calcite[3]

Analcime = calcite

In thin section, analcime microlites are seen to be converting to small calcite grains similar to those shown in Plate 2.7a. Under a scanning electron microscope, analcime is found to be coated by platy, foliated clays. (Plate 2.3d).

In the upper member, discrete analcime phenocrysts other than those found in blairmorite fragments are rare. Hexagonal crystal forms, in some cases with remnant zonation, are replaced by a fine chert like aggregate composed almost entirely of adularia with minor sericite (Plate 2.2c, d). Usually the entire crystal has been replaced. Despite the similarity in crystal forms between garnets and analcime, it is not likey that adularia would replace a garnet. It would seem that discrete analcime phenocrysts were unstable in the matrix of the upper member and probably recrystallized during cooling. The alteration of analcime in the upper section is summarised by the assemblage:

Analcime = adularia ± calcite ± fibrous mass (sericite/zeolite).

In many blairmorite fragments of the upper member, analcime also exhibits these features, though they are less pronounced.

Plagioclase

Plagioclase is a common yet minor component found only in the lower member where it averages up to 1% (Table 2.1). In some beds, discordant pipes of about 0.5 mm width contain almost exclusively euhedral andesine crystals associated with abundant clays, pyroxene and minor quartz. These features are thought to be degassing pipes.

---

[3]According to Hebner *et al.* (1985), at lower temperatures and neutral pH analcime will convert to smectite and calcite.

Plate 2.2

A. Photomicrograph of a euhedral aegirine-augite (A) phenocryst which is being pseudomorphically replaced by Fe calcite (Ca). Lower member, wch-44, field of view 1 x 1mm, X-polars.

B. Photomicrograph of an anhedral (rounded) analcime (An) phenocryst showing the yellow hue and fractured texture common in analcimes of the lower member, wch-48, field of view 2.7 x 2.7mm, P-polars.

C. Photomicrograph of a hexagonal phenocryst showing remnant zoning. It is composed of a fine aggregate of adularia and sericite. Analcime (An) is suspected to be the precursor. Lower member, wch-75, field of view 1 x 1mm, P-polars.

D. Photomicrograph of "C" under crossed polars. Note the resemblance to chert. Lower member, wch-75, field of view 2.7 x 2.7mm, X-polars.

E. Photograph of an angular blairmorite fragment with its characteristically porphyritic analcime (An) and subordinate sanidine (Fp) crystals. Upper member at Willoughby Ridge.

F. Photomicrograph of a finely prophyritic (aphanitic to glassy) blairmorite fragment (Fg). The analcime microlites are the small, dark grains. The clast is plastically deformed. This type of clast is only found in the lower member. wch-15, field of view 1 x 1mm, P-polars.

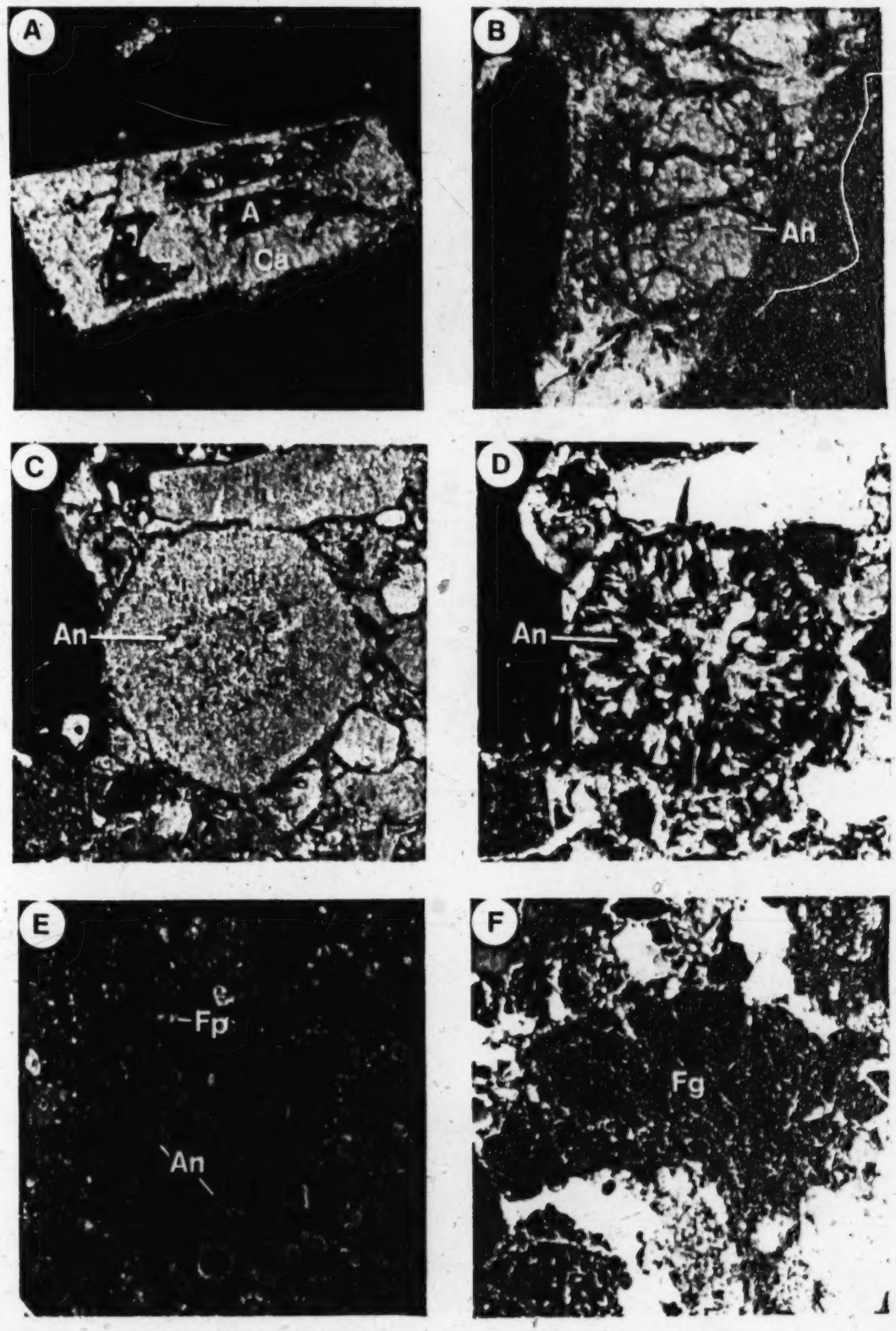
A
A
Ca
B
An
C
An
D
An
E
Fp
An
F
Fg

The composition of the plagioclase ranges from An 31 to An 50 with an average around An 40, andesine. Crystals occur as both large phenocrysts and as micro-phenocrysts in the matrix. Both types are euhedral and show excellent albite and simple twinning.

A unique occurrence of plagioclase is as euhedral, zoned inclusions with sharp crystal boundaries in large zoned sanidine crystals. The composition is again An 44. These features suggest that the crystals are inclusions rather then perthitic exsolution. In some cases a perthitic texture was identified; however the plagioclase showed no crystal shape or zoning. The composition in these cases was not determined.

In almost all cases, plagioclase crystals are relatively unaltered, showing only minor sericite development.

Accessory Minerals

Sphene is the most abundant accessory mineral in both members, where it has been found in trace amounts in all but a few beds (Table 2.1). It occurs as euhedral, well twinned crystals up to 4mm in size and may be found both as small microphenocrysts and inclusions. Elongation in the "c" crystallographic direction is common. It generally alters to carbonate.

Amphibole is a relatively rare mineral found only in the upper beds of the lower member. It occurs as an aggregate usually with a rim of Fe oxide, and rarely as discrete phenocrysts. Both hornblende and basaltic hornblende were identified. Alteration of aegirine - augite may be a likely source.

Apatite is a common accessory found as very small crystals in the matrix and as inclusions in garnets. It is abundant in the upper section in rock fragments which have been altered to adularia aggregates, and rare as phenocrysts.

Zoisite and clinozoisite have been identified in clasts of the upper member. They are likely secondary minerals. Epidote has been observed as inclusions in an unaltered feldspar which suggests it may also occur as a primary component. The most common association is with feldspar aggregate recrystallization of rock fragments.

Biotite occasionally occurs in the upper member where it is found to alter to chlorite. If the presence of chlorite is any indication, biotite may initially have been present in much greater abundances.

Metallic minerals are common throughout the section but are most abundant in the upper member. Titanomagnetite, hematite, ilmenite and pyrite were found to be the most common. In the lower member they may concentrate with other heavy non-metallic minerals in density-stratified deposits, (Chapter V). The crystals border the size range between micophenocrysts and matrix phases.

B. Rock Fragments

Rock fragments make up a major part of the Crowsnest suite. Their abundances range from 0 to 73% throughout both the lower and upper members (Table 2.1). Virtually all fragments are cognate and juvenile, though a number of accidental clasts were identified.

The textures of the fragments suggests an origin as previously erupted flows or plugs. They are very commonly porphyritic, with the feldspar and sphene phenocrysts characteristically exhibiting a trachytic texture. Coarser or equigranular rocks may reflect plutonic or hypabyssal origin. Most fragments contain sanidine feldspar, plus or minus melanite, aegirine - augite and analcime. The original mineralogy of many fragments has been obliterated by alteration, recrystallization and pseudomorphic replacement. In many cases, the original textures are preserved.

A detailed description and classification of all clasts present in the Crowsnest suite is well beyond the scope of this study. However, their presence as an integral component warrants some discussion. For general purposes, the majority of fragments may be divided into five groups, based in part on the descriptions given by Ferguson and Edgar (1978) and Pearce (1967) for primary rock types. The reader is referred to these works for comparative descriptions of relatively fresh, primary lava flows which survived the eruptions which produced and emplaced fragments of similar mineralogy and texture.

1. Trachytes. Trachyte fragments of the Crowsnest are those whose mineralogy consists of sanidine, aegirine - augite, sphene, melanite, plagioclase and lesser amounts of magnetite, ilmenite, apatite, amphibole and analcime. Sanidine is by far the most abundant constituent, followed by aegirine - augite. All other components are confined to the matrix phase, with some, notably sphene, achieving micophenocryst status.
2. Phonolites. Phonolite fragments may be categorized under the name analcime phonolite due to occurrence of analcime as a primary magmatic constituent (Ferguson and Edgar,

1978). Generally, such rocks contain approximately equally amounts of sanidine and analcime. Pearce (1967) noted abundances of about 18% of each in the phenocryst phase. Other common constituents are aegirine - augite, aegirine, melanite, sphene, biotite, chlorite, amphibole and Fe,Ti - oxides. Apatite was identified in most fragments, sometimes becoming fairly abundant. Sanidine, pyroxene, analcime and melanite are notably porphyritic.

3. Blairmorite. This unusual rock type, first named by Knight in 1904, has since been the focus of many studies; Mackenzie (1914), Pearce (1967, 1970) and Ferguson and Edgar (1978). The most common occurrence as noted by this study and those mentioned above is as fragments in the thick beds of the upper member (Plate 2.2e). They are also quite common as small glassy or aphanitic fragments in many beds of the lower member. Such fragments are composed of small analcime microlites in a fine glass matrix (Plate 2.2f). These fine-grained varieties probably represent a juvenile phase. Characteristically, analcime occurs as large euhedral phenocrysts up to 4cm. Small euhedral crystals may also be abundant in the matrix. They may constitute 60 to 85% of the phenocryst phase. Sanidine was observed to be present in substantially lesser amounts than in other rock types. Melanite garnet, aegirine - augite, sphene and Fe - Ti oxides are found in variable amounts in the matrix. The former two may occur as small phenocrysts along with the analcime.

4. Crystal Aggregate Fragments. In rare instances, fragments containing crystal aggregates of a single mineral were identified. Amphibole-rich fragments containing almost entirely coarse hornblende crystals averaging .25mm were recognized in the upper beds of the lower member, and more abundantly in the upper sequences. An Fe-oxide rim about the whole fragment was observed in a number of cases. Such rims were not found around individual crystals within the aggregate.

   Pure aegrine aggregates were identified only in the upper section. They are easily recognized by their brilliant, high birefringence and the radiating habit of the crystals which average about 1mm in length. There appears to have been little or no alteration.

5. Accidental Fragments. Accidental fragments are occasionally found throughout the deposits of the proposed type section. They are totally absent in many beds and make up no more than about 2% in those in which they occur.

In the lower most beds of the lower member, sandstone, shale and, in one case, limestone were identified. Sparry calcite fragments found in the upper section are thought to be accidental. Occurrences of accidental igneous or metamorphic clasts were not documented.

Alteration

In many welded beds of both members, fragments commonly exhibit an alteration assemblage. It is thought that the fragments of the type section have undergone multiple alteration processes during their history. Initially deposited as fresh, viscose, primary lava flows or plugs immediately surrounding the vent, the deposits were probably subjected to alteration during subsequent eruptions. Further disruption and redeposition as a component of a hot, pyroclastic deposit may have overprinted the initial assemblage.

In thin section, most clasts have suffered mineralogical changes. In the lower member, the alteration is dominated by clays and pink albite alteration of the constituent sanidines. A common alteration of clasts of the upper member is the apparrent recrystallization of both the matrix and phenocrysts (feldspar and analcime) to a fine, chert-like, adularia/sericite aggregate. This aggregate also contains varying amounts of epidote, apatite, carbonate and minor zeolite. (Plate 2.6a). The transformation may not destroy crystal outlines.

In many fragments of both members, small round spheroids filled with radiating fibers are common. In some cases, adularia appears to accompany the radiating forms. It is probable that these forms may have been remnant vesicles.

A reflection of the alteration/recrystallization which has taken place in many fragments from both members is the presence of baked and/or resorbed rims around many clasts (Plate 2.7f). This is almost always accompanied by a marked color change and evidence of plastic deformation indicating emplacement at elevated temperatures.

C. Matrix

The matrix of the Crowsnest suite is dominated by a highly complex mixture of mineral species. Many of these species are the result of intense alteration. As with the phenocryst phase, there is a notable difference between the matrix phases of the upper and lower members, indicating that the origin, mineralogy and conditions of diagenesis varied between the two sequences. In the lower member, the matrix is composed of fine-grained pyroclastic material

consisting of small crystals, crystal fragments, rock fragments and their subsequent diagenetic assemblages. The matrix of the upper member, however, consists almost entirely of finely-crystalline assemblages dominated by adularia. Matrix components were determined by petrographic, scanning electron microscope and X-ray diffraction analyses.

Original Material: Glassy and Aphanitic Components

Original glassy/aphanitic components are those components of the matrix which have retained their original compositions and textures after the alteration which has clearly taken place in both members. Despite intense devitrification, rare, fine, glassy and aphanitic fragments are preserved in some rock types. It is likely that glass was a major component of the matrix in some beds of the lower member before alteration. Ferguson and Edgar (1978) and Pearce (1967) identify an abundant glass component in the flows of the formation. In the pyroclastic rocks, true glasses were not generally identified; however, it is thought that the abundant aphantic fragments of the lower member represent a slightly coarser crystalline counter-part. In the upper member, recrystallization has overprinted virtually all of this original material.

Bubble walls and glass shards likely composed a portion of many deposits in the lower member. Despite the highly altered nature of many of these beds, the occurrence of very fine fibers and crescent shapes indicate their original presence. These forms are now composed of clays and other alteration assemblages. In many cases the original shapes have been destroyed by alteration.

In general, fine sanidine laths and sanidine-rich aphanites dominate these original phases. Sodium cobaltinitrite staining was used to determine that the extremely fine-grained varieties contained essentially potassium feldspar as the dominant mineral phase.

The matrix of the lower member was probably composed of primary glass and/or aphanitic fragments and crystal fragments which have been intensely altered, obliterating the original mineralogy and texture. Alteration to clay minerals and calcite is very common and will be further discussed in the following sections. Most alteration occurs in beds that are unwelded, and therefore susceptible to devitrifying waters. This alteration is observed to some extent in all beds, with some showing almost complete alteration of the original material.

In contrast, alteration of the matrix to clays in the upper upper member is much less pervasive. This may have been due to the impervious nature of the welded rocks. The matrix of the upper member characteristically shows recrystallization to a fine adularia/sericite aggregate and, in rare cases, zeolite. Serpentine, chlorite, Fe-calcite and Fe -Ti oxides are found in abundance with occasional epidote group minerals and apatite.

Clay Minerals

The abundance of clay and clay-sized material within the Crowsnest Formation is apparent upon first inspection of the lower member at the type section. They represent the most common alteration assemblage of the pyroclastic rocks in these lower beds.

X-ray diffraction (XRD), scanning electron microscopy (SEM) and energy dispersal analysis (EDA) were used to identify the mineralogies in this size range for both members. Sample preparation and analytical procedures may be found in appendix B.

Lower Member

Clay minerals may be observed in both hand specimen and thin section. Beds with a non-welded character tend to have a higher abundance of clay minerals, likely due to their permeable nature. Clays are present in all beds in the lower member, although their whole rock abundances vary (Table 2.1). They are distinguished in thin section from glass and zeolites by their foliated nature, low to moderate birefringence and length slow orientation (Plate 2.6b).

Clays are most abundant in the matrix where devitrification of the original glass has occurred. Large, zoned sanidine crystals have altered to clay minerals around their boundaries, along fractures throughout their interior and preferentially within specific zones. The overall abundance of clays can be attributed to devitrification of matrix glasses, alteration of sanidine phenocrysts and probably the alteration of analcime to clays and carbonate.

X-Ray Diffraction

Four clay mineral species were identified from the lower member. Illite, mixed-layer illite/smectite, chlorite and kaolinite were found in decreasing order of abundance in the clay-size fractions (Table 2.2). The term "illite" is used for all mica species with a 10Å *001* peak and subsequent integral diffractions.

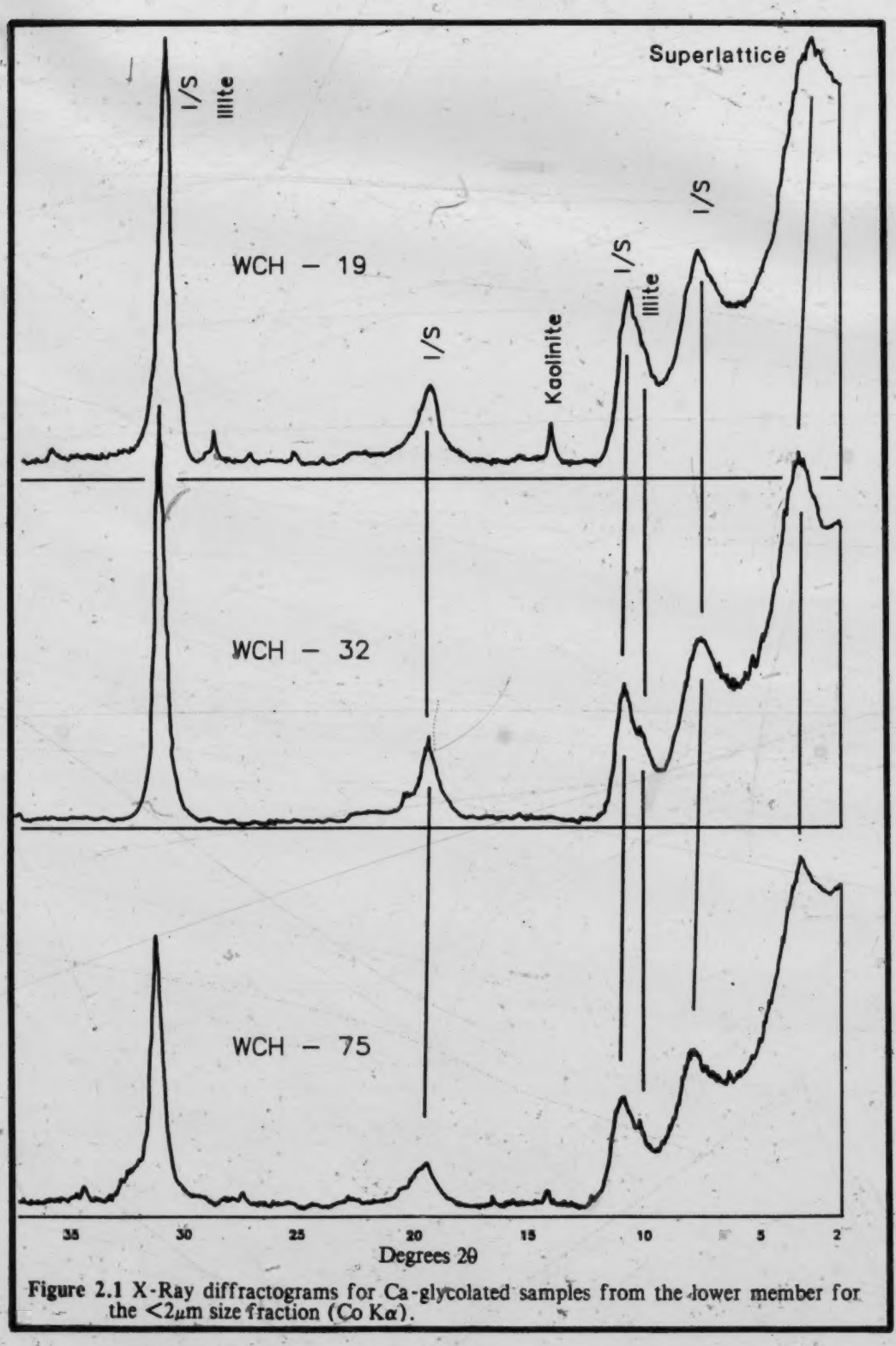

Figure 2.1 X-Ray diffractograms for Ca-glycolated samples from the lower member for the $<2\mu m$ size fraction (Co Kα).

A series of charts for <2μm Ca^{2+}-glycolated samples from the lower member are shown in Figure 2.1. Each sample represents the signature of a single bed. The two most pronounced characteristics of these samples are their purity (i.e. they contain only clay minerals) and the compositional similarity between samples in the same size range (Figure 2.1).

The pronounced non-integral diffractions at about 13.0Å, 9.4Å, 5.2Å and 3.3Å are identified as mixed-layer illite/smectite after methods proposed by Reynolds (1980), Hower (1981), and Brindley (1981). The relative percentages in the mixed-layer are discussed below.

Discrete illite is identified by d - spacings between 9.8 and 10.2Å and subsequent integral diffractions (Figure 2.1). Deviation of the 10.0Å, *001* reflection to 9.8Å is suggested by Srodoń (1980, 1984) to be the result of small percentages, up to 5%, of expandable layers mixed randomly with illite.

Chlorite and kaolinite diffractions occur together. The presence of a 3.54Å *004* diffraction distinguishes chlorite from kaolinite which has a 3.58Å *002* diffraction. Enhanced diffractions at 14.2Å, 7.1Å and 3.54Å upon heating to 550°C confirms the presence of chlorite as kaolinite is destroyed at this temperature.

Discrete illite and the illite/smectite mixed-layer are the dominant mineral species, comprising about 90 to 98 percent of the clay-size fraction (Table 2.2). Chlorite and kaolinite make up the remainder. These latter two phases are likey a reflection of composition, namely the availabilty of iron and aluminium. A detailed analysis of a green crystal ash, (WCH -32, see Chapter IV) for the size ranges <2μm, 2 to 5μm and 5 to 20μm indicate that clays dominate the finer size range up to 5μm, at which size other mineral constituents such as melanite and sanidine begin to appear (Table 2.3).

Table2.3 Detailed analysis of the <2μm, 2 to 5μm and 5 to 20μm size fraction for sample wch-32.

	Illite/smectite	Illite	Kaolinite	Sanidine	Garnet	Analcime
<2μm	M	M	-	-	-	-
2-5μm	M	M	m	m	m	m
5-20μm	M	M	m	m	M	m

M = major component, m = minor component

These data indicate a virtually complete conversion to clay minerals in <2μm size range.

TABLE 2.2 RELATIVE CLAY MINERAL ABUNDANCES (%) IN THE <2μm SIZE FRACTION

SAMPLE NUMBER	KAOL.	ILLITE	SMEC.	CHLOR.	ILLITE/ SMEC.
WCH-1	-	70	-	1	28
WCH-9	-	70	-	2	27
WCH-14	-	49	-	4	46
WCH-17	-	65	-	3	32
WCH-18	3	55	-	-	42
WCH-19	10	52	-	-	38
WCH-31	-	66	-	-	34
WCH-32A	-	54	-	-	46
WCH-32B	-	52	-	-	48
WCH-33	-	60	-	4	35
WCH-40	-	67	-	4	30
WCH-52	-	63	-	6	31
WCH-59	22	51	-	12	15
WCH-62	4	62	-	2	32
WCH-75	4	54	-	-	42
UPPER SECTION					
WCH-88	-	68	-	32	-
WCH-92	-	54	-	46	-
WCH-98	-	61	-	39	-

The nature of the mixed-layer clays, especially those in bentonites, has been investigated by Reynolds (1980), Hower (1981) and Srodon (1984). Their percentage determinations for illite and smectite in the mixed-layer are based upon the shift of the non-integral diffractions with changing percentages of illite and smectite in the mixed-layer. The schemes also determine the order and stacking arrangement (i.e. IS versus ISII types and their variations). All three systems are utilized in this study to compare the compositions of each bed. The results of all methods are given in Table 2.4.

In Figure 2.2 the $(001)_{10}/(002)_{17}$ and the $(002)_{10}/(003)_{17}$ diffractions of the mixed-layer are plotted to determine their composition. As two sets of data are plotted on two different standard curves, the overlap between plotted samples is taken as a better representation of the compositional range and the average. This assumption excludes data points on the upper and lower extremes. The Crowsnest suite clusters between 55% and 74% illite for allevardite ordering (Figure 2.2). Allevardite ordering is favored due to the highly pronounced superlattice diffraction on all calcium glycolated charts (Srodon, 1984). The average composition from this method is around 64% illite.

The method proposed by Srodon (1984) for $(002)_{10}/(003)_{17}$ and $(003)_{10}/(005)_{17}$ diffractions (Figure 2.3) shows the Crowsnest rocks to range between 20 and 50 % smectite, clustering around 30%. Ordering type is determined by plotting percent smectite (Figure 2.3) versus the $(001)_{10}/(001)_{17}$ reflection (Figure 2.4). According to this scheme, the illite/smectites of the Crowsnest Formation have IS ordering type, with slightly transitional values towards IIS type. No samples indicated random ordering.

Based upon these three schemes, the illite/smectite clays of the Lower Crowsnest Formation contain between 55 and 75% illite with an IS ordering type. Discrepancies between the values listed in Table 2.4 may be caused by interference of the mixed-layer diffraction by the discrete illite diffraction and by broad, rounded mixed-layer diffractions. For such diffractions, an estimated center of the diffraction was used to determine the d - spacing.

Scanning Electron Microscopy

The morphology and chemistry of selected samples from the lower member were investigated by scanning electron microscope (SEM), and energy dispersive spectrometry (EDS).

TABLE 2.4 COMPOSITIONAL DETERMINATIONS FOR ILLITE/SMECTITE MIXED LAYER CLAYS

WCH #	Reynolds, (1981) % Illite		Hower (1980) % Illite		Srodon (1984)	
	(002)	*(003)*	*(002)*	*(003)*	% Illite	Ordering Type
WCH-1	60%	53%	42%	53%	80%	IS
WCH-9	80%	60%	67%	60%	78%	IS
WCH-14	70%	63%	55%	63%	70%	IS
WCH-17	71%	63%	56%	63%	70%	IS
WCH-18	65%	68%	50%	68%	65%	IS
WCH-19	69%	67%	54%	67%	70%	IS
WCH-31	60%	62%	42%	62%	71%	IS
WCH-32	69%	66%	54%	66%	65%	IS
WCH-33	63%	64%	47%	64%	72%	IS
WCH-40	60%	60%	42%	60%	77%	IS
WCH-52	55%	71%	35%	71%	51%	IS
WCH-59	55%	63%	35%	63%	73%	IS
WCH-62	72%	61%	57%	61%	75%	IS
WCH-75	65%	67%	50%	67%	63%	IS

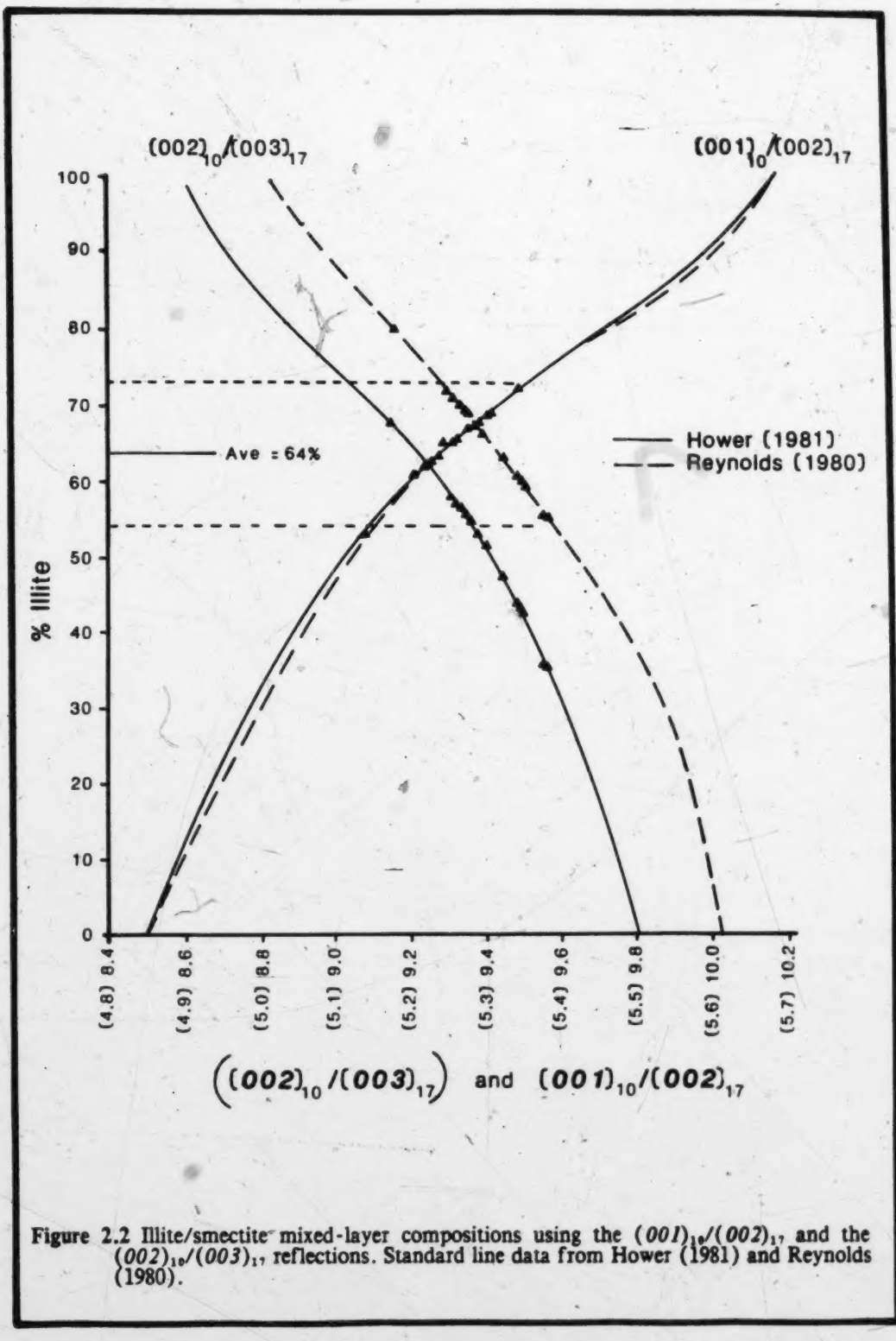

Figure 2.2 Illite/smectite mixed-layer compositions using the $(001)_{10}/(002)_{17}$ and the $(002)_{10}/(003)_{17}$ reflections. Standard line data from Hower (1981) and Reynolds (1980).

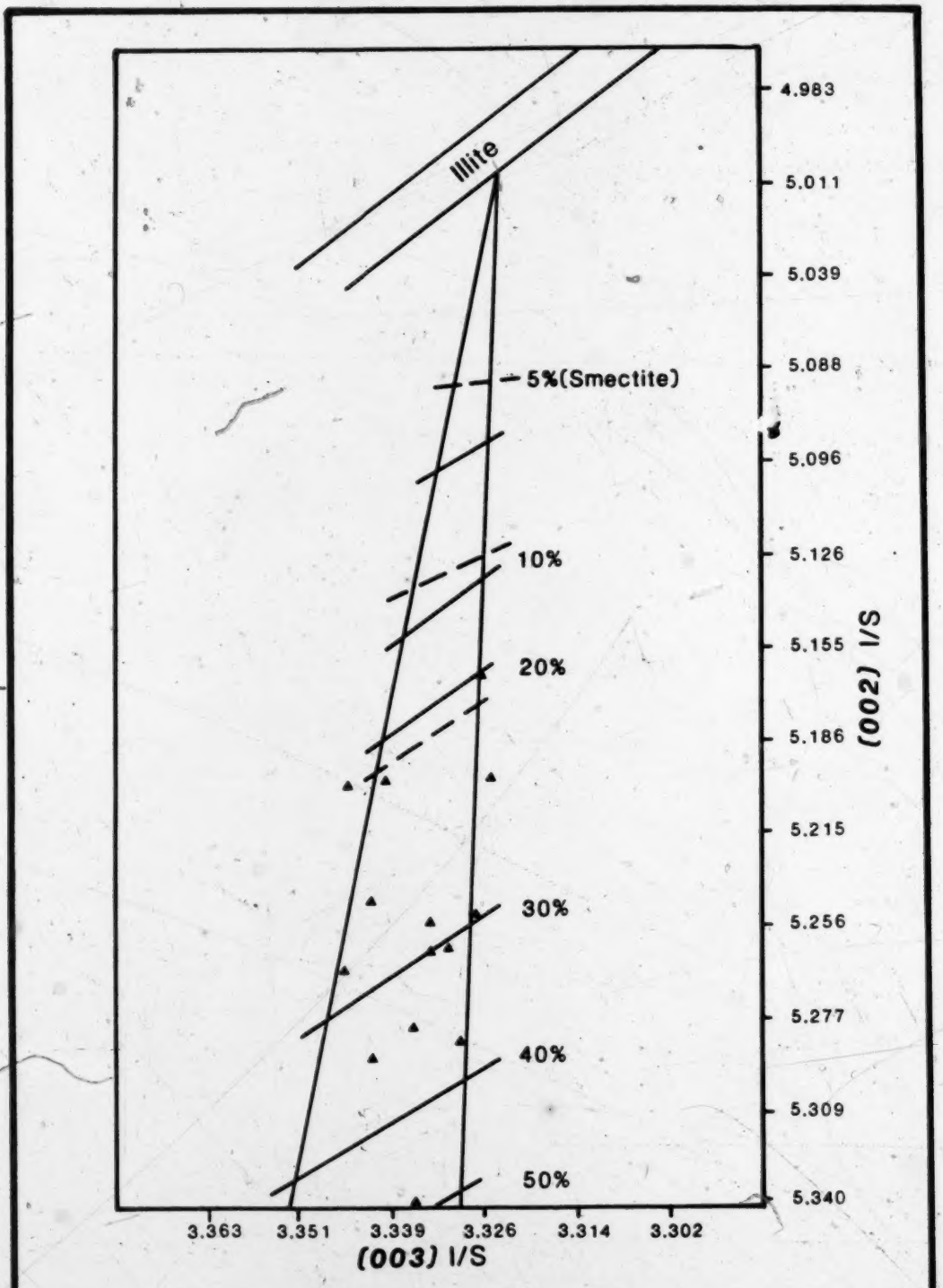

Figure 2.3 Illite/smectite mixed - layer compositions using the $(002)_{10}/(003)_{17}$ and the $(003)_{10}/(005)_{17}$ reflections, after Srodon (1984).

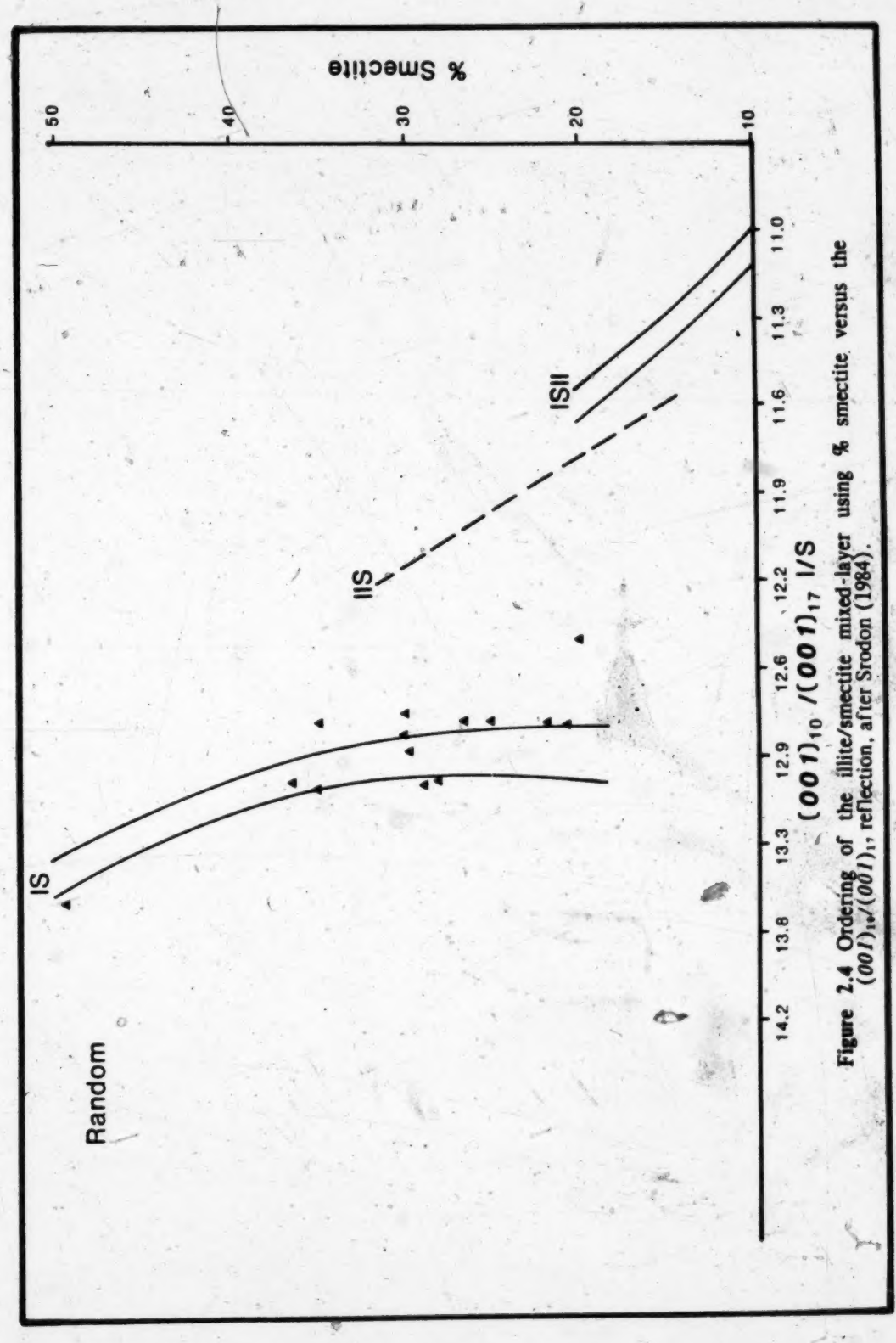

Figure 2.4 Ordering of the illite/smectite mixed-layer using % smectite versus the $(001)_{10}/(001)_{17}$ reflection, after Srodon (1984).

Illite/smectite can be recognized by its foliated nature, best exhibited in cross-section (Plate 2.3c,f,g,h and 2.4a). Planes perpendicular to the foliation show a smooth, hummocky surface. A marked foliation is often developed around larger crystal and rock fragments (Plate 2.3h. Plate 2.4a).

Discrete illite overgrowths are observed to be an authigenic phase which developed after the formation of the illite/smectite. It occurs as overgrowths on illite/smectite, as pore fillings, and commonly exhibits a ropy to fibrous texture (Plate 2.4c,d,e).

Chlorite occurs as platelets and poorly developed rosettes (Plate 2.4g).

Upper Member

Except for chlorite, clay minerals are not abundant in the massive sequences of the upper member. Texturally, there is little resemblance to the beds of the lower part of the formation. The processes which have encouraged the formation of clays elsewhere have not influenced these upper beds. Their massive, seemingly impermeable nature has apparently reduced the effect of the devitrifying waters which have substantially altered the more permeable, less massive beds of the lower member.

X-ray Diffraction

Diffractograms of calcium glycolated samples from the upper member show a marked change in the clay signature from that of the lower member (Figure 2.5). Chlorite and illite[4] are identified by diffractions at 14.2Å and 10.2Å respectively. Both exhibit integral diffractions. The presence of the 10Å peak is partially due to the presence of biotite, identified in thin section.

In contrast to the $<2\mu$m size fraction in the lower member (Figure 2.1), the samples of the upper section are not composed solely of clay minerals. Adularia, analcime, mica group minerals and calcite are also present (Figure 2.5). Of the clay minerals, 10Å minerals are the dominant, averaging around 55% (Table 2.2). Chlorite abundance averages around 39% (Table 2.2).

Chlorite is likely the iron rich variety (chamosite) as manifested by the presence of a subdued *001* diffraction, an enhanced 7.1Å *002* diffraction and a 3.54Å *004* diffraction (Figure 2.5). The *001* peak is enhanced upon heating to 550 °C.

[4]Illite includes illite and sericite.

Plate 2.3

A. SEM micrograph of a sanidine crystal (**Fp**) in sharp contact with a clay (**Cl**) matrix composed of illite and illite/smectite. Lower member, wch-16.

B. SEM micrograph of a sanidine crystal (**Fp**) showing a corroded contact with a clay (**Cl**) matrix composed of illite and illite/smectite. Lower member, wch-31.

C. SEM micrograph of a euhedral garnet (**Gr**) showing smooth unaltered crystal faces. Impact chips (**ch**) can be seen on both crystal faces and edges. The crystal is supported by clay (**Cl**) matrix composed of illite and illite/smectite. Lower member, wch-32.

D. SEM micrograph of a euhedral analcime (**An**) coated in clay minerals. It is supported by a clay (**Cl**) matrix. Lower member, wch-77.

E. EDA graph of the analcime crystal in "D" showing the sodium aluminosilicate compostion[1].

F. SEM micrograph of massive illite/smectite showing a foliated texture in cross-section and a smooth hummocky surface perpendicular to the foliation. Lower member, wch-32.

G. SEM micrograph of showing a platy habit of illite/smectite. Lower member, wch-32.

H. SEM micrograph of foliated clays (**Cl**) between crystal fragments (**Cf**). Lower member, wch-52.

---

[1] Au and Ag were introduced during sample preparation.

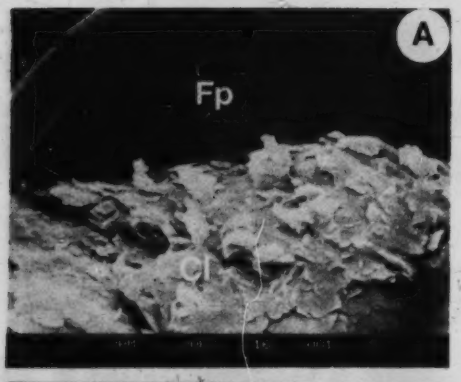
A
Fp
Cl

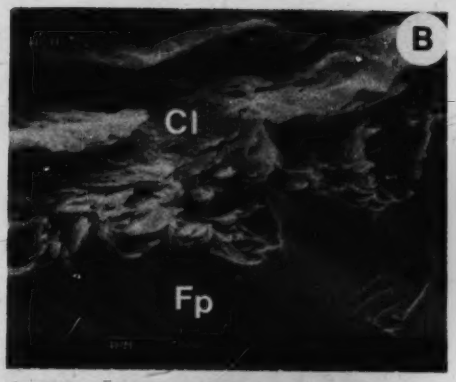
B
Cl
Fp

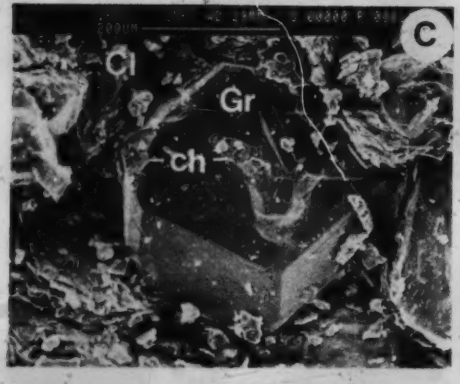
C
Cl
Gr
ch

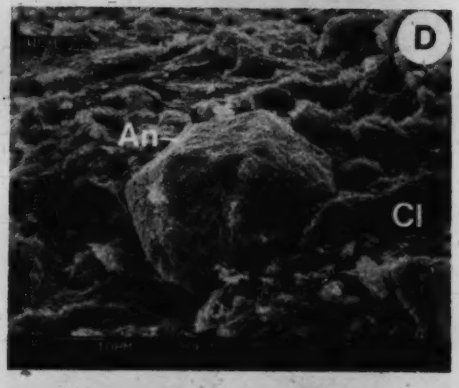
D
An
Cl

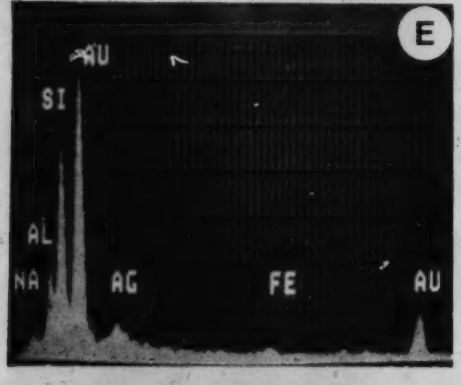
E
AU
SI
AL
NA
AG
FE
AU

F

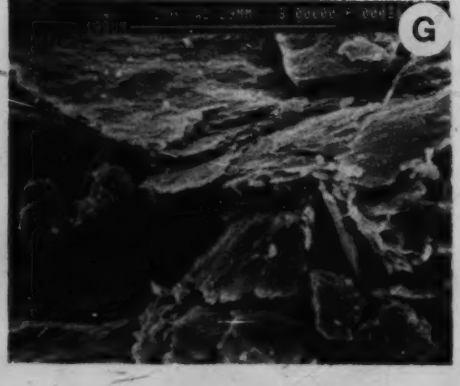
G

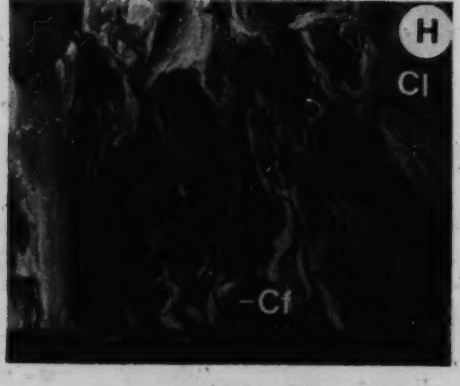
H
Cl
Cl

Plate 2.4

A. SEM micrograph of massive illite/smectite (I/S) supporting a euhedral garnet (Gr) phenocryst. Lower member, wch-32.

B. EDA graph of a <0.2μm separate of typical illite/smectite from the Crowsnest Formation showing calcium as the probable interlayer cation.

C. SEM micrograph of ropy, honeycomb-like illite (I) overgrowths on illite/smectite (I/S) and other fragmental components. Lower member, wch-62.

D. SEM micrograph of wispy illite (I) overgrowths on massive illite/smectite (I/S). Lower member, wch-32.

E. SEM micrograph of honey comb illite (I) as a pore filler. Lower member, wch-74.

F. EDA graph of the ropy illite in "E" showing its potassic composition.

G. SEM micrograph of chlorite (Chl) from the lower member exhibiting a platy habit and poorly defined rosettes, wch-74.

H. SEM micrograph of honeycomb illite (I) from the upper member, wch-98.

171X 25KV WD 30MM S 00000 P 00026
200UM
A

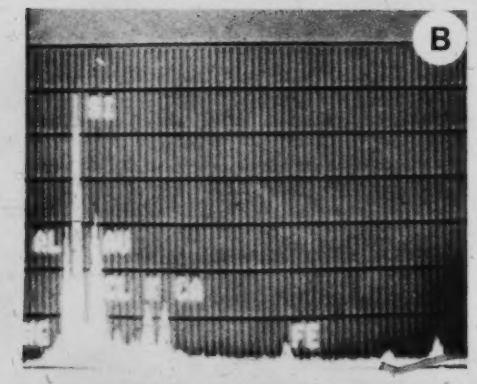
B
AL
FE

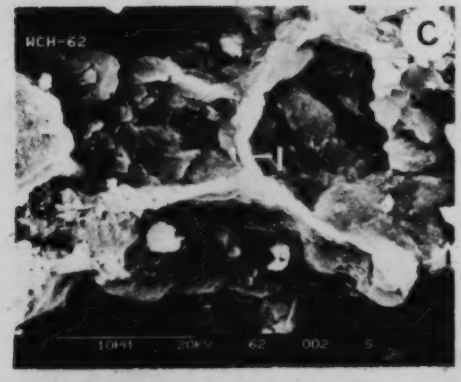
WCH-62
C
I
10MM 20KV 62 002 S

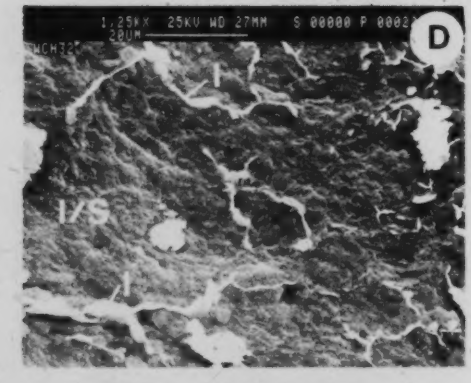
1.25KX 25KV WD 27MM S 00000 P 0002
20UM
D
I
I/S
I

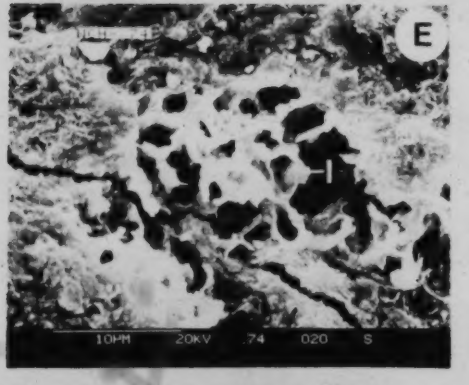
E
I
10MM 20KV 74 020 S

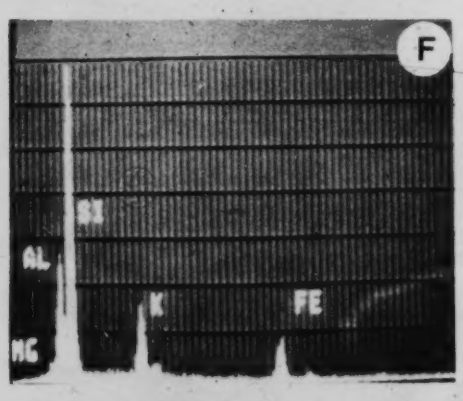
F
SI
AL
K
FE
MG

G
Chl

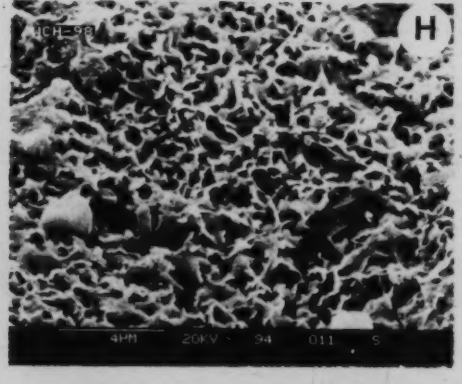
H
4MM 20KV 94 011 S

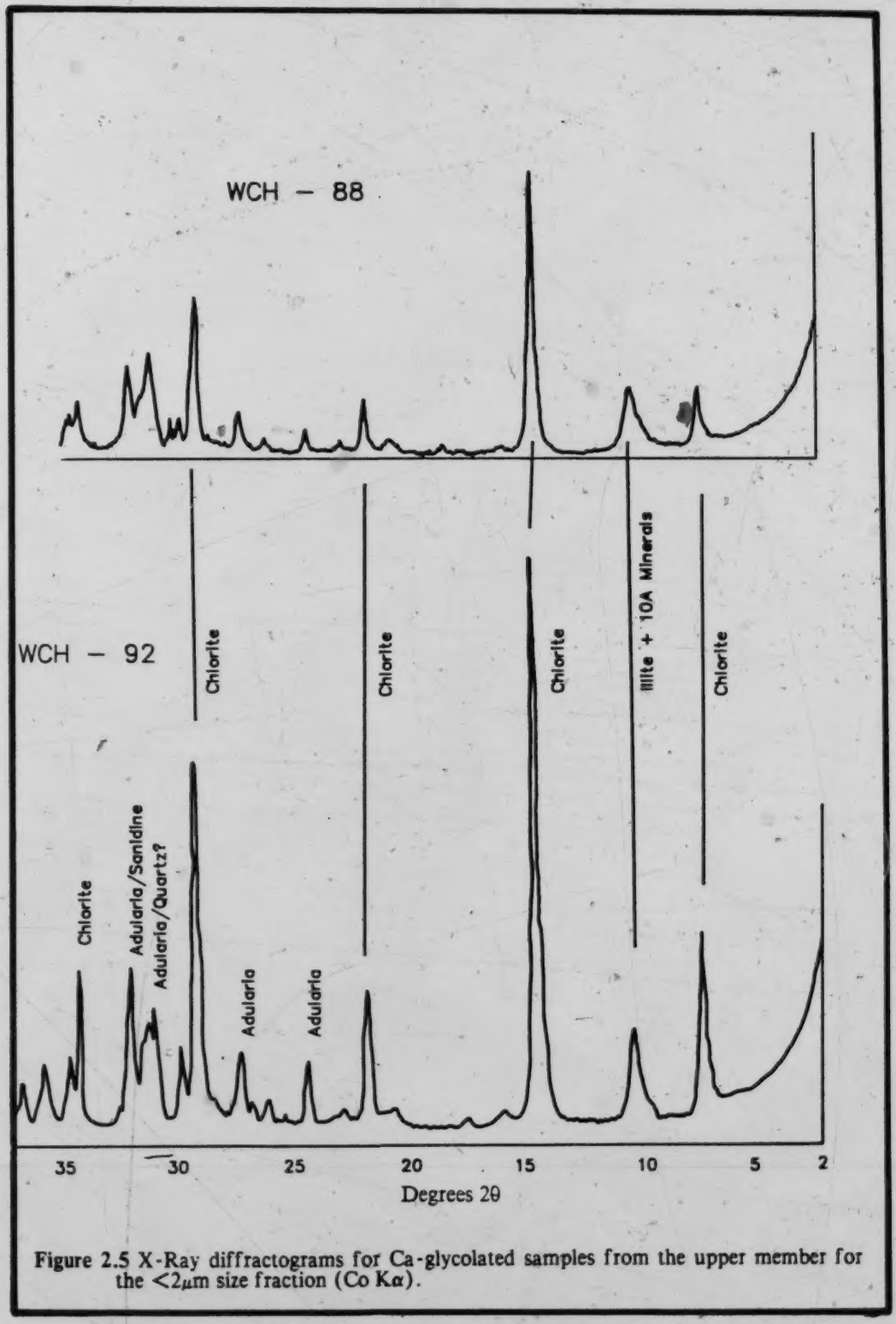

Figure 2.5 X-Ray diffractograms for Ca-glycolated samples from the upper member for the $<2\mu m$ size fraction (Co Kα).

Scanning Electron Microscopy

Both illite and chlorite were recognized by SEM and EDA. Illite is similar in appearence to that of the lower member, occurring as a foliated mass or as rope-like fibers arranged in a honeycomb pattern (Plate 2.4h). It occurs with adularia aggregate and as secondary overgrowths on chlorite.

Chlorite formed as blade-like aggregates and as long fibrous to platy masses (Plate 2.5a,b). Partial rosettes which grew in very tight pore spaces formed radiating crystals (Plate 2.5b).

Carbonate

Carbonate is an abundant matrix component after fine pyroclastic components and clay minerals in the lower member. In the upper member, it is the second most abundant matrix phase after adularia recrystallization assemblages (Table 2.1). Staining using Alzarin red S ($K_3Fe(CN_6)$) mixed with 1.5% HCl and XRD analysis indicate an iron-rich calcite. Similar results were obtained from both members. Calcite may comprise up to 50% of the matrix in certain beds of the lower member and up to 20% in the upper member (Table 2.1). In many cases, the carbonate is found to support the other constituents. An anomalous situation was encountered in the upper beds of the lower member where bombs (samples CB and CB_1), were found to be composed of 70% radiating Fe-carbonate (Table 2.1). Bombs from other exposures of the Crowsnest Formation also exhibits this calcareous nature. In many cases, the bombs are supported by non-calcareous tuffs suggesting that in situ calcite replacement has not occurred.

Throughout the section, numerous textures are exhibited by carbonate. They are divided into six types based upon morphologies exhibited in thin section and SEM.

1. Rims. Thin rims are found in many cases to surround euhedral sanidines, garnets and pyroxenes. It is not certain if the carbonate is primary though its presence as a coating suports the assumption.
2. Coarse, Radiating Crystals. This very unique texture is primarily restricted to bombs found throughout the formation. The crystals grow as long fan-shaped, radiating aggregates which may comprise the entire matrix (Plate 2.6d). The aggregates surround and support crystals, crystal fragments and both juvenile and cognate clasts. Larger crystals show only minor replacement on their margins suggesting that the origin of the carbonate was not by

Plate 2.5

A. SEM micrograph of platy chlorite (**Chl**) from the upper member, wch- 94.

B. SEM micrograph of radiating (rosettes) chlorite (**Chl**) crystals growing in tight pore spaces. Upper member, wch-94.

C. SEM micrograph of calcite (**Ca**) growing in a pore. Lower member, wch-74.

D. SEM micrograph of authigenic adularia (**Ad**) from the lower member growing with small amounts of clay (**Cl**) minerals in a pore space. Lower member, wch-52.

E. SEM micrograph of massive chert-like adularia common as a recrystallization assemblage throughout the upper member, wch-74.

F. EDA graph of massive adularia. This potassic signature is common to both pore filling and massive varieties.

G. SEM micrograph of well formed titanomagnetite (**Mg**) crystals which are very common throughout the upper member. The crystals occur with chlorite (**Chl**), wch-88.

H. EDA of the titanomagnetite crystals in "G" showing the Ti content.

A
Chl

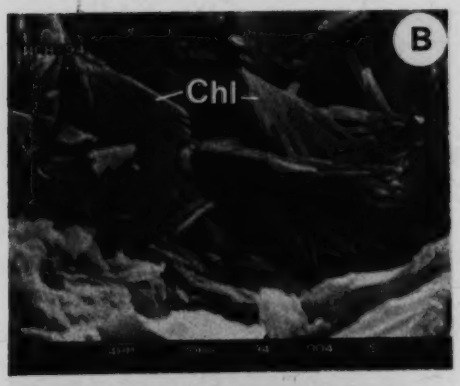
B
Chl

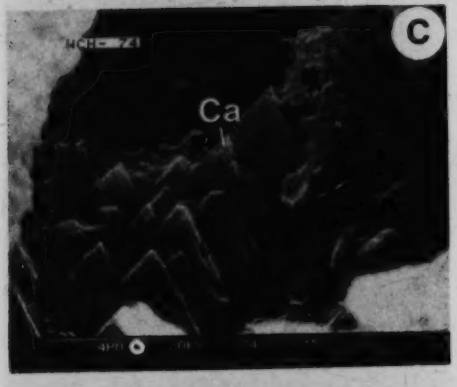
C
Ca

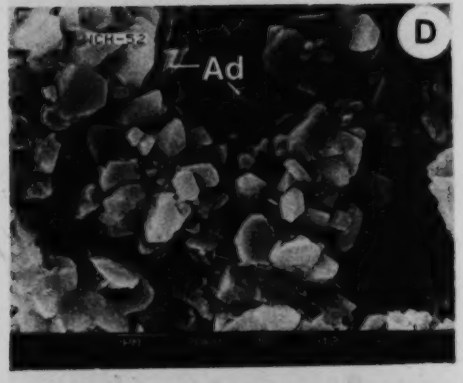
D
Ad

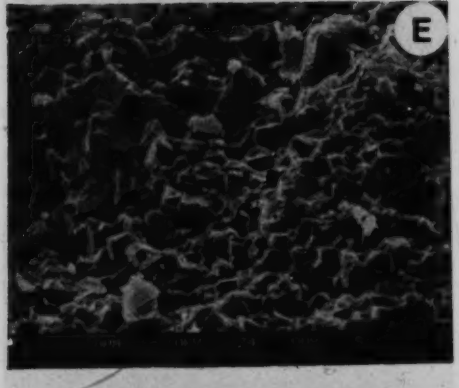
E

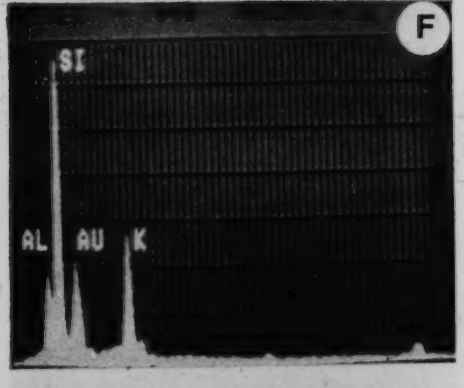
F
SI
AL
AU
K

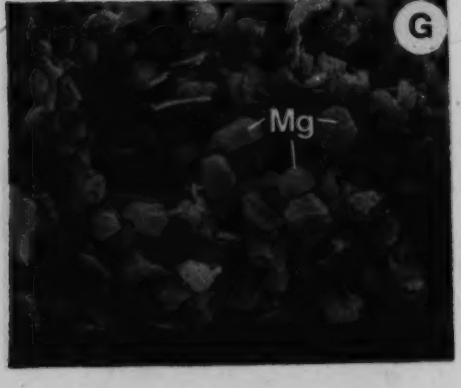
G
Mg

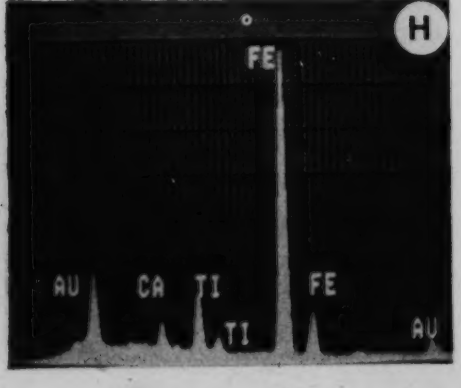
H
FE
AU
CA
TI
TI
FE
AU

replacement of the coarser crystal component. In most cases, fine, cognate and juvenile fragments are replaced by a more massive, non-radiating carbonate in the presence of the radiating forms (Plate 2.6d).

In all bombs, a remnant glass or aphanite phase was replaced by the massive, radiating carbonate matrix (Plate 2.6d,e,f). This texture favors the wholesale replacement of the original glass component. Further, fibrous, radiating feldspar crystals comprising a fine matrix are replaced pseudomorphically (Plate 2.6f).

The source of the abundant carbonate is difficult to assess. The other components of the bombs show good evidence of emplacement as a viscose semi-solid mass at elevated temperatures. With this evidence, it is probable that the carbonate was in part primary. The origin of carbonate is further investigated by geochemical methods in Chapter III.

3. Coarse, sparry crystals. Coarse, sparry carbonate crystals are common in both members but are better developed in the upper section. This morphology is most common in the dense deposits of the upper member. It is probable that this texture is the result of recrystallization or vein filling. It may exhibit replacement characteristics (Plate 2.6c).
4. Fine crystal mass. Carbonate is often found as a fine-grained matrix in the beds of the lower member. It is observed to replace finely crystalline components of rock fragments, especially blairmorite and rock fragments in bombs, discussed above (Plate 2.6d,e). Larger crystals do not seem to be affected, though there may be some reaction around their rim.
5. Granular mass. Occasionally small grains or spheres occur in some beds of the lower member (e.g. wch-14). The spheres are commonly separated by foliated clay minerals (Plate 2.7a). The spheroids apparently form, in part, by replacement of small analcime microlites commonly present in many glassy phases, and in the matrix. In some beds, notably wch - 67, these small grains define beds suggesting a strictly pyroclastic origin.
6. Pseudomorphs. Single crystal pseudomorphs of Fe-calcite after aegirine-augite and sphene are common where they occur as phenocrysts in rock fragments and as inclusions in other crystals. This is documented in the descriptions of the phenocrysts in the previous section (Plate 2.2a).
7. Veins and fractures. Calcite veins and fractures are common in both members. In some fragments, veins end abruptly at their edges suggesting a previous fracturing event.

Plate 2.6

A. Photomicrograph of adularia/sericite recrystallization of the matrix of a rock fragment from the upper member. Twinned, porphyritic garnets (**Gr**) show fracture infill and recrystallization of inclusions. Epidote, chlorite, apatite and Fe - Ti oxides accompany the adularia. Upper member, wch-93, field of view 0.6 x 0.6mm, X-polars.

B. Photomicrograph of foliated clay minerals (**Cl**), illite and illite-smectite, comprising the matrix between sanidine (**Fp**), hornblende (**Hb**) and garnet (**Gr**) phenocrysts. Remnant aphanitic (glassy ?) (**Ap**) phases still remain. Lower member, wch-32, field of view 1 x 1mm, X-polars.

C. Photomicrograph of coarse, sparry Fe calcite (**Ca**) replacement and possibly pore or fracture filler. Fe - Ti oxides (**Ox**) comprise the rest of the picture. Upper member, wch-93, field of view 1 x 1mm, X-polars.

D. Photomicrograph of coarse, radiating Fe calcite (**Ca**) supporting relatively fresh sanidine (**Fp**), plagioclase and aegirine-augite (**A**) crystal fragments. Less radiating, fine grained Fe calcite appears to have replaced aphanitic or glassy fragments (**Ap**). These textures are common to bombs where they occur. Pipeline section bomb, field of view 1 x 1mm X-polars.

E. Photomicrograph of fine grained Fe calcite (**Ca**) replacing an aphanitic to glassy matrix (**Ap**). The circular forms may be remnant vesicles. The sample is taken from a bomb. Lower member, wch Cb_1, field of view 1 x 1mm, X-polars.

F. Photomicrograph of Fe calcite (**Ca**) pseudomorphically replacing fine, fiberous sanidine laths (**Fp**) in the matrix. Other notable constituants are garnet (**Gr**) and plagioclase (**Pl**). The sample comes from a bomb at the Pipeline section. Pipeline section, field of view 0.6 x 0.6mm, X-polars.

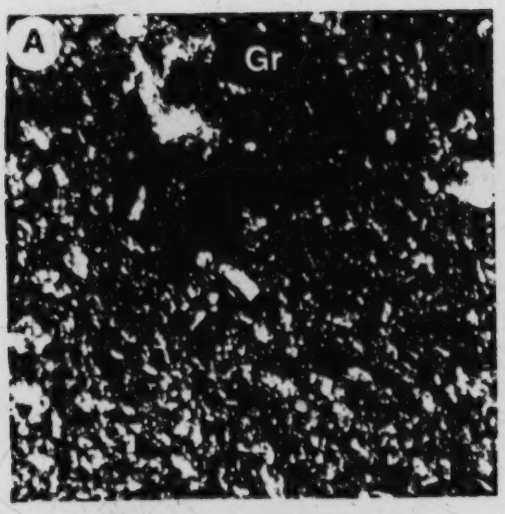
A
Gr

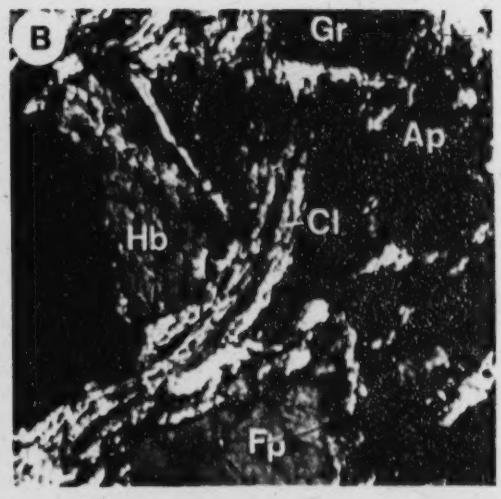
B
Gr
Ap
Hb
Cl
Fp

C
Ox
Ca

D
Fp
Ca
Ap

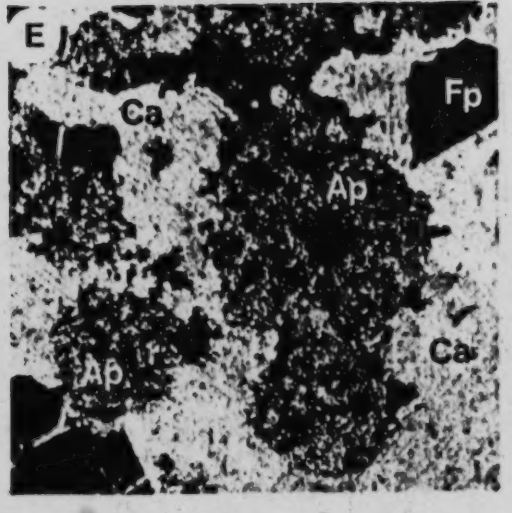
E
Ca
Fp
Ap
Ca
Ap

F
Pl
Gr
Ca

Calcite is seen to preferrentially replace feldspar, pyroxene and analcime-rich glasses. This is perhaps exemplified by its iron-rich nature. In a number of cases, calcite comprises the entire matrix. Wholesale replacement of a pre-existing matrix is indicated by the coarse nature of the calcite, and, in most cases, the matrix supported nature of the rock. Radiating calcite crystals may totally engulf smaller crystals or rock fragments, reflecting subsequent recrystallization. Under SEM, calcite is observed as euhedral pore fillers and as a massive matrix component (Plate 2.5c). In the latter case, secondary solution is indicated by a pitted texture.

Feldspar Aggregate

Fine feldspar aggregates may be observed as both replacement and authigenic components in both members. Texturally, they strongly resemble chert. Staining with sodium colbaltinitrite indicated that they are almost entirely composed of potassium feldspars. The low temperature form adularia was identified by XRD , SEM and EDA. It is found as a recrystallization product of fine, feldspathic glass/aphanite, feldspar-rich or glassy rock fragments and sanidine phenocrysts (Plates 2.1b, and 2.7c,d and 2.6a). In many cases remnants of the original component remain. Two types were identified.

1. Pore fillers. Crystal masses composed of fine authigenic adularia were found to occasionally coat pore spaces in the middle of the lower member and in the upper member (Plate 2.5d,e). Individually, the adularia crystals are tabular to platy with multiple crystal faces. They occur as overgrowths on pore walls and phenocrysts along with clay minerals. This evidence suggests that they were precipitated from potassic pore fluids as an authigenic phase.
2. Dense aggregates. Dense chert-like masses of adularia containing abundant sericite (10Å mica), apatite, epidote group minerals and Fe-Ti oxides are very common in the upper member and comprise the major matrix phases (Plates 2.2c,d, 2.5f and 2.6a). Recrystallization of feldspar phenocrysts to aggregate begins to occur in the upper beds of the lower member. In the upper member, the matrix, phenocryst and rock fragment phases show intense recrystallization. In many cases, the original crystal or fragment shape is preserved (Plates 2.1b, 2.2c,d). The grain size ranges from $<$ 0.1mm to as much as 3mm in extreme cases. It is thought that this dense phase adularia aggregate represents

recrystallization of high temperature minerals (eg. sanidine, and feldspathic glasses) and metastable minerals (eg. analcime at high temperatures) during slow cooling. This seems to have occurred pervasively througout the upper member and may reflect the type of deposit and its emplacement. This problem is further addressed in Chapters VI and VII.

Replacement of the aggregates by calcite occurs in both members.

Zeolites and Trace Minerals

Zeolites are rarely found throughout both members at the type section. Two crystal morphologies found in the matrix of both members were interpreted as being zeolites.

A tabular form exhibiting excellent cleavage was found as a vein filler with calcite (wch-60). It was identified as heulandite and is associated with calcite and hematite. A second form was characterized by its fibrous, radiating crystal habit and is tentatively identified as thompsonite.

Titanomagnetite was observed to occur as small, euhedral crystals, primarily in the upper member (Plate 2.6g). Polished sections indicate that it is associated with ilmenite, hematite and pyrite.

D. Textures

Many phases exhibit textural features which are unique to pyroclastic rocks. The following descriptions are based on those features exhibited by phases of the Crowsnest Formation which may attest to the conditions under which they were emplaced.

Uniquely pyroclastic textures are common throughout the type section on both outcrop and microscope levels. In most cases, they provide evidence of emplacement at elevated temperatures, though welding is not always indicated. The mechanisms and energies of the emplacement process may be reflected by some textures.

Plastic Deformation Structures

In the absence of bubble wall shards, the best indication of welding is the plastic deformation of juvenile or cognate rock fragments. Evidence that such components were emplaced by high temperature pyroclastic eruptions is best established by the shapes of the fragments.

In thin section, glassy and aphanitic juvenile fragments, cognate fragments and crystals may exhibit compaction textures between more competent, coarse crystals and lithic phases (Plates 2.2f, 2.7b,c). In some fine-grained beds, apparently juvenile clasts may have an amoeba-like outline (Plate 2.7b). They likely represent primary magma that was ejected as liquid clots. The presence of the above features suggest that the fragments were hot and malleable during deposition. The more solid clasts may exhibit only slight deformation along their edges. In many cases these features are associated with sutured boundaries and bent crystals.

In the majority of cases, plastic deformation textures are found in the presence of more solid, undeformed lithic components, which often exhibit rounded forms with baked margins, also indicating high temperatures (Plate 2.7c).

Plastic deformation features occur in the massive resistant beds of the lower member, and throughout all beds of the upper member. In recessive beds, these features are not generally found.

Suture Boundaries

Many phases in thin section exhibit sutured contacts with other phases. This usually occurs at contacts between sanidine crystals or crystal fragments and between lithic clasts (Plate 2.7d,e). Sutures are thought to represent a welding effect, rather than pressure solution for the following reasons:

1. They are associated with plastic deformation structures, bent crystals and clasts with baked margins.
2. They are not pervasive throughout the beds in which they occur.
3. They occur in massive, resistant beds.
4. Recessive beds, apparently unwelded, rarely contain suture features.

Alone, suture boundaries are not used as criteria for welding due to their relative rarity even in favorable horizons.

Plate 2.7

A. Photomicrograph of Fe calcite granules from the lower member, wch-14, field of view 0.6 x 0.6mm, X-polars.

B. Photomicrograph of intensely deformed aphanitic, fragments (Fg) supported by a fine tuff matrix composed of fine crystal and rock fragments, wch-77, field of view 1cm x 1cm, P-polars.

C. Photograph of large, plastically deformed blairmorite fragment which has been flattened in a pyroclastic breccia, Pipeline section.

D. Photomicrograph showing sutured contacts (sc) between two sanidine (Fp) crystals in a welded crystal tuff, wch-33, field of view 2.7 x 2.7mm, X-polars.

E. Photomicrograph showing sutured contacts between lithic fragments in a welded lithic lapilli tuff, wch-75, field of view 2.7 x 2.7mm, P-polars.

F. Photograph of a green trachyte clast showing a marked baked margin, wch-13.

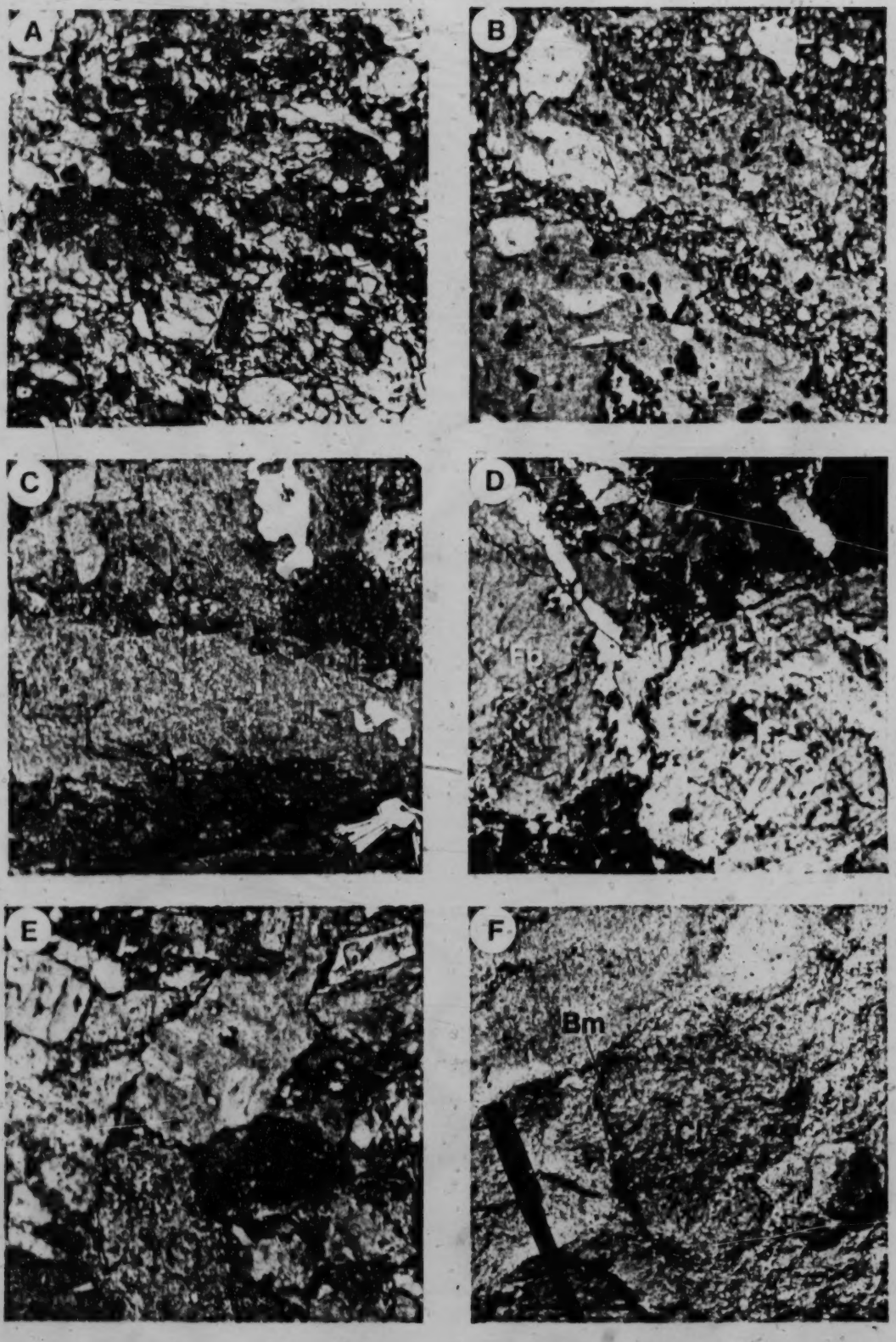
A
B
C
D
Fb
E
F
Bm

Baked Margins

Many coarse beds contain cognate fragments, mostly from earlier primary flows, that are rounded to subrounded and exhibit a baked rim which is marked by a sometimes dramatic color change (Plate 2.7f). This change is a reflection of recrystallization and/or alteration around the rim of the fragment. It is found around the entire perimeter of the clast and is therefore thought to have occurred during, or shortly after deposition.

Rounding occurred prior to the baking of the margin.

E. Summary

The previous descriptions reveal that the phases, their mineralogical composition and distribution vary between the two members. Further, the alteration assemblages which comprise a major part of the matrix of both members is markedly different between the two.

Generally, the lower member is characterized by a well defined phenocryst assemblage which is not as well developed in the upper member. For the most part the phenocrysts of the lower member occur in a matrix composed of finer crystal and rock fragments along with an abundant and marked alteration assemblage. This assemblage is dominated by clay mineral species and calcite.

The upper member is dominated by rock fragments and matrix phases with a less well defined phenocryst assemblage. Intense recrystallization has destroyed original compositions and textures. The matrix resembles that of a melanocratic dyke which cuts the member, suggesting the presences of a fluid.

Figure 2.6 depicts the relative occurrence of the mineralogical phases and their components within the type section. The marked change between the lower and upper members is clearly depicted.

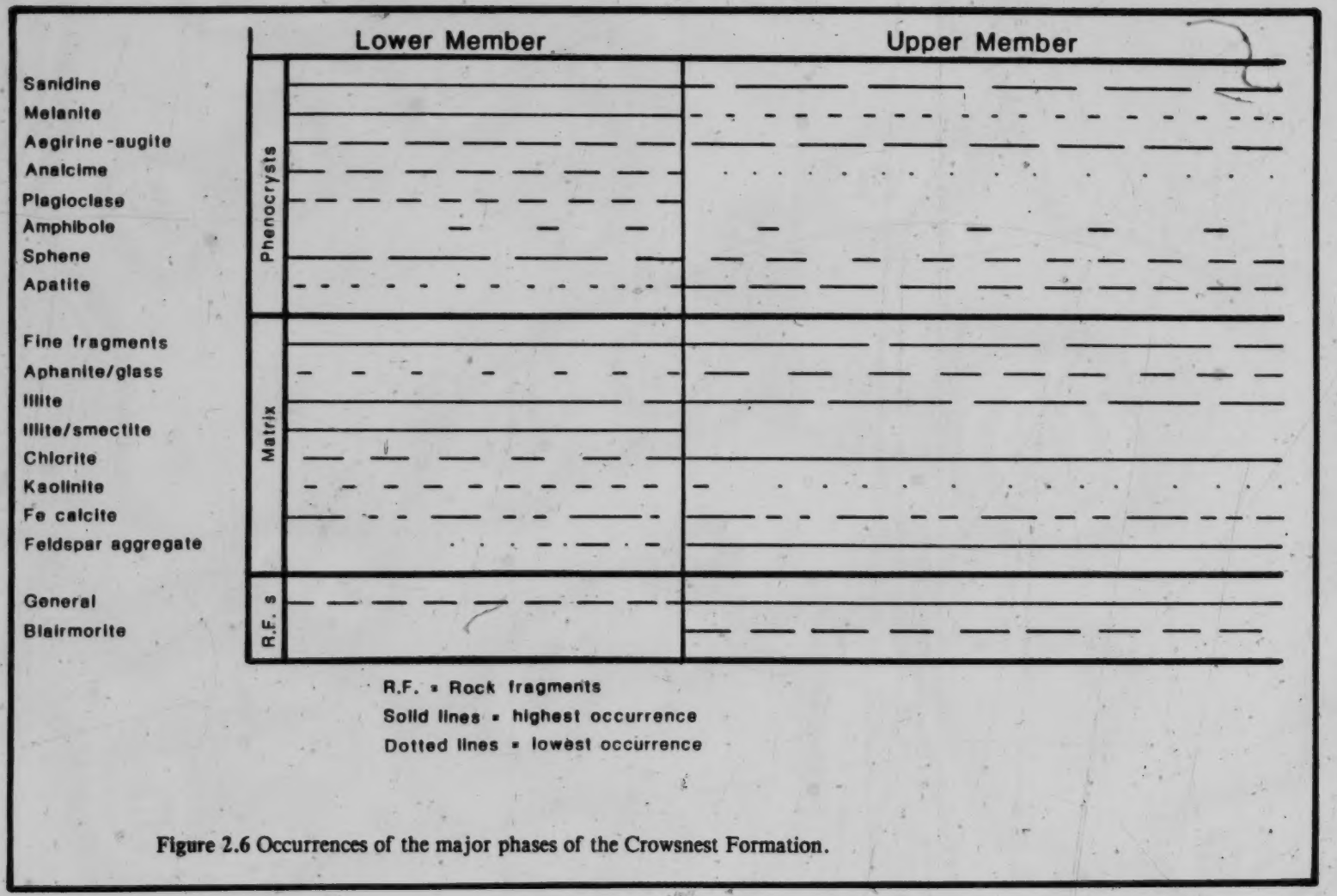

Figure 2.6 Occurrences of the major phases of the Crowsnest Formation.

III. GEOCHEMISTRY

A total of thirty samples were selectively taken from the type section west of Coleman to be analyzed for whole rock abundances of the major oxides, five trace or minor elements, sulfur, CO_2 and loss on ignition at 1040°C. The major element oxides SiO_2, Al_2O_3, Fe_2O_3 , MgO, CaO, Na_2O, K_2O, TiO_2, MnO, P_2O_5 and the minor elements Rb, Sr, Y, Zr and Nb were determined by X-ray fluorescence at McMaster University in Hamilton Ontario, Canada (Table 3.1). The thirty samples chosen for these analyses were taken from the lower member of the Crowsnest formation at the type section. A complete cross-section of the member, and the various rock types within it were sampled. An analysis of a dyke found to intrude the pyroclastic breccias of the member is also included and is plotted with the primary rocks. This rock type has not been identified by any previous workers. Further, two analysis of carbonate-rich bombs are included and will be discussed separately. The massive upper sequence was not analysed due to the problems of obtaining a representative sample of the coarsely fragmental rock type.

The accuracy of McMaster XRF determinations is determined by comparison with a standard sample[5] analyzed at the University of Alberta by classical wet chemical methods. The results are given in Table 3.2.

A series of analyses presented by Pearce (1967) and Ferguson and Edgar (1978) for fresh primary flows and intrusives will be used to compare the pyroclastic rock sequences with their primary counterparts. The results from Pearce (1967) were determined from the matrix glasses of Crowsnest igneous rocks. The samples are suggested by the author to represent the liquid fraction of the melt, excluding the analcime and sanidine crystals which are likely to have been removed by fractionation. No data is available as to the accuracy of these analyses. They are therefore used to determine an approximate field into which the Crowsnest matrix glasses fall.

Ferguson and Edgar (1978) present whole rock data for three petrologically different suites; trachytes, analcime phonolites and blairmorites. Results were obtained using X-ray fluoresence methods. No accuracy data was obtainable. The samples are again used to determine a field for the compositions of the three rock types. In total, 54 samples of primary rocks from the Crowsnest formation are compared with those of this study.

---

[5]The standard sample is a composite sample from the basement of Alberta.

TABLE 3.1 CHEMICAL ANALYSIS OF SELECTED CROWSNEST ROCKS FROM THE TYPE SECTION

WCH #	MAJOR ELEMENT OXIDES %										TRACE ELEMENTS PPM					VOLITILES %		
	SiO_2	Al_2O_3	Fe_2O_3	MgO	CaO	Na_2O	K_2O	TiO_2	MnO	P_2O_5	Rb	Sr	Y	Zr	Nb	S	CO_2	L.O.I.
1	62.57	17.94	5.51	1.78	3.31	1.81	6.33	0.56	0.00	0.07	166	1510	26	298	20	0.01	1.53	5.44
9	61.48	18.88	4.88	1.20	3.11	3.25	6.43	0.55	0.12	0.01	140	2069	26	303	19	0.04	0.46	2.89
12	60.76	21.09	3.77	0.06	2.46	3.15	8.21	0.34	0.10	0.04	166	2412	21	308	24	0.01	0.20	3.35
14	51.58	19.30	5.93	1.45	12.09	2.16	6.72	0.36	0.41	0.00	124	1980	19	252	18	0.04	7.15	10.80
16	60.72	20.10	4.00	0.06	2.71	4.23	7.57	0.40	0.15	0.05	137	2679	25	138	17	0.01	0.34	2.76
17	58.98	21.94	4.49	0.96	1.87	2.29	8.99	0.34	0.11	0.02	197	2357	17	313	30	0.25	0.61	5.15
18	57.50	21.41	5.80	1.15	2.57	1.93	9.02	0.43	0.14	0.05	217	2255	19	308	35	0.01	0.44	5.24
19	58.10	19.26	6.30	0.08	5.15	2.17	7.73	0.90	0.21	0.09	160	2427	32	351	33	0.01	0.35	4.08
31	61.37	19.36	4.03	0.07	3.81	2.72	8.00	0.42	0.14	0.06	151	2584	21	309	37	0.01	0.29	3.03
32	57.44	20.64	5.20	1.14	5.70	2.07	7.06	0.53	0.20	0.03	103	3441	28	382	23	0.08	0.22	3.97
33	62.57	18.66	3.74	0.06	4.14	3.78	6.37	0.40	0.14	0.03	100	3379	27	349	24	0.04	0.36	2.46
36	57.74	21.41	6.54	1.07	2.39	3.09	6.99	0.55	0.14	0.08	215	1610	25	357	25	0.01	0.29	3.91
38	60.44	20.43	3.68	0.86	3.43	3.58	6.61	0.41	0.18	0.06	145	2200	25	323	22	0.01	1.39	3.89
40	59.78	18.30	6.21	0.94	4.51	4.44	4.88	0.61	0.22	0.09	111	2453	28	330	25	0.06	0.98	2.65
41	60.59	21.49	3.40	0.92	2.02	4.90	6.24	0.30	0.12	0.03	134	1911	18	353	21	0.06	0.63	4.81
45	61.06	19.99	3.81	0.95	2.90	3.82	6.96	0.33	0.11	0.06	145	3771	24	410	18	0.08	0.34	3.39
51	59.47	20.01	4.46	0.86	3.46	3.25	7.82	0.45	0.18	0.04	158	2400	19	296	21	0.01	1.06	4.92
52	58.74	17.60	8.80	0.96	2.52	2.80	7.64	0.60	0.25	0.08	244	2099	19	251	18	0.01	0.51	3.05
53	61.44	18.54	5.94	0.07	1.84	3.18	7.99	0.61	0.23	0.15	163	1922	24	270	17	0.01	0.59	3.00
54	60.16	20.02	4.51	0.87	2.689	4.20	6.85	0.50	0.12	0.09	150	2202	24	319	25	0.09	0.38	2.88
60	63.78	18.79	4.10	0.80	2.96	4.46	4.32	0.56	0.12	0.12	94	2248	25	290	15	0.20	0.30	2.02
66	58.64	18.76	6.70	1.23	3.20	3.64	6.74	0.74	0.15	0.21	163	2122	28	284	19	0.01	0.34	2.81
69	59.81	20.78	4.61	1.03	1.86	3.88	7.41	0.45	0.10	0.06	187	1957	27	306	16	0.01	0.14	3.15
71	58.05	17.89	6.72	1.22	5.75	4.08	5.14	0.73	0.25	0.16	104	2707	29	315	16	0.28	0.55	2.84
75	53.15	17.05	5.49	0.07	14.07	3.32	5.62	0.64	0.48	0.08	122	2242	33	282	20	0.01	8.42	10.03
77	55.12	19.84	8.21	2.03	4.25	3.24	6.25	0.56	0.14	0.34	219	1301	22	246	117	0.01	0.46	6.34
78	60.62	17.92	6.04	0.88	3.53	3.73	6.20	0.76	0.17	0.14	134	3459	29	352	25	0.01	0.35	3.40
CB	41.26	13.43	4.87	1.44	30.33	2.20	4.84	0.36	1.34	0.01	121	1598	20	155	10	0.06	19.78	21.52
B1	41.37	13.47	4.97	0.07	30.61	2.74	5.01	0.37	1.36	0.03	120	1605	20	148	9	0.06	19.72	21.50
85	56.05	16.89	6.67	1.23	3.50	0.32	14.33	0.56	0.21	0.23	448	1442	5	195	55	0.01	3.57	5.47

TABLE 3.2 ACCURACY OF MCMASTER X-RAY FLUORESENCE TECHNIQUES

	Sample R-122* Ave. of 4 "Wet chemical" Analyses	Sample R-122 McMaster XRF**	Change	% Error
SiO_2	68.38	67.56	-.82	-1.19%
Al_2O_3	14.27	13.80	-.47	-3.29%
TiO_2	.55	.54	-.01	-1.82%
Fe_2O_3	4.76	5.52	+.76	+15.96%
MgO	1.73	2.29	+.54	+30.8%
CaO	2.77	3.08	+.31	+11.19%
Na_2O	2.91	2.73	-.18	-6.18%
K_2O	4.32	4.27	-.05	-1.15%
MnO	.06	.08	+.02	+33.33%
P_2O_5	.17	.15	-.02	-11.76%

* Re-calculated as H_2O free analysis.

** Calculated to total 100% without H_2O.

To date the Crowsnest volcanic suite has been classified by petrological descriptions and limited chemical analyses. None of these results have been applied to modern classification schemes for the major oxides and trace elements. It would seem appropriate to discuss these major classifications in the light of their applicability to the altered volcanic rocks of the Crowsnest, specifically the lower member.

Irvine and Baragar (1971) have presented a well known, and widely used system for the classification of common volcanic rocks based upon the use of CIPW norms. This classification is best suited for unaltered volcanic rocks, and assumes that all altered rocks have been removed or that the nature of the alteration has been identified and taken into account.

The rocks of the lower pyroclastic member of the type section are intensely altered to clays and in some instances carbonate. It would seem that the use of the CIPW norm classification is inappropriate unless an approximation of the degree of alteration and metasomatism can assessed.

The movement of sodium and potassium would cause the greatest problem when using CIPW norms. A scheme presented by Hughs (1973) defines an "igneous spectrum" based upon the relative percent of K_2O in the total alkalies. All fresh igneous rocks fall within this spectrum. As such, it may be used to test the degree of sodic and potassic metasomatism in altered igneous rocks. This scheme does not allow for the movement of calcium, magnesium, aluminum, iron, manganese and phosphorus which are known to be mobile during low-grade metamorphism (Cann, 1970; Pearce and Cann, 1971 and Goff, 1984). The degree of metasomatism which has occurred may therefore be tested.

Trace element schemes are very useful when trying to classify altered igneous rocks. Pearce and Cann (1971), Wedepohl (1978) and Goff (1984) have shown that Rb, Sr become highly mobile with K and Ca during alteration while Zr, Ti, Y, Nb and others are relatively immobile. Classifications which utilize these latter elements would seem best suited for the pyroclastic rocks of the Crowsnest Formation. Winchester and Floyd (1977) provide a scheme based on the minor elements Ti, Zr, Y, Nb, Ce, Ga, and Sc which are shown to vary during differentiation. Plotted against each other, immobile elemental ratios define fields into which the common igneous rock types fall. Discrimination between alkaline, subalkaline and their various differentiates can be made, based upon the variation in the minor element ratios.

Two diagrams used in this scheme incorporate the degree of silica saturation (SiO_2 wt.%) as a parameter. It has been shown by Blatt *et al.* (1980) that silica becomes mobile during the devitrification process, and may migrate locally within the system. Comparison with unaltered samples will determine the degree of silica migration during devitrification.

The devitrified nature of the lower member causes serious problems in classification, especially with regard to the norm system utilized by Irvine and Baragar (1971). In an attempt to determine the degree of alteration and metasomatism, the rocks of the lower Crowsnest will be plotted against their primary counterparts on all diagrams.

Further, the compositions of the pyroclastic beds are thought to be more closely representative of the phenocryst phase, as the processes which emplaced the deposits have been shown to concentrate the crystal fraction (Walker, 1971).

A. Igneous spectrum

Low grade metamorphism and/or alteration will initially involve the movement of the primary alkalies, sodium and potassium. Calcium also becomes very mobile under such conditions (Goff, 1984). The "Igneous Spectrum" defined by Hughes (1973), (Figure 3.1) delineates a trend which encompasses the alkali compositions of common igneous rocks. Rocks whose compositions fall within this spectrum may be considered fresh or to have suffered closed-system metasomatism. Rocks which suffer "open system" metasomatism may readily fall outside the spectrum depending upon sodium or potassium.

This system has good potential to accommodate feldspathoidal volcanic rocks. Hughes (1973) points out that leucite-bearing rocks would tend to fall to the right of the spectrum, while rocks with significant nepheline composition would fall in the middle of the spectrum. Rocks with high percentages of It would seem apparent that, in light of the Crowsnest mineralogy, fresh rocks bearing significant analcime would plot to the left or sodium-enriched side of the spectrum.

Figure 3.1a shows plots of the primary rocks from Pearce (1971) and Ferguson and Edgar (1977). Those from the Crowsnest type section are plotted in Figure 3.1b. The primary samples from Ferguson and Edgar (1978) form three fields trending from potassic trachytes through intermediate analcime phonolites to sodic blairmorites (Figure 3.1a). The fields defined by the samples fit the previous argument as is indicated by their mineralogy. The

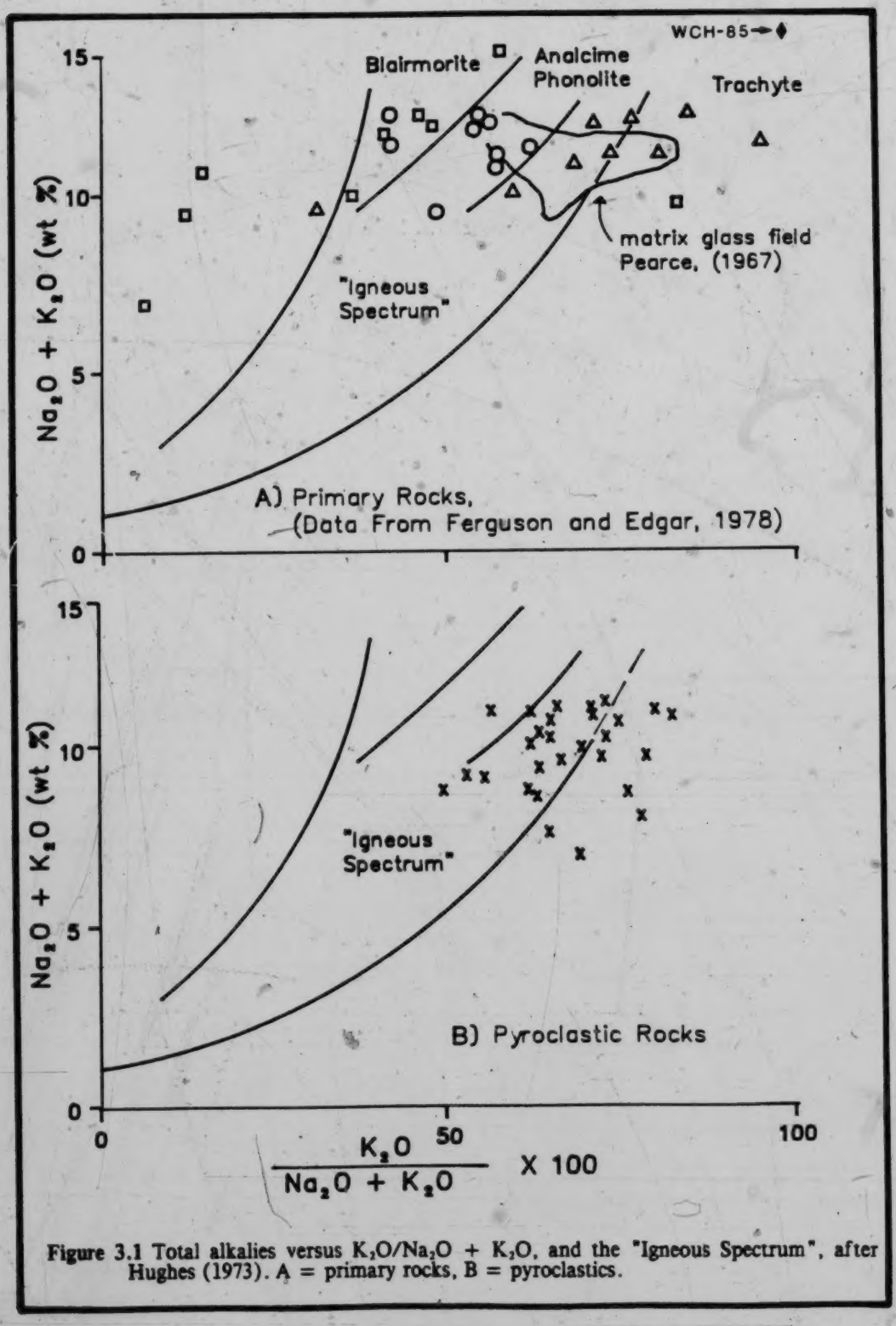

Figure 3.1 Total alkalies versus $K_2O/Na_2O + K_2O$, and the "Igneous Spectrum", after Hughes (1973). A = primary rocks, B = pyroclastics.

matrix glasses of Pearce (1971) are found to cluster within the trachyte field (Figure 3.1a). The primary samples probably represent the entire compositional range of the Crowsnest rocks. Samples which fall to the right and left of the spectrum likely reflect the abundance of sanidine and analcime respectively. Extreme cases may be the result of highly fractionated varieties. Such a case is exhibited by the dyke which cuts the upper member at the proposed type section (wch-85) which is strongly potassic (14.33 wt%, Table 3.1). The possibility of leucite occurring in the dyke may be a significant influence on the potassium content.

The analyses from the rocks of the lower pyroclastic horizons are plotted in Figure 3.2b are found to straddle the right hand boundary of the igneous spectrum. The majority of samples falling within the "igneous spectrum" closely mimic those of the matrix glasses analyzed by Pearce (1967). None of the samples collected were analcime-rich, i.e. blairmorites, and therefore were not expected to fall dramatically to the right of the spectrum within the blairmorite field.

The majority of rocks sampled have been shown to be substantially altered to clay minerals via devitrification of the ground mass or glassy/aphanitic fragments. The nature of this alteration would render both potassium and sodium mobile. Estimates from this diagram suggests that metasomatism has taken place in all rocks showing even minor alteration. The shift to the right of the spectrum suggests that sodium has been removed while potassium was either less mobile or remained in the system. This is consistent with the formation of potassium-bearing illite and illite/smectite as the major diagenetic phases.

Initially, the original composition of the pyroclastic beds was probably approximated by the trachyte and analcime phonolite fields, which represent an average composition for the suite due to the relative rarity of blairmorite. It is probable that the eruption of the pyroclastics homogenized the composition by mixing cognate and juvenile components to the extent that an approximation of the average composition was achieved.

B. Whole Rock Classification

The following whole rock classification is based upon the norm system of Irvine and Baragar (1979). The use of norms is especially susceptible to error when dealing with altered rocks such as those of the Crowsnest Formation. It was shown in Figure 3.1 that the ash and tuff beds have suffered sodium depletion causing an effective removal of nepheline from the

norm. This renders the use of the Ol'-Ne'-Q' diagram problematical. However, constituent minerals such as the calcic aegirine-augites of the Crowsnest impart an alkaline nature to these rocks.

Total Alkalies versus Silica

The alkali - silica variation diagram was first used by MacDonald and Katsura (1964) to divide alkaline and subalkaline rocks. It was subsequently modified by Irvine and Baragar in 1971 to its present form.

Figures 3.2a,b and c show all suites of Crowsnest rocks to be broadly alkaline in character. The primary rocks define three fields based on changing silica content (Figure 3.2b). All rocks show a relatively uniform alkali concentration, with a marked silica depletion from trachytes to blairmorites. The matrix glasses plot within all three fields, but are notably clustered with the trachytes and analcime phonolites (Figure 3.2a).

The pyroclastics of the lower Crowsnest are slightly depleted in alkalies relative to the primary rocks (Figure 3-2c). All but two samples plot as alkali rocks within the trachyte field. The anomalous samples are likely the result of alkali depletion, especially sodium, by metasomatism. Two samples from the cores of calcite-bearing bombs are very silica under-saturated.

Discrimination between sodic and potassic series for the altered volcanics is made very difficult by the removal of sodium. However, the only primary rocks that are shown to be relatively saturated in sodium are the blairmorites, while trachytes and analcime phonolites are substanially more potassic (Figure 3.1a).

An - Ab - Or Plot

Upon concluding that the rocks of the Crowsnest volcanics lie within the alkali basalt series, the degree of differentiation can be determined. Based upon a compilation by Muir and Tilley (1961, in Irvine and Baragar, 1971) the An - Ab' - Or ternary plot is used to distinguish between sodic and potassic differentiates of an alkali olivine basalt. Figures 3.3a and b classify all but the blairmorites in the potassic field. The ash and tuff beds tend to be slightly more An normative than the primary rocks which again show a well defined trend from the potassic trachytes to the sodic blairmorites. The highly potassic dyke (wch-85) is strongly Or normative.

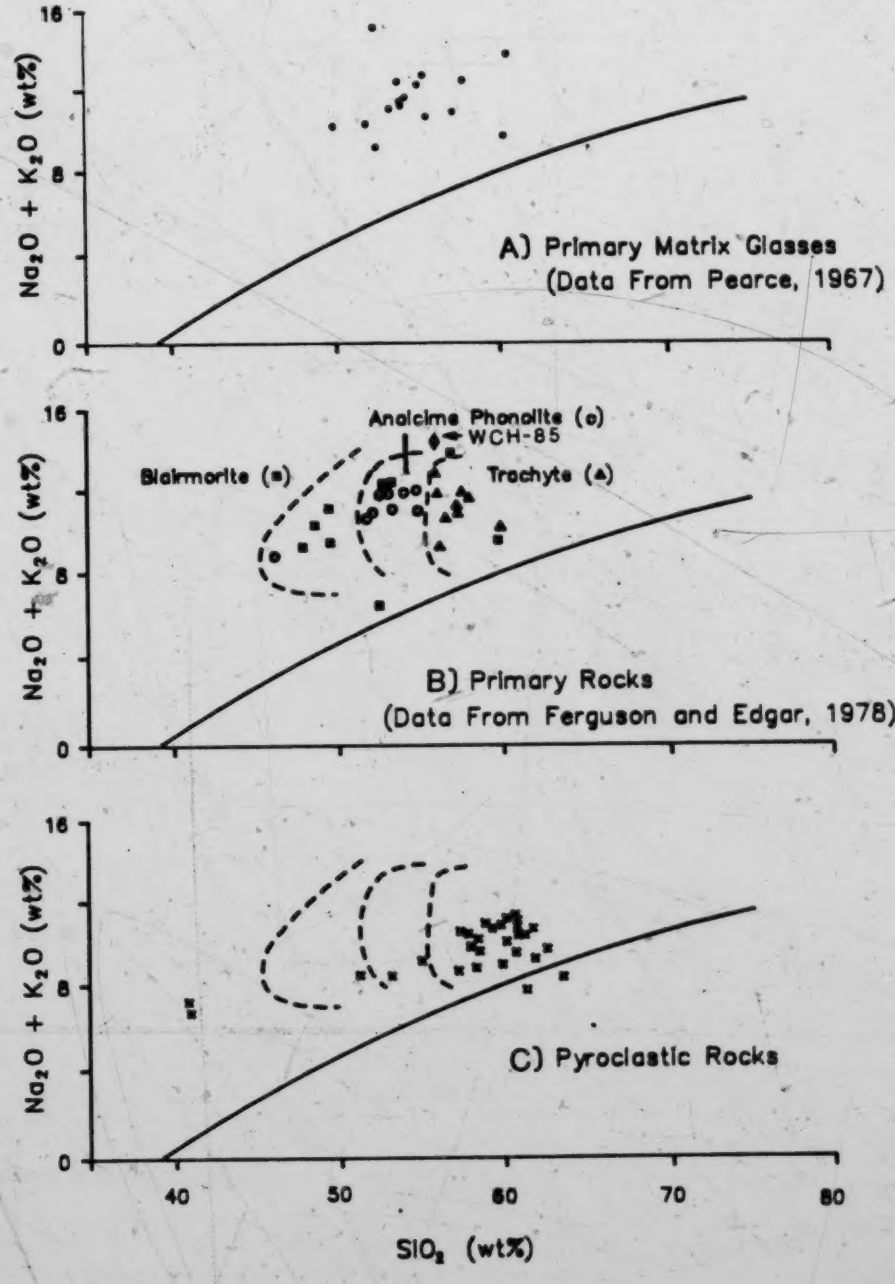

Figure 3.2 Total alkalies versus silica, after Irvine and Baragar (1971). A = matrix glasses, B = primary rocks, C = pyroclastics.

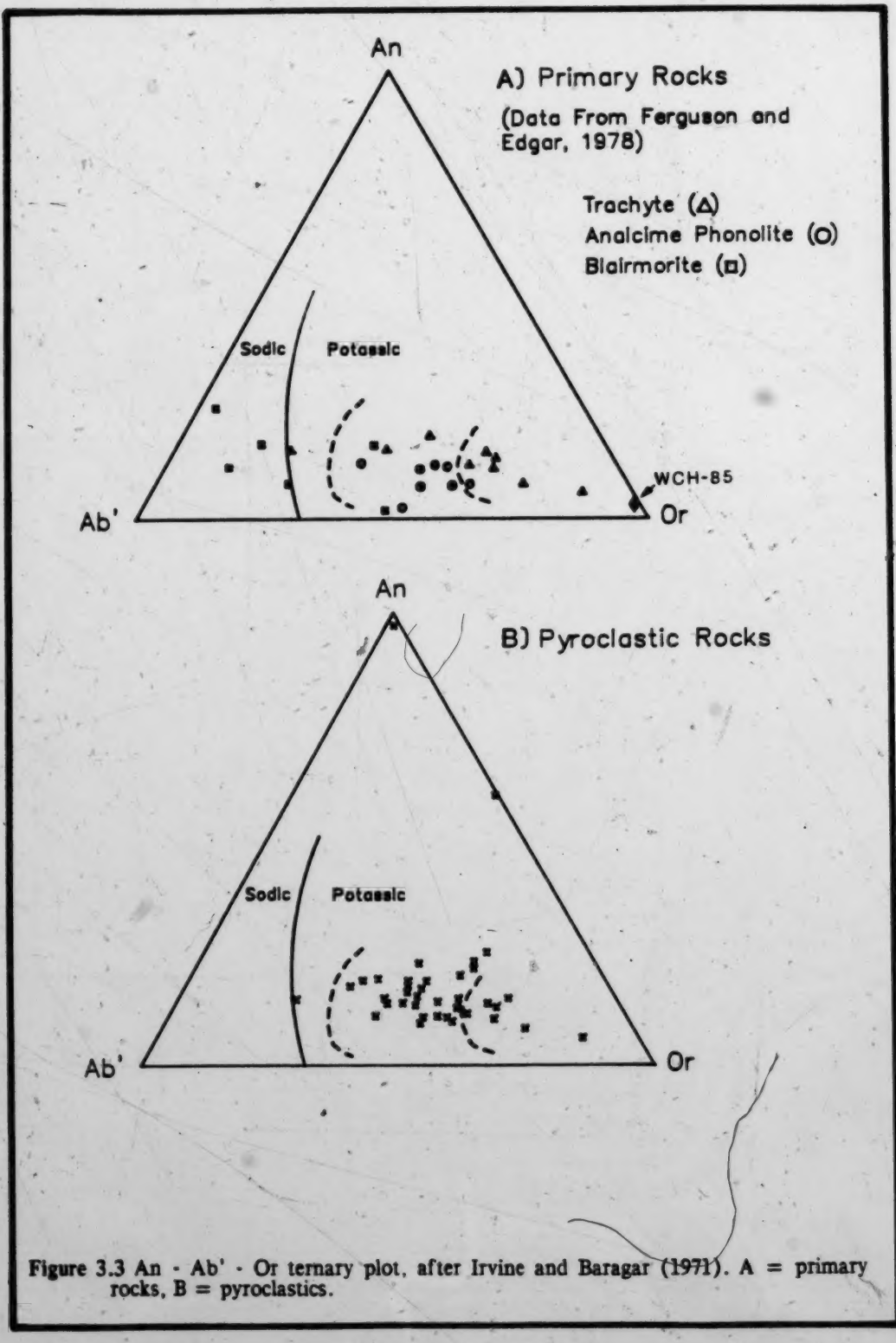

Figure 3.3 An - Ab' - Or ternary plot, after Irvine and Baragar (1971). A = primary rocks, B = pyroclastics.

The presence of carbonate has shifted the pyroclastic suite to a more An normative composition. The bombs of the formation, with their abundant carbonate, are entirely An normative.

Normative Color Index versus Normative Plagioclase Index

Excluding the blairmorites which plot as sodic series, all Crowsnest samples of this study and those of Pearce (1967) and Ferguson and Edgar (1978) plot as intermediate to felsic potassic series. Figures 3.4a and b show the primary rocks to classify as tristanites and trachytes. The composition of the ignimbrite beds is again found to closely mimic that of an analcime phonolite and/or trachyte as defined by Ferguson and Edgar (1978). The matrix glasses of Pearce (1967) also fall within this range. According to this scheme, the average composition of the Crowsnest suite, including the pyroclastics, may be classified as tristanite or trachybasalt of the potassic alkaline basalt series. Blairmorites classify as benmorites of the sodic series.

C. Minor Element Geochemistry

Perhaps the most useful classification of altered igneous rocks is one that is based upon the relatively immobile elements found in refractory minerals. Of these, Zr, Y, Ti and Nb will be used to classify the lower ash and tuff horizons. These analyses will be compared with those of Furguson and Edgar (1978) for primary rock types.

Wedepohl (1978) and Goff (1984) points out that the immobility of an element is the result of its ability to be incorporated into the lattice of stable minerals. These minerals must show resistance to breakdown during alteration and metamorphism. In some instances these elements may remain relatively immobile even after breakdown of the host mineral due to their inability to go into solution (Wedepohl, 1978).

The common alteration of the lower Crowsnest is one of intense devitrification of the glassy ground mass of the ash or tuff beds. It is not known what affect on mobility such an intense conversion of glass to clay minerals has on the mobility of Ti, Y, Zr and Nb. Cann (1970) suggests, however, that during devitrification of pillow basalts they suffer only minor mobility. It seems that the progressive hydration of volcanic glass will not affect trace element mobility to a significant degree.

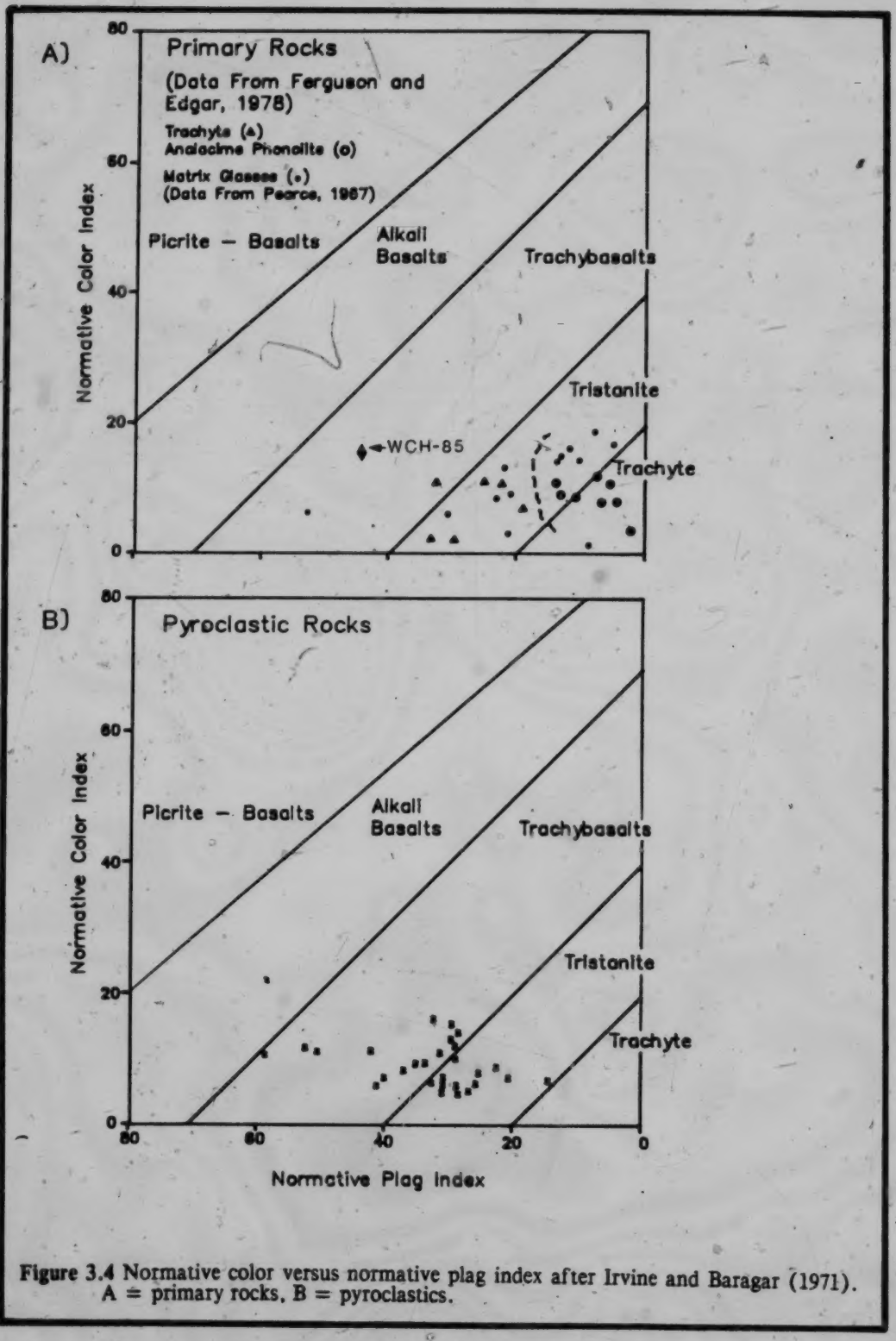

Figure 3.4 Normative color versus normative plag index after Irvine and Baragar (1971). A = primary rocks, B = pyroclastics.

The occurrence of Ti, Y, Zr, and Nb in the common rock forming minerals is especially important in light of the relatively unique mineralogy of the Crowsnest. It is essential to determine which mineral carries which element as the mineral distribution throughout the sequence may have an affect upon the elemental ratios used in many classifications.

Titanium is commonly found in the minerals ilmenite and augite. It also occurs in the relatively rare andradite garnet commonly associated with alkaline igneous rocks (Wedepohl, 1978). Dingwell and Brearly (1985) have found rare occurrences of Fe-Ti oxides as inclusions in garnets from a sample of the lower Crowsnest. Their study (Dingwell and Brearly, 1985) shows the garnets to be titanium-bearing, especially in the dark zones.

Dunn *et al.* (1981) have shown that the clinopyroxenes, aegirine and aegirine-augite are capable of fractionating zirconium during the magmatic process. The highly charged nature of zirconium usually results in the residual formation of zircon and to some extent ilmenite. The absence of the latter mineral in the Crowsnest suite suggests that the concentration of Zr lies with the clinopyroxenes.

Niobium, like zirconium and titanium, may be found in biotite, amphiboles and a host of titanium-bearing minerals. It is principally found in sphene, pyroxene and ilmenite (Wedephol, 1978). Aegirine-augite and sphene are the minerals which would likely carry the greatest abundances of niobium in the Crowsnest suite.

Yttrium and the associated lanthanides are principally found in minerals where substitution for Ca^{2+} can take place, (Wedepohl, 1978). Apatite, sphene and calcic agirine-augite will have the greatest abundance of yttrium. Minor amounts may be found in potash feldspar due to initial crystallization trapping of yttrium, (Wedepohl, 1978).

Upon identifying the minerals species which carry Ti, Y, Zr, Nb, a few observations on their distribution throughout the sequence can be made. The most striking feature can be found in table 3.3 which lists the Crowsnest mineral suite and their densities.

TABLE 3.3. Trace element-bearing minerals and their densities

Mineral	Density	Trace Elements
Apatite	2.71	Y
Sanidine	2.55 - 2.63	Y(tr.)
Sphene	3.45 - 3.55	Ti,Y
Aegirine-augite	.3.45	Zr, Nb, Ti
Melanite	3.7 - 4.1	Ti
Ilmenite	4.72	Ti, Nb
Titanomgnetite	5.17	Ti

All of the trace elements excepting Y are found to occur in the minerals with notably higher densities.

During a pyroclasitic eruption, either air-fall or pyroclastic flow, a degree a fractionation will take place. Separation of the Y, Zr, Ti and Nb-bearing heavier minerals from the lighter mineral species, the feldspars and analcimes, has occurred in many beds which exhibit strong density-stratification. Zones enriched in the denser minerals will have a much higher concentration of trace elements relative to other zones composed chiefly of lighter minerals. This type of fractionation may also take place with respect to the distance from the vent. The deposits farthest from the vent would be depleted in trace elements relative to those in proximal areas.

With this in mind, all samples analyzed by this study were collected so that all fractions within a single bed were represented. A comparison of samples from Ferguson and Edgar (1978) with this study should determine the degree to which fractionation has taken place.

Winchester and Floyd (1977) have presented a number of classifications based on immobile element composition. The three diagrams Zr/TiO_2 vs Nb/Y, SiO_2 vs Nb/Y and SiO_2 vs Zr/TiO_2 will be utilized to classify the Crowsnest rocks. With these classifications only a broad distinction can be made between alkaline and subalkaline rocks. The line dividing the two suites is taken as only approximate. There is also no division between the potassic and sodic series. However, basanite, tristanite/benmorite, phonolite and trachyte differentiates can be distinguished.

Trachyandesite is taken to be synonymous with tristanite on all diagrams, as is suggested by Irvine and Baragar (1977).

Zr/TiO_2 versus Nb/Y

Three fields are again defined by the trachytes, analcime phonolites and blairmorites of Ferguson and Edgar (1978), (Figure 3.5a). They are divided on the relative increases in the Nb/Y ratio progressing from trachyte to blairmorite. The ratio of Zr to TiO_2 is shown to be quite variable within each group.

The rocks of the lower Crowsnest are plotted in Figure 3.5b. Numerous samples cluster just within the subalkaline field based upon their Nb/Y ratios, while the majority classify as tristanites. Again most cluster near values of the primary trachytes.

The enrichment of yttrium and the depletion of niobium-bearing minerals by crystal fractionation may cause the anomalous samples to fall in the subalkaline fields.

SiO_2 versus Nb/Y

Blairmorite, analcime phonolite and trachyte fields are again well defined (Figure 3.6a). The pyroclastics plot as tristanites along with the trachytes (Figure 3.6b). The ignimbrite beds show a slight enrichment in SiO_2 relative to their primary counterparts. As expected some samples plot within the subalkaline field.

SiO_2 versus Zr/TiO_2

No discrete fields are delineated by the primary rocks on the basis of Zr/TiO_2 ratio (Figure 3.7a). The trachytes do show a tendency to be slightly more silica-rich and plot as tristanites and phonolites, while the analcime phonolites and the blairmorites plot as phonolites and basanites respectively.

The pyroclastic suite is slightly enriched in silica, but plots as trachytes and tristanites along with the primary trachytes (Figure 3.7b).

D. Bomb Geochemistry

The occurrence of carbonate in the Crowsnest has been documented since the formation was first discovered. Pearce (1967) first predicted the occurrence of carbonatite based on the presence of 6 to 10 inch carbonate pisoliths in some beds. Similar forms are identified as bombs in this study.

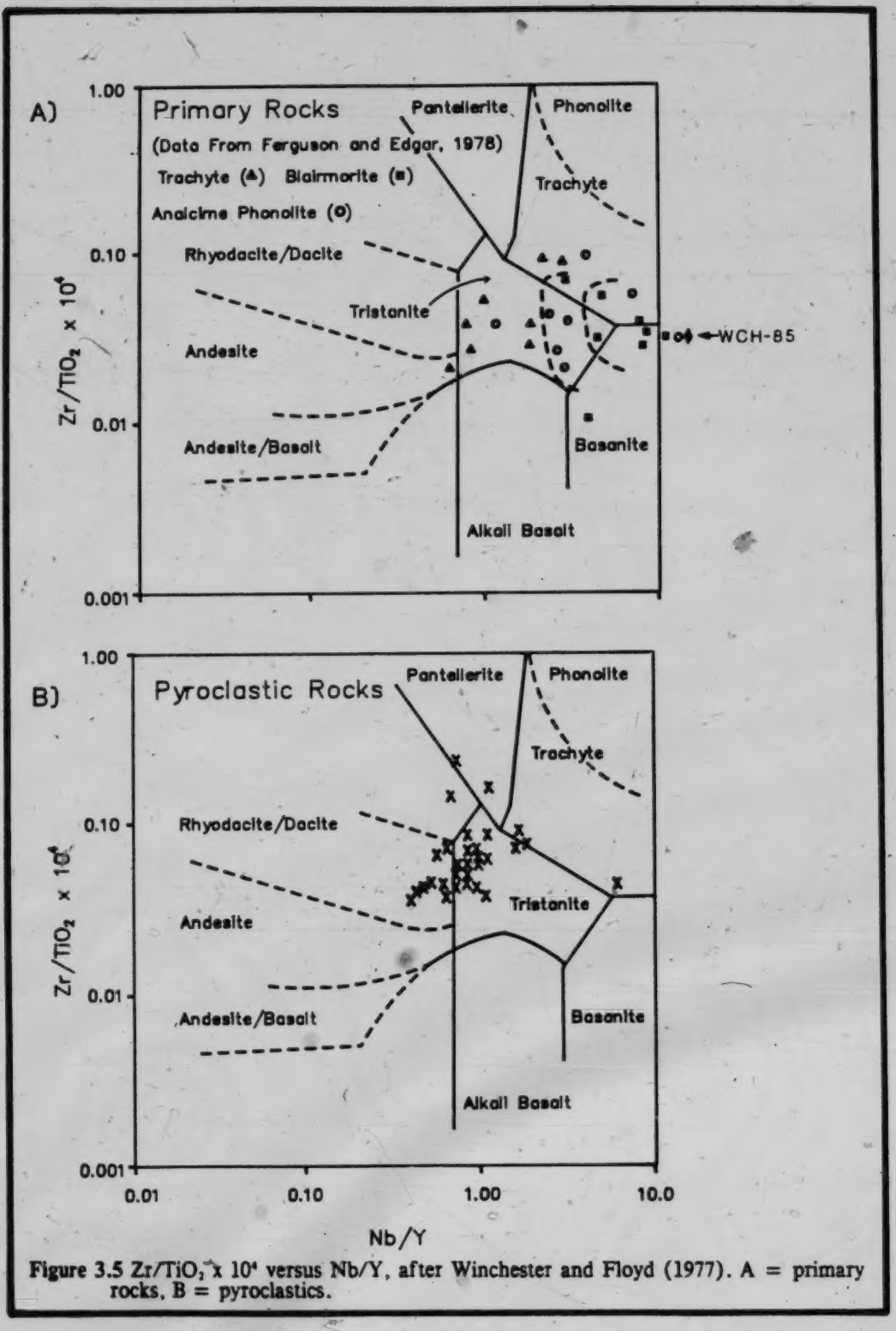

Figure 3.5 $Zr/TiO_2 \times 10^4$ versus Nb/Y, after Winchester and Floyd (1977). A = primary rocks, B = pyroclastics.

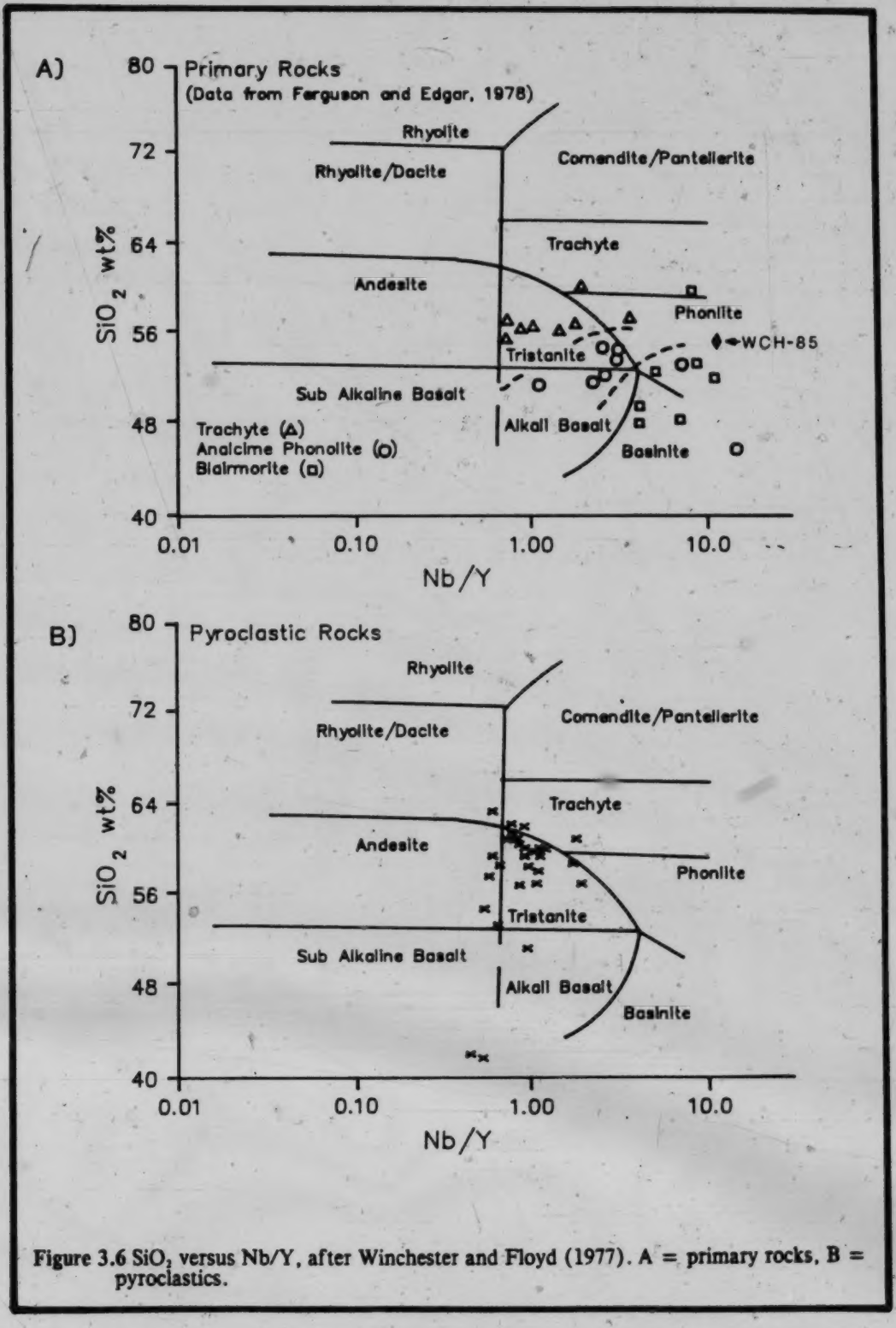

Figure 3.6 SiO_2 versus Nb/Y, after Winchester and Floyd (1977). A = primary rocks, B = pyroclastics.

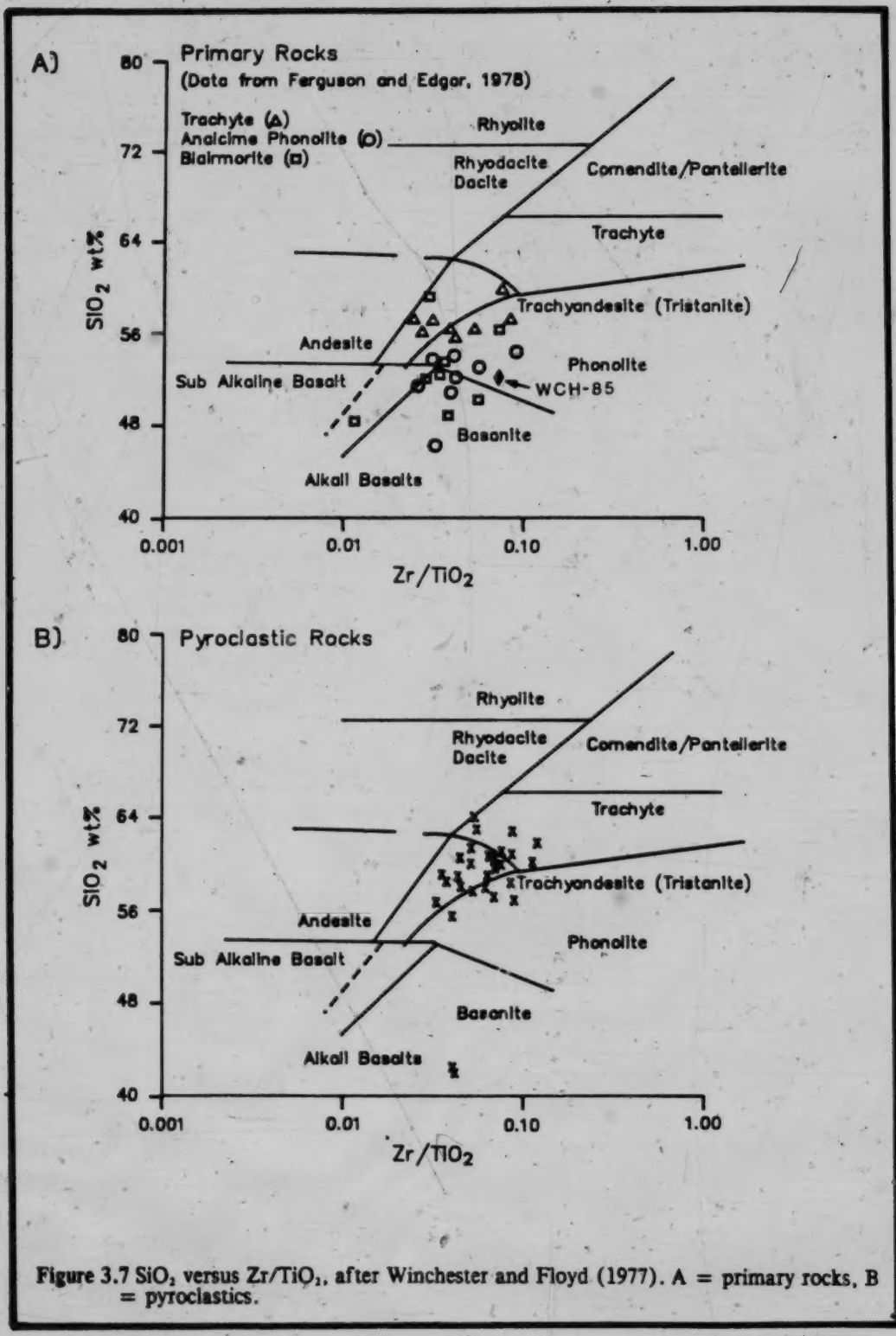

Figure 3.7 SiO_2 versus Zr/TiO_2, after Winchester and Floyd (1977). A = primary rocks, B = pyroclastics.

Textural evidence (Chapter II) suggests that much of the presence of carbonate is due to the replacement of glass, glassy fragments, small analcime microlites and larger phenocrysts. The identification of bombs, which are dominantly composed of carbonate (Plate 2.6d,e,f), at three locations provides interesting new evidence on the occurrence of a carbonatite phase.

The highly differentiated composition and the unusual mineralogy of the Crowsnest Formation is similar to compositions associated with carbonatites described by Moorhouse (1959), Gold (1963) and Heinrich (1966). The similarity is exemplified by the presence of the minerals melanite, apatite, sphene, aegirine-augite and magnetite.

Gold (1963) and Heinrick (1966) have shown that carbonatites may be distinguished on the basis of the geochemical abundances of P, Ba, Sr, Nb, Y, Zr, K, Na, rare earth elements and oxygen isotope data. The average carbonatite composition is compared with those for alkaline igneous rocks, standard igneous rocks, limestones and seven Ca-rich samples from the Crowsnest (Table 3.4). These seven samples represent two from carbonate-rich bombs, two from carbonate-bearing pyroclastic beds, and one from each of the rock types defined by Ferguson and Edgar (1978). The samples from pyroclastic beds contain small round spheroids (Plate 2.7a) which were probably deposited as pyroclastic fragments.

A comparison given in Table 3.4 shows that the compositions of the bombs closely mimics the compositions of both the pyroclastic and primary Crowsnest suites. SiO_2 and CaO were predictably variable.

The major element compositions for Ti, Na, K, P, and Sr for the Crowsnest rocks approximates the composition for alkaline igneous rocks. Exept for P_2O_5, the bombs show no chemical similarities with limestones, suggesting that the source is not in situ replacement. The trace element composition for Nb, Y, Zr again show a marked igneous signature. The Crowsnest compositions are transitional between alkaline and standard igneous rock types. The is no marked similarity with limestones or true carbonatites.

The source of the abundant calcium in these rocks and others throughout the Crowsnest is uncertain. Further studies involving oxygen and carbon isotopes may define a source, though the occurrence of carbonate in primary bombs, and the igneous compositional signature, point to a magmatic source.

TABLE 3.4 CHEMICAL COMPOSITIONS FOR CARBONATITES AND CROWSNEST ROCKS

	Standard rocks*				Crowsnest Rocks						
					Pyroclastic			Primary			
	I	II	III	IV	V	VI	VII	VIII	IX	IX	X
Wt%											
Si_2O	11.99	49.65	63.16	5.14	41.37	41.26	53.18	51.58	56.24	51.99	59.91
TiO_2	.079	1.46	10.74	.067	.37	.36	.64	.36	.9	.94	.68
Na_2O	.42	6.13	3.27	.03	2.74	2.20	3.32	2.16	3.15	4.81	6.31
K_2O	1.48	3.69	3.17	.16	5.01	4.84	5.62	6.72	8.58	6.32	3.63
P_2O_5	2.04	.2-2		.045	.01	.08	0	.06	.03	.02	-
SrO	.4	.1-1	.03	.07	.16	.15	.22	.19	.31	.17	.10
CaO	34.80	7.00	4.90	42.30	30.33	30.61	14.70	12.09	4.43	4.20	5.42
PPM											
Nb	1951	35	20	.3	9.0	10	20	18	20	40	25
Y	96	20	20	30	20	20	33	19	23	17	3
Zr	1120	500	17	19	148	155	282	252	260	220	188

* Data from Gold (1963) and Heinrick (1966)

I = Carbonatites, II = Alkaline Igneous Rocks, III = General Igneous, IV = Limestones

V = CB_1, VI = CB, VII = WCH-75, VIII = WCH-14, IX = Trachyte X = Analcime Phonolite, XI = Blairmorite

E. Discussion

The movement of potassium, sodium and calcium during devitrification has has had some affect on the classification of the Crowsnest pyroclastic suite. Elemental movement is illustrated in the diagrams of this chapter and also in the abundance of the alteration/authigenic phases illite, illite/smectite, calcite and adularia. Fortunately, the data for the fresh, primary rocks have provided a standard to which the pyroclastics can be compared.

According to the classification of Irvine and Baragar (1971) both the primary and pyroclastic rocks of the Crowsnest are potassic differentiates of an alkaline olivine basalt, excluding the blairmorites which are sodic differentiates. The former classify dominantly as tristanites while the latter classify as benmorites.

A significant feature of many diagrams is the marked differentiation between the trachytes, analcime phonolites and the blairmorites of Ferguson and Edgar (1978). These rocks were probably erupted from a strongly zoned or fractionated magma chamber and therefore represent progressive differentiation of the melt. More study is needed to reach any further conclusions.

The unusual occurrence of carbonate bombs suggests the presence of a carbonatite phase. Geochemically, however, the signatures of these bombs do not match those of standard carbonatites. They do show a strong igneous character suggesting that they recrystallized[6] from magmatic components, perhaps CO_2 and calcium-bearing feldspathic glass[7].

---

[6]Based on textural observations in thin section, Plate 2.6d,e,f.
[7]Holland and Borcsik (1976) show that a decrease in pCO_2 reduces the solubility of calcite under favorable conditions. The study is limited to temperatures below 200°C.

IV. CLASSIFICATION AND NOMENCLATURE

Pyroclastics are one of the most diverse type of volcanic rock. There is an extremely wide variety of deposits, which often grade freely into each other. Classification has progressed substantially over the last fifteen years and has now reached a point where deposit types, their eruptive origins and emplacment mechanisms are understood.

Fisher (1961, 1966), Williams and McBirney (1979), and Schmid (1981) have provided classifications of pyroclastic components and the rocks in which they are constituents. Deposit types, their origin, and emplacement mechanisms have been discussed by Sparks (1976), Fisher (1979, 1983), Sparks (1982), Sparks *et al.* (1976) and Sparks (1982), among others. These studies have described many important pyroclastic eruptions.

The Crowsnest Formation provides an excellent opportunity to apply the modern understanding of pyroclastic rocks to an ancient pyroclastic deposit. For this reason the following brief review of pyroclastic rocks is presented. It is intended as a reference to be used during the discussions and interpretations of the Crowsnest Formation and its deposits.

A. Pyroclastic Components

Individual pyroclastic components may be classified on the basis of their origin, which is often useful in the interpretation of the deposit. Three types are now recognized

1. Juvenile Components. Juvenile components originate from the erupting magma. They may consist of crystals, glassy fragments, bombs and magma clots.
2. Cognate Components. Cognate components originate from previously ejected volcanic rock. They may consist of fragmented flows, plugs, intrusives or pyroclastics.
3. Accidental Components. Accidental components originate from the rocks into which the rising magma penetrates. Such rocks are incorporated and eventually ejected as pyroclastic debris. They may consist of any rock type.

An improtant system of grainsize classification has been developed by Fisher (1961, 1966) and Schmid (1981). This system divides pyroclastic components into three sizes; ash (<2mm), lapilli or lapillus (2-64mm) and blocks or bombs (>64mm) (Figure 4.1a) . The corresponding deposits of such components are called tuff, lapillistone, pyroclastic breccia, and/or agglomerate respectively. Further division may be made on the basis of coarse or fine grainsize subdivisions as defined by Schmid (1981) in Figure 4.1a. Mixture terms are available

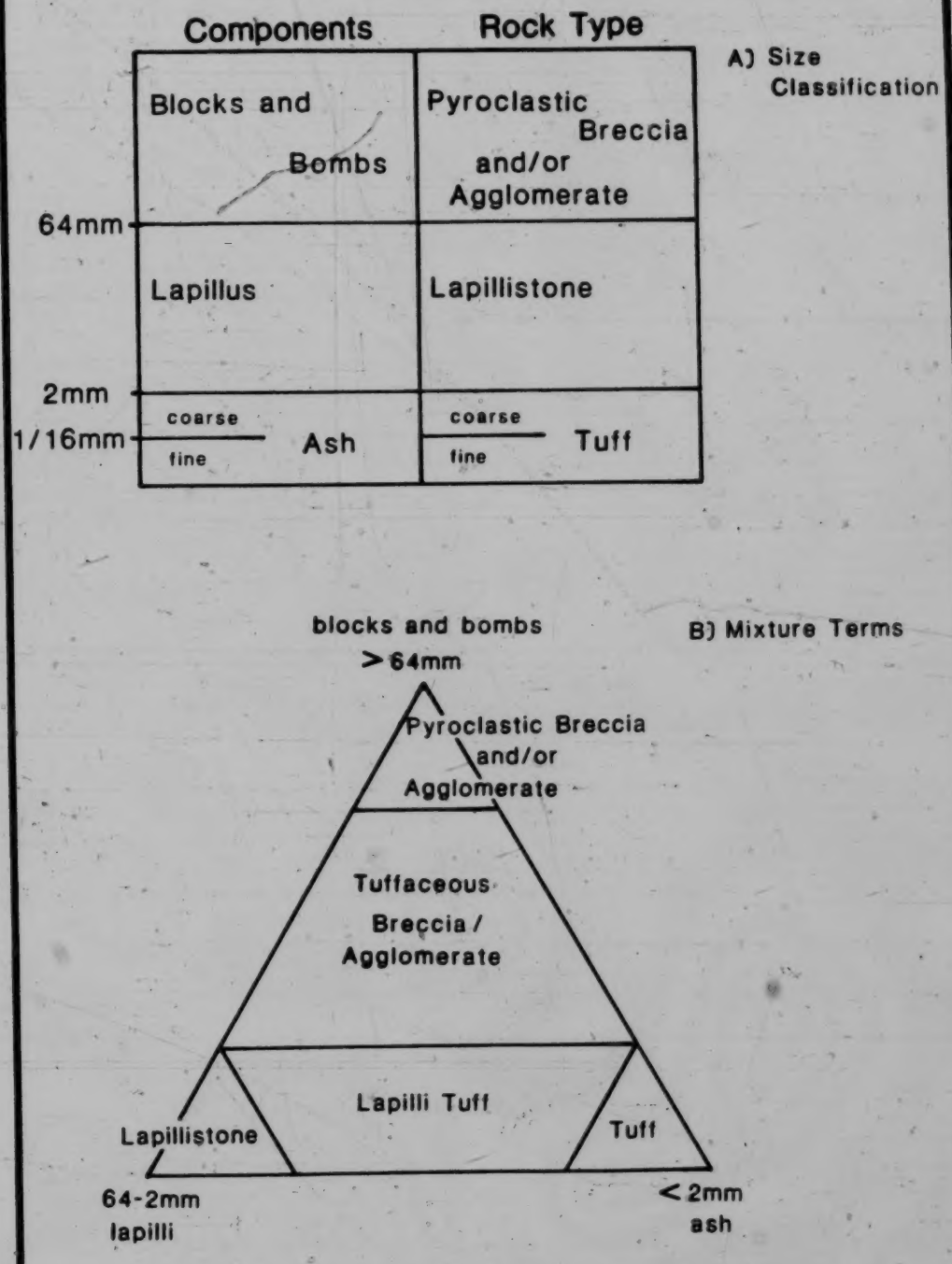

Figure 4.1 Classification of pyroclastic rock components, after Fisher (1961, 1966) and Schmid (1981). A) Size classification, B) Mixture Terms.

and are defined in Figure 4.1b by Fisher (1966) and Schmid (1981). Descriptions of different types of ash, lappilus and bombs or fragments are fully described by Williams and McBirney (1979) and Fisher and Schmincke (1984) and need not be discussed here.

The problematical term "agglomerate" was initially defined with broad criteria and has been used to describe a number of different deposit types. Unfortunately it seems that the use of the term is still relatively unrestricted in both the academic and industrial sense. In the past, it has been used to describe a rock composed of an "agglomeration" of very coarse pyroclastic ejecta, either homogeneous or heterogeneous. Fisher and Schmincke (1984) suggests the term be restricted to a coarse deposit consisting entirely of bombs, while Williams and McBirney (1979) place a restriction of an intermediate to basaltic composition on such bomb deposits. Many deposits do not readily classify under the term pyroclastic breccia because they consist of virtually round pyroclastic fragments which do not exhibit the characteristics of bombs. In such cases the use of agglomerate may be appropriate.

For the purpose of this paper the term agglomerate will be used for a pyroclastic deposit consisting of coarse, rounded fragments. This would include rocks whose components initially may have been angular (breccia) but were rounded during flow. The term *bomb agglomerate* is applied to the appropriate deposits as is defined by Fisher and Schmincke (1984). The term pyroclastic breccia will be used for deposits which are essentially composed of angular fragments.

B. Eruptive Origins of Pyroclastic Rocks

Until the last decade, the understanding of how, why and under what conditions pyroclastic deposits were formed was limited. It is now known that such deposits are produced by a number of different types of eruption.

Factors which may initiate pyroclastic eruptions are quite numerous. However, Sparks (1976, 1982) and Fisher and Schmincke (1984) point out that expansion of magmatic gases and/or vaporization of water are the two most critical. Generally, two types of eruptions are identified:

1. Magmatic Eruptions. Magmatic eruptions occur when gases within the magma expand explosively as the melt reaches the surface. Variations in the intensity and violence of the eruption depend on the amount of gas in the melt. This has profound implications on the

formation of pyroclastics as will be discussed later.

2. Hydroclastic Eruptions. Hydroclastic eruptions involve the reaction between external water and the rising magma or magmatic gases. The eruptions can be divided into two types according to Fisher and Schmincke (1984).
   a. Phreatic eruptions occur when external water (formational or surface) is rapidly converted to steam by heat generated from the magma. The resultant explosion disrupts the country rock, producing deposits which are rich in accidental fragments.
   b. Phreatomagmatic eruptions result when ascending magma contacts a water source of any kind. Such deposits contain abundant juvenile, cognate and accidental components.

   Large volumes of steam are produced by hydroclastic eruptions which emplace deposits at substantially lower temperatures than their magmatic counterparts.

Generally, eruptions are classified by their relative intensity which is directly reflected by the dispersal of the deposits. Dispersal (D) is defined by Walker (1973) as the area enclosed by the 0.1 Tmax[1] isopach. The classifaction is as follows:

	D (km^2)
Hawaiian	0 - 0.05
Strombolian	0.05 - 5
Sub - Plinian	5 -500
Plinian	500 - 50,000
Ultra Plinian	> 50,000

Sparks (1982) notes that increasing column height and eruption intensity correspond to increasing values of D.

Observations of recent and historic eruptions have helped to define five major eruptive origins (listed below) for pyroclastic rocks. Four are discussed here in limited detail. Any and all of these may occur during an eruption or eruptive phase (Figure 4.2).

1. Convective Column and Gravitational Column Collapse (Sparks and Wilson, 1976).
2. Boiling over (Williams and McBirney, 1978).
3. Dome Collapse (Schmincke and Johnston, 1977).
4. Inclined Blast (Perret, 1939).

---

[1]10% of the maximum thickness.

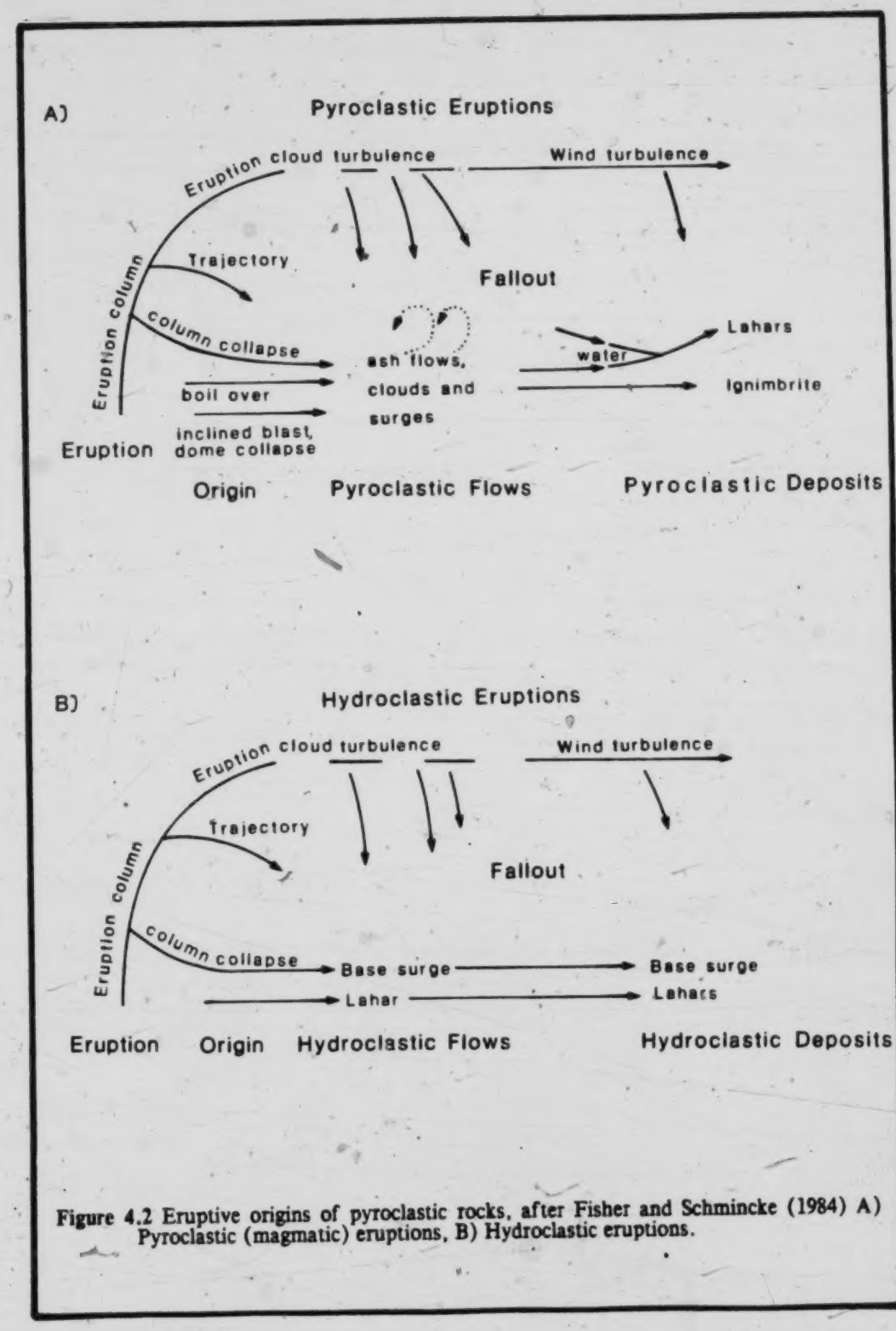

Figure 4.2 Eruptive origins of pyroclastic rocks, after Fisher and Schmincke (1984) A) Pyroclastic (magmatic) eruptions, B) Hydroclastic eruptions.

5. Explosive disruption of lava fronts (Rose *et al.*, 1977).

Convective Columns and Gravitational Column Collapse

A major model developed over the last decade is that of convective columns and gravitational column collapse described by Sparks and Wilson (1976) and Sparks *et al.* (1978). Based upon numerous observations, the model allows for the formation of air-falls and/or pyroclastic flows from vertical eruption columns. The formation of such columns is summarized in stages by Sparks (1982):

1. Explosive Stage. Gas exsolution and expansion at relatively shallow depths in the vent initiates the eruption. Solid and liquid components achieve "peak velocities" between 100-600 m/s (Sparks and Wilson, 1976) as they leave the vent. Velocity and other factors depend upon the depth of the explosion and the morphology of the vent (Sparks and Wilson, 1976; Sparks *et al.*, 1978 and Sparks and Sparks, 1983).
2. Gas Thrust. Sparks (1982) describes an area immediately above the vent where momentum of the particles gradually takes over from thrust, creating a decrease in velocity. As the column spreads from the vent, a peripheral zone develops where violent mixing with air occurs. The zone gradually moves inwards towards the core of the jet. Within this mixing zone, the velocity and temperature of the particles and magmatic gas decrease as cooler air is mixed and heated.

The two following models have been developed by Sparks and Wilson (1976) and Sparks *et al.* (1978). They describe two columns, one forming dominantly air-fall deposits and the other forming dominantly pyroclastic flows (Figure 4.3). There is a full gradation between the two types.

1. Convective Plume. The heated air and particles in the peripheral mixing zone become less dense than the atmosphere and rise as a result of a density or buoyancy effect. Complete penetration of the column by this turbulent mixing zone produces a tall column, rising well up into the atmosphere, producing dominantly air-fall deposits.
2. Column Collapse. Should mixing not penetrate the entire column, the unmixed core remains more dense than the surrounding atmosphere. As gravitational forces take over from momentum, it collapses and spreads as pyroclastic flows about the vent. Large heavy clasts fall near the vent forming co-ignimbrite lag deposits as described by Wright and

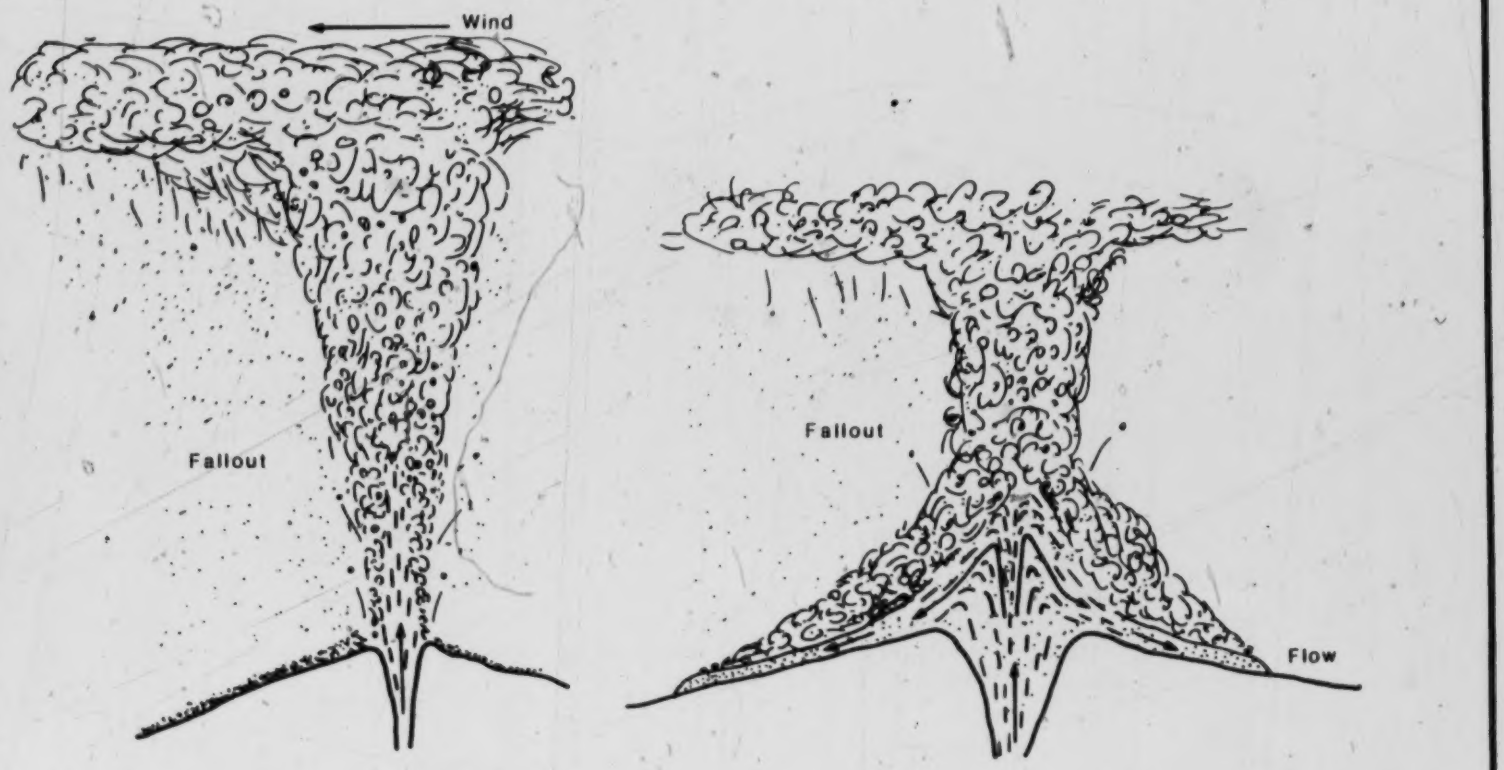

Figure 4.3 Schematic diagrams of a fully convective column and a collapsing column, after Sparks (1982).

Walker (1977).

Exceptionally gas-charged eruptions produce violent mixing zones, favoring fully convective columns[9] and subsequent air-falls. Eruptions of lesser gas concentration would tend to produce pyroclastic flows (Sparks, 1982). Further, wide vents and high discharge rates would also favor the formation of pyroclastic flows (Sparks and Wilson, 1976; Sparks *et al.*, 1978; and Sparks, 1982).

Boiling Over

Such eruptions are essentially the least gas charged equivalent of the convective plume eruptions. Described in detail by Williams and McBirney (1979) as Krakatoan types, these eruptions tend to be more fluid and less gas charged. The eruptions are interpreted to be shallow (Taylor, 1958) and may have resulted from intense vesiculation of magma, providing a buoyancy mechanism. Such eruptions cause very fluid flows to essentially spill or well up over the crator rim (Williams and McBirney, 1979; Fisher and Schmincke, 1984). The eruptions may or may not be associated with a vertical column (Fisher and Schmincke, 1984). Similar eruptions from fissures associated with calderas, and those not related to active volcanoes, are described as Valley of Ten Thousand Smokes type and Valles type respectively by Williams and McBirney (1979).

Dome Collapse

The gravitational collapse or disintegration of domes, dome flanks and summit spines have been described by Perret (1937), Schmincke and Johnson (1977), Williams and McBirney (1979) and Fisher and Schmincke (1984). Williams and McBirney (1979) have identified two fundamental types of dome collapse;

1. Merapi (non-explosive). Merapi types form from the gravitational collapse of over-steepened dome flanks or spines.
2. Pelean (explosive). Pelean types may be gas-rich or gas-poor and occur during active growth of the dome. Internal eruptions disrupt the dome during its growth. Such types are often associated with lateral blasts.

---

[9] Termed "Plinian eruption collumns".

The deposits of dome collapse have been described as "block and ash flows" by Perret (1937). In the Pelean types magmatic components occur in the form of bombs, pumice and lapillus, while those of Merapi type are essentially composed of cognate material with lesser juvenile components. It would seem possible if not probable to have liquid magma as a component of some Pelean types.

Inclined Blast

First described by Perret in 1937, lateral or directional blasts may occur during most types of eruption and produce a variety of deposits. As has been observed at Mt. St Helens, such blasts eject material laterally, usually from the base of a vertical column or from the flank of the volcano (Fisher and Schmincke, 1984)

C. Flow Mechanics

Miller (1978) defines a pyroclastic flow as a mobile fluidized mass that contains hot, dry debris and gas, synonymous with the hot gaseous particulate density current of Fisher and Schmincke (1984). The flows are composed essentially of coarser fragments which are dispersed in fluidized fines (Sparks, 1976). The gases which are responsible for the buoyancy and hence mobility of the flows are derived from magmatic gases and the atmosphere. The latter is incorporated and heated during the formation and subsequent movement of the flow.

Movement and emplacement of pyroclastic flows occurs by a number of complex mechanisms. These mechanisms rely heavily upon the interaction between gas and solids to yield a mass of particles that behave much like a fluid body (Sparks, 1982). In turn, the morphology of the deposits reflect the mechanisms by which they were emplaced. A comparative analogue is a sediment density current. The main body of a pyroclastic flow moves as a dense particulate mass along the ground. The initial energy is provided by the eruption (Sheridan, 1979) and later by gravitational forces. As they advance, flow fronts develop a "cleft and lobe" shape (Fisher, 1979; Fisher and Schmincke, 1984), the lobes resulting from more rapidly advancing currents within the flow (Fisher and Schmincke, 1984).

Initially, on mountain slopes, flows may follow pre-existing channels, spreading out as lobes or fans away from the vent. (Sparks *et al.*, 1973; Rowley *et al.*, 1981 and Fisher and Schmincke, 1984). They are observed by Fisher and Schmincke (1984) to almost completely

drain the upper slopes, leaving the greater thicknesses to be deposited away from the source, in lower regions. Lag levees and proximal bedded deposits may remain where the main body has drained away (Rowey *et al.*, 1982; Rowley *et al.*, 1985). It seems reasonable to find pyroclastic deposits better preserved in the low lying areas flanking a vent.

Pyroclastic flows are known to have great mobility (Fisher and Schmincke, 1984 and Miller and Smith, 1977). Some documented flows (see Fisher and Schmincke, 1984) have covered distances of up to 600 km and surmounted topography as high as 300 meters (Mt. St. Helens). An extreme example occured in New Zealand where the Taupo ignimbrite climbed a height of 1500 meters (Walker and Wilson, personal com., in Sparks, 1982). Miller and Smith (1977) suggest that such flows may have been thick, inflated, dilute clouds which attained high altitudes and simply overrode topography.

Velocities have been measured from 14 km (Fisher and Schmincke, 1984) to 230 km/h (Moore and Melson, 1969 in Fisher and Schmincke, 1984). Sparks (1982) suggests that velocities of flows average between 10-30 m/s or about 30-110 km/h. High volume flows tend to travel greater distances (Miller and Smith, 1977).

The mobility of flows relies upon the buoyancy and fluidizing effect provided by hot gas or heated air. The gases are provided by original magmatic gas, exsolution of gas from juvenile fragments (Sparks, 1979), gas release during breakage of solid fragements and incorporation of air at the front of flows. From these observations, Sparks (1982) has devised a model for the various types of flow movement (Figure 4.4):

1. Poorly Fluidized Viscous Flows. Essentially a viscose flow, these types tend to have high yield strength and viscosity with a non-turbulent flow front. Deposits are poorly-sorted and may carry very large clasts. Movement is by shearing along a basal zone.
2. Strongly Fluidized Viscous Flows. Such flows are intermediate between strictly turbulent and viscous types. They are fluidized over part of their length as a result of overriding of air or water. This results in a loss of shear strength and a more fluidized effect.
3. Fluidized, Turbulent Flow. This flow type is entirely turbulent; the fluidizing affect is caused by the rapid mixing of air at the head, resulting in an inflated flow.

Fisher (1982) identifies four types of flow transformation which may occur along the length of a flow as shown in Figure 4.5. Such transformations result in textural variations within a flow (Fisher, 1983). Rowley *et al.* (1985) provide evidence that inflation and deflation

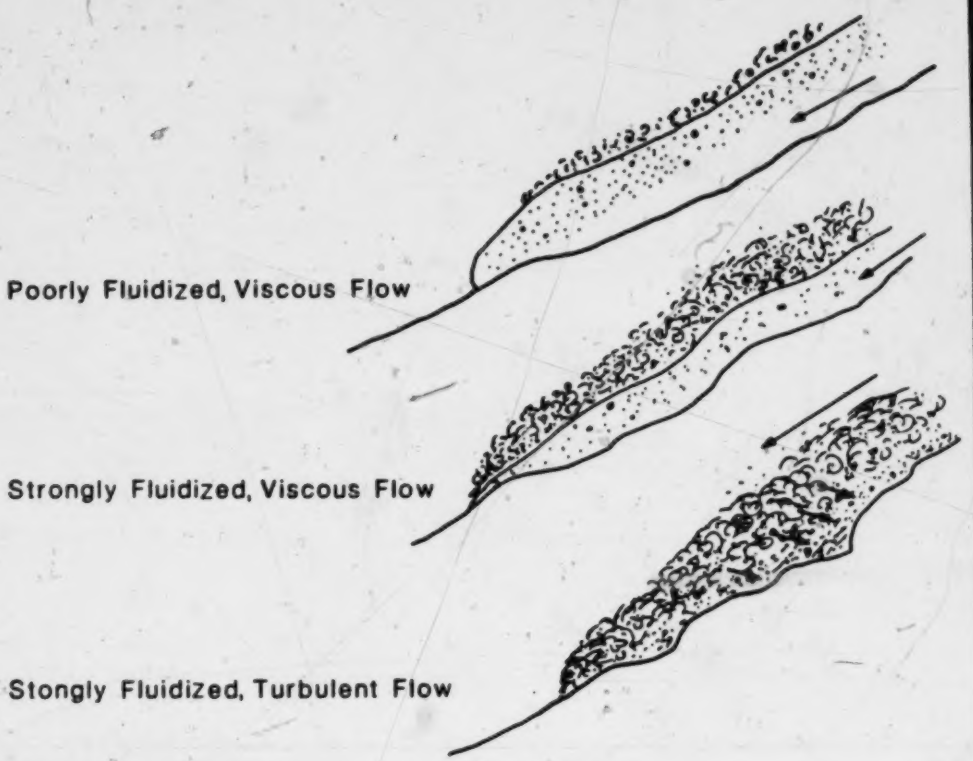

Figure 4.4 Mechanisms of pyroclastic flow, after Sparks (1982).

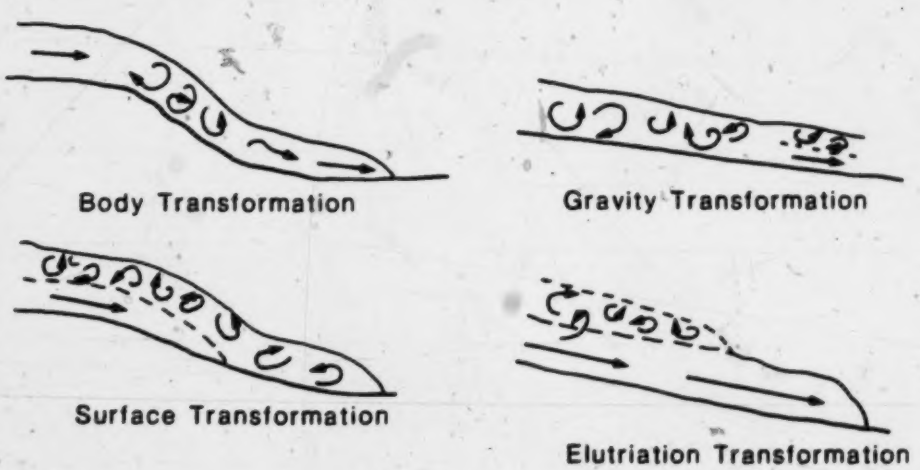

Figure 4.5 Flow transformations, after Fisher (1982).

transformations may occur as a flow moves down the flank of the volcano. They note that on steep, rough slopes, rapidly moving flows may incorporate air, becoming inflated, subsequently developing a turbulent, inflated flow. On lower slopes, they may deflate and produce nonturbulent flows. The resulting deposits suggest that there is a complete gradation between dense, non-turbulent and dilute, turbulent flows (Rowley *et al.*, 1985).

Flows usually develop a two layer cross-section, which is described by Williams and McBirney (1979), Sparks (1982) and Fisher and Schmincke (1984) (Figure 4.4). The basal layer is denser with a high particle concentration, while the upper zone consists of a turbulent, lower concentration cloud (ash-cloud). The flow of the lower part is, for the most part, controlled by topography, while the upper may move outward from the lower flow and may separate from it entirely, usually after movement of the lower has stopped. Fisher (1975) suggests that there is a *critical zone* which exists between the dense and turbulent phases developing textural discontinuities in the resulting deposit.

Pyroclastic flows originate by column collapse, lateral blast, dome collapse and boiling over (Figure 4.2). During a given eruption, more than one mechanism may operate to generate pyroclastic flows.

D. Pyroclastic Deposits

Many criteria are used to distinguish different deposits and their components. In turn, identification of deposit type allows for the interpretation of the mode of emplacement and the origin. The most complete description of pyroclastic rocks, flow types, mechanisms and origins is given by Fisher and Schmincke (1984). Deposits can be divided up into four major types: pyroclastic flows from magmatic eruptions (ignimbrites), pyroclastic flows from hydroclastic eruptions (base-surges), air-fall deposits and lahar deposits. Flows from magmatic eruptions can be divided into flows and surges. During an eruption, more than one type may be emplaced.

Ignimbrites

The term *ignimbrite* will be defined for the purpose of this paper as being an individual pyroclastic flow deposit consisting primarily of juvenile and cognate fragments, originating by pyroclastic flows from magmatic eruptions. The flows may be emplaced at high temperatures,

though welding is not implied. An ignimbrite deposit would therefore constitute an assemblage of flows which resulted during the course of a single eruption (after Sparks, 1982). The term does not include flow deposits of hydroclastic or laharic origins.

The products of pyroclastic flows can be classified into two types, which represent the two end members of a gradational series. These deposits are emplaced by nonturbulent, laminar (viscous) flows at one end, and highly turbulent diluted flows at the other. Recently, evidence from deposits at Mount St. Helens (Rowley *et al.*, 1985) suggest that a complete gradation between the two may occur both vertically and laterally during the course of the flow. The deposits representing these two end members are discussed below followed by standard models which relate the two types.

1. Massive Deposits from Dense, Non-Turbulent Flows. Generally, massive beds are poorly-sorted and often exhibit few features aside from marked normal grading of the lithic fragments and reverse grading of pumaceous fragments (Sparks, 1976). Discontinuous lenses or *trains* of crystals or rock fragments may occur and are proposed by Fisher and Schmincke (1984) to result from inter-tonguing *streams* of variable flow regime. Occasionally, local areas of thin lamination and low-angle cross-stratification may develop. Alternating coarse to fine layers can occur due to changing conditions in the eruption column (Fisher and Schmincke, 1984). Gas escape pipes (Fisher and Schmincke, 1984) may occur along with draping structures (Sheridan, 1979) during degassing and deflation of a flow. Gas escape structures may be associated with hydroclastic explosion pits (identified by Rowley *et al.*, 1982) where a pyroclastic flow has overridden a body of water. Welding may or may not occur.

   The massive beds may show gradational or sharp contacts with other types of flow deposits, notably surges. Rowley *et al.* (1985) provide evidence that massive or "main facies" deposits are the deflated counterpart of turbulent flows which produce surge deposits.

2. Surge Deposits. Surge deposits are often intimately associated with the massive beds of denser pyroclastic flows. They represent a turbulent phase, the deposits of which may overlie, underlie, grade into or extend beyond the massive main body of flow (Fisher, 1979; Sheridan, 1979; Sparks, 1982 and Rowley *et al.*, 1985). The origins of surge deposits, especially the ground surge, are debatable and are discussed below. Surges are hot, and

hence are distinguished from the wet, cooler base surges of hydroclastic eruptions.

Surge deposits are generally more fine-grained than flow deposits and usually exhibit moderate to good sorting with large clasts being notably absent (Sparks, 1982). Thin, well-defined planar and lenticular beds are found in vertical and lateral association with low-angle cross-beds (5-15°) and occasionally sand wave or dune forms (Sparks *et al.*, 1973; Sparks, 1982; Fisher and Schmincke, 1984 and Rowley *et al.*, 1985). Rowley *et al.* (1985) identify plane parallel-beds as the dominant bed form of proximal surge deposits at Mt St. Helens. Scours often occur between deposits (Rowley *et al.*, 1985). Surges have a notably higher crystal concentration than pyroclastic flows (Walker, 1971; Sparks, 1976, 1983 and Fisher and Schmincke, 1984), thought to result from the disintegration of pumice and subsequent concentration of phenocrysts. Pumaceous fines are removed during eruption and movement of the flow (Walker, 1971 and Fisher and Schmincke, 1984). Two main types of surge are known.

a. Ground surges. These types tend to underlie pyroclastic flows (Fisher, 1979; Sparks, 1982 and Fisher and Schmincke, 1984). They exhibit all the features of surge deposits and may also tend to pinch and swell, usually caused by uneven lower topography (Sparks, 1976). The origin of the ground surge is debatable.

   Wilson (1980) and Wilson and Walker (1982) suggest that they form as the result of cool air being infolded at the turbulent head of the flow, causing a turbulent cushion to form at the base. Arguments that ground surge deposits become coarse breccias in proximal areas are supportive. However, the co-ignimbrite, lag-fall deposits of Wright and Walker (1977) may be an alternative explanation.

   Sparks (1976), Fisher (1979) and Sheridan (1979) suggest that the ground surge forms from plug explosions, changing vent conditions and directed blasts during Plinian eruptions. It is suggested by Sparks *et al.* (1973) and Sheridan (1979) that the ground surge may mark the onset of a pyroclastic event, with turbulent flows moving out radially from the vent during the beginning of the eruption.

b. Ash Cloud Surges. Ash cloud surge deposits contain the standard surge textures and features. They are formed by "elutriation" (Fisher, 1979) from the top of a moving pyroclastic flow. The deposits occur as discontinuous lenses which overlie and extend beyond the main body of the flow. Ash cloud surges have a tendency to separate

entirely from the main body of the flow forming deposits which, in select areas, are not associated with a massive flow (Sparks *et al.*, 1973; Fisher, 1979; Sheridan, 1979 and Sparks, 1982).

Ignimbrite Depositional Models

A standard ignimbrite flow model is presented by Sparks *et al.*, (1973) along with amended versions by Sparks, (1976), Fisher (1979), Sheridan (1979) and Fisher and Schmincke (1984). Figure 4.6 depicts the idealized flow units of an ignimbrite deposit and the origins of each. The facies are presented for both proximal and distal areas. Unit 1 (Figure 4.6) is the ground surge facies which is often found in assocciation with pyroclastic flows. It may not always be present between flow units, especially in cases where the flows of a single eruption rapidly followed each other (Sheridan, 1979).

The flow itself is defined by units 2a-2d in Figure 4.6. Unit 2a is a pronounced basal zone or layer which is usually thin compared to the main body. It is fine grained and exhibits a poorly-sorted nature. The grain size distribution is similar to the main body, only over a smaller size range, lacking large clasts (Sparks *et al.*, 1973 and Sparks, 1976). Reverse grading is identified in most cases by Sparks (1973, 1976). With the reverse grading in clast size towards the top, the basal unit is abruptly transitional into the main body, usually over a few centimeters (Sparks *et al.*, 1973; Figure 4.6). Fisher and Schmincke (1984) believe that this basal zone was formed by the ingestion of air at the flow front, while Sparks *et al.* (1973) suggest the basal layer forms by forces of shear and grain size distribution which occur at the base of the flow.

Layers 2b-2d (Figure 4.6) represent the main body of the flow. It is estimated by Sparks *et al.* (1973) to contain approximately 90% of the bulk of the flow. The deposits are generally poorly-sorted and may contain some very large rock fragments. A marked grading results from the density contrast of the more massive and denser lithic fragments and the lighter pumice fragments (Sparks *et al.*, 1976, Sparks, 1976). Lithic fragments tend to be normally graded concentrating in unit 2b, while pumaceous clasts tend to "float" and concentrate at the top of the flow (unit 2d). The center of the flow, unit 2c, is a transitional zone between the two.

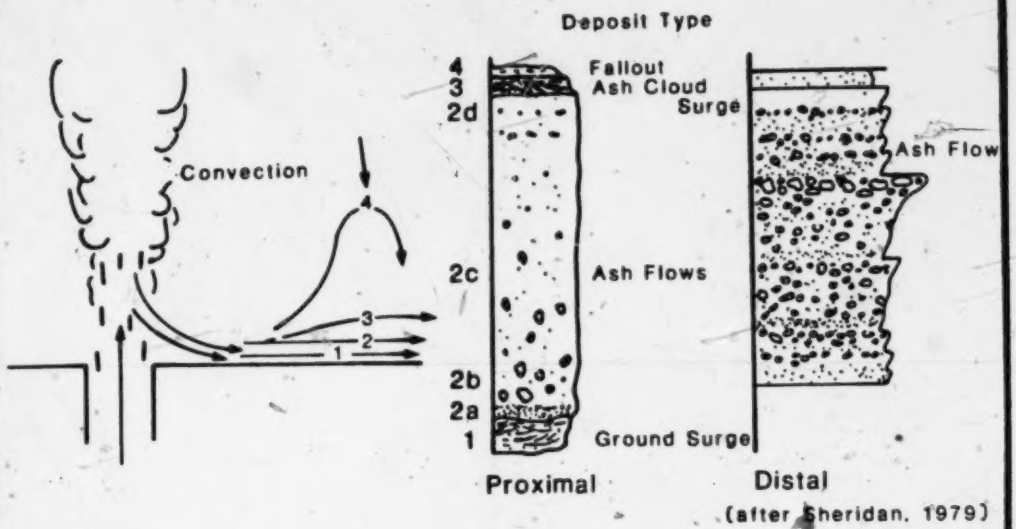

Figure 4.6 Standard ignimbrite depositional model and accompanying distal facies, after Fisher and Schmincke (1984) and Sheridan, (1979) respectively.

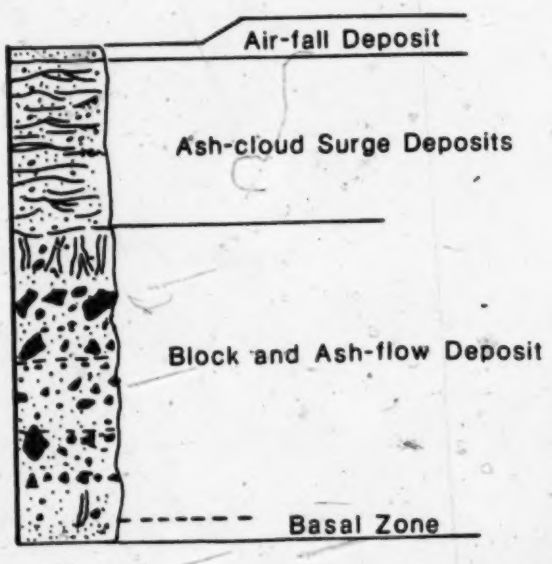

Figure 4.7 Deposit from a block and ash flow, after Fisher *et al.*, (1980).

The mechanisms of movement have a profound effect on sorting, as the denser flows inhibit the formation of graded zones (Sparks, 1976). The main body of the flow is often overlain by fine ash or ash cloud surge deposits (unit 3, Figure 4.6) which form by "elutriation" of the upper part of the flow (Fisher, 1979).

This ideal section or unit does not fit all types of flow. Two models have been produced for similar deposits in proximal and distal regions.

1. Proximal Regions. Areas immediately adjacent to the vent on the steep flanks of the volcano contain ignimbrites which are unique and do not fall under the standard flow model presented above. Generally, such deposits are characterized by well defined parallel-bedding with occasional dunes and chute and pool structures. Scour is often noted between beds (Rowley *et al.*, 1985).

   Such deposits have been termed ignimbrite veneer deposits by Wilson and Walker (1982) and proximal bedded pyroclastic flow deposits by Rowley *et al.* (1985). Rowley *et al.*, (1985) suggest that the deposits were emplaced by pyroclastic flows which had become inflated and turbulent on the steeper flanks. They further suggest that these deposits are the inflated equivalent to the more massive main facies (standard ignimbrite) and that there is a full gradation between the two. They note that these closely proximal beds grade into massive beds where there is a decrease in topography.

2. Distal Deposits. Sheridan (1979) suggests that proximal facies are gas inflated relative to distal areas where less pronounced flow facies occur (figure 4.6). Generally, grain size tends to fine in distal areas.

Figure 4.7 shows that flows resulting from different eruptions may result in other than idealized sections.

The sequence: ground surge - flow - ash cloud - air fall (standard ignimbrite flow model) is suggested by Sparks *et al.* (1973) and Sheridan (1979) to represent the following sequence:

1. Explosive or blast stage, producing ground surges (according to the interpretations of Fisher, 1979 and Sheridan, 1979).
2. Avalanche or flow stage, producing pyroclastic flows, ground surges (according to interpretation of Wilson and Walker, 1982) and ash cloud surges.

3. Effusive Stage (Sheridan, 1979), erupting gas-poor primary lavas. -

It is suggested that the sequence represents the tapping of progressively deeper levels in the magma chamber, (Sparks *et al.*, 1973).

The deposits formed by ground surges, ash cloud surges and basal, reversely graded zones may be helpful in defining flow boundaries. In situations where numerous flows directly follow one another, forming a sequence of massive flow beds without surge deposits, the basal zone and the grading of lithic and pumice fragments may be helpful in defining individual flow deposits.

The Base Surge

Base surge flows account for a major part of hydroclastic deposits. They develop where a mixture of dense steam and solid components are combined to form a turbulent, fluidized flow associated with hydroclastic eruptions (Fisher and Schmincke, 1984). The condensed steam supports and fluidizes the flow and imparts a cohesive nature to the particles (Fisher and Schmincke, 1984). This cohesiveness may have profound effects on the formation of bed forms, as discussed by Allan (1982).

The flows form at the base of collapsing vertical eruption columns and travel radially outward from its base (Waters and Fisher, 1971 and Crow and Fisher, 1979). They move with a cleft and lobe style flow front similar to pyroclastic flows (Fisher and Schmincke, 1984). Fisher (1977) identifies "U-shaped channels" which are cut into underlying deposits by rapidly advancing turbulent lobes on steeper topography. In many cases, the channels were originally V - shaped channels which previously incised the slope.

The deposits thin rapidly (exponentially) away from the source though local thickening may result from topography changes (Wohletz and Sheridan, 1979). They have also been observed by Crow and Fisher (1979) to pinch and swell over their length.

In general the deposits are poorly-sorted. Bedding is usually thin and very well defined, resulting from short multiple blasts common in hydroclastic eruptions (Fisher and Schmincke, 1984). Soft sediment deformation of the deposit due to its cohesive nature has been described by Fisher and Schmincke (1984). The deposits of base surge flows are characterized by plane parallel-beds, dunes, ripples and chute and pool structures. The bed forms have been described by Fisher and Waters (1970), Schmincke *et al.* (1973), Sheridan and Updike (1975) and Crowe

and Fisher (1979). Allan (1982) comments that these forms may depend on cohesive forces rather than flow regime.

A unique occurence of surge deposits has been documented by Rowley *et al.* (1981). They describe phreatic explosion pits on the upper surface of hot ignimbrites which have overridden a water source at Mount St. Helens. Steam explosions resulted in the formation of pits on the surface of the flow. Local deposits around the pits, from remobilized ignimbrite, have bedforms characteristic of base surge or hydroclastic origin.

Air-Fall Deposits

Air-falls are the most widely known pyroclastic deposit. These deposits may be distinguished by their overall geometry and their internal characteristics. Circular or fan shaped lobes are the most common morphology of airfall deposits. They are strongly influenced by wind acting upon a convecting column and are subsequently deposited down-wind from the vent (Sparks *et al.*, 1976; Sparks, 1982 and Fisher and Schmincke, 1984). The relative thickness of a single deposit may increase with proximity to the vent, though Sarna-Wojcicki *et al.* (1981) show the presence of a secondary thickening which developed down-wind from the vent during eruptions of Mt. St. Helens on May 18, 1980.

Unlike those emplaced by flow, air-fall deposits tend to be moderately to well-sorted (Williams and McBirney, 1978; Sparks, 1982 and Fisher and Schmincke, 1984). The beds are plane parallel and notably mantle topography (see Fisher and Schmincke, 1984 for excellent examples). Sharp to gradational bedding contacts reflect the eruption energy, volume, rate of deposition, wind direction and time between eruptions (Fisher and Schmincke, 1984). Color (composition) diagenetic features, sorting or grain size may also define beds. Other than various styles of grading, reflecting eruption intensities, the beds are relatively featureless (Fisher and Schmincke, 1984). Sparks (1982) explains that a "pulse like" eruption or series of eruptions develop the well stratified deposits. Continuous explosive activity decreases the stratification.

Transportation is by ballistic trajectory (coarse fragments) and by turbulent suspension in convecting columns (Sparks and Wilson, 1976; Sparks *et al.*, 1978; Sparks, 1983 and Fisher and Schmincke, 1984; see also discussion on convective column collapse). Intensely convective plumes, resulting from exceptionally gas-charged eruptions, produce few flows while

transporting fines well up into the atmosphere. Air-fall deposits may also occur during a pyroclastic flow when fine particles are elutriated from the top of the flow (Fisher and Schmincke, 1984) and during other types of eruption which may suspend particles in the atmosphere, for however brief a time.

Welding has been identified in air-fall deposits by Sparks and Wright (1979). It is controlled by numerous factors, the most important of which are the rate of discharge and accumulation. High rates tend to discourage heat loss, therefore allowing welding to occur in the thicker areas of the deposit.

Lahars

Lahars are essentially sediment gravity flows with larger clasts being supported or suspended in a matrix of water and finer particles. In the words of Fisher and Schmincke, 1984, ". . . they behave like plastic materials similar to wet concrete."

The flows may originate concurrently with eruptions or by later erosion of a volcanic pile (Crandell, 1971 and Williams and McBirney, 1979). Exceptionally wet eruptions of loose material associated with lakes, ice, snow, or areas of intense rainfall are the more prolific producers of lahars (Fisher and Schmincke, 1984 and Williams and McBirney, 1979). Some have been noted to originate as pyroclastic flows which have later been transformed by incorporation of water (Crandell, 1971 and Janda *et al.*, 1981) (Figure 4.2).

The flows are tongue-shaped, being initially confined to pre-existing channels or valleys and later fanning out into broad lobes in areas of lesser relief. They may fill valleys to depths of hundreds of feet (Crandell, 1971). Janda *et al.* (1981) mention that streams beds on Mt. St. Helens were all at one time subject to laharic flows.

The mobility depends upon the water content and steepness of slope (William and McBirney, 1979). Flows with higher water content, and therefore Smith (1986) describes three types of debree flow based on particle concentration during flow and deposit characteristics. lower particle concentration, would have greater mobility.

The upper surfaces of single deposits are described as hummocky (Fisher and Schmincke, 1984 and Janda *et al.*, 1981), while the lower surfaces are concordant and show no erosion (Fisher and Schmincke, 1984). The beds tend to be thick, poorly-sorted and lack internal stratification. Reverse and normal grading may occassionally occur (Fisher and

Schmincke, 1984). Progressive stacking of flows may result in very thick massive deposits with individual bedding contacts being ill-defined. Ricketts (1982) describes the presence of thin, red shale veneers on the top of laharic beds of the Crowsnest Formation. Similar features may be of use in defining other deposits.

The deposits of lahars may strongly resemble those of massive, poorly-sorted pyroclastic flows. Hoblith *et al.* (1979) distinguish the two by the remnant magmatism which forms in hotter deposits.

E. Summarized Classification

Table 4.1 gives a summarized account of the physical features and origins of pyroclastic rocks based on the preceeding discussion and descriptions by the authors mentioned. It is intended as a quick reference check and not as a detailed classification. The reader is referred to the work of Fisher and Schmincke (1984) for further descriptions.

TABLE 4.1 SUMMARY CLASSIFICATION OF PYROCLASTIC DEPOSITS AND THEIR ORIGINS

Textures and Features	Pyroclastic Flows	Pyroclastic Surges	Hydroclastic Base Surge	Air Falls	Lahars
Deposits	lobes sheets	lobes sheets	lobes sheets	fans	tongues lobes
Components	J,C	J,C	J,C,A	J,C	C,A
Sorting	poor	moderate	moderate	good	poor
Bedding	thin to thick	thin	thin	thin	thick
Stratification					
Parallel beds	tr	X	X	X	-
laminations	tr	X	X	X	-
dune forms	-	X	X	-	-
chute & pool	-	X	X	-	-
massive - beds	X	-	-	-	X
Deflation Structures	x	X	X	X	-
Mantle Bedding	-	x	x	X	-
Grading					
normal	X	X	X	X	x
reverse	X	X	X	X	-
multiple	X	X	X	X	-
Temperature	hot	hot	cool	Var.	cool
Welding	Var.	Occ.	-	Occ.	-
Gas Escape Structures	X	x	-	-	-
Origin	CCl, LB, DCl, BO	CCl, El, LB	CCl, LB	CC	

J = juvenile, C = cognate, A = accidental, X = major, x = minor

CCl = column collapse, LB = lateral blast, DCl = dome collapse

BO = boiling over, El = elutriation, CC = convective column

V. DEPOSITS

Pyroclastic deposits comprise an estimated 90% of all exposures of the Crowsnest Formation. The remaining 10% are primary lavas and volcanogenic sediments. In areas removed from the type section, sediments derived from the Crowsnest pile become dominant and interfinger with the sediments of the Blairmore Formation (Mellon, 1967).

Surprisingly, little attention has been focussed on the pyroclastic deposits and their depositional history. The only study conducted on such rocks was by Ricketts (1981) who identified lahar deposits south of the type section. This study also suggests that cross-stratified deposits were short-lived stream deposits, an interpretation which is not favored by this study.

The new exposures at the type section allow for the investigation of the deposits of the Crowsnest Formation as a whole unit. This in turn provides evidence for the eventual interpretation of the depositional history of the formation.

A. Pyroclastic Flow Deposits: Ignimbrites

Agglomerates

Coarse, poorly-sorted beds, composed primarily of large rounded clasts, are identified as agglomerates in the lower member and the base of the upper member (Foldout A & B). No true pyroclastic breccias were found in the lower member. Agglomerates characteristically consist of rounded clasts in a matrix of crystals, crystal fragments and small rock fragments, generally less than 0.5 cm (Plate 5.1a, b). Cognate fragments may comprise up to 75% of the rock and often exhibit a strongly trachytic alignment of feldspar phenocrysts, attesting to a primary flow origin (Plate 5.1a,b). They range in size from 1 cm to as much as 50 cm and may show normal grading. The presence of baked rims around many clasts suggest emplacement at elevated temperatures.

The matrix is composed of euhedral crystals of sanidine, garnet and aegirine-augite with minor occurrences of other minerals characteristic of the Crowsnest Formation. The majority of crystals have been broken and/or intensely fractured and show slight rounding. Microscopically, sanidine crystals may be bent and in some instances show sutured boundaries. The beds are considered to be welded.

The lower boundaries of these deposits are generally abrupt and may be roughly planar or show substantial relief as shown in the type section about 17 m from its base (Foldout A). In this case, the lower contact is erosional and exhibits approximately 2 meters of relief (Foldout A).

Upper contacts may or may not be gradational into overlying surge deposits which are discussed below (Plates 5.1a, 5.2b, 5.3d). In many instances these agglomerates are present as a coarse basal deposit of the following cyclic sequence (Plate 5.1a, 5.3d):

agglomerate - surge - agglomerate

The agglomerates are much coarser than the surge deposits.

The appearence of these deposits is sometimes remakably similar to a conglomerate. The following features attest to their pyroclastic origin:

1. Welded textures.
2. Occasional draping of large fragments by surge deposits (Plate 5.1a).
3. Grading structures.
4. Sheet-like deposits which often show parellel contacts with air-fall and other flow deposits.

The occurrence of these deposits with those identified as surge deposits suggest an intimate relationship between the two. It is thought that the deposits result from explosions which disrupt and fragment plugs and/or primary flows deposits producing coarse pyroclastic flows. It is thought that these agglomerates are essentially a coarse lag, composed of large clasts which dropped out of a turbulent, inflated block and ash flow. The remaining finer material was deposited as cross-stratified surges which overly and extend beyond this coarser fraction. The agglomerates themselves probably moved as a dense, non-turbulent flow. Rounding probably occurred during emplacement; however, plastic deformation textures suggest some clasts may initially have been malleable.

Except for the rounded nature of the clasts, they resemble the deposits of a block and ash flow as described by Fisher *et al.*, (1980) (Figure 4.7). Gas transport is indicated by association with surge deposits which occasionally contain gas deflation features.

Pyroclastic Breccias

The major portion of the upper member is characterized by thick beds of pyroclastic breccia which can be distinguished from the previously discussed agglomerates by their dark

Plate 5.1

A. Photograph of cyclic agglomerate (**Ag**) - surge (**Sg**) deposits. Larger clasts are rounded. Surge deposits show cross-stratifcation and deflation drape structures (**Ds**). Pipeline section.

B. Photograph of a cut and polished slab of an agglomerate from the lower member. Cognate clasts are rounded and show well defined trachytic textures (**T**). The matrix is composed of sanidine and garnet crystals, wch-13.

C. Photograph of a cut and polished slab of pyroclastic breccia from the upper member. Clasts show baked margins and flow imbrication.

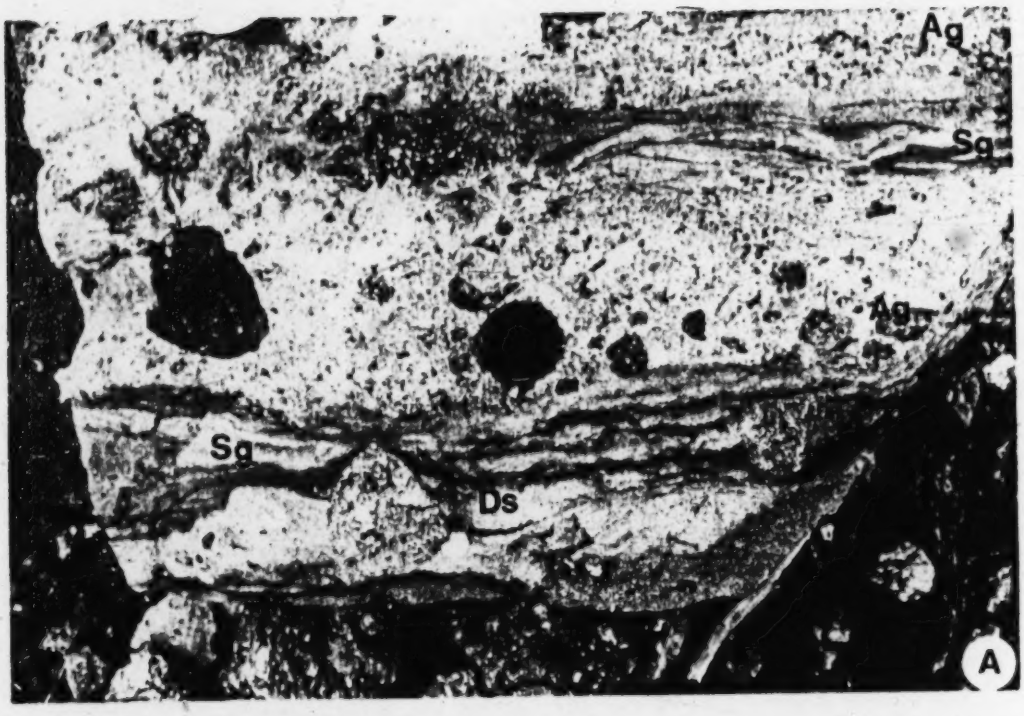
Ag
Sg
Ag
Sg
Ds
A

B
T

C
Bm

green - grey color, their massive nature and the increased angularity of the clasts (Plates 5.1c, 5.2a, 6.1b). They are not generally associated with surge deposits.

Individually, the beds are composed of cognate and juvenile clasts with subordinate accidental fragments. Trachytic textures in many fragments indicate their origin as plugs or flows. The blairmorite fragments, common to these upper beds, may be both cognate and juvenile, as the latter are often intensely deformed by stretching and flattening (Plate 2.2e, 2.7c). Other juvenile clasts are represented by fine-grained aphanitic fragments, many of which are intensely deformed relative to their cognate counter parts. Fragments composed of older pyroclastic debris, surges, flows and agglomerates, suggest that earlier erupted material has been incorporated in these flows.

The sizes of the fragments range dramatically between less than half a centimeter to as much as three meters. They constitute between 25 and 85% of the rock, though, in most cases, the matrix is the more dominant and supporting phase (Plate 5.1c). Pronounced normal size grading of fragments is common in a number of beds. Baked and/or resorbed margins occur with plastic deformation structures and may occasionally be associated with imbrication and/or flow stretching.

The matrix is dominated by a phase showing substantial alteration and/or recrystallization which obliterates many original textures. It is characteristically fine to medium-crystalline, containing abundant Fe-Ti Oxides (titanomagnetite, ilmenite, pyrite) and recrystallization assemblages (calcite, chlorite, adularia) (see Chapter II). The matrix may comprise up to about 75% of the rock.

It is the contention of this study that this phase represents a substantial liquid magmatic component (lava) as it exhibits a texture and composition simmilar to a dyke which is seen to intrude the upper member. This liquid fraction would provide mobillity to the flow. No structures were found in these dense beds indicating gas transport. On the whole, bedding contacts are relatively obscure, but may be defined by slight color changes and abrupt changes in clast size (Plate 6.1b). The latter reflects normal grading throughout the whole bed.

The presence of plastic deformation, baked or resorbed margins, charred wood and the extremely massive, sometimes jointed character of these beds provides evidence that they were emplaced as high temperature flows with the presence of a liquid as a supporting and mobilizating phase. Poorly defined jointing may also be developed, a good example of which

occurs towards the top of the type section. These beds probably represent a mix between a pyroclastic and a true lava flow.

The resemblance of these beds to those of block and ash flows described by Perret (1939), Williams and McBirney (1978) and Fisher and Schmincke (1984), suggest that they originated by the disruption and/or fragmentation of a dome or summit spine. In the case of the Crowsnest, disintegration was induced and probably enhanced by an explosion followed by the influx of magma and accompanying juvenile components which incorporated the more solid cognate material. The resulting flows appear to have been very dense with a primary liquid supporting and carrying large clasts derived from the dome and surrounding debris pile. It appears that the flows were fairly mobile as their deposits are found farthest from the vent. These types of beds generally comprise the upper 4/5 of the upper member. Williams and McBirney (1979) suggest that such eruptions and their deposits represent mature stages of volcanic activity.

Ash Flow Deposits

Both lapilli tuffs and tuffs represent pyroclastic flow emplaced deposits in the lower member where they may be found in discrete beds or graded sequences. They are not found in the upper member though some agglomerates and pyroclastic breccias may fine to this size range. Throughout the lower member, there is a full gradation between flow emplaced tuffs and agglomerates, sometimes within the same bed. The following descriptions are concerned strictly with ash flows. Surge deposits are discussed separately due to their unique origin and bed forms.

Generally, the flow deposits of the lower member are dominated by crystal-rich varieties containing abundant whole and broken phenocrysts of sanidine, garnet, aegirine-augite and other crystal components. Lithic varieties, dominantly composed of cognate fragments are, however, well represented. The deposits are compositionally similar to those deposited by air-falls but can be distinguished by depositional textures (cross-stratification), thickness, sorting, grain size and the presence of associated surge deposits.

The deposits are generally pink, reflecting the abundance of sanidine phenocrysts and sanidine-rich rock fragments, though finer-grained varieties become purple. Sanidine, garnet and other crystal constituents comprise the coarser fraction along with variable amounts of

rock fragments. The crystals may be whole, fractured or broken and may show variable degrees of rounding. Cognate rock fragments are most common though juvenile aphanitic types may also be present. This coarse fraction may reach 70% of the rock.

The matrix is dominated by fine crystal fragments, whole microlites and small rock fragments. Aphanitic fragments are also usually present. The matrix is considered to be a finer, more pulverized equivalent of the coarser component. Sorting is generally poor to moderate with a range in size from <0.1 mm (matrix) to 6 cm, for lithic types. Crystal-rich varieties usually do not exceed 1 cm.

The bedding contacts are generally abrupt and may be parallel or pinch and swell slightly. Basal contacts are not generally erosional and may be distinguished by the following:

1. A marked color change, usually from green or purple ash or tuff beds (air-fall) to the pink color of the crystal-rich tuffs emplaced by flow.
2. Abrupt changes in grain size.
3. A marked change in the competency of the bed reflecting the more massive, sometimes welded nature of flow emplaced deposits (Foldout A) (Plate 6.1a).
4. The presence of a reversely graded basal zone similar to that described for the standard ignimbrite (Figure 4.6).

The contacts may also be gradational where the bed overlies or underlies surge deposits.

The thicknesses of the flow deposited lapilli tuff or tuff beds at the type section range from thick beds, up to 7 meters, to thin beds of less than half a meter (Foldout A, Plate 6.1a). Some of the thinner varieties are seen to pinch out laterally on the scale of the outcrop.

Many beds exhibit features that resemble the standard ignimbrite flow unit described by Sparks *et al.* (1973), Sparks (1976), Sheridan (1979), Fisher (1979) and Fisher and Schmincke (1984) (see Chapter IV, Figure 4.6). The following features of the standard ignimbrite flow unit were identified in the flow deposits of the lower Crowsnest Formation:

1. Ground Surges. Deposits of surge origin, discussed below, were often identified directly below thick, massive flow deposits. They may show pinch and swell bedding and, in some cases, appear to be scoured by the main body of the flow. They may not, however, always be present.
2. Basal Zone. A thin basal zone is often developed below the main body of the flow. It is difficult to distinguish in many cases, as the grain size is only slightly less than that of the

main body. The basal zone often exhibits reverse grading into the main body of flow. This is consistent with the standard ignimbrite flow model (see unit 2a, Figure 4.6).

3. Main Body. The bulk of such deposits is made up of thickly-bedded, pink, coarse crystal/lihtic tuffs and fine crystal lapilli tuffs (Plate 6.1a). They are massive and are generally featureless; however, the following bed forms were observed:
   a. Zones of density-stratified garnets and dense crystal components. These may be discrete layers, lenses or trains.
   b. Massive zones which grade laterally into density-stratified parallel- laminations which in turn grade into zones of low-angle cross-bedding.
   c. Normal grading of lithic fragments and occasionally crystals.
   d. Lenses of green, crystal-rich ash occur at the top of many thick deposits, probably of air-fall or ash cloud origin.

   The absence of very coarse rock fragments may suggest that these massive flows are the deflated, more distal equivalent of a highly inflated surge after it has lost its coarser fraction during turbulent flow. In such cases, they would be similar to the *main facies* deposits of Mount St. Helens as described by Rowley *et al.* (1985). It may also be that the flow originated with a finer fragment constsituent. Low density, pumaceous clasts were not observed in any beds. Welding features are usually present, though the degree of welding is variable.

4. Ash Cloud Surges and Air-falls. Commonly overlying the thick, massive beds which comprise the main body of the flow are surge deposits and/or air-falls, both of which are described below (Plate 6.1a).

The deposits which exhibit the features described above are interpreted to have been emplaced by pyroclastic flows at elevated temperatures. For the most part the main body of the deposits were emplaced by non-turbulent flow which produced the massive beds with only limited bed forms. Internal flow transformations (see Fisher, 1983) probably produced the zones of density-stratification, cross-lamination and crystal trains.

Other types of lapilli tuff beds exhibit features that suggest emplacement by flow under different conditions; however, they differ from the deposts of a standard ignimbrite. Most display complex grading features while others may be totally massive. The presence of low-angle cross-lamination distinguishes these types from air-fall deposits. In many instances

the finer fractions show good evidence for surge deposition. Massive flow tuff and lapilli tuff beds may periodically develop faint cross-stratified zones at their base. In this case, the dense beds may exhibit grading but are otherwise void of structures. The deposits were probably emplaced by a viscous, non-turbulent flow which developed a turbulent zone at its base.

Welding features are usually present in all types of flow deposited lapilli tuffs and tuffs, although the degree is certainly variable. The thicker massive beds generally show the higher degrees of welding.

Surges

Surge deposits may be categorized under the terms coarse crystal tuff, crystal lapilli tuff and lithic lapilli tuff. They are discussed separately because they represent a deposit which is distinct from those previously described. Surge deposits are emplaced by the same mechanisms as their ash flow counterparts; however, they are deposited from turbulent clouds which inevitably form distinct depositional structures. They are found in intimate association with massive agglomerates, tuffs, lapilli tuffs and to a much lesser extent breccias throughout the lower member and the base of the upper member (Plate 5.2a,b). Such deposits often grade both vertically and laterally into surge deposits.

Surge deposits of the Crowsnest are easily distinguished by their abundant bed forms and their darker, red-pink color. The deposits are composed of primary crystals, sanidine and garnet being dominant, and roughly equal amounts of rock fragments, both cognate and juvenile. They are generally clast and/or crystal supported with a noticeable lack of very fine components. Sanidines and garnets tend to be both euhedral crystals and crystal framents. Rock fragments are generally round to sub-rounded, and may show plastic deformation. The size of the fragments is variable but is usually less than 2 cm. Large fragments may occasionally appear within surge deposits. In such cases, they may be draped (deflation) by the finer components.

Individual surge beds are found to underlie, overlie and grade into other flow deposits (Plates 5.1a, 5.2a,b, 5.3b,d). Bedding of a flow unit is generally planar though it often exhibits a pinch and swell morphology and may pinch out over a few meters (Plates 5.1a; 5.2a). Bedding was not observed to exceed a meter, though composite beds may reach thicknesses of 5 meters. Sorting is generally poor, but shows some increase in the density-stratified horizons.

Plate 5.2

A. Photograph of cyclic agglomerate (**Ag**) - surge (**Sg**) deposits at the base of the upper member. The cyclic sequences occur between two thick pyroclastic breccias (**Br**) carrying angular fragments, Pipeline section.

B. Photograph of parallel-bedded surge deposits and underlying agglomerates, upper member, Pipeline section.

A
Br
Ag
Sg
Ag
Ag
Sg
Br
B

Plate 5.3

A. Photograph of a cut and polished slab of fining upward surge deposit. The specimen exhibits dune forms (**Df**) which lack internal stratification. Top of the lower member.

B. Photograph of a cut and polished slab of a dense pyroclastic flow overlain by an ash-cloud surge deposit. The surge deposit shows progressive fining to the top. Structures observed in the surge deposit are parallel-beds (**Pb**), cross- stratification (**Cs**) and remobilization structures (**Rs**), lower member.

C. Photograph of a cut and polished slab of a parallel-bedded/laminated surge deposit. Lower member.

D. Photograph of a cut and polished slab of a cyclic agglomerate (**Ag**)- surge (**Sg**) deposit, lower member, wch-14.

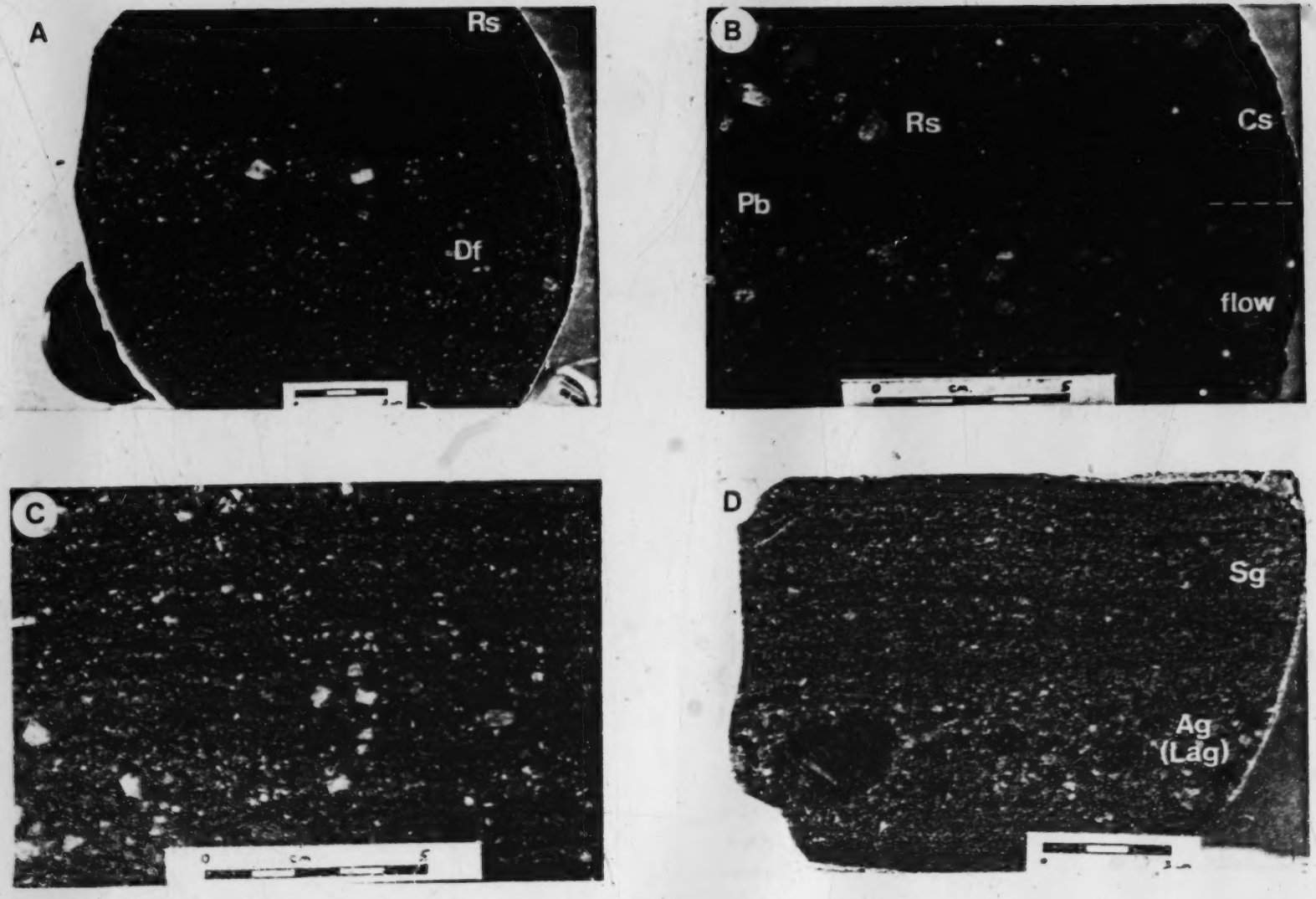
A
Rs
Df
B
Rs
Cs
Pb
flow
C
D
Sg
Ag
(Lag)

Over a given surge bed, a progressive fining of the components may occur towards the top of the bed (Plate 5.3a,d). The fining is thought to represent decreasing flow energy.

Plane parallel-laminations, low amplitude ripples, dune forms and zones of low-angle cross-bedding/lamination are characteristic of the deposits and are discussed in detail below. These bedforms are defined and enhanced by a marked density- stratification of garnets, sphene, aegirine-augite, titanomagnetite and ilmenite. Invariably, the forms show scour at their bases. Size grading and component composition may also define forms.

The prominent bed forms which occur in surge deposits may be categorized into groups based on morphology.

Parallel-Beds/Laminations. Beds and/or laminations which show roughly parallel boundaries are the most common bed form found in surge deposits (Plates 5.2b, 5.3c,d, 5.4a, 5.5c,d. Figures 5.1, 5.2a) They range in thickness from <1 mm to as much as 5 cm. Each bed exhibits scour at its base. Many deposits are lensoid as a result of truncation followed by depostion during a subsequent flow or pulse. Most have a strong tendency to pinch and swell over their length, and may pinch or lens out entirely. The deposits resemble a series of interfingering lenss with light, coarse interiors bounded by dark, fine, density-stratified horizons. They are often seen to grade laterally from slightly thicker, more massive deposits.

These deposits strongly resemble modern proximal bedded pyroclastic flow deposits[10] from Mount St. Helens. Plate 5.4 compares the surge deposits of the Crowsnest Formation with those of Mount St. Helens.

The upper and lower boundaries are usually smoothly undulating surfaces which may drape over coarse, underlying components (Plate 5.1a). Occasionally, poorly defined low amplitude ripples may develop in some finer-grained boundaries. A given bed or lamination is distinguished by the following cross-section (Figures 5.1, 5.2a):

a. A black, fine-grained density-stratified zone which underlies the coarser main body of the bed and shows an abrupt or sometimes gradational contact with lower deposits. It generally does not exceed 2 mm in thickness. This zone may lens in and out over the length of the bed. A marked reverse grading into the coarser, lighter main body of the

---

[10]Proximal pyroclastic flow deposits are described by Rowley *et al.* (1985) as follows: "*Individual beds range from 2 mm to more than 1 m thick and are mainly 1 to 20 cm thick. Beds typically show pronounced lateral variations in thickness, generally within a distance of a few meters.*" they occur within 3 km of the vent.

Plate 5.4

A. Photograph of cut and polished slab of a surge deposit from the Willoughby Ridge section. The photograph shows parallel- beds similar to those found in surge deposits at Mount St. Helens.

B. Photograph of a proximal bedded pyroclastic flow deposit (surge) from Mount. St. Helens. Photograph shows well defined 1 - 5cm thick parallel-bedding. Reproduced with permission (Rowley *et al.*, 1985).

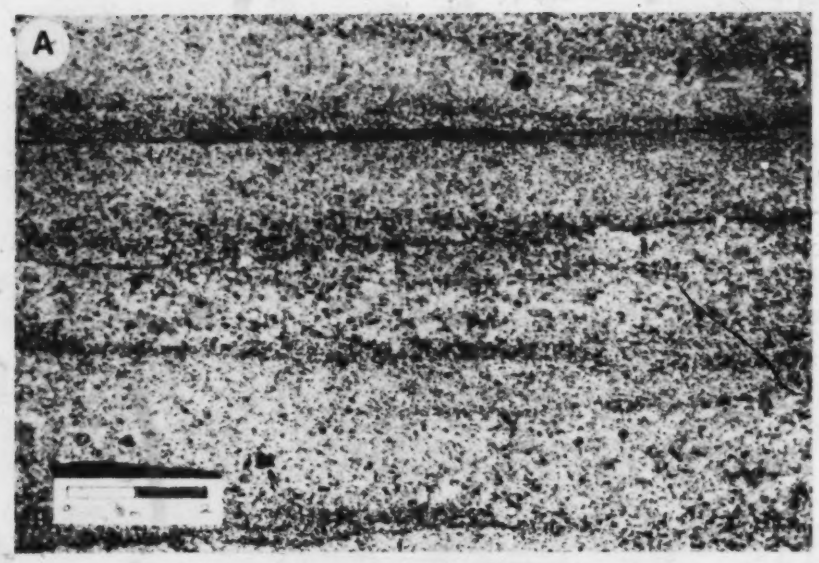
A

B

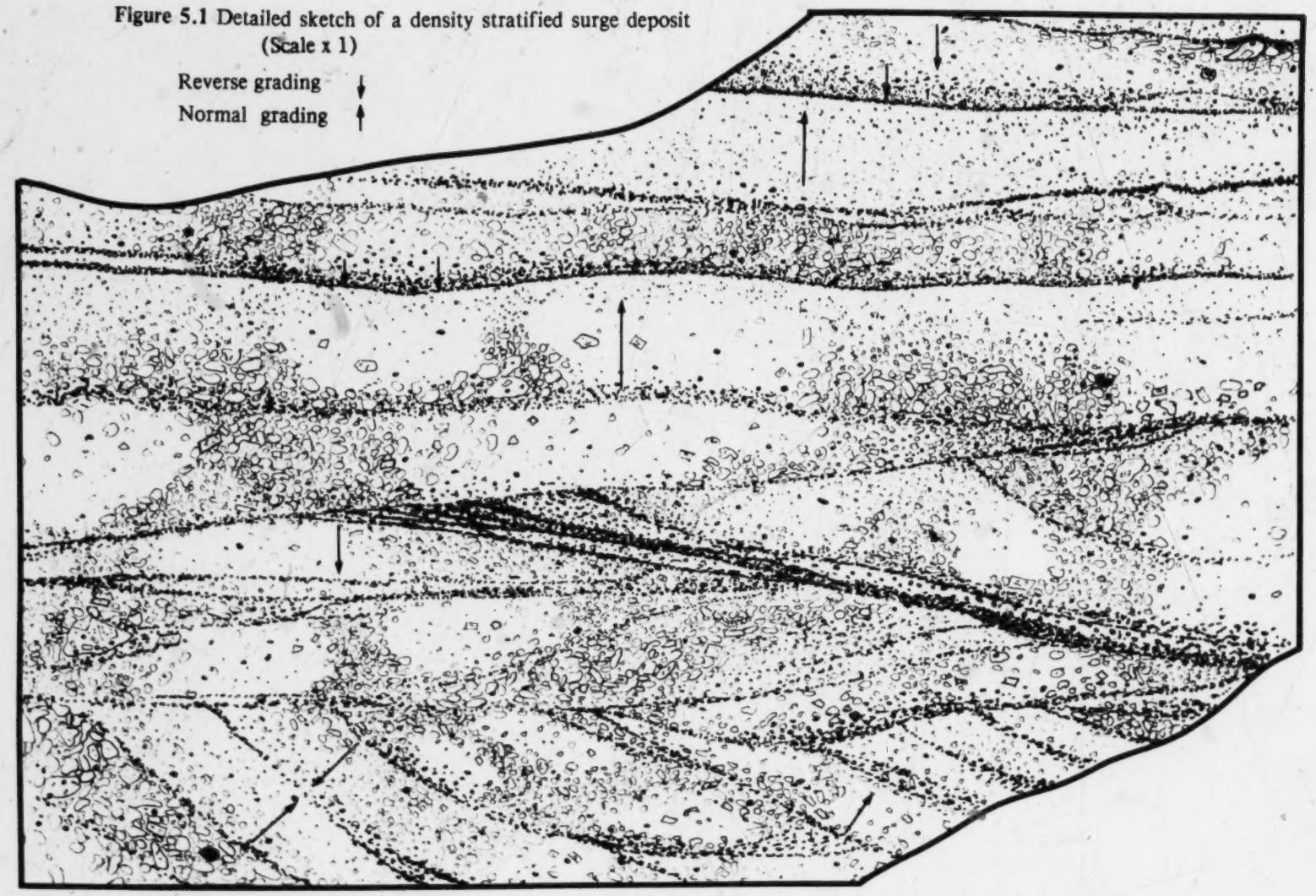

Figure 5.1 Detailed sketch of a density stratified surge deposit (Scale x 1)

bed/lamination occurs over a few millimeters. Larger garnets (2 mm) are generally concentrated just above this basal zone (Figures 5.2, 5.2. Plates 5.4a, 5.5c,d).

b. The main body of the bed is composed of much coarser crystals and rock fragments. Sanidine crystals are generally large, up to 1 cm, and exhibit euhedral crystal shapes. Many are broken and show slight rounding. Rock fragments are round and may exhibit plastic deformation in both hand specimen and thin section. Sorting is poor.

Three types of grading were identified in the main body (Figire 5.1):

1) Normal grading of garnet crystals from just above the density stratified basal zone to the top of the bed.
2) Normal grading of fragments and sanidine crystals.
3) Reverse grading of sanidine crystals.

Large crystals and fragments at the top of a bed may be draped by a subsequent zone of density-stratification (Plate 5.5c,d).

On occasion, the coarse main body may exhibit low-angle cross-laminations, 2-10°, and/or thin, parallel- laminations, again defined by density-stratified heavy minerals. These zones often represent pinchouts of individual beds/laminations within a larger lens.

Dune Forms. Dune forms may be observed in most surge deposits but to a much lesser extent than parallel and/or lensoid beds with which they are associated. Again, the shapes and features are defined by thin zones of marked density- stratified heavy minerals. They may also be defined by changes in grain size.

Such forms may range in size from 5-70 cm. Much larger forms, up to 3 m, have been observed (wch-40). Generally they have rounded peaks and gently sloping sides at angles between 10-20° with extremes of 5-30°. They may or may not be symmetrical.

Two types of dune forms may be distinguished by their internal characteristics (Figure 5.2b,c).

a. Dune forms exhibiting internal low-angle cross-stratification, usually in one direction, are often associated with other bed forms (Figure 5.2c). The cross-stratification comprises a whole dune, and is often truncated by subsequent deposits. Structures are well defined by marked density-stratification of the denser minerals. The grain size is generally finer and sorting is improved. Coarser, poorly-sorted partings and/or lenss

separate density-stratified equivalents.

Such deposits are interpreted as being the result of migration of dunes during flow and subsequent deposition.

b. Dunes which exhibit no internal stratification, apart from a complex system of grading, are also observed with parellel beds and migrating dunes (Figure 5.2b. Plate 5.3a). A single, thin zone of density-stratification marks each side and the base of the dune form. The base is usually uneven and may form a trough which cuts into and truncates underlying structures. The density-stratified basal zone often drapes larger clasts or crystals in the top of lower beds. The density-stratified zones that define the sides of the form also drape coarse particles within the form.

Internally, these dune forms exhibit a complex system of grading as follows (Figure 5.2b):

1) Reverse size grading of garnets from the base up into the center of the form.
2) Reverse grading of lithic clasts from base to the top of the form.
3) Feldspar concentration in the lower part of the form.

These dune forms are thought to represent scour and erosion of previous, coarser flow deposits and therefore are not true dunes. Reworking probably enhanced the concentration of heavy minerals on top of eroded deposits, producing the basal and flanking zones.

Zones of Cross-Stratification. Zones of low-angle and trough cross-stratification are associated with plane parallel-beds, dune and ripple forms (Figure 5.1. Plate 5.5a,b) The angle of inclination is variable, but usually less than 30°. Density-stratification and associated coarser horizons again define the features. Four general types are distinguished.

a. Density cross-stratification associated with dunes and/or scour features. Such types have occurred as a result of dune and/or ripple migration.

b. Density cross-stratification in lateral association with plane parallel and lensoid beds, generally in the absence of scour.

c. Density cross-stratification associated with erosional channels or trough scours in the absence of dunes or dune forms (Plate 5.5a,b). Such features were probably formed as earlier deposits were scoured or remobilized. Truncation of previous bed forms is common in the presence of scours and subsequent cross-stratification.

Plate 5.5

A. Photograph of a cut and polished slab of a welded surge deposit from the Willoughby Ridge section. The sample shows parallel-bedding (**Pb**), scour cross-stratification(**Cs**) and possibly dune forms. Density-stratification enhances all features. Garnets show a marked reverse size grading within most features. A detailed sketch of this slab is presented in Figure 5.1. Lower member.

B. Photograph of "A" showing a close-up of trough cross-stratification (**Cs**) which has been truncated by a parallel-bed. Again, garnets show a marked reverse grading in some cases superimposed on a normally graded bed.

C. Photograph of "A" showing a close-up of a parallelbed showing slight reverse grading of sanidine phenocryst fragments and rock fragments. Garnets also show reverse grading. A large clast (**Dc**)in the top of the bed is draped by the overlying bed.

D. Photograph of "A" showing a close-up of a 1cm drop clast (**Dc**) which is draped by a zone of density- stratification.

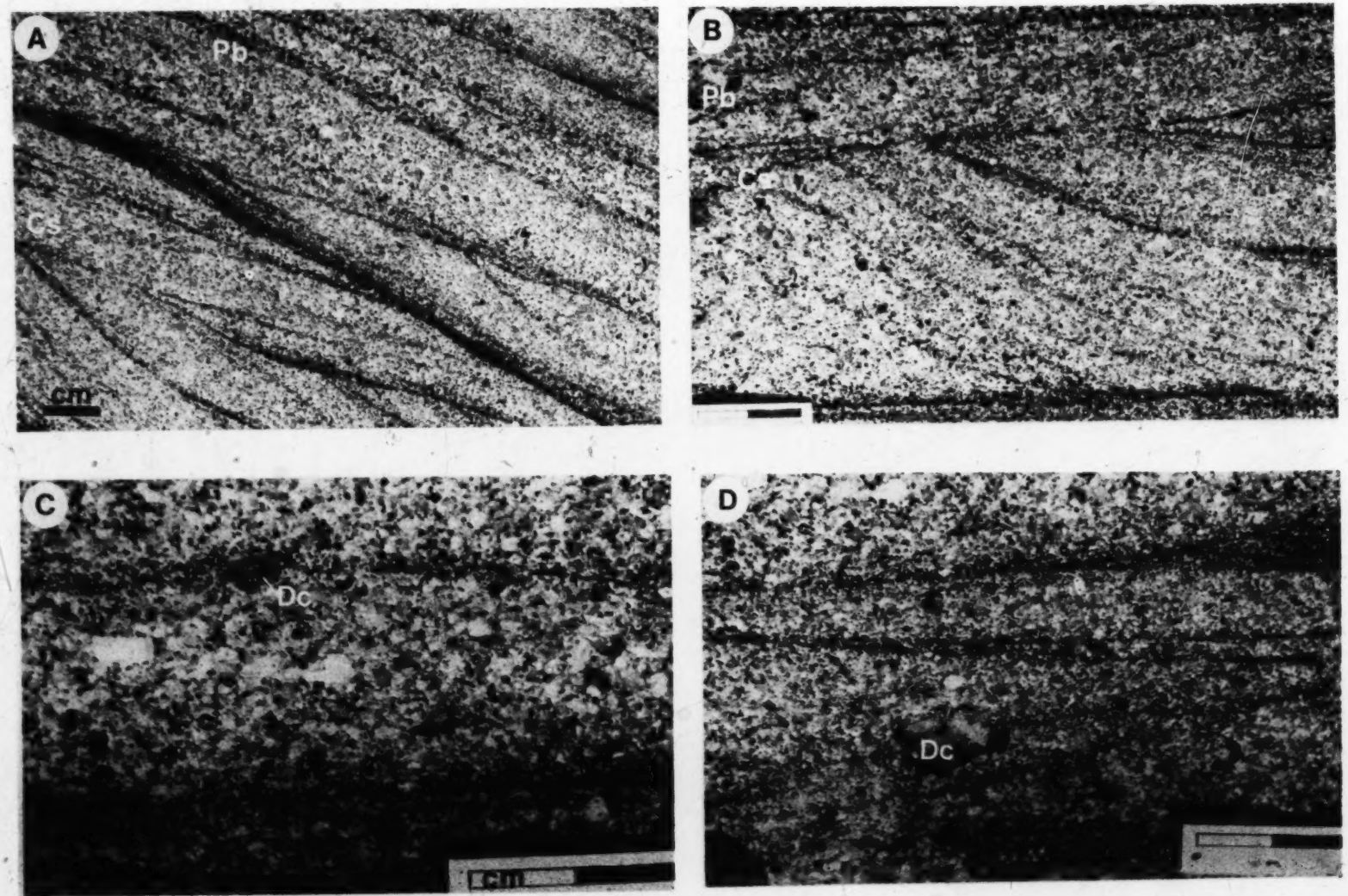
A
Pb
cm
B
Pb
C
Dc
cm
D
Dc

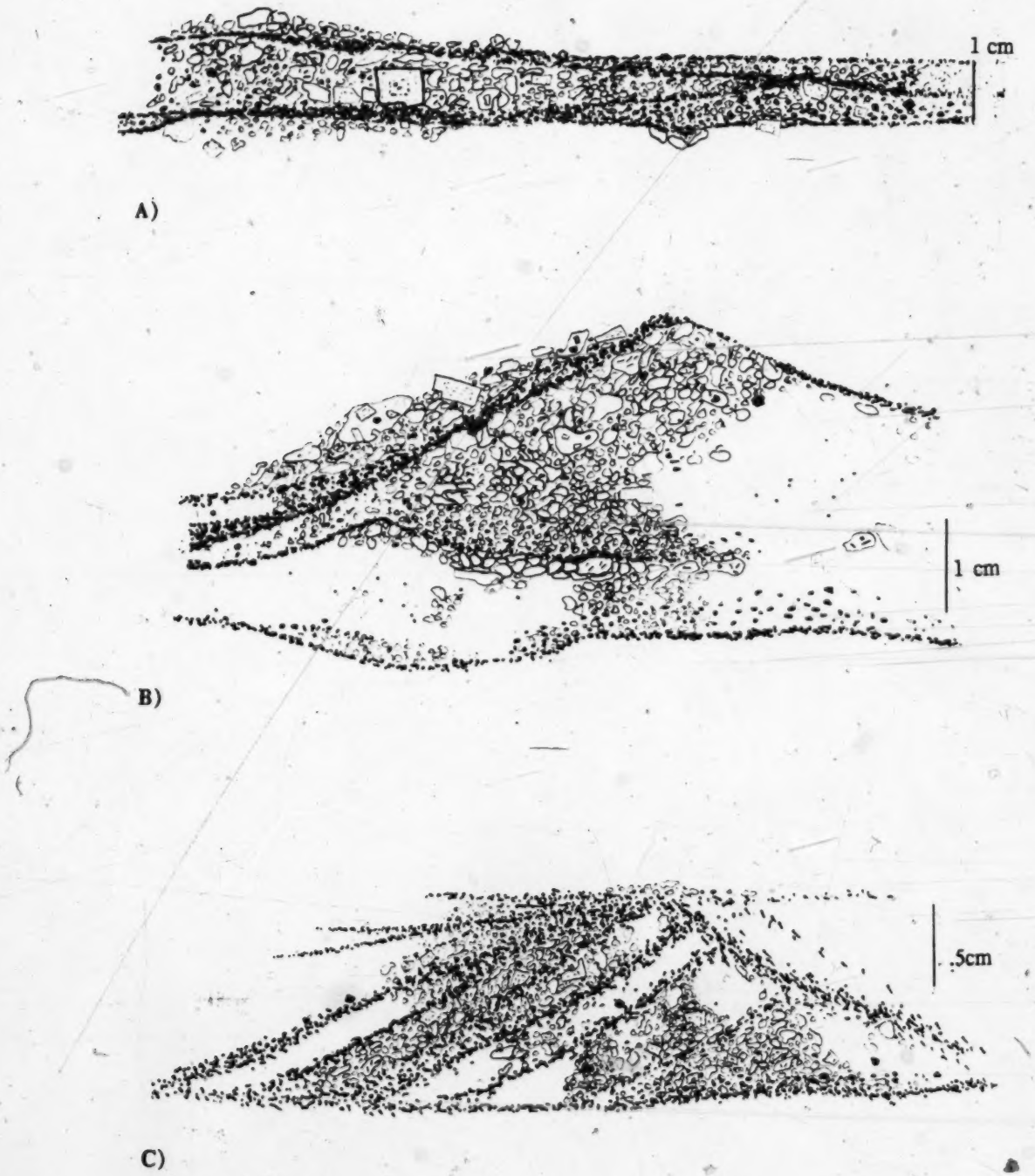

Figure 5.2 Detailed sketch of paralell, lensoid beds (A), erosional dune shapes (B) and true dunes (C).

d. Low angle cross-stratification at the base of massive flow deposits. In such cases, the stratifiction was probably formed by a turbulent cushion at the base of the flow.

Ripples. Good ripple forms are generally rare; however, they are observed in fine-grained tops of surge deposits and occasionally in fine-grained density stratified zones. At best, they are poorly defined. Lengths are small, generally less than 3 cm, with heights not exceeding 1 cm. Small scale, internal cross-lamination, indicating migration, maybe observed.

Remobilization Structures. Apart from trough-like scours, small, relatively featureless channels are often seen to truncate other structures (Plate 5.3a,b). They invariably occur in the finer-grained components at the top of the flow. Remobilization of fines during deflation would seem a probable explanation for these structures.

Beds and bed forms from modern deposits similar to those described above are interpreted as being emplaced by high energy, turbulent flows by Fisher (1979, 1983,), Sheridan (1979), Sparks *et al.* (1973), Sparks (1982) and Rowley *et al.* (1985). Ricketts (1982) previously identified these cross-stratified deposits as deposits of short lived streams which drained the upper slopes of the vent. The presence of plastic deformation and suture boundaries indicate emplacement at high temperatures expected during higher temperature pyroclastic flows, a feature which could not form by sedimentary processes.

The bed forms, (dunes, plane parallel-beds/laminations and cross-laminated zones) represent high flow regime according to Blatt *et al.*, (1980) and Rowley *et al.*, (1985); however, flow regimes in pyroclastic rocks are not well understood. The observation that one bedform is not formed consistently throughout the deposit is thought to represent the abruptly changing conditions of flow, energy and turbulence which may be present in a surge flow. Thus the conditions of stability of one form may be only temporarily achieved. Conditions probably favored parallel and lensoid forms as they are dominant in surges deposits of the Crowsnest Formation. This is consistent with modern examples at Mount St. Helens (Rowley *et al.*, 1985) and other surge deposits described throughout the world.

The origins of the density-stratification characteristic of surges is uncertain. The morphology of density-stratified zones suggests some possible origins.

1. Fallout from turbulent, inflated suspension may produce draping structures and graded zones. Reverse size grading could be facilitated by denser particle concentrations in the

flow, allowing only the finer, dense components to sink.

2. Heavy minerals may be left behind as a lag deposit during scour. Further traction may produce structures in the lee of large particles, and a better-sorted deposit.

It is probable that both processes may have acted at once.

Overall, three types of surge deposits were identified in the lower member of the Crowsnest Formation:

Ground Surges. Surge deposits which form discrete beds immediately beneath less turbulent, massive flow deposits are identified as ground surges (Plates 5.2a). Such deposits may not always be present.

Ash Cloud Surges. Surge deposits which are in vertical or lateral contact with agglomerates and non-turbulent pyroclastic flows are identified as ash cloud surges (Plates 5.3b, 6.1a). The contact may be sharp or gradational.

Discrete Surge Deposits. Surge deposits which are not directly associated with massive flows are interpreted to be the result of deposition by surges which have over-shot and become detached from the massive flows with which they were associated.

B. Air-Fall Deposits

Deposits interpreted as air-falls are abundant in the lower member, but do not occur with the massive beds of the upper member. They are distinguished from flow deposits by the following characteristics:

1. Lack of internal stratification, i.e. bedforms, etc.
2. Draping structures.
3. Generally better sorting; ranging from poor to good between, and within beds.
4. Fine matrix containing angular crystal fragments. The slight rounding observed in flows is not evident.
5. Grading sequences, described below.
6. Stratigraphic association with flow deposits. They may occur immediately after flow and/or surge deposits.
7. Occurrence of bombs in many fine-grained tuff horizons.
8. Sharp contacts with flow deposits and gradational contacts with other air-falls.

Generally, the matrix of most tuffs is composed of very fine crystals and crystal fragments and small rock fragments. Much of this fraction is too small to be identified by optical methods. It is thought to be dominated by feldspar fragments. Crescent shapes were occasionally observed but they were too small to be firmly identified as remnants of devitrified glass shards.

The coarser fractions, generally less than 2 mm, are composed chiefly of crystals or angular crystal fragments, dominantly sanidine and melanite, and varying amounts of cognate and juvenile rock fragments. Many fragments are plastically deformed, sometimes intensely. This usually occurs in the absence of other welding structures, reflected by the recessive nature and intense alteration of air-falls.

Bedding of air-fall deposits is generally thin and usually does not exceed half a meter. Average thicknesses are less than 20 cm, with extremely thin varieties measuring less than 5 cm. They are parallel-bedded, however some slight pinch and swell may occur. This may be mantle bedding; however, the size of the exposure is too small to make a valid interpretation. Small scale mantle bedding is identified and discussed below.

Grading represents changing intensities in the eruption column according to work by Williams and McBirney (1978). Further, sharp contacts represent separate eruptions.

Five types of air-fall deposits are identified at the Crowsnest type section. The first three described below are often found in association with each other, defining what is termed a trilogy.

Pink beds: Crystal Lapilli Tuffs

Pink, crystal lapilli tuffs represent the coarsest, most poorly-sorted air-fall deposits, excluding varieties which contain bombs (Plate 5.6a). They are chiefly composed of crystals, crystal fragments and both juvenile and cognate rock fragments. The grain size does not exceed 0.75 cm. The sanidine crystals and rock fragments often show pronounced normal grading and may accompany a weak density-stratification of garnets.

Bedding thicknesses range between 5 cm and 50 cm. Contacts with other air-fall deposits are generally gradational, but may also be sharp. Purple tuffs and green ashes are seen to grade freely into pink beds. Small scale mantle bedding was observed.

Welding features were observed in most pink beds, though some were distinctly unwelded. The degree of welding is noted to be variable within, and between beds. The greater the intensity the more resistant the bed is observed to become.

Pink, crystal lapilli tuffs are interpreted to be a proximal air-fall deposit produced by high intensity eruptions. The lack of flow features sets them apart from massive flow deposits with a similar grain size. They essentially represent a deposit which may have been formed under conditions where sorting was not yet well developed. Continually changing intensities and conditions are reflected by internal grading and grading between other air-fall deposits. Sharp boundaries suggest separate eruptions.

The welding features observed suggest high rates of deposition which preserved heat and the initial plastic nature of many components.

Green beds: Coarse Crystal Ashes

Green, coarse crystal ashes are intermediate in size between purple tuffs and pink crystal lapilli tuffs. They are chiefly composed of feldspar and garnet crystals and angular crystal fragments, with lesser amounts of rock fragments. Sizes range from <1 mm to 3 mm. The matrix is often very intensely altered to the clay minerals illite and illite/smectite, giving the deposit its light green appearance. For the most part, the original matrix does not survive. Glassy fragments and aphanitic shards were probably the original constituent as some remnents were observed in thin section. The deposits of green, crystal ash are very loose and recessive (Plate 6.1a). Sorting is moderate, in the absence of the original matrix phases.

The thicknesses of these beds may range from <2 cm to as much as 40 cm, (wch-32). They may pinch and swell slightly, perhaps representing mantle bedding.

Internally they are void of depositional structures excluding different types of grading as follows:

1. Normal or reverse grading of feldspar crystals and crystal fragments.
2. Faint, poorly defined density-stratification of garnets.
3. Normal to reverse symmetrical grading with a very fine, clay- rich ash (brown bentonite) representing the finest component.

Bedding contacts may be either sharp or gradational with all of the other types of air-fall deposits. Sharp contacts are also observed. The deposits are interpreted to be crystal-rich ash

falls, again with grading suggesting changing intensities. Moderate sorting and thick deposits suggest proximity to the vent.

Purple beds: Crystal tuffs

Purple crystal tuffs are dominated by fine (<1 mm) components, many of which are too small to identify optically. These finer components may exhibit crescent shapes as mentioned above, though their origin as pumice shards could not fully be demonstrated. The identifiable components were dominated by angular feldspar and garnet fragments and/or whole crystals. Rock fragments, especially juvenile types, and other crystal components were, however, common. For the most part, this finer fraction is moderately-sorted.

Many beds carry a distinctly bimodal assemblage with the presence of a coarse, <1.5 cm, phenocryst assemblage, usually consisting of whole and broken euhedral sanidine crystals and occasionally garnets, which are supported by the fine fraction. Phenocrysts do not usually comprise more than 10% of the rock and may show normal or reverse grading (Plate 5.6b).

A second unusual case is the occurrence of large carbonate bombs (described below and in Chapters II & III) supported by a fine, non-calcareous, purple tuff, generally without the phenocryst phase.

In all cases, bedding is thinner than a meter, with average thicknesses generally around 15 cm. Again, they may grade freely into the pink and green beds or exhibit a sharp contact. They may also pinch and swell slightly, however they are generally parallel-bedded.

Purple crystal tuffs are thought to represent deposits of less intense eruptions which deposited finer material. Coarse crystals or bombs were thrown out in varying amounts during deposition of the tuff.

Bomb Agglomerates

Beds containing bombs were found at both the type section and at the pipeline section (Foldout A). The size of the supporting material is often much too fine to be classified as an agglomerate; however, the presence of bombs as the only coarse phase leads to this classification. The beds contain up to 20% bombs.

The bombs are chiefly composed of carbonate, up to 70%, which supports whole and broken crystals and both small cognate and juvenile clasts. The carbonate often exhibits

Plate 5.6

A. Photograph of a cut and polished slab of a "pink" air-fall deposit showing normal grading of the sanidine phenocrysts and slight density-stratification of the heavier minerals. The base reversely grades into the main body of the deposit, lower member, wch-33.

B. Photograph of a cut and polished slab of a purple air-fall tuff showing strong normal grading, lower member, wch-67.

C. Photograph of carbonate bombs taken from various locations.

   a. Spheroidal bomb, Pipeline section.

   b. Bulbous, kidney-shaped bomb, wch-78.

   c. Bulbous, kidney-shaped bomb, wch-78.

   d. Spheroidal bomb, showing poorly defined ribs, wch-78.

   e. Bulbous, kidney-shaped bomb, wch-78.

   f. Bulbous, kidney-shaped bomb, wch-78.

   g. Spindle bomb, wch-78.

   h. Almond-shaped bomb, Oldman River Bridge. Collected by D.A. White in 1966.

   i. Bulbous, kidney-shaped bomb, wch-78.

   j. Almond-shaped bomb showing logitudinal ribs, wch-78.

D. Photograph of a cut and polished slab of a conglomerate, probably from Ma Butte. Clasts show strong porphyritic and trachytic textures. The clasts are supported by a fine silty-sand matrix.

A

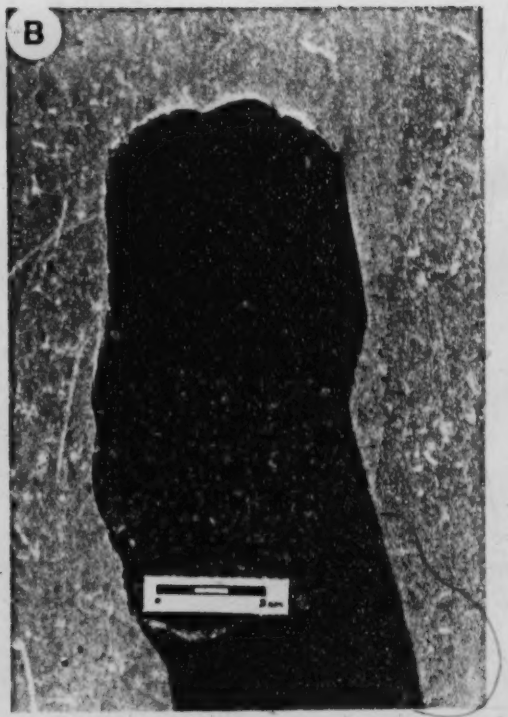
B

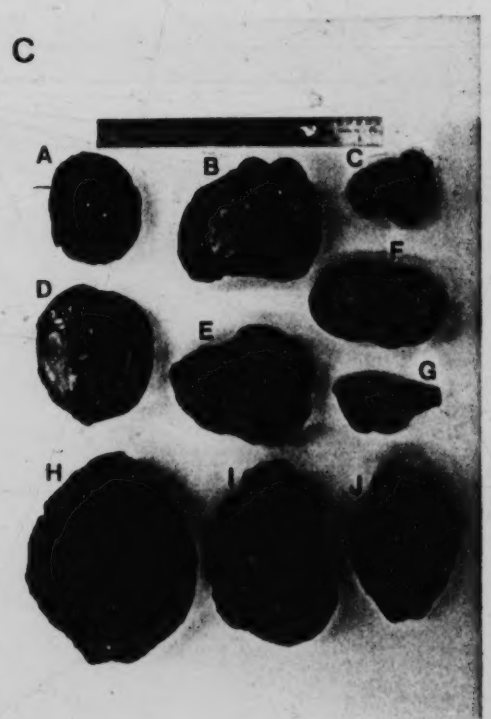
C
A
B
C
D
E
F
G
H
I
J

D

replacement textures though geochemical evidence does not rule out a primary source. The other constituents, especially the aphanitic clasts, exhibit plastic deformation structures.

The following types of bombs were identified (Plate 5.6c):

1. Spheroidal bombs, exhibiting an equatorial ridges, ribs or flutes.
2. Spindle bombs.
3. Almond bombs, (bipolar fusiform), often exhibiting flutes and/or ridges.
4. Bulbous or kidney-shaped bombs.

At the pipeline section some spheroidal bombs were found to be flattened on one side by impact. The sizes of the Crowsnest bombs are variable between 2 and 25 cm.

Supporting components are variable throughout different beds. At the type section, the beds containing bombs are comprised of a fine, purple tuff which, unlike the bombs, is not appreciably calcareous, ruling out in situ carbonate replacement. At the pipeline section, bombs are found in a coarse lithic, lapilli tuff with a carbonate matrix in the vicinity of the bombs. In both sections these beds occur towards the top of the lower member, though they are not correlateable. The bombs were apparently high temperature projectiles which were emplaced during air-falls and/or flows.

Clay beds: Bentonite

Thin, very fine beds or laminations consisting almost entirely of the clay minerals illite, illite/smectite and minor kaolinite are observed in graded, green crystal ash beds, in the upper part of the lower member. They are the finest component of the graded sequences and within the whole of the formation.

If truly vitric tuffs were formed by the Crowsnest eruptions they would produce such deposits after devitrification. Their association with green crystal tuff would support this idea in as much as the matrix of the crystal tuff has a strong resemblance to the bentonites. They are also recessive. Emplacement of such fine deposits was by weak, or waning stages of eruptions.

C. Lahar Deposits

Lahar deposits are relatively rare in the three sections investigated during this study. Only one flow or series of small flows were identified at the very base of the formation at its type section (see Chapter 6) (Foldout A).

They are characterized by their massive, very poorly-sorted nature and the occurrence of red and/or green shale clasts and partings; similar to those identified by Ricketts (1982). The matrix is clay-rich and may or may not support cognate clasts which range in size from <1 cm to as much as a meter. Crystal components are also common. Bedding is usually poorly defined, however, deposits appear to be thick. Shale partings may define a boundary or contact.

The deposits suggest that laharic mud flows drained the summits, incorporating cognate fragments and crystals as it moved. The shale clasts may represent water flow between laharic events. It is also expected that the flow followed previously existing channels on the mountain slope and may have later fanned out in areas of less relief.

D. Primary Flows and Intrusives

Most of the occurrences of primary rocks in the Crowsnest have been well documented by Pearce (1967, 1970) and Ferguson and Edgar (1978) and need not be discussed again here. It is well documented, however, that flows are rare. Two occurrences not previously described are herein briefly discussed.

A relatively fresh trachytic[11] flow was identified on the Willoughby Ridge section. It lies within the top of the upper member and exhibits strongly trachytic textures defined by euhedral feldspar laths.

In the upper member at the type section, a thin (0.5 - 1 meter) dyke was found to intrude between two massive breccia flows. It exhibits a chilled margin and has incorporated what seem to be cognate clasts. The clasts exhibit baked and/or resorbed rims.

Mineralogically it is composed chiefly of recrystallized feldspars, Fe-Ti oxides (titanomagnetite, ilmenite, pyrite and hematite). The high potassium composition, (K_2O wt% = 14.33) suggests the occurrence of a late differentiate (Chapter 4, wch-85). Texturally, it shares a close resemblance to the matrix of many pyroclastic breccias of the upper member.

---

[11] Classified according Ferguson and Edgar (1978).

E. Volcanogenic Sediments

Sediments derived from the Crowsnest volcanic pile are, in the vicinity of Coleman, rare and have been identified in only two cases:

1. Sandstone and Shales. Within the first 150 meters below the first outcrop of the Crowsnest Formation on Willoughby Ridge a series of quartzofeldspathic sandstones and shales were found to contain rounded to sub-rounded melanite garnets, sphene and sanidine. The main components of the deposits are characteristic of sands from the Upper Blairmore Group as described by Glaister (1958, 1959), Stott (1963) and Mellon (1967). This strongly implies that an earlier phase of Crowsnest volcanism occurred before the emplacement of the pyroclastics in the Coleman area. The implications of this observation are discussed more fully in Chapter 6.
2. Conglomerates. A conglomerate from unknown location was provided by Dr. R.A. Burwash at the University of Alberta (Plate 5.6d). The sample contains large, well rounded cognate cobbles and pebbles of trachyte, analcime phonolite and blairmorite. They range in size between 1 cm and about 20 cm. The rock is clast supported with fine sands comprising the rest of the matrix. White calcite is found to cement parts of the rock. Some identifiable crystals in the matrix suggest the fines were derived from pyroclastic deposits. Similar deposits have been reported from Ma Butte by Pearce (1967) , some carrying clasts estimated at 15 tons.

   The deposits were likely emplaced by high energy streams draining the mountain face. The origin of the streams was in areas dominated by primary flows or plugs.

   There is a likelihood that the streams which drained the slopes of the vents also produced finer-grained deposits. Such occurrences were not identified in the vicinity of Coleman.

Discussion

The compositions of any or all of the above deposits may change with either crystals or rock fragments becoming dominant. It is probable that some clasts were incorporated into the deposits as hot, semi-molten bombs or molten clots, a fine equivalent to bombs.

The moderately poor sorting and the thicknesses of the deposits point strongly to deposition in proximal areas. The characteristics of many deposits, such as surges and massive

ash flows, also suggest proximal deposition. Gradational contacts of air-fall deposits suggest that many were emplaced by continuous eruptions which varied in intensity. This concept is more fully developed in the next chapter. The implication for the deposition of air-falls over greater areas, i.e. Alberta basin, is also addressed.

Pearce (1967, 1970) and Ricketts (1982) have suggested that a substantial part of the Crowsnest Formation is composed of volcanogenic sediments. The evidence presented in this chapter strongly suggests that many such deposits are the direct result of pyroclastic volcanism which produced air-falls, pyroclastic flows and lahars. At the type section, no sedimentary deposits were identified.

VI. STRATIGRAPHY

A. Detailed Stratigraphy of the Proposed Type Section

The Crowsnest Formation at its type section is divided into an upper and lower member. The lower member is characterized by thinly to thickly-bedded tuffs, lapilli tuffs and agglomerates, representing deposition by pyroclastic flow, air-fall and minor lahars (Plate 6.1a). The deposits range in color from pink to light green to purple. Despite their recessive nature, they are over 75% exposed on highway No.3 west of Coleman Alberta

The upper member is characterized by very thickly -bedded, massive pyroclastic breccias and minor agglomerates, forming resistant cliffs in the area. The beds are commonly dark green to grey (Plate 6.1b). The division between the two members is placed at the base of the first continuous occurrence of the massive beds of the upper member (Foldout B). This division is not intended to be time stratigraphic, nor may it occur at the base of the same bed throughout the formation. It is taken to represent a marked change in the type and conditions of the eruptions which produced the deposits of the Crowsnest Formation.

Lower Member

Foldout A provides a detailed stratigraphic column of the lower 85 meters of the lower member. The remaining 40 meters of the member are not included in the column as they are largely covered. They are, however, discussed below and are well represented in Foldout B.

The lower member is divided into six units based upon the physical and depositional characteristics of the beds and their inferred mode of origin (Foldout A).

Unit I

The basal unit of the Crowsnest Formation (16 meters) lies in apparent contact with maroon shales of the upper Blairmore Group. These are exposed 20 m stratigraphically below unit I.

The unit is entirely composed of thickly-bedded lahar deposits similar to those identified by Ricketts (1982) at other localities. The deposits are very poorly sorted and contain abundant cognate fragments. Commonly, accidental fragments are found as red or purple shale lenses and clasts which may or may not define a bedding plane. The lenses or clasts often

Plate 6.1

A. Photograph of the middle of the lower member at the proposed type section. Units and samples are marked for position. The photograph shows the thinly, parallel-bedded air-fall deposits of unit III and the thick pyroclastic flow beds of unit IV. Thin beds are characteristic of the lower member. (See foldout A and appendix B for full descriptions)(looking north)

B. Photograph of the thick pyroclastic breccia beds of the upper member. Bedding contacts are marked in white along with their position in the section. A thin mafic dyke (wch-85) cuts the upper contact. (Looking north)

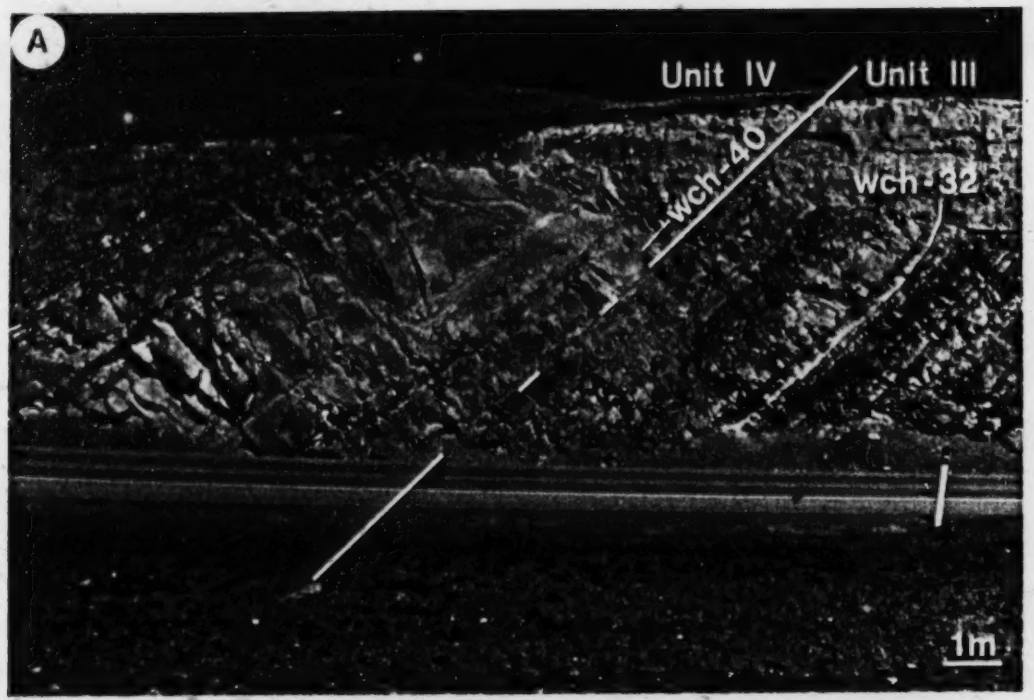
A
Unit IV
Unit III
wch-40
wch-32
1m

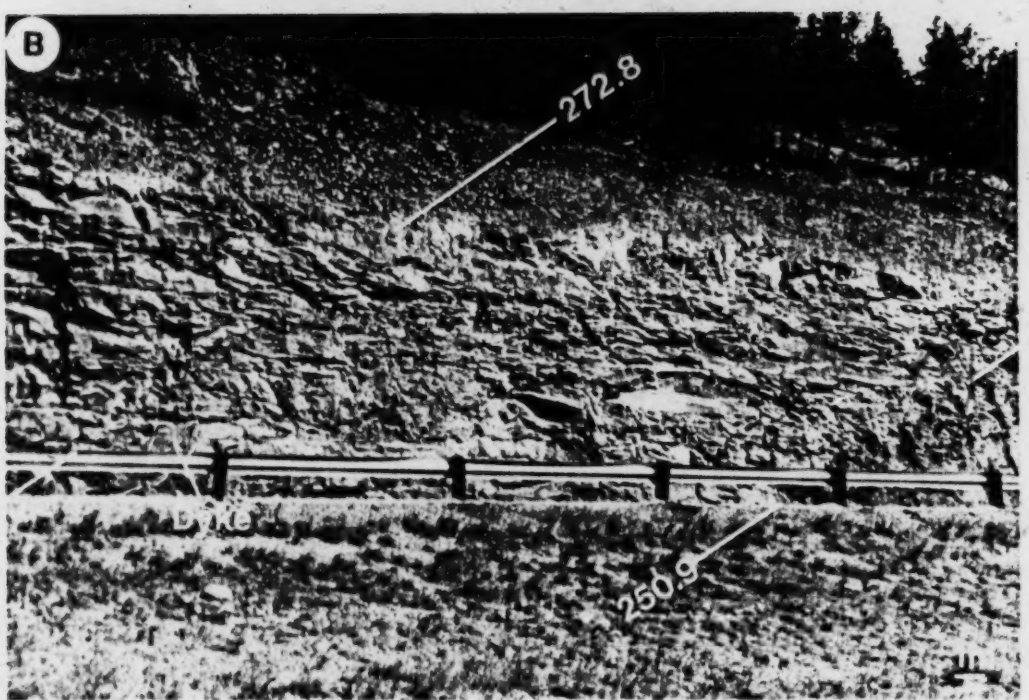
B
272.8
250.9

exhibit soft sediment deformation. The upper contact with unit II is defined by a bed of discontinuous shale lenses (Foldout A). Bedding is poorly defined, but may be distinguished by shale lenses, and, in one case, a thin, purple crystal tuff (wch-9).

The presence of previously ejected effusive material as clasts (cognate), and crystal phenocrysts as primary constituents of these basal lahars strongly suggests that Crowsnest volcanism had been occurring elsewhere before the emplacement of the deposits at the type section. The implications of this observation are discussed under regional stratigraphy.

Unit II

The deposits of unit II are more massive than those of unit I and III, though the lower contact does not show an abrupt change in competency. Generally, the unit is dominated by flows and surges. Three types of deposit were identified (Foldout A).

The base of the unit is comprised of thinly-bedded, purple and pink crystal tuffs and crystal lapilli tuffs. Depositional structures, mostly subtle normal and reverse grading, suggest an air-fall origin, though thin ash flows cannot be ruled out.

Some beds are notably calcareous and contain Fe - carbonate which comprises most of the groundmass in the dominantly matrix supported rock. It exhibits both a replacement texture and a granular texture. The latter may suggest a pyroclastic origin as no analcime microlites were seen to be replaced by carbonate as previously mentioned in Chapter II. The contact with the overlying agglomerate is sharp and shows substantial relief of up to 3m.

Massive agglomerates occur periodically throughout most of unit II and often occur as part of a cyclic fining upwards sequence. The rock type has been described in Chapter V (Plates 5.1b, 5.3c). A thick agglomerate is seen to truncate lower strata and shows an abrupt basal contact with substantial relief (Foldout A). This agglomerate grades upward abruptly into overlying surge deposits. A similar agglomerate without erosional contact caps the unit.

The upper half of unit II is composed of the following fining upwards, cyclic sequences:

Basal agglomerate - surge - agglomerate

The thickness of a given cycle is variable between about 10 cm and 50 cm (Plate 5.3d). Contacts are abrupt to gradational over a few centimeters. The agglomerates and tuff are massive and show poor sorting. The surges are only slightly better sorted and show

parallel-bedding/lamination, low-angle cross-stratification and lensoid bedding. All types may drape larger fragments in the lower deposits. Such deposits probably formed during turbulent, inflated surges.

Deposition of unit II was initially by air-fall followed by an agglomerate-surge flow which may have scoured a stream valley. This was followed by cyclic flows which produced the thin agglomerates and surge cycles. All types show welding, though the degree decreases from agglomerates to surges.

The upper contact is abrupt and marks a change in competency.

Unit III

Most of unit III is dominated by purple crystal tuffs, green crystal ashes and pink crystal lapilli tuffs. They are interpreted as air-fall deposits in Chapter V (Plate 6.1a). Three types of bed, pink tuff/lapilli tuff, purple tuff and green ash grade into each other or, in the case of green ashes, form lenses within the other types. Where all three occur together they form trilogies. Three types have been identified:

1 Purple tuffs grading reversely into green ashes and normally back into purple tuffs.
2 Purple tuffs grading reversely into green ashes and normally into pink crystal lapilli tuffs.
3 Pink lapilli tuffs grading normally to green crystal ashes which in turn grade into purple tuffs.

Other combinations were observed, however they were minor.

In cases where bedding contacts are gradational, deposition occurred during a single eruption where changing intensities produced the different beds. Where contacts are sharp, pulse-like eruptions or abruptly changing intensities are inferred. Welded pink crystal lapilli tuffs suggest high rates of accumulation.

Although the unit is dominated by air-fall deposits, flows are also present. A small agglomerate, similar to those described in unit II is found in the middle of the unit. Classically, it is overridden by a surge deposit. Towards the top of the unit, thick tuffs and lapilli tuffs occur with occasional surges suggesting an increased pyroclastic flow influence. In these upper beds, lenses of green crystal ash are common but only occur at the top of a flow.

It appears that the unit was emplaced by air-fall processes with occasional interfingering pyroclastic flows. Preservation of the poorly consolidated beds, the presence of

welding in pink beds and the lack of erosional features suggest high, continuous rates of deposition. The coarse, poorly sorted nature of many beds reflects proximity to the vent. Towards the contact with unit IV, processes favouring flow deposits seem to be increasing (Plate 6.1a).

Unit IV

Unit IV is characterized by thick ignimbrite deposits (ash flow tuffs and lapilli tuffs with intermittent surges) and air-fall beds (green ashes, purple tuffs, pink tuffs and occasional thin bentonites). The flow deposits range in thickness between <1 meter and 7 meters, while surges are relatively thin and rarely exceed a meter. The air-fall deposits are thinly-bedded, generally less than 30 cm. Ignimbrites tend to be resistant, while air-fall deposits are recessive (Foldout A, Plate 6.1a).

The thick flow deposit which dominates the unit from 39 m to 47 m (Foldout A, Plate 6.1a) exhibits the classical features of the standard ignimbrite flow unit described by Sparks *et al.* (1973), Sheridan (1979) and Fisher and Schmincke (1984) and resembles the massive facies of Rowley *et al.* (1985). An initial ground surge is found at the base of the deposit, exhibiting both low-angle cross-stratification and lensing features (Plate 6.1a). It is seen to pinch and swell laterally. The surge grades abruptly upward into a fine-grained reversely graded basal unit approximately 20cm thick. The unit is finer-grained than the main body of the flow into which it reversely grades. The main body is massive and exhibits few features. Petrographic studies show it to be welded. The top of the unit contains green ash lenses immediately below the upper boundary, probably of air-fall origin.

The other flows are similar though well defined surge deposits are not generally present. The thickness of the flows tends to decrease towards the top of the unit.

Thinly-bedded air-fall deposits ranging in combined thickness between 1.5 and 4 meters separate each successive flow. Towards the top of the unit, air-fall deposits become thicker, though they may contain thin surges and flows. The presence of the air-fall deposits with the emplacement of ignimbrites is consistant with the standard ignimbrite flow model. The unit was emplaced by pyroclastic flow processes with subordinate air-falls.

Unit V

The base of unit V is dominated by air-fall beds composed of purple tuffs, green ashes and pink crystal lapilli tuffs similar to unit III. The green ashes have a slightly higher garnet content. Occasional thin flow deposits are found interbedded with the air-fall deposits. The beds on a whole contain the greatest abundance of analcime crystals and juvenile blairmorite fragments in the lower member.

Overlying the air-fall beds is a 5 m sequence of bomb-bearing bearing purple tuffs, as described in Chapter V (Plate 5.5c), with green ash air-fall deposits separating the beds. Thicker flows, surges and air-fall deposits overly the deposits.

Unit VI

Unit VI encompasses the deposits lying between unit V and the base of the upper member. Most of the unit is recessive and poorly exposed (Foldout B). Test pits and trenches helped expose some areas as most of the outcrop was found to be covered by up to two feet of overburden. Wind erosion is quickly removing the remaining cover.

The base of the unit consists of massive pink agglomerate beds and accompanying surge deposits. The rest of the unit, the covered interval, is apparently dominated by purple and pink crystal tuffs. Pink, welded agglomerates and coarse lapilli tuffs are common but their abundance could not be determined. Thickly-bedded, massive agglomerates and lapilli tuffs characteristic of the upper member occur towards the top of the covered interval. The first continuous deposits of this type begin at 124 meters up section where the base of the upper member is placed (Foldout B).

All samples collected from the pits and trenches contained only pyroclastic ejecta. No sediments or reworked pyroclastics were found suggesting that there was not an extensive period of erosion in the covered interval. The unit is dominantly composed of ignimbrites and subordinate air-fall deposits, the latter apparently decreasing towards the base of the upper member.

Upper Member

The upper member comprises about 70% (276 m) of the Crowsnest Formation at its type section. In other areas away from Coleman (i.e. Lynx Creek and Oldman River) it appears to comprise the entire formation in the absence of the the lower member. In the vicinity of the type section, the upper member seems to form a resistant cap over the deposits of the lower member.

Despite its thickness, the type of deposits throughout the upper member are uniform. Pyroclastic breccias are the dominant deposit. Two discrete units were defined at the type section (Foldout B). For continuity the numbering is continued from the lower member.

Unit VII

The basal zone of the upper member is characterized by massive agglomerates, pyroclastic breccias and surges ranging up to 10 meters in thickness. It is, for the most part, dominated by agglomerates with their characteristically round clasts. In all cases, the beds exhibit good welding. Colors range from pink to brown to green. Internally they exhibit occasional normal grading, trachytic alignment of sanidine phenocrysts in the matrix and rarely, internal cross-lamination. Surge deposits are often associated in small numbers.

The approximate equivalent, 1.2 km south on the pipeline section, Foldout B, exhibits strongly defined sequences of agglomerates grading vertically and laterally into pronounced surge deposits, similar to the deposits of unit II (Plate 5.2a,b). Laterally, these beds become coarse agglomerates and/or well defined pyroclastic breccias. In the absence of surge deposits the bedding is defined by normal grading of clasts. The deposits of the upper member strongly resemble those of modern block and ash flows which form during dome collapse as outlined in Chapter IV. Gas inflated flows and air-falls appear to have only occurred at the base of the upper member.

It may be that the beds present in both sections can be correlated. The changeable character of pyroclastic deposits would make this extremely difficult without more exposure. No attempt to correlate single beds was made.

Unit VIII

The upper 230 meters of the proposed type section is composed of thick, massive pyroclastic breccias as described in Chapter V (Plates 2.2e, 5.1c, 5.2b, 6.1b). Bedding is at best vague with contacts being distinguished by slight color changes and/or abrupt changes in grain size (Plate 6.1a). The beds are very thick, ranging from 20 meters to 120 meters. It is probable that the thick beds are composite deposits with individual beds being indistinguishable.

A dyke, previously described in Chapter V, intrudes along the contact of a bed at about 270 meters up section (Foldout B). It may be associated with brecciation found in the immediate vicinity.

Towards the top of the section, a densely welded tuff, possibly of air-fall origin, is sandwiched between two dense green breccias which contain intensely charred wood fragments. The bed is tan colored and occurs approximately 10 m below the upper contact with the Blackstone Formation.

The coarse nature and in some cases the angularity of the fragments in these upper beds indicate emplacement as coarse, block flows. Chapter IV more fully describes the mode of emplacement of these beds.

B. Local Stratigraphy

The correlation of the formation, even in the type area, is made difficult by the lack of marker beds either within the formation itself, or within the bracketing Mill Creek and Blackstone Formations. Indeed, the same problem exists with positioning the formation with respect to the Middle Cretaceous sequences of the foothills and the Alberta basin. This problem is further discussed under regional stratigraphy.

Foldout B is a stratigraphic cross-section which incorporates the measured sections of the type section, the Pipeline section and the Willoughby ridge section. Correlation between the three sections is only made at the contact between the upper and lower members. As mentioned, it is not taken to be time stratigraphic nor may it lie at the base of the same bed or deposit. It is, however, thought to mark a dramatic change in eruptive conditions between the ash falls and flows of the lower member and the block flows of the upper member. Other correlations are entirely schematic and are intended as a model for the deposit.

The section is hung on the approximate position of *Inoceramus labiatus* which lies directly on the Crowsnest Formation in the Coleman area (Glaister 1958, 1959 and Mellon, 1967). Glaister (1958, 1959) notes that the distance between the top of the Crowsnest and the *I. labiatus* zone increases both to the north and south.

Other factors taken into account during the construction of this section are as follows:

1. Thinning/wedging of pyroclastic deposits away from the source area causes a net decrease in the thickness of the formation. This is exemptified by a thin 1 meter deposit of only the upper member on the Oldman River, north of the proposed type section.
2. The upper contact is disconformable (Glaister 1958, 1959; Stott, 1963; Norris, 1964 and Mellon, 1967).
3. The deposition rates of the volcanics near their vents logically exceeded those of the upper Blairmore Group, inhibiting interfingering near the source during continuous eruptions.

The basal contact of the Crowsnest Formation is seen to be gradational at the Willoughby ridge section. Typical Blairmore sandstones and shales may carry abundant mineralogy characteristic of the Crowsnest Formation up to 150 m below the first occurrence of unreworked Crowsnest. Not all beds however contain these characteristic minerals.

At the type section, the contact appears abrupt, however the first Blairmore sediments observed occur below a 24 meter covered interval in which no samples were retrieved.

Regardless of where the Willoughby ridge section is correlated, the lowest Blairmore sediments bearing minerals derived from the Crowsnest Formation apparently occur well below the base of the proposed type section (Foldout B). This seems to suggest the presence of volcanic activity before deposition at the type section.

Further evidence for earlier eruptive events is found in the basal lahars of the type section, where the majority of clasts are cognate, being formed by previous eruptions. The presence of a lahar suggests that relief was already built up around the vicinity of the vent before deposition at the proposed type section.

The Crowsnest Formation in Foldout B is drawn to depict the depositional features which may result by overlaping fan-shaped pyroclastic deposits in the vicinity of the vent or vents. Multiple vents have already been suggested by Pearce (1967). Erosional channels which, although not observed except where they have been infilled by subsequent pyroclastic flows, probably drained the mountain slope. Their presence is substantiated by the occurrence of the

conglomerates previously described in Chapter V.

C. Age and Correlation

Regionally, the Crowsnest Formation is restricted to the southwestern corner of Alberta. Its exposure has been well documented by an excellent map of the area produced by R.A. Price in 1959. The thickness of the formation is readily observed to thin rapidly in all directions from the local area around the type section and eventually becomes a member of the upper Blairmore Formation (Mellon, 1967). To the west however, its extent is obscured by the rocks of Precambrian and Paleozoic age which have been overthrust along the Lewis fault (Figure 1.2). The thickest known sections are found in the vicinity of Coleman at Iron Ridge and Ma Butte (Figure 1.3) (This study, MacKenzie, 1956; Norris, 1964 and Pearce, 1967). In these areas the formation achieves a maximum thickness of about 450 meters[12] (1600 feet).

To the southwest of the study area a group of mineralogically similar trachyte plugs may be found in the vicinity of Howell Creek B.C., where it empties into the Flathead River (Figure 1.1). Gordy and Edwards (1962), Norris (1964) and Currie (1976) suggest a genetic similarity; however, no study has yet confirmed the relationship.

In all areas of its exposure, the Crowsnest Formation is underlain by the continental sediments of the upper Mill Creek Formation and overlain by the marine shales of the Alberta Group, specifically the Blackstone Formation.

The Blairmore Formation has been described in detail by Carr (1946), Glaister (1958, 1959), Norris (1964) and Mellon, (1967). The flora has been described and identified by Bell (1956). The upper Blairmore, as defined by Glaister (1958, 1959), includes all rocks which lie between the calcareous ostracod marker horizon and the marine shales of the Alberta Group and/or rocks of the Crowsnest Formation. Mellon (1967) identifies the Mill Creek Formation at the top of the Blairmore Group. This formation is distinguished by the occurrence of Dicotyledonous flora which also occurs in the Crowsnest Formation. As such, the volcanics were considered the upper member of the Mill Creek Formation. However, their distinct lithology in the vicinity of the Crowsnest Pass certainly warrants formational status.

The rocks of the upper Blairmore Group (Mill Creek Formation) are characterized by the abundance of green feldspathic sandstones and greywackes (Glaister, 1958, 1959 and

---

[12]The total thickness of the proposed type section is 404 meters (1362 feet), (see appendix A).

Mellon, 1967), the latter becoming more abundant towards the top of the formation. Numerous igneous pebble conglomerates containing granite, granophyre, vitrophyre and other types of possible calc-alkaline affinities were identified in the middle of the upper Blairmore by Glaister (1958) and Norris (1964). These were interpreted as being the result of the unroofing of the Nelson granitic complexes to the west (Carr 1946, Glaister 1958, 1959, Norris 1964). The upper part of the Upper Blairmore is composed dominantly of arkosic greywackes (Carr 1946, Glaister 1958, 1959).

In the vicinity of the type section, the Crowsnest Formation lies in gradational contact with the sediments of the upper Blairmore Formation. These sediments, especially the sandstone were found to be quartzofeldspathic, containing abundant volcanic components not related to the Crowsnest Formation. The rocks are indicative of lower to middle beds of the upper Blairmore as described by Glaister (1958, 1959). The arkosic greywackes Carr (1946) and Glaister (1958, 1959), which characterize the top beds of the upper Blairmore were not found, suggesting that the base of the Crowsnest lies within the middle of the upper Blairmore Formation.

Poor stratigraphic control inhibits the exact positioning of the Crowsnest Formation. The occurrence of the following flora have been identified in the Crowsnest Formation by Bell (1956):

Platanus
Sequoia condita
Celastrophophyllum acutedens
Cinnamomoides sp.
Cinnamomoides ovalis

He suggests an Albian age for the suite.

Melanite garnets identical to those of the Crowsnest Formation are found consistently in the fine-grained sands and shales of the Viking Formation from the Caroline field northwest of Calgary[13]. Their presence logically suggests a Crowsnest source, placing the beginning of volcanism at or near Viking time. The garnets may have been emplaced by air-fall or by erosion. Their presence only as very fine grains, <0.05 mm, and the occurrence of bentonites within the formation (Amajor, 1978, 1985) favor the latter. Further, Amajor (1978) describes

[13] Samples were provided by Mike Dean, (pers. comm.) and descriptions of the Viking Formation may be found in Dean (1985)

five bentonite horizons which occur in the Viking Formation. At least three of these bentonites originated in the southwest and a Crowsnest source is inferred (Amajor, 1978, 1985).

The duration of Crowsnest volcanic activity is difficult to assess. The deposits at the type section suggest rapid deposition rates over a short time span. The apparent absence of uncomformities and the presence of welded air-fall deposits in the proposed type section confirm this observation. On the other hand, Blairmore sediments containing Crowsnest material suggest earlier eruptive phases.

The possibility of a more extended period of volcanism may also be suggested by the occurrences of correlated volcanic horizons in the following stratigraphic sequences of the Alberta basin:

1. As previously mentioned, the occurrence of black melanite garnets in the Viking Formation strongly suggests correlation with the Crowsnest. The prominent bentonite horizons in the formation further point to the same source as has been suggested by Amajor (1978, 1985).
2. Potassium-argon dates have been determined for Crowsnest rocks by Folinsbee *et al.* (1957) and Folinsbee *et al.* (1961). The dates achieved ranged between 93.9 Ma to 101 Ma and suggest an Albian age. This evidence is coincident with the paleontological data provided by Bell (1956).

   The spread of dates, 93.9 Ma for the type section, to 101 Ma for Mill Creek, suggest that total volcanism occurred over a span of 7 my. with individual deposits, i.e. the type section being deposited over a shorter time span.

   Tizzard and Lerbekmo (1975) dated sandine and biotite from Viking bentonites in the Suffield area of Alberta. Their results range from 94 to 105 Ma These data are compared with dates for the Crowsnest in Figure 6.1 and show an excellent correlation.
3. The "redspeck marker" found in the top of the Bow Island Formation and equivalent Colorado shales contains a characteristically high abundance of the zeolite heulandite. Thompson and Axford (1953) and Glaister (1959) suggest they were formed indirectly by volcanism and correlate the zone with the Crowsnest Formation.
4. Carr (1946) and Glaister (1958, 1959) identify tuffaceous horizons in the top of the Blairmore Formation where the distinct beds of the Crowsnest are missing. Carr (1946) notes that tuffaceous horizons occur in the upper 600 feet of the formation and are concentrated in the upper 200 feet. In most cases, they are mixed with clastic components

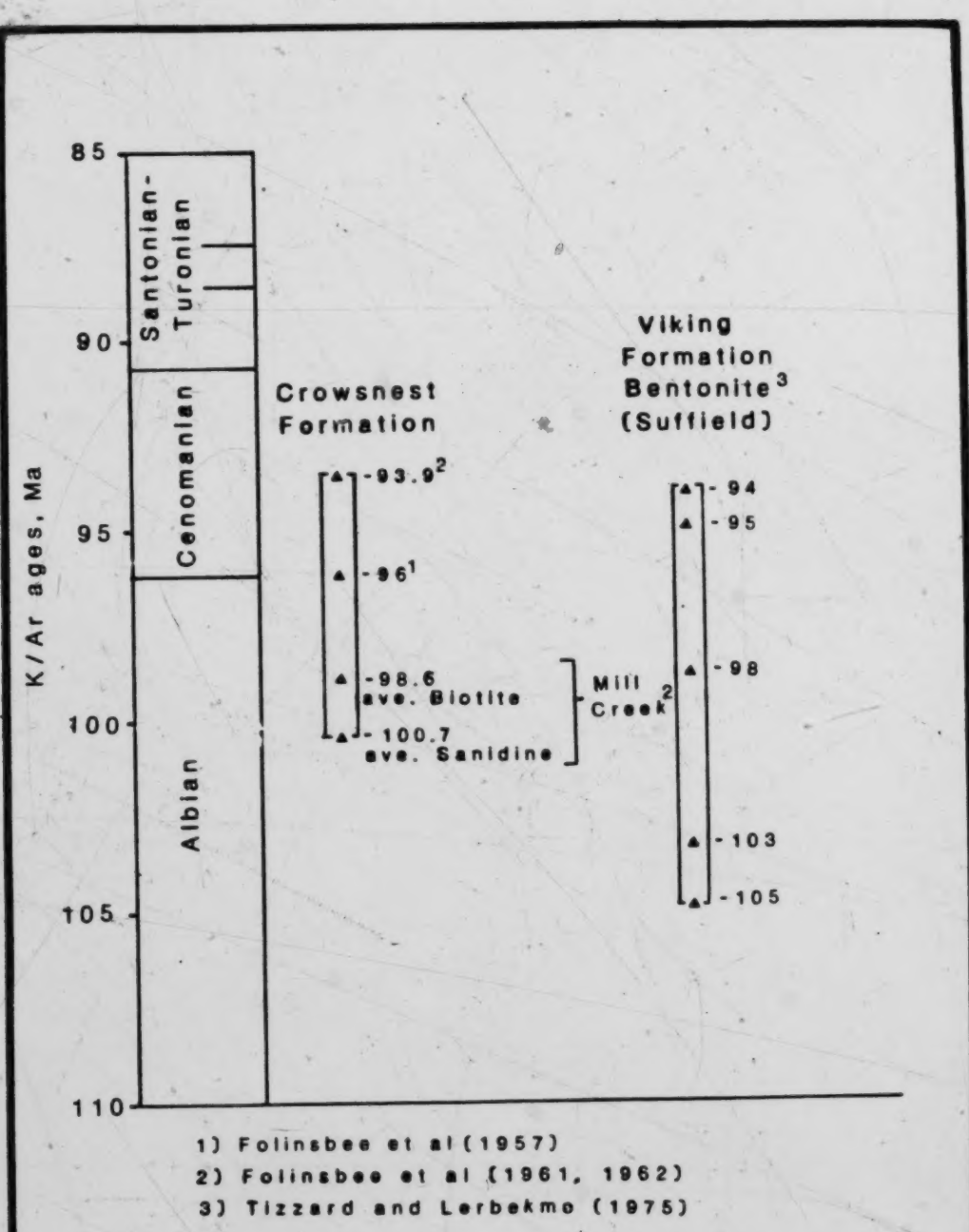

Figure 6.1 K/Ar ages for the Crowsnest Formation and a bentonite from the Viking Formation.

and may contain orthoclase (sanidine?), plagioclase, biotite, garnet, chlorite and apatite, showing some resemblance to Crowsnest mineralogy. Carr (1946) also describes the presence of a feldspathic marker bed 600 feet below the top of the Blairmore on the Highwood river. The bed contains well formed feldspar crystals which are correlated with the Crowsnest (Carr, 1946).

5. Bentonites have been identified in the lower marine Blackstone Formation in the vicinity of the Crowsnest Formation by Stott (1963) and Norris (1964). It is not known what relation these beds have with the Crowsnest. However, Carr (1946) describes a tuffaceous horizon in the lower Blackstone Formation on the Highwood River which contains garnet, analcime and apatite, again suggesting a genetic link with the Crowsnest.

The upper contact of the Crowsnest Formation is marked by a profound change from the massive agglomerates of the upper member to the fine-grained marine shales of the Blackstone Formation. The contact is thought to be disconformable (Carr, 1946, Glaister, 1958, 1959 and Norris, 1964). This view is also favored by this study.

It is clear that this boundary marks the cessation of the Crowsnest volcanism, though it may not have occurred simultaneously throughout the whole formation. Also, small sporadic eruptions following deposition of the upper agglomerates and breccias cannot be ruled out. The exact time and position of the final eruptive episodes is ambiguous, again due to poor stratigraphic control.

The upper contact represents a maximum build-up of volcanic debris on the continental sediments of the Blairmore Group. In all areas the contact with the Blackstone Formation suggests that the volcanic pile was built up before transgression of the Blackstone sea during Cenomian-Turonian time. The relief of the Crowsnest pile, herein termed the Crowsnest high, has been determined to be a maximum of 120 feet by Norris, (1964) based upon a bentonite marker at the base of the Vimy member of the Lower Blackstone Formation. Three observations suggest a greater relief on the Crowsnest high.

1. The base of the Blackstone Formation in the vicinity of the Crowsnest is composed of the Sunkay Member, containing the index fossil *Dunveganoceras* on Mill Creek and the overlying Vimy member, containing the index fossils *Watinoceras* and *Inoceramus labiatus* (Stelck *et al.*, 1956, Glaister 1958, 1959 and Stelck, pers. comm.). Both members thin substantially over the Crowsnest high. The Sunkay member thins by 97% from 631 feet at

its type section to 15 feet in the vicinity of the Crowsnest (Stott, 1963). It does not appear to be present in areas of maximum Crowsnest buildup.

The Vimy Member thins by 74% from 605 feet at its type section to 154 feet in the area of Crowsnest Pass (Stott, 1963), where it may lie directly on the volcanics (Glaister, 1959). Stott (1963), observes that the members rapidly thicken away from the Crowsnest high.

2. Folinsbee *et al.* (1961) noted that *Inoceramus labiatus* occurs 200 feet above their K-Ar dated Crowsnest bed on Mill Creek. In accordance with observations made by Glaister (1959) and Mellon (1885), that the same zone lies directly on the volcanics at their type section, the known relief is 200[14] feet. Further, Folinsbee *et al.* (1961) state that *Dunveganoceras* occurs 15 feet above the same volcanic bed at Mill Creek. The previous evidence provided by *I. labiatus* suggests this horizon pinches out against the Crowsnest high.
3. The "fish scale" marker is not present in the Crowsnest Pass, suggesting it pinched out against the Crowsnest high.

In all of the above cases, the relationships not only depend upon the maximum relief of the Crowsnest high, but also on the time of non-deposition between cessation of volcanism and transgression of the Blackstone sea. The true maximum relief of the Crowsnest high may be still greater as the maximum would occur at the vents, none of which are exposed.

D. Interpretive Stratigraphy

Mineralogical, paleontological and radiometric data define a stratigraphic bracket within which the Crowsnest event falls, although exact positioning is not yet known.

The earliest eruptions occurred at or near Viking time which has been well defined by Stelck (1958, 1975). The deposition of the Viking occurred during minor regressions of the inland sea (Hein *et al.*, in press). Whether local regressions reflected uplift in the vicinity of the Crowsnest is not known.

---

[14]The absence of nearly 1000 feet of lower Blackstone Formation may suggest much greater relief.

The latest possible age for major eruptions was probably pre-Dunvegan as evidenced by *Dunveganoceras* 15 feet above the volcanics on Mill Creek (Folinsbee *et al.*, (1961); however, later small-scale events may have occurred after Dunvegan time. The disconformable upper contact of the Crowsnest may represent a much older date for the cessation of volcanism which was followed in the immediate area by a substantial period of non-deposition prior to the transgression of the Blackstone sea. The occurrences of tuffs and bentonites throughout Blairmore/Colorado time suggest that eruptions may have dumped material periodically into the Alberta basin.

Figure 6.2 gives a schematic cross-section of southern Alberta which incorporates the previous observations. The diagram suggests that volcanism occurred throughout Colorado time starting approximately during deposition of the Viking Formation. Whether eruptions were constant over that time or whether a very active, short lived eruptive period was preceeded, or followed by small subordinate eruptions is not known. The continuous beds at the type section may favor the latter, however active vents may have developed periodically through late Albian time.

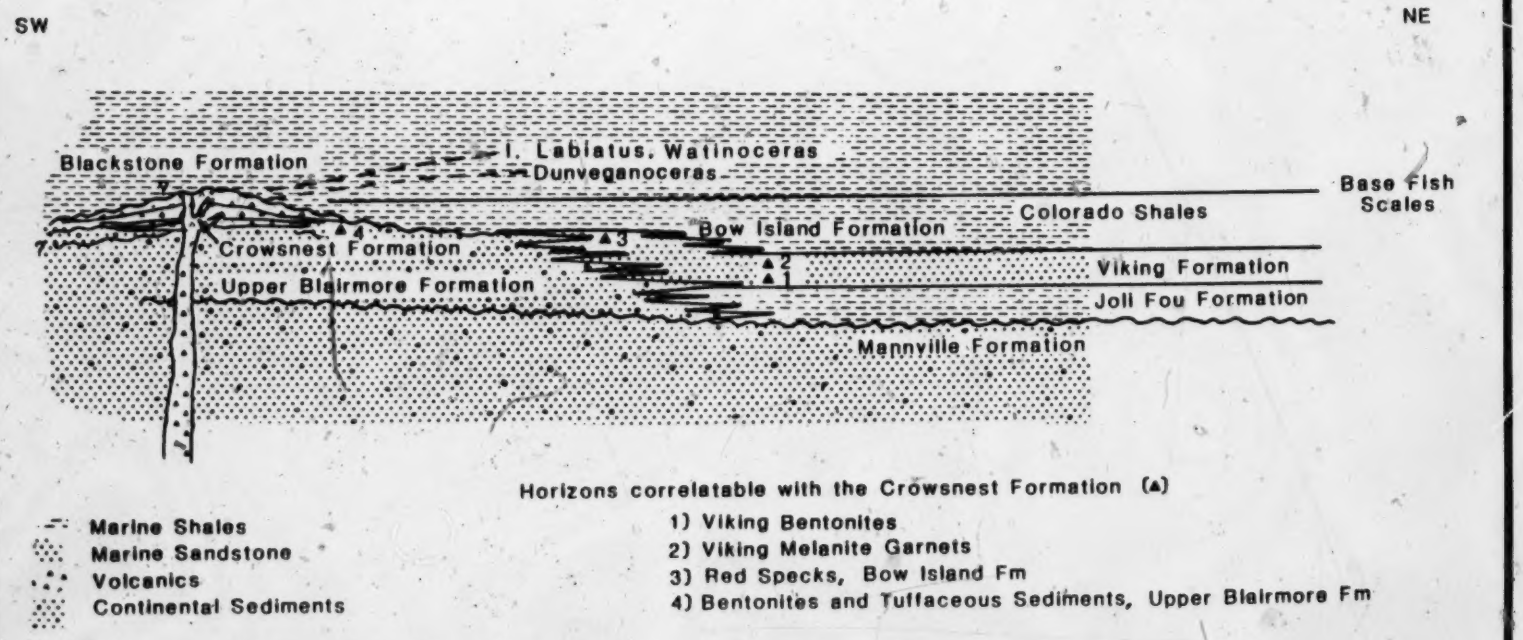

Figure 6.2 Schematic stratigraphic cross section through southwestern Alberta showing Upper Albian to Turonian strata and their correlation with the Crowsnest Formation.

VII. HISTORY OF THE CROWSNEST FORMATION

During mid to upper Albian time, structural discontinuities in the basement below Cranbrook, B.C.[15] resulted in the formation of a hydrous, trachyte melt (Pearce, 1967, 1969 and Ferguson and Edgar, 1978). Differentiation of this melt probably occurred by crystal fractionation of sanidine, analcime, pyroxene and garnet (Pearce, 1967, 1970 and Ferguson and Edgar 1978) at depths between 23 and 35 km (Ferguson and Edgar, 1978). It appears that sanidine, aegirine - augite and sphene were first to crystallize followed by garnet and analcime. This assumption is based on their occurrence as inclusions in other minerals. These observations are consistent with those of Pearce (1967) and Ferguson and Edgar (1978). Ferguson and Edgar (1978) suggest that the melts were rapidly propelled to the surface by H_2O and CO_2 gas and quickly cooled, preserving the analcime under extrusive volcanic conditions.

Geochemically, both the primary and pyroclastic flows show similar and sometimes identical signatures despite the intense devitrification, metasomatism and recrystallization which has occurred in the pyroclastics, especially in the lower member. Both types classify readily as tristanites of the alkali basalt, potassic differentiate series with blairmorites representing a sodic end member, classified as a benmorite. This suggests that the differentiation trend was from potassic to sodic as the melt evolved. These results are somewhat contrary to Ferguson and Edgar (1978), who suggest a completely sodic path of differentiation.

Surface eruptions of Crowsnest material occurred on the flood plain flanking the east side of the Cordilleran uplift with the inland Joli Fou seaway lying to the east (Figure 7.6a,b). The dominantly pyroclastic eruptions were subaerial, depositing air-falls, ignimbrites, lahars and subsequent sediments on the continental deposits of the Blairmore Group.

Pearce (1967) suggested the presence of multiple vents in the vicinity of Coleman, Ma Butte and George Creek, based on the presence of minor intrusives and the thickest occurrences of the volcanics. The suggested volume of debris ejected has been estimated at about 50 cubic miles (Pearce, 1967) although the effects of erosion are hard to define. These views are accepted by this study.

The eruptive events of the Crowsnest are divided into stages based upon the distinct character of the deposits of the lower and upper members of the formation. As no vents have been exposed, their morphologies are only interpretive and are based upon modern examples

[15]Pre-laramide position of the Crowsnest Formation according to Norris (1964).

provided by Green (1971), Williams and McBirney (1979) and Fisher and Schmincke (1984).

A. Early Eruptions

The distinctive nature of the deposits of the lower member suggest that the eruptions and eruptive conditions which prevailed during early Crowsnest time were different from those which later emplaced the upper member.

The deposits of the lower member show their thickest accumulation in the vicinity of Coleman, where a maximum of about 124 meters was measured on highway No.3 (Foldout A and B). The deposits thin rapidly to the south and are not found to the south at Lynx Creek or to the north on the Oldman River. The strike length is estimated at about 20 km north and south of Coleman for a total of about 40 km.

The deposits of the lower member at the type section are almost entirely composed of air-fall and ignimbrite, with subordinate lahars. Little evidence of erosion is present aside from the probable presence of an erosional channel which has been subsequently filled by ignimbrite (Unit II, Foldout A).

In areas away from the type section where the member notably thins, i.e. Willoughby Ridge section, lower-laying Blairmore sediments carry mineral suites characteristic of the Crowsnest Formation, suggesting that erosion, at least in areas removed from the vents, has occurred. Stratigraphic evidence suggests this erosional debris has come from both earlier deposits and those represented by the type section.

Three types of pyroclastic deposits were identified a the type section. Air-falls and ignimbrite were dominant, followed by subordinate lahars. Ignimbrites are identified by their depositional character which ranges from massive to cross-laminated beds. Many deposits strongly resemble the standard ignimbrite flow unit which sees a cross-bedded ground surge followed by a massive flow and subsequent ash cloud surges and/or air-falls respectively (Foldout A and Chapter V).

Air-fall deposits are identified by their parallel-bedded nature, their grading sequences and the absence of flow features (cross-stratification). In some cases, mantle bedding on a small scale is observed.

As seen in Foldout A, air-fall deposits and ignimbrites may occur together (upper unit IV and unit V) or as deposits dominated by one type, unit II (flow), unit III (air-fall),

suggesting that eruption conditions favored the formation of one or both types. Comparison of the lower deposits at the type section with those described by Rowley *et al.* (1985) from Mount St. Helens suggest a close proximity to the vent or vents.

The abundance of cognate and juvenile rock fragments which exhibit well defined trachytic flow textures strongly favors the presence of lavas, plugs and probably intrusives. Such clasts may constitute up to 80% of the rock.

Eruptive Model for Lower Crowsnest

The presence of air-fall deposits and interbedded ignimbrites in the lower Crowsnest Formation provide powerful evidence that the eruptions which produced the deposits of the lower member were gas-charged varieties which favor air-fall deposits and may or may not have produced ash flows. This interpretation is compatable with the genetic interpretations of Pearce (1967, 1970) and Ferguson and Edgar (1979).

The eruptions were violent, as ascending magma propelled by H_2O and CO_2 gas (Ferguson and Edgar, 1978) reached the surface, disintegrating plugs, flows and pyroclastics which were previously deposited in the direct vicinity of the vent. Such eruptions produced deposits which were composed of juvenile crystals and both cognate and juvenile components. According to modern observations, these gas-charged eruptions would favor the formation of a vertical eruption column, (Sparks and Wilson, 1976; Sparks *et al.*, 1978 and Sparks, 1983)

The occurrence of the air-fall and ignimbrite deposits described in Chapters V & VI suggest that varying conditions of eruption produced both a completely convective column and/or a convective column suffering different stages of collapse. Three scenarios are postulated:

Highly Gas-Charged Eruptions. Eruptions of a highly gas-charged nature are suggested by Williams and McBirney (1979), Sparks (1982) to favor the production of air-fall deposits by the convective plume theory proposed by Sparks and Wilson (1976) and Sparks *et al.* (1978). Such eruptions during Crowsnest time would favor the thick sequences of air-fall beds found within unit III, upper unit IV and unit V of the type section (Foldout A). Figure 7.1a gives a graphical representation of this type of eruption with respect to the Crowsnest deposits.

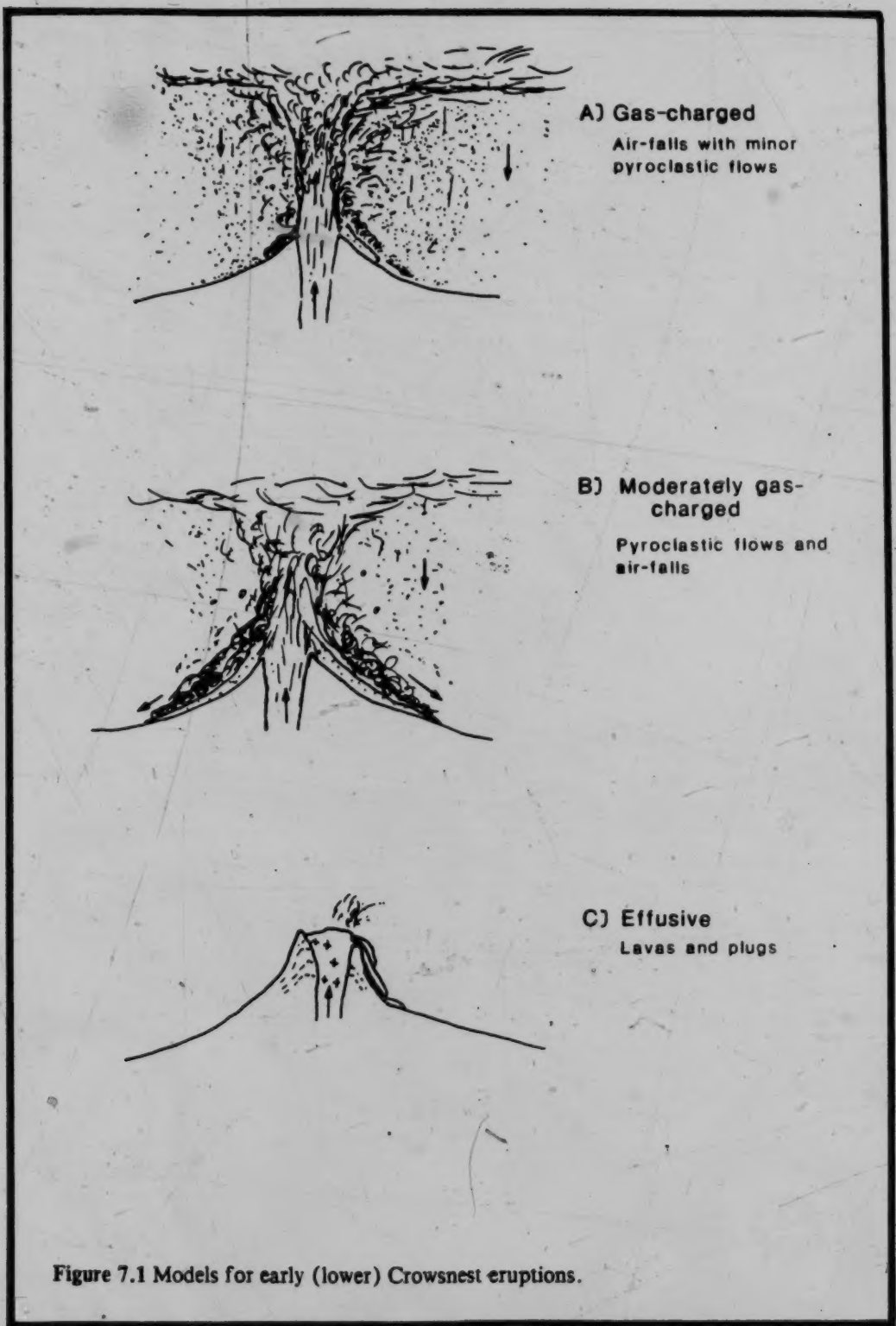

Figure 7.1 Models for early (lower) Crowsnest eruptions.

In such a model, the relatively coarse air-falls of the type section would be deposited in proximal areas, (near the flanks of the vent) essentially representing a deposit composed of coarser crystals and lithic fragments which were too heavy to be carried to great heights. The intensities of the eruptions dictate where these deposits are emplaced. Violent eruptions would eject coarser debris greater distances, while less intense eruptions would deposit finer material in similar areas. The marked grading readily observed in many air-fall beds reflects the changing intensity during eruptions. Air-fall beds with gradational contacts are thought to be deposited during a single eruption, while those with sharp contacts may have been emplaced by separate pulse-like eruptions. The eruption column was undoubtably affected by wind, resulting in the deposition of air-falls in lobes downwind from the vent.

Minor pyroclastic flows are found within thicker sequences of air-fall deposits, suggesting that some gravitational column collapse had occurred. Small scale lateral blasts cannot, however, be ruled out.

Moderately Gas-Charged. Eruptions which are moderately gas-charged have a tendency to produce a vertical eruption column, the core of which may collapse to form ash flows (Williams and McBirney, 1979 and Sparks 1982, see Chapter I). The presence of deposits in the type section which fit the standard ignimbrite flow model strongly suggest that this type of eruption occurred in early Crowsnest time (Units II and IV, Foldout A).

Figure 7.1b graphically describes this eruption model where moderately gas-charged eruptions would form a vertical eruption column with a collapsing core. The ensuing flows moved rapidly down the mountain slope and fanned out as they reached the lower relief flanks of the volcano. Ground surges and ash cloud surges accompanied these flows as evidenced by the associated deposits at the type section.

Contemporanious with the collapse of the core, a convective zone in the eruption column produced air-falls in a similar manner to those described above. The air-falls followed the emplacement of the ignimbrite (Figure 7.1b) as evidenced by the overlying deposits of the type section (Unit IV, Foldout A). Again, the air-fall deposits were probably strongly affected by prevailing winds, producing lobe-like deposits downwind from vent, with eruption intensities controlling grading.

The eruptions described above would likely favor the finer ash flows of unit IV, which carry few large lithic fragments. In contrast, the coarse agglomeratic flows which characterize unit III probably formed under somewhat different situations exemplified by the high concentrations of lithic cognate fragments commonly present. The origin postulated for these flows is one where fragments from disrupted plugs, domes, lava flows and possibly coarse, co-ignimbrite or co-air-fall deposits are remobilized and incorported as part of both turbulent and dense pyroclastic flows with juvenile material. In the former case, turbulence would favor the formation of a coarse, basal lag deposit composed of larger, rounded rock fragments which dropped from the flow during movement. The deposits which were emplaced after this "density stratification" would be finer grained, and depleted in coarse fragments. The resultant deposits would be coarse agglomerates which grade into fine-grained surge deposits (Plates 5.1a, 5.2a,b and 5.3d.). In the latter case, density stratification would be less pronounced. Violent eruptions disrupted the pile and formed flows containing a wide range of component sizes. Similarly, a lateral blast would have the same effect. Such flows are seen to be followed by thick sequences of ash cloud surge which commonly overly such deposits suggesting gas transport.

Effusive Eruptions. The prominent presence of cognate clasts in all but the bentonites of the lower member is strong evidence for effusive eruptions. Many of these lithic fragments exhibit strongly developed trachytic flow textures. By the sheer numbers of these clasts, it is postulated that a gas-depleted phase may have occurred during waning stages of gas-charged eruptions, producing lavas and vent plugs which were subsequently disintegrated by later gas-charged eruptions (Figure 7.1c). Cycles where gas-charged eruptions evolve into gas poor effusive phases have been suggested by Sheridan (1979).

The rarity of primary lavas in the exposed sections of the Crowsnest Formation would suggest that they were viscous "toothpaste - like" lavas which did not flow far from the crater. The postulation of a plug is speculative, however, the presence of clasts which exhibit coarser crystallinity and no flow fabric is supportive.

In all of the above eruptions primary components occurred in the form of crystal phenocrysts, aphanitic fragments and probably coarser-grained fragments. Cognate components are represented by lithic clasts and probably crystals re-incorporated from the pile.

The eruptions are postulated to have been subaerial by Pearce (1967), based on the presence of pisoliths which have since been identified as bombs by this study. Further evidence for subaerial deposition is as follows:

1. Abundant air-fall and ignimbrite deposits with features consistent with modern analogies, i.e. graded bedding, surge deposits, etc.
2. Welded character of many beds with plastically deformed clasts suggesting slower cooling rates.
3. Presence of lahar deposits.
4. Deposition of the suite on continental sediments carrying non-aqueous plant remains.
5. Lack of reworking which may have occurred in higher energy aqueous environments.

With such a limited exposure of the Crowsnest terrain, erosion between early eruptive events is difficult to assess. At the type section, there is very little evidence for erosion. The lahars at the base of the section suggests that some erosion, i.e. water saturation, has occurred, but other than the channel filled by deposits of unit III (Foldout A) evidence is lacking. The lack of erosion channels and soil horizons in this section implies a relatively short eruptive episode which produced the deposit at the type section. In other areas, the presence of coarse volcanic conglomerates (i.e. Ma Butte) suggest erosion of steeper mountain slopes.

In the more distal areas, Blairmore sediments may carry abundant minerals derived from the volcanics suggesting erosion and redeposition by Blairmore rivers and streams.

Vent and Deposit Morphology

The interpretation of the morphology of early Crowsnest vents is made difficult by the lack of better exposure. However, the eruptions discussed above produce deposits which may form vents similar to those observed today (see Williams and McBirney, 1979). The following discussion describes a type vent for the Crowsnest with the knowledge that variations are bound to occur.

The ignimbrite and air-fall producing eruptions emplace deposits with well documented morphologies (Chapter III). Pyroclastic flow deposits may be emplaced down any side of the vent, though directional blasts favor deposition in a restricted direction (e.g. Mt. St. Helens). In cross-section, a deposit consists of many overlapping and inter-tonguing lenses of variable thicknesses. Air-fall deposits form large scale lobes down wind from the deposit. In proximal

areas the deposits probably have a similar morphology to flows.

A combination of air-falls, pyroclastic flows and lahars would produce a deposit of interfingering lenses. Add to this the deposits of multiple, relatively closely spaced vents, as postulated for the Crowsnest, and one is left with a very complex deposit with few correlatable horizons.

The deposits of the lower Crowsnest at the type section and throughout its exposure are dominated by pyroclastic debris with very minor lava flows (Foldout A and B). Williams and McBirney (1979) suggest that deposits dominated by pyroclastics, and especially those in continental regions would favor the development of a symmetrical composite cone or cones. The geomorphology of such cones are well documented by Green (1971).

Figure 7.2 gives a schematic representation of a possible lower Crowsnest vent. Three facies are postulated according to evidence from the type section.

Vent facies. The vent facies is delineated by the deposits which probably occurred within the vent of the proposed lower Crowsnest volcano. The facies is thought to be characterized by primary lavas which had formed a plug or small dome in the vent. Williams and McBirney (1979) have noted the formation of such plugs in other composite cones. Whether spines were formed is purely conjectural.

Proximal Vent Facies. A proximal vent facies is postulated to be dominated by viscous, toothpaste lavas, coarse pyroclastic lag deposits and subordinate pyroclastics (Figure 7.2). The rarity of flows in the exposed Crowsnest Formation combined with the abundance of cognate lithic clasts showing a trachytic flow texture provides evidence for the presence of the proximal, lava dominated facies. Further, the dominant pyroclastic suites of the Crowsnest would favor the formation of coarse, co-ignimbrite or co-air-fall deposits, similar to those described by Wright and Walker (1977). Such deposits would contain coarse blocks, boulders and bombs, forming coarse deposits close to the vent. High intensity eruptions may, however, remobilize such deposits.

Distal facies. The proposed distal facies would include deposits found on the flanks and lower slopes of the vent which are dominated by pyroclastic rocks of air-fall, pyroclastic flow and lahar origin. The type section along highway No.3 is thought to represent the distal facies; however, it is thought to lie close to the source, as erosional features and interfingering with the Blairmore Group are not well developed. It is thought that

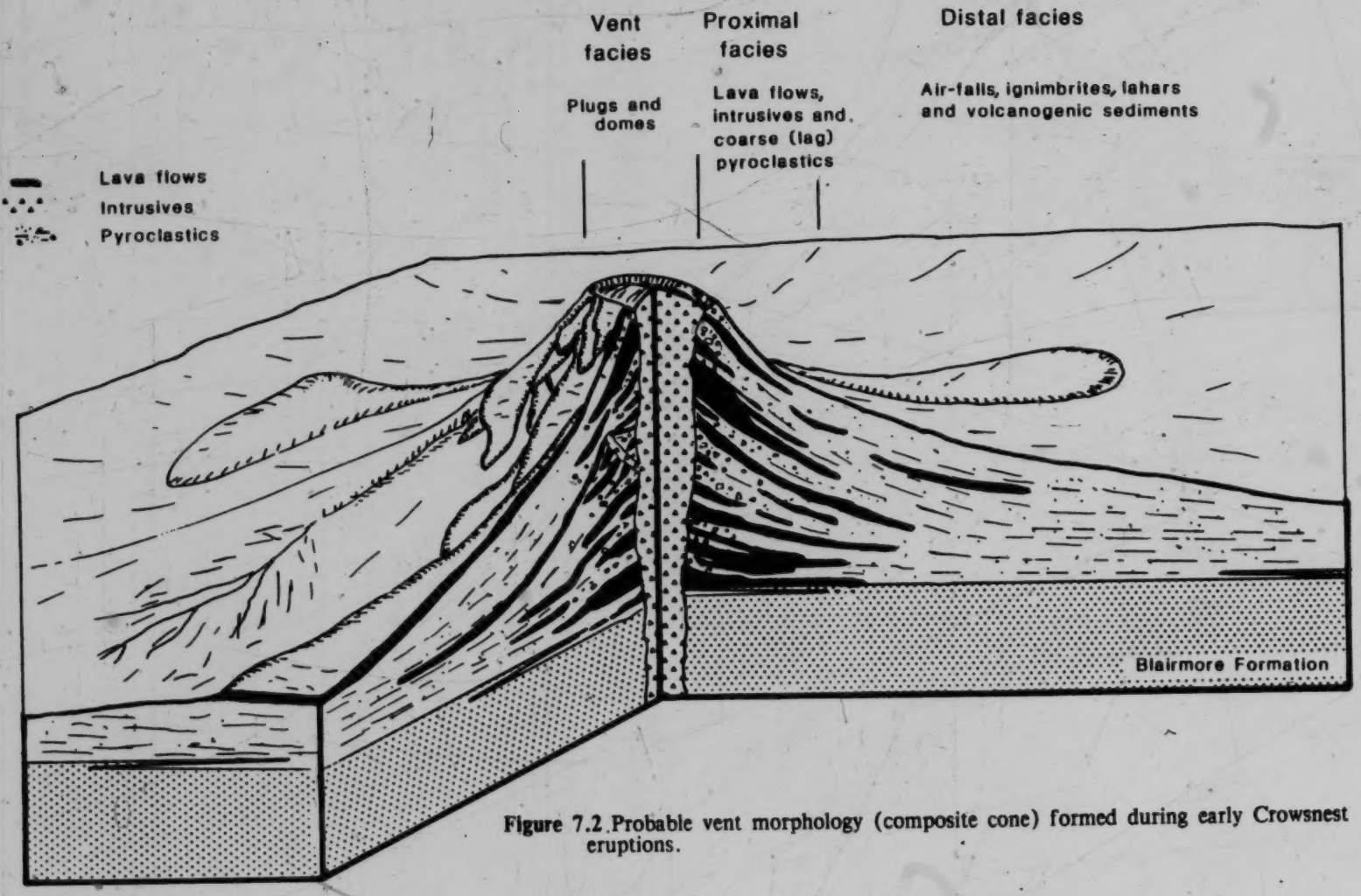

Figure 7.2 Probable vent morphology (composite cone) formed during early Crowsnest eruptions.

pyroclastic deposits lying on the steeper flanks may be more dissected by run off, while deposits well removed from the source would be reworked by Blairmore streams, e.g. Willoughby Ridge.

The surface of the cone was likely covered by drainage gullies which dumped fan-shaped deposits on the lower lying areas (Figure 7.1).

B. Late Eruptions

The distinctive character of the beds which comprise the upper member strongly resemble the block and ash flows first described by Parret (1937) and suggests the occurrence of late stage dome building eruptions which commonly occur in mature volcanoes (Williams and McBirney, 1979 and Fisher and Schmincke, 1984).

Eruption Model for the upper Crowsnest

Two eruptive phases are postulated to have occurred during the deposition of the upper member.

Moderately Gas-Charged Eruptions The base of the upper member is marked by what is here termed a transition zone (Foldout B). The deposits in this zone mark a change between the dominantly air-fall and ash flow tuff deposits of the lower member, and the massive agglomerates and pyroclastic breccias of the upper member. The deposits are similar to those of unit II from the lower member and consist of coarse to very coarse agglomerates and breccias accompanied by abundant surge deposits and subordinate air-falls (Plates 5.1a, 5.2a) The whole deposit is composed of apparently cyclic sequences of a basal agglomerate which grade vertically and laterally into surges, see Chapter V and VI.

According to modern observations, the deposits represent moderate to poorly gas-charged eruptions favoring pyroclastic flows over air-falls. In the transition zone at the base of the upper member, the deposits suggest that the eruptions were of this nature.

An idealized eruption model for the basal transition zone of the upper member is given in Figure 7.3a. The model implies moderate to poorly gas-charged, explosive eruptions which produced ash flows and block and ash flows in pulse like eruptions which resulted in the deposition of the observed cyclic squences. The eruptions mixed juvenile crystals, lithic fragments (blairmorite) and magma (bombs) with cognate material from

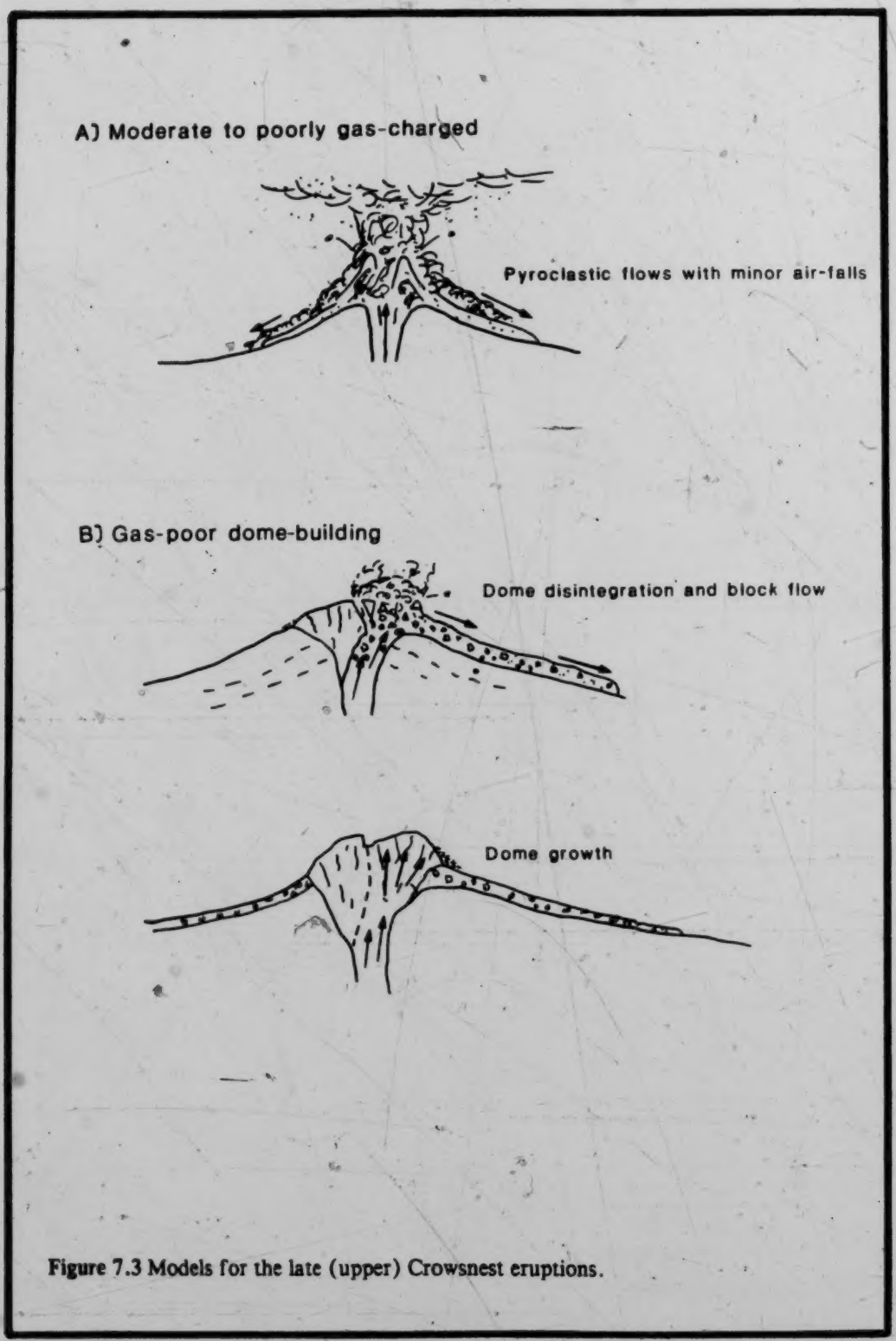
A) Moderate to poorly gas-charged
Pyroclastic flows with minor air-falls
B) Gas-poor dome-building
Dome disintegration and block flow
Dome growth

Figure 7.3 Models for the late (upper) Crowsnest eruptions.

domes, plugs, flows and pyroclastic debris from proximal areas about the vent. Air-fall components were minimal (Figure 7.3a).

Dome Eruptions The major portion of the upper member is composed of deposits which show a marked contrast from those which they overlie and suggest a major change in the type eruption. As described in Chapters V & VI, the deposits of the upper member consist of thickly-bedded, massive pyroclastic breccias. Deposits similar to those of the lower member and the transition zone are not present. The beds of this upper member are chiefly composed of cognate clasts (flows, early pyroclastics, blairmorite) and juvenile clasts (blairmorite and both hypabyssal and extrusive rocks). The matrix, although strongly altered and recrystallized, is finely crystalline and strongly resembles that of a dyke which is seen to intrude the sequence at the type section. This suggests the presence of a magmatic liquid as a supporting phase.

The deposits may be categorized as block flows which are characteristic of dome building eruptions, (Chapter III).

Figure 7.3b gives an idealized model for the eruptions which produced the thick flows of the upper member. By such a scenario, a dome building period would evolve from the early gas-charged eruptions. Eruptions would occur when magma, moving up the conduit, pushed through the dome fragmenting it and subsequently incorporating large blocks of the dome material (Figure 7.3b). The presence of fragments from earlier pyroclastic deposits (ash flows, surges, agglomerate and pyroclastic breccias) shows that parts of the earlier deposited cones were also incorporated. It appears that the fluid component was fairly high, and produced thick flows which were apparently mobile as evidenced by their exposure over great distances. The occurrence of multiple vents logically had substantial influence on the distances travelled. The resulting deposits represent a combination of a truly magmatic lava flow and a pyroclastic rock.

The presence of eruptions which may have occurred other than those described above is difficult to assess. It appears that some explosive activity may have been coincident, as a densely welded tuff has been identified at the top of the section sandwiched between two massive pyroclastic breccias. The deposit is thought to be air-fall, although evidence for this interpretation is inconclusive. Further, bombs up to 20cm long were found at the Oldman River section approximately 37 km north of the type section. It

is likely that the bombs originated by explosive eruptions, landed close to the vent and were later carried by the flow into which it dropped.

The time span over which these eruptions took place is difficult to determine on the basis of petrologic and geomorphologic evidence. With such thick, densely welded flows, the effects of surface erosion would be less dramatic than for the softer deposits of the lower member. At the type section, the contacts between flows are ambiguous and are only defined by faint color changes and abrupt changes in the size of the clasts. The presence of abundant charred plant remains in the upper member throughout the Crowsnest Formation suggests some time between eruptions. The upper member, at least at the type section, appears to have been fairly quickly deposited.

Vent and Deposit Morphology

The morphologies of vents dominated by domes have been well documented by Green (1971) and Williams and McBirney (1979). Based upon their observations an ideal vent for the upper Crowsnest is presented in Figure 7.4. The model depicts the vent morphology after substantial dome building eruptions. Once again variations are likely to occur.

The model depicts a vent dominated by a large dome which formed over the main conduit. By shear volume of the flows, it is probable that such domes achieved large sizes. It is not known if earlier domes were removed completely during subsequent eruptions.

Local debris pile are postulated to immediately flank the dome as a result of spalling during cooling. As shown, large scale fan-shaped flows representing those of the upper member run out from all sides of the summit.

In cross-section, the dome and its deposits are seen to truncate the earlier strata near the summit. This truncation is postulated due to the occurrence of early pyroclastic debris as clasts in the thick upper flows. Further, the upper flows are again seen to interfinger with each other and those from other vents. In areas removed from the immediate vicinity of the vent, the upper beds are found to conformably overly those of lower member. The type section is postulated to occur in these areas (Figure 7.4).

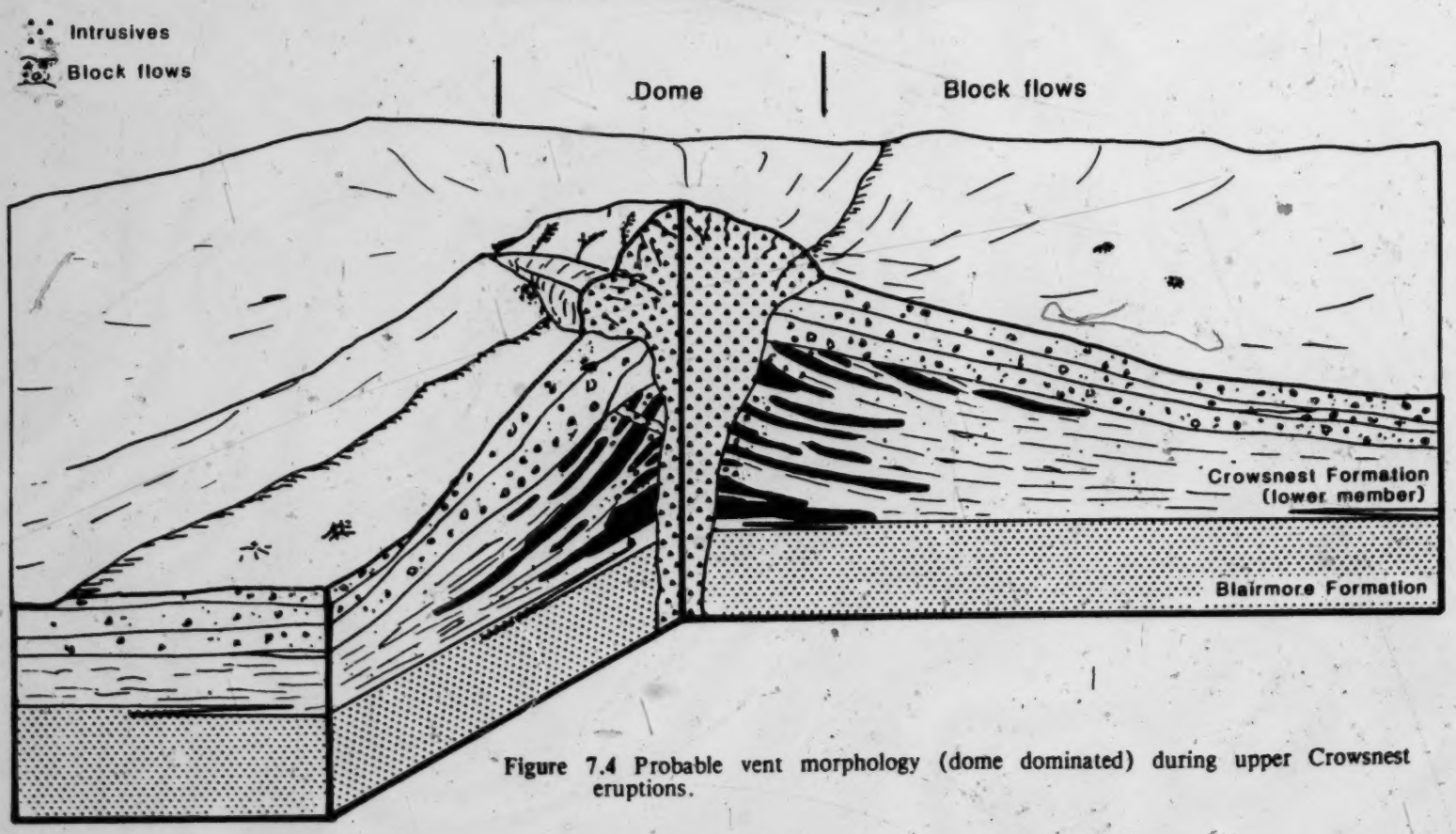

Figure 7.4 Probable vent morphology (dome dominated) during upper Crowsnest eruptions.

Discussion

Logically, the eruptions of the Crowsnest Formation followed an evolutionary path common to many modern volcanoes. Based upon evidence provided by the deposits of the Crowsnest, the above interpretations of the eruptives have been made.

Williams and McBirney (1979) describe the formation and evolution of a composite volcano. Classically the early stages are characterized by gas- charged eruptions which become increasingly less gas-charged until dome building stage is reached.

The deposits of the Crowsnest seem to represent just such an evolution (Figure 7.5). The early or youthful eruptions, proposed to be highly gas- charged, produced abundant air-falls and ignimbrites. Further, such eruptions show a cyclic evolution where single eruptions are initially gas-charged and give way to effussive late phases, producing plugs and flows. These types of eruptions have been described by Sheridan (1979).

With increasing age, the early gas-charged eruptions eventually gave way to moderately gas-charged eruptions and finally to relatively gas-poor dome-building eruptions characteristic of mature volcanoes (Williams and McBirney 1979).

If the thickness of the deposits formed by such eruptions are indicative of the length of time the process has occurred, then mature, dome building phases have clearly dominated the eruptive history of the Crowsnest (Figure 7.5). Certainly, the higher volumes of erupted material in the upper member may bias this approximation.

C. Geological History of the Crowsnest Formation

The evidence presented in the previous sections and chapters provides insight into the history of the eruptions which produced the deposits of the Crowsnest formation now visible at its type section. They are therefore discussed in relation to their geological setting.

Pre-Crowsnest: Early Upper Albian

During pre-Crowsnest time, erosion of the uplifted Cordilleran rocks to the west produced the thick sequences of continental sediments which make up the upper Blairmore Group (Glaister 1958, 1959; Norris 1964 and Williams and Stelck, 1975). To the east, the Joli Fou sea had begun its transgression into the interior of the continent, depositing the marine shales of the Joli Fou and equivalent formations (Figure 7.6a), (Williams and Stelck, 1975).

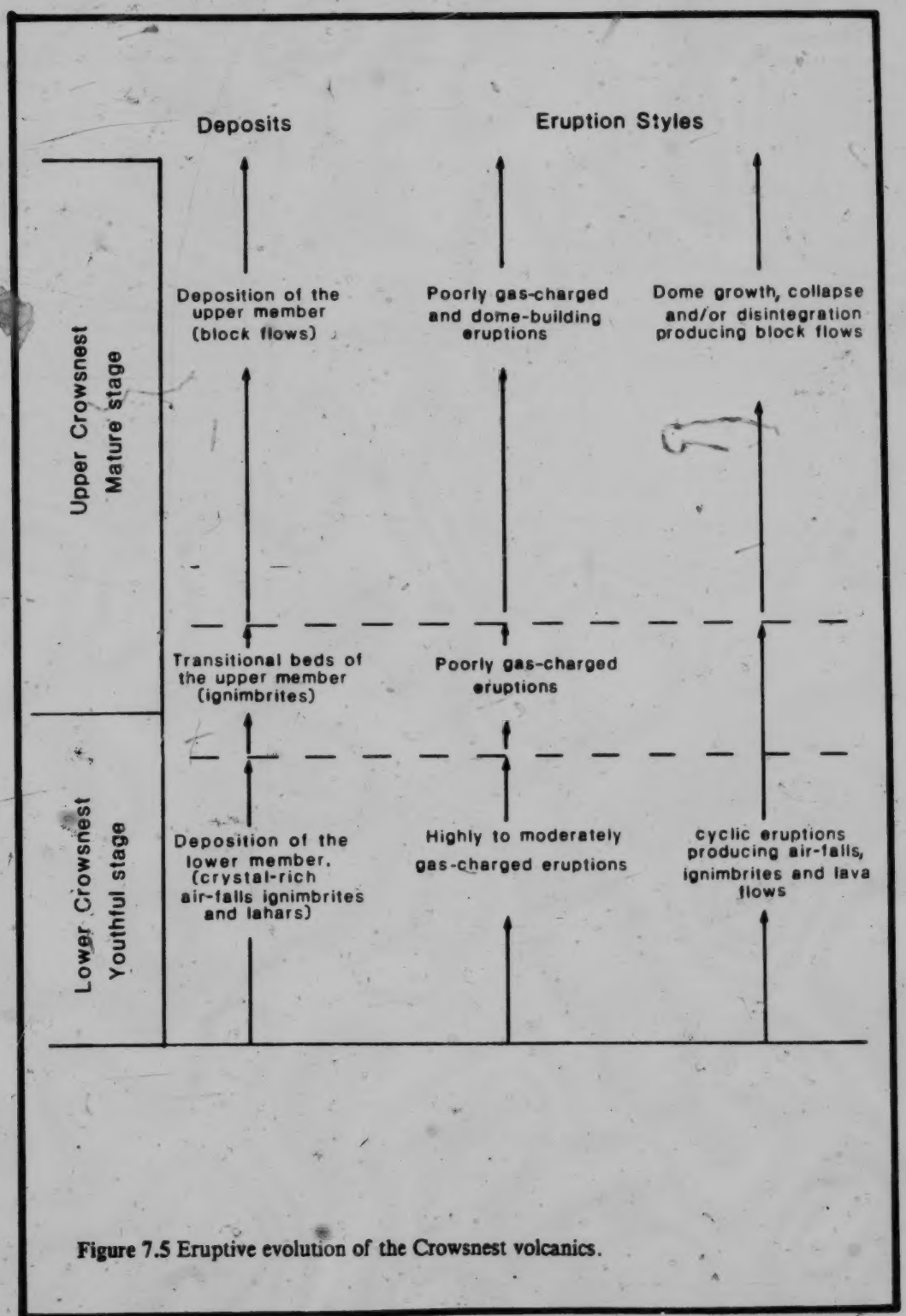
Deposits
Eruption Styles
Upper Crowsnest
Mature stage
Deposition of the upper member (block flows)
Poorly gas-charged and dome-building eruptions
Dome growth, collapse and/or disintegration producing block flows
Transitional beds of the upper member (ignimbrites)
Poorly gas-charged eruptions
Lower Crowsnest
Youthful stage
Deposition of the lower member, (crystal-rich air-falls ignimbrites and lahars)
Highly to moderately gas-charged eruptions
cyclic eruptions producing air-falls, ignimbrites and lava flows

Figure 7.5 Eruptive evolution of the Crowsnest volcanics.

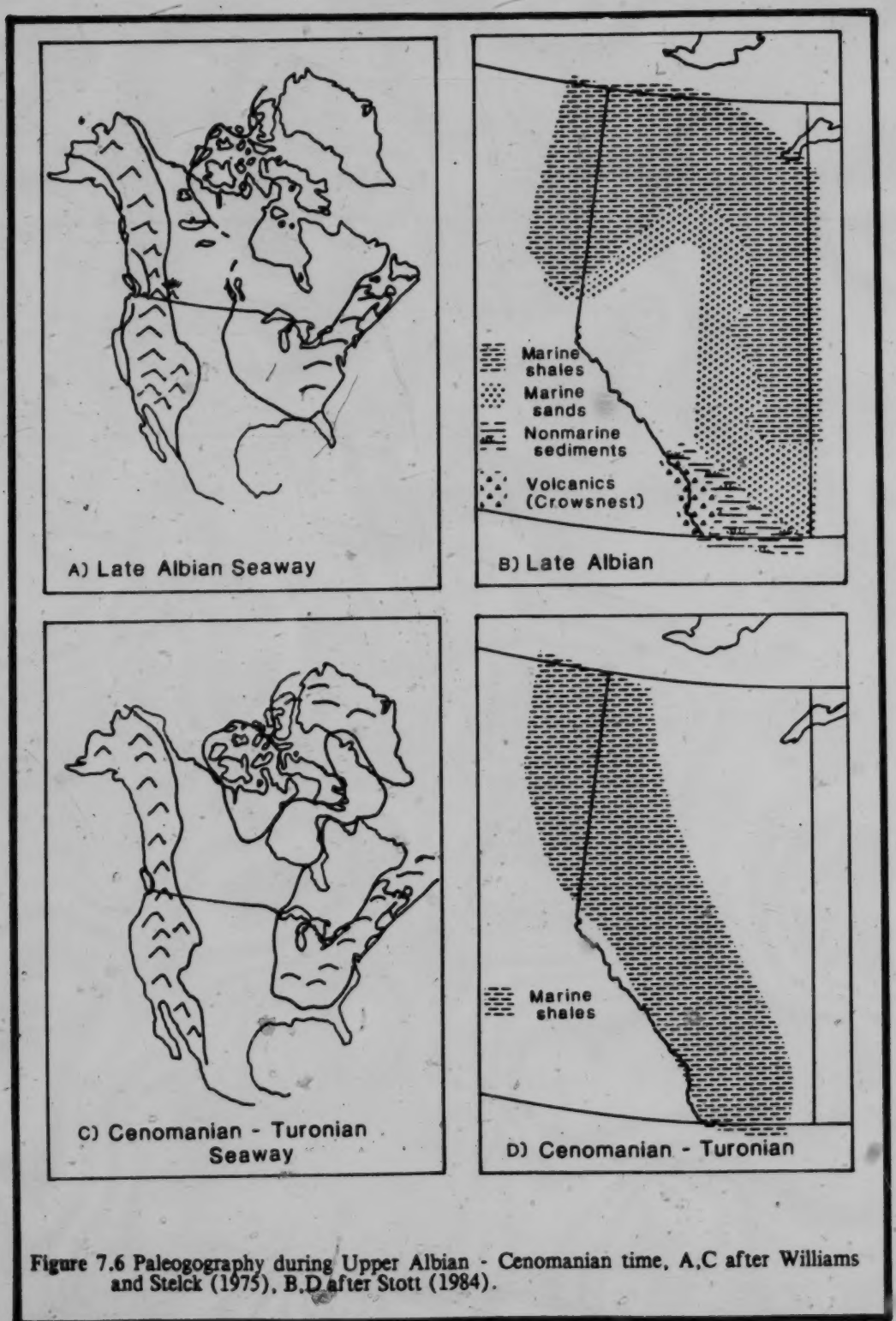

Figure 7.6 Paleogography during Upper Albian - Cenomanian time, A,C after Williams and Stelck (1975), B,D after Stott (1984).

The lack of bentonites in the Joli Fou Formation (Stelck pers. comm.) suggests local volcanism had not yet begun.

The sediments of the pre-Crowsnest Blairmore Group represent flood plain, lowland and littoral marine environments (Norris, 1964) which flanked the east side of the rising Cordillera. The surface of the flood plain was dominated by angiosperms, and conifers from fossil evidence provided by Bell (1956) and Norris (1964). Towards the beginning of Crowsnest time, minor shallowings of the inland sea initiated the deposition of the Viking Formation (Hein *et al.*, in press).

Crowsnest time: Middle Upper Albian

Crowsnest eruptions began around the time of the deposition of the Viking Formation (Figure 7.6a,b). The initial gas-charged, youthful eruptions formed composite cones on the flood plain east of the rising Cordillera (Figure 7.7). It is probable that different vents developed independently of each other (i.e. earlier or later) although their deposits almost certainly interfingered. Evidence indicates that fine ashes were probably ejected well up into the atmosphere and subsequently formed bentonites in areas far removed from the Crowsnest vents (see Amajor, 1985).

The eruptions eventually evolved into a mature, dome forming stage which produced the thick, massive deposits of the upper member. In local areas at least, these deposits capped those of the lower member, causing alteration while it cooled (Figure 7.8). This cap essentially shielded the softer rocks of the lower member from erosion.

Over the active phase of the Crowsnest, air-fall deposits were produced and probably resulted in the eventual deposition of ash well out into the Alberta basin. Deposits to the west are not expected to have survived due to erosion as the highlands continued to rise. The air-falls were likely most numerous during the early eruptive phases; however, the presence of a probable welded air-fall deposit at the top of the upper member suggests they may have been formed during mature eruptions. The following deposits may be a reflection of this airborne debris out in the Alberta basin:

1. Viking Bentonites (Amajor, 1978, 1985 shows three principle bentonites)
2. "Reds specks" in the Vaughn member of the Bow Island Formation. (Axford, 1953 and Glaister, 1959)

Figure 7.7 Paleogeography of southwestern Alberta during early (lower) Crowsnest time.

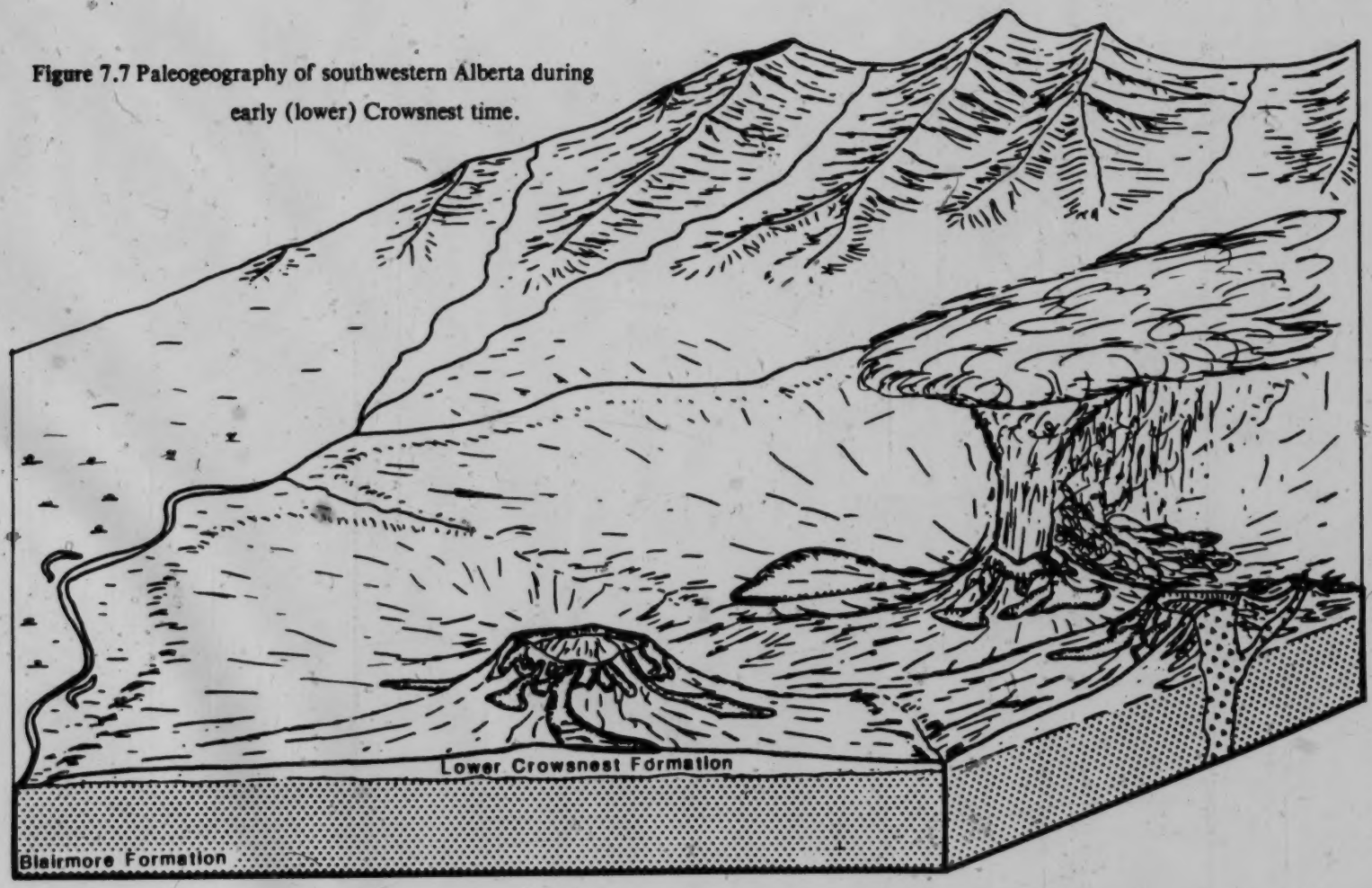

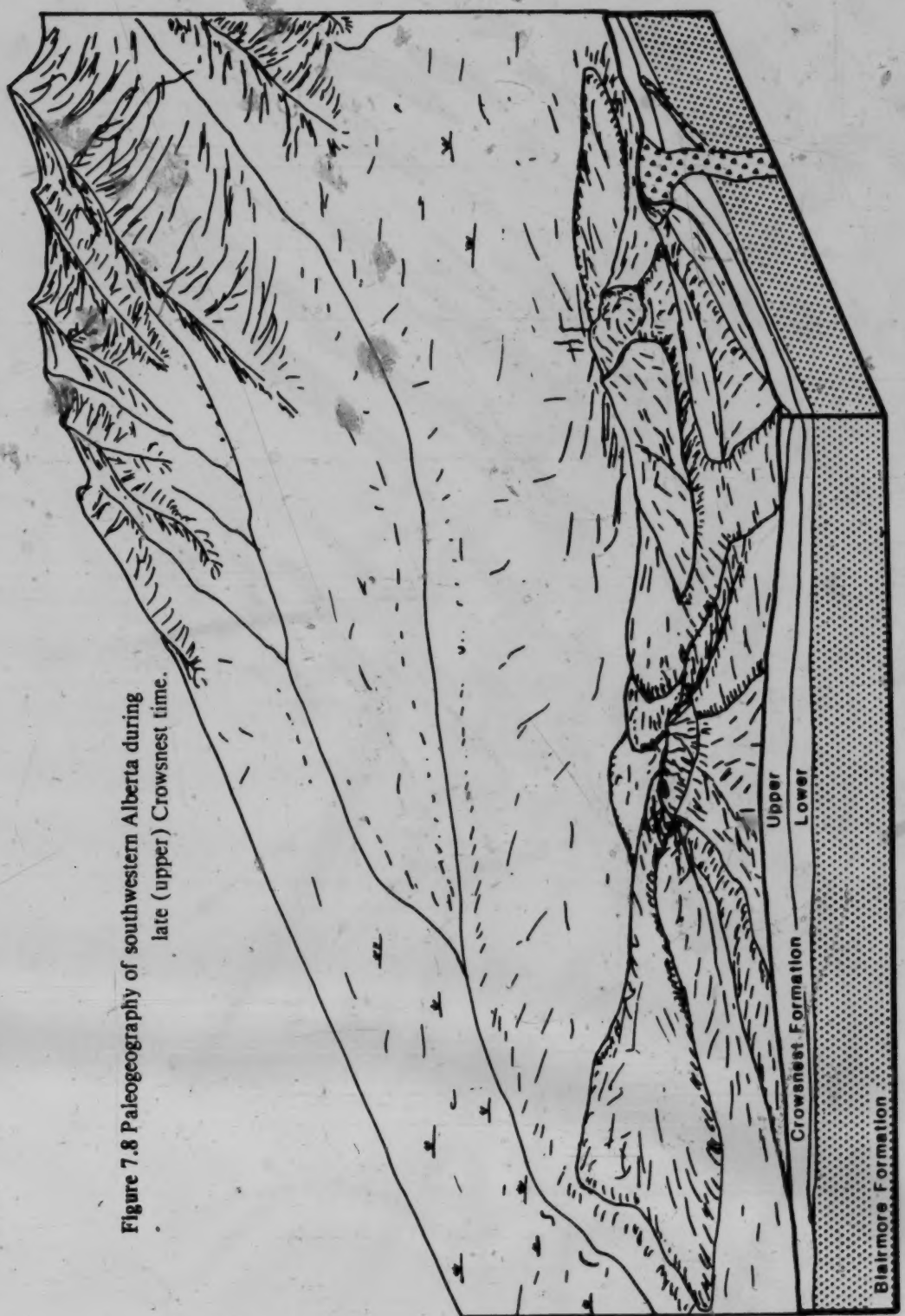

Figure 7.8 Paleogeography of southwestern Alberta during late (upper) Crowsnest time.

Figure 7.9 Paleogeography of southwestern Alberta during post Crowsnest time.

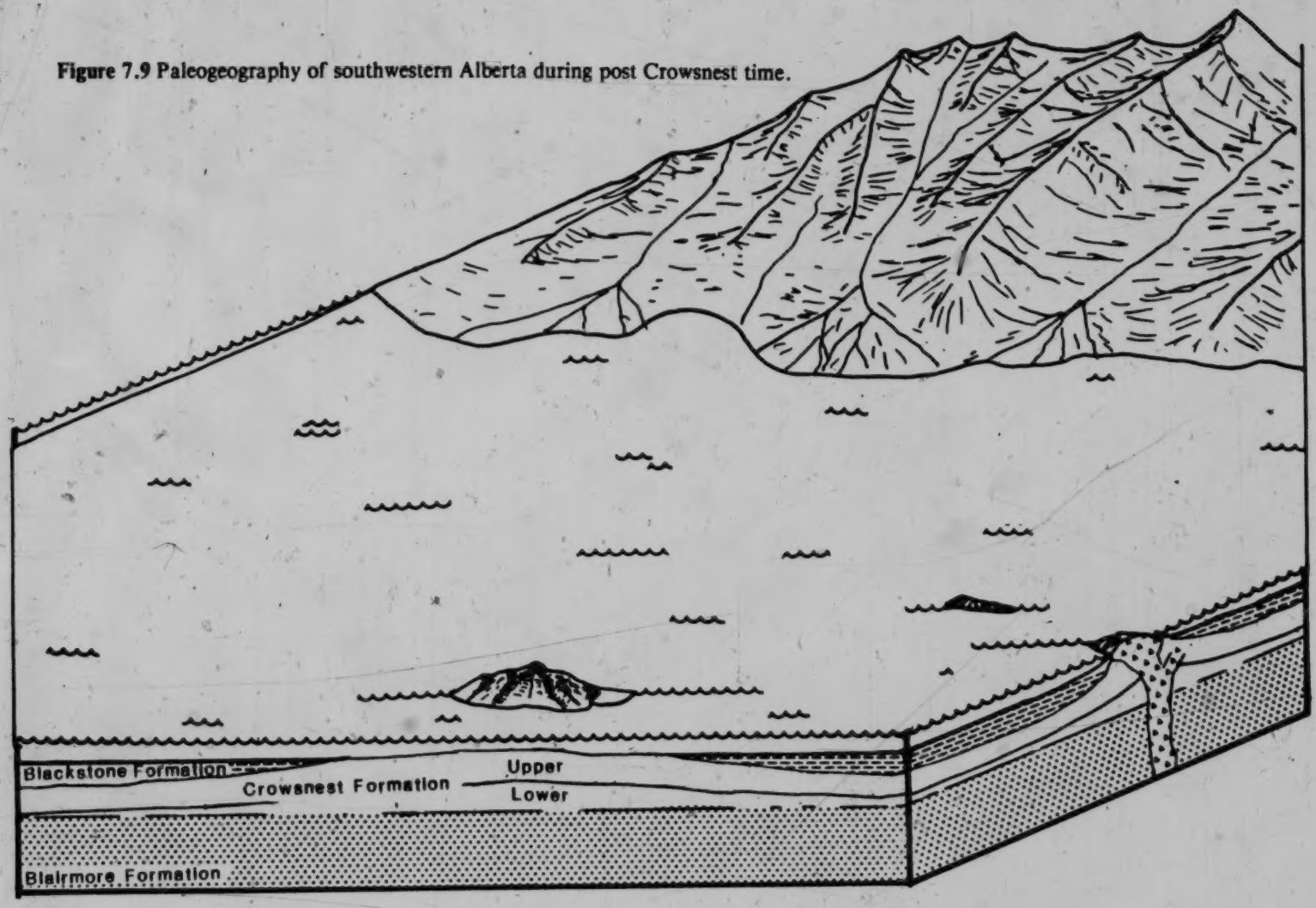

3. Bentonite beds and tuffaceous horizons in the top of the upper Blairmore Group (Carr, 1946).

The close of volcanic activity is difficult to determine. It is likely to have occurred before the transgression of the Cenomanian - Turonian sea in the area, (Figure 7.6c). It must have been pre-latest Cenomanian as the index fossil *Dunveganoceras* is found above the Crowsnest Formation on Mill Creek.

Post Crowsnest: Cenomanian-Turonian Time

Following the cessation of volcanism, the inland seaway transgressed during Cenomanian - Turonian time (Figure 7.6c). In all areas of its occurrence, the Crowsnest is overlain by marine shales suggesting a depositional hiatus between the end of volcanic activity and the transgression of the inland sea. Small sporadic eruptions may have produced some of the bentonites and tuffaceous horizons within the base of the Blackstone Formation; however, evidence for a direct association is lacking.

The transgression did not completely submerge the Crowsnest vents until at least Turonian time as the occurrence of *Inoceramus labiatus* directly above the Crowsnest Formation at its type section suggests. As the vents, probably representing maximum build-up of the volcanic pile, are not exposed, this submergence occurred after the minimum age provided by *I. labiatus*. Throughout the early transgression of this sea, therefore, the vents of the Crowsnest probably formed small, extinct volcanic islands immediately east of the Cordillera (Figure 7.9).

VIII. BIBLIOGRAPHY

Allen, J.R.L. 1982, Sedimentary Structures. Their character and physical basis. Volume 2, Elsivier, Amsterdam, 663p.

Amajor, L.C. 1978, A regional correlation of some bentonite beds in the lower Cretaceous Viking Formation of south-central Alberta, Canada. unpublished M.Sc. thesis, University of Alberta, 82p.

Amajor, L.C. 1985, Biotite grain size distribution and source area of the Lower Cretaceous Viking bentonites, Alberta Canada. Bulliten Canadian Petroleum Geology, 33, pp. 471 - 478.

Bell, W.A. 1956, Lower Cretaceous floras of western Canada. Geolgical Survey of Canada Memoir 285, pp. 15 - 17.

Best, M.G. 1982, Igneous and Metamorphic Petrology. 630 p. (pp. 204 207), W.H. Freeman and Company, San Fransisco.

Blatt, H., Middleton, G., Murry, R. 1980, Origin of Sedimentary Rocks, 2nd ed., pp. 292-293, Prentice - Hall Inc., Englewood, N.J.

Brindley, G.W. 1981, Clay mineral structures.*in*: Longstaffe, F.J. (ed), Short Course in Clays and the Resourse Geologist, Mineralogical Association of Canada Short Course 7 pp. 1 - 21.

Caldwell, W.G.E., North, B.R., Stelck, C.R. and Wall, J.H. 1978, A foraminiferal zonal scheme for the Cretaceous System in the interior planes of Canada. *in* Western and Arctic Biostratigraphy, C.R. Stelck and B.D.E. Chatterton eds, Geological Association of Canada, Special Paper 18, pp 495 - 475.

Cann, J.R. 1970, Rb, Sr, Y, Zr and Nb in some ocean floor basaltic rocks. Earth Planetary Science Letters, 10, pp.7-11

Carey, A. 1982, Mineralogical study of a sill in the Crowsnest Pass area, southwestern Alberta. Unpublished B.Sc. thesis, Univertsity of Calgary, 14p.

Carr, J.L. 1946, The geology of the Highwood-Elbow area, Alberta. unpublished M.Sc. thesis, University of Alberta, 200p.

Clow, W.H.A., and Crockford, M.B.B. 1951, Geology of the Carbondale River area, Alberta. Research Council of Alberta, Report 59, pp 20 -40.

Crandell, D.R. 1971, Post glacial lahars from Mount Rainer volcano , Washington. U.S. Geological Survey Professional Paper 677, pp.1-75.

Crowe, B.M. and Fisher, R.V. 1973, Sedimentary structures in Base surge deposits with special reference to cross bedding, Ubhebe Craters, Death Valley, California. Geological

Society of America Bulletin **84**, pp.663-682.

Currie, K.L. 1976, The alkaline rocks of Canada. Geolgical Survey of Canada Bulletin **239**, 228p.

Dean, M.E. 1985, Diagenesis of the Viking Formation. Unpublished M.Sc. Thesis, University of Alberta, 195p.

Dingwell, D.B., Brearly, M. 1985, Mineral chemistry of igneous melanite garnets from the analcite-bearing volcanic rocks, Alberta, Canada. Contributions to Mineralogy and Petrology **90**, pp. 29 - 35.

Dawson, D.M., 1885, Preliminary report on the physical and geological features of that portion of the Rocky Mountains between lattitudes 49° and 51°30'. Geology and Natural History Survey of Canada, pt. B, Annual Report, pp. 67-69B.

Dunn, T. and McCallum, I.S. 1981, The partitioning of Zr and Nb between diopside in melts in the system diopside - albite - anorthite. Geochimica et Cosmochimica Acta, **46**, pp. 623-629.

Eberl, D. 1978, Reactions for dioctahedral smectites. Clays and Clay Minerals, **26**, pp.327-340.

Ferguson, L.J. and Edgar, A.D. 1978, The petrogenesis and origin of the analcime in the volcanic rocks of the Crowsnest Formation, Alberta. Canadian Journal of Earth Science, **15**, pp. 69-77.

Fisher, R.V. 1960, Criteria for recognition of laharic breccias, southern Cascade Mountains, Washington. Geological Society of America Bulletin **71**, pp.127 - 132.

Fisher. R.V. 1961, Proposed classification of volcanoclastic sediments and rocks. Geological Society of America Bulletin **72**, pp. 1409 - 1414.

Fisher, R.V. 1966, Rocks composed of volcanoclastic fragments. Earth Science Review **1**, pp. 287 - 289.

Fisher, R.V. 1977, Erosion by volcanic base - surge density currents: U-shaped channels. Geological Society of America Bulletin **88**, pp. 1287-1297.

Fisher, R.V. 1979, Models for pyroclastic surges and pyroclastic flows. Journal of Volcanology and Geothermal Research **6**, pp. 305-318.

Fisher, R.V. 1983, Flow transformations in sediment gravity flows. Geology **11**, pp. 273-274.

Fisher, R.V. and Schmincke, H.U. 1984, Pyroclastic Rocks. Springer - Verlag, Berlin, Heidleburg, New York, Tokyo, 472p.

Fisher, R.V., Smith, A.L. and Roobol, M.J. 1980, Destruction of St. Pierre, Martinique by

ash cloud surges, May 8, and 20, 1902. Geology 8, pp. 472-476.

Folinsbee, R.E., Ritchie, W.D. and Stansberry, G.F. 1957, The Crowsnest volcanics and Cretaceous geochronology. Alberta Society of Petroleum Geologists, 7th Annual Field Conference Guidebook, pp. 20-26.

Folinsbee, R.E., Baadsgaard, H. and Cumming, G.L. 1963, Dating of volcanic ash beds (bentonites) by the K-Ar method. in Nuclear Geophysics Proceedings of a Conference, Woods Hole, Mass., June 7-9 1962. Nat. Acad. Sci, Nat. Res, Coun., pub 1075, pp. 70-82.

Folinsbee, R.E., Baadsgaard, H., Lipson, J.,1961, Potassium-argon dates of Upper Cretaceous ash falls, Alberta, Canada. Annals N.Y. Academy of Science 91, pp. 352-359.

Foscolos, A.E., Reinson, G.E. and Powell, T.G. 1982, Controls on clay-mineral authigenesis in the Viking sandstone, central Alberta. 1. shallow depths. Canadian Mineralogist 20, pp. 141-150.

Glaister, R.P. 1959, Lower Cretaceous of southern Alberta and adjoining areas. American Association of Petroleum Geologists 43, pp. 590-640.

Glaister, R.P. 1959, Petrology of the Blairmore sandstones. Alberta Society of Petroleum Geologists 6, pp. 43-49.

Green, J. and Short, N.M., (eds) 1971, Volcanic Landforms and Surface Features: A Photographic Atlas and Glossary. Springer - Verlag, 519p.

Goff, S.P. 1984, The magmatic and metamorphic history of the East Arm, Great Slave Lake, N.W.T.. Unpub. Ph.D. Thesis, University of Alberta.

Gold, D.P. 1963, Average chemical compositions of carbonatites. Economic Geology, 58, pp. 988 - 991.

Gordy, P.L. and Edwards, G. 1962, Age of the Howel Creek intrusives. Journal Alberta Society of Petroleum Geologists 10 pp. 369-372.

Grim, R.E. and Guven, N. 1978, Bentonites, Geology, Mineralogy, Properties and Uses. Elsevier Sciientific Pub. Co., 256p.

Hebner, B.A., Longstaffe, F.J. and Bird, G.W. 1985, Fluid - pore mineral transformation during simulated steam injection: implications for reduced permeability damage. Petroleum Society of Canadian Institute of Mining Paper 85-36-17.

Hein, F.J., Dean, M.E., Delure, A.M., Grant, S.K., Robb, G.A. and Longstaffe, F.J., In press, Regional sedimentology of the Viking Formation, Caroline, Garrington and Harmatten East Fields, western south - central Alberta: storm and current - influenced shelf settings. Bulletin Canadian Society of Petroleum Geology.

Heinrich, E. Wm. 1966, The Geology of Carbonatites. 555p. Rand McNally, Chicago.

Hoffman, J. and Hower, J. 1979, Clay mineral assemblages as low grade metamorphic geothermometers, application in the thrust faulted disturbed belt of Montana, U.S.A. *in:* Aspects of Diagenesis, P.A. Scholle and P.R. Schluger, eds. Society of Ecomonic Paleontologists and Mineralogists Special Publication **26**, pp. 55-79.

Hoblitt, R.P. and Kellogg, K.S. 1979, Emplacement temperatures of unsorted and unstratified deposits of volcanic rock debris as determined by paleomagnetic techniques. Geological Society of America Bulletin (part 1) **90**, pp. 633 - 642.

Holland, H.D. and Brocsik, M. 1965, On the solution and deposition of calcite in hydrothermal systems: Symposium on the problems of post magmatic ore deposition. Prague **2**, pp. 364 - 374.

Hower, J. 1981, X-Ray diffraction identification of mixed layer clay minerals. *in:* Short Course in Clays and the Resource Geologist, F.J. Longstaffe ed. Mineralogical Association of Canada Short Course 7, May 1981.

Hughs, C.J. 1973, Spillites, Keratophyres and the igneous spectrum. Geological Magazine **109**, pp. 513-527.

Ignasiak, T.M., Kotlyar, L. Longstaffe, F.J.L., Strauss, O.P. and Montgomery, D.S. 1983, Separation and characterization of clay from Athabasca asphaltene. Feul, **62**, pp. 353 - 362.

Irvine, T.N. and Baragar, W.R.A. 1971, A guide to the chemical classification of the common volcanic rocks. Canadian Journal of Earth Science **8**, pp. 523-548.

Janda, R.J., Scott, K.M., Nolan, K.M. and Martinson, H.A. 1981, Lahar movement, effects and deposits. *in:* The 1980 eruptions of Mount St. Helens, Lipman, P.W. and Mullineaux, D.R., eds. U.S. Geological Survey Professional Paper **1250**, pp. 461 - 478.

Kastner, M. and Siever, R. 1979, Low temperature feldspars in sedimentary rocks. American Journal of Science **279**, pp. 435-479.

Knight , C.W. 1904, Analcime - trachyte tuffs and breccias from southwest Alberta, Canadian Record of Science **9**, pp. 265-278.

Larson, E.S., and Buie, B.F. 1938, Potash analcime and pseudoleucite from the Highwood Mountains of Montana. American Mineralogist **23**, pp. 837-849.

Leach, W.W. 1902, Annual Report, Geological Survey of Canada XV, p. 171A.

Leach, W.W. 1912, Geology of the Blairmore map area, Geological Survey of Canada, Summary Report 1911, pp. 192-200.

LeBas, H.M. 1977, Carbonatite - Nephelinite Volcanism, an African Case History, Wiley Interscience, New York, 347p.

Lerbekmo, J.F. and Campbell, F.A. 1969, Distrabution, composition and source of the White River Ash, Yukon Territory. Canadian Journal of Earth Science **6**, 109-116.

Loranger, D.M. 1951, Useful Blairmore microfossil zone in central and southern Alberta, Canada. American Association of Petoleum Geologists Bulletin **35**, pp. 2348-2367.

Mackenzie, J.D. 1913, Southfork coal area, Oldman river, Alberta. Geological Survey of Canada, Summary Report 1912.

Mackenzie, J.D. 1914, Geological Survey Canada Museum Bulletin **4**, Series 20, Nov 19, 1914, pp. 1 - 30.

MacKenzie, J.D. 1915, The primary analcite of the Crowsnest volcanics. American Journal of Science **39**, pp. 571-574.

MacKenzie, H.N.S. 1956, Crowsnest Volcanics. Journal Alberta Society of Petroleum Geologists **4**, pp. 70-74.

Mellon, G.B. 1967, Stratigraphy and petrology of the lower Cretaceous Blairmore and Mannville Groups, Alberta foothills and plains, Research Council of Alberta Bulletin **21**, 269p.

Miller, C.D. 1978, Holocene pyroclastic flow deposits from Shasta and Black Butte, west of Mount Shasta, California. Journal of Research, United States Geological Survey **6**, pp. 611 - 624.

Miller, T.P. and Smith, R.L. 1977, Spectacular mobility of ash flows around Aniakchak and Fisher calderas, Alaska. Geology **5**, pp. 173-176.

Norris. D.K. 1964, Cretaceous of the southeastern Canadian Cordillera. Canadian Petoleum Geology Bulletin **12**, Field Conference Guidebook, pp.512-535.

Pearce, J.A. and Cann, J.R. 1971, Ophiolite origin investigatedby discriminant analysis using Ti, Zr, and Y. Earth and Planetary Sciences, Letters **12**, p 339.

Pearce, T.H. 1967, The analcite-bearing rocks of the Crowsnest Formation. Ph.D. thesis, Queens University , Kingston Ontario, 181p.

Pearce, T.H. 1970, The analcite-bearing volcanic rocks of the Crowsnest Formation, Alberta. Canadian Journal of Earth Science **7**, pp.46-66.

Perret, F.A. 1937, The eruption of Mt. Pelee 1929 -1932. Carnegie Institute of Washington Publication **458**, pp. 1 - 126.

Pevear, D.R., Williams, V.E. and Mustoe, G.E. 1980, Kaolintite, smectite and K-rectorite in bentonites, relation to coal rank at Tulameen, British Columbia, Clays and Clay Minerals **28**, pp.241-254.

Pevear, D.R. Dethier, D.P. and Frank, D. 1982, Clay minerals in the 1980 deposits from Mount St. Helens. Clays and Clay Minerals **30**, pp. 241-252.

Price, R.A.,1959, Flathead British Columbia - Alberta. Geological Survey of Canada, map 1-1959. Price, R.A.,1962, Fernie map-area, east half, Alberta and British Columbia. Geological Survey of Canada Paper 61-25, 65p.

Ricketts, B.D. 1982, Laharic breccias from the Crowsnest Formation, southwestern Alberta. Current Research, part A, Geological Survey of Canada Paper 82-1A, pp. 83 - 87.

Reynolds, R.C. 1980, Interstratified clay minerals. *in*: Crystal structures of clay minerals and their X-ray identification. G.W. Brindley and G.W. Brown, eds., Min. Soc. London.

Reynolds, R.C., and Hower, J. 1970, The nature of interlayering in mixed-layer illite - montmorillonites. Clays and Clay Minerals **18**, pp. 25-36.

Roberson, H. E. and Lahann, R.W. 1981, Smectite to illite conversion rates, effects of solution chemistry. Clays and Clay Minerals **29**, pp. 129-135.

Rose, W.I., Jr., Pearson, T. and Bonis,S. 1977, Nuee ardente eruptions from the foot of a dacite lava flow, Santiaguito Volcano, Guatemala, Bulletin of Volcanology **40**, pp. 1 - 16.

Rowley, P.D., Kuntz, M.A. and Macleod, N.S. 1981, Pyroclastic flow deposits. *in:* The 1980 eruptions of Mount St. Helens, Washington. Lipman, P.W. and Mullineaux, D.R., eds. U.S. Geol. Survey Prof. Paper **1250**, pp. 489 - 512.

Rowley, P.D., MacLeod, N.S., Kuntz, M.A. and Kaplan, A.M., 1985, Proximal bedded deposits related to pyroclastic flows of May 18, 1980, Mount St. Helens, Washington. Geologicl Society of America Bulletin **96**, pp. 1373 - 1383.

Rutherford, R.L. 1938, Crystal habit of the orthoclase in the Crowsnest volcanics at Coleman, Alberta. University of Toronto, Studies, Geological Survey **41**, pp. 67-70.

Sarna-Wojcicki, A.M., Shipley, S., Waitt, R.B., Jr., Dzurisin, D. and Wood, S.H. 1981, Areal distribution, thickness, mass, volume and grainsize of air- fall ash from six major eruptions of 1980. *In:* The 1980 eruptions of Mount St. Helens, Washington. Lipman, P.W. and Mullineaux, D.R., eds. U.S. Geological Survey Professional Paper **1250**, pp. 577 - 600.

Schmid, R., 1981, Descriptive nomenclature and classification of pyroclastic deposits and fragments: Recommendations of the IUGS Subcommission on the Systematics of Igneous Rocks. Geology **9**, pp. 41 - 43.

Schmincke, H.U., Fisher, R.V. and Waters, A.C. 1973, Antidune and chute and pool

structures in the base surge deposits of the Laacher Sea area Germany, Sedimentology 20, pp. 553-574.

Sheridan, M.F. 1979, Emplacement of pyroclastic flows: A review. Geological Society of America Special Paper 180, pp.125 - 136.

Sheridan, M.F. and Updike, R.G. 1975, Sugarloaf Mountain tephra - a Pleistocene rhyolitic deposit of base - surge origin. Geolgical Society of America Bulletin 86, pp.571 - 581.

Smith, G.A. 1986, Coarse-grained nonmarine volcaniclastic sediment: Terminology and depositional process. Geological Society of America Bulletin 97, p 1 - 10.

Sparks, R.S.J. 1976, Grainsize variations in ignimbrites and implications for the transport of pyroclastic flows, Sedimentology 23, pp.147-188.

Sparks, R.S.J. 1979, Gas release rates from pyroclastic flows: An assessment of the role of fluidization in their emplacement. Bulletin of Volcanology 41, pp.1-9.

Sparks, R.S.J. 1982, Modern silicic volcanism, development of facies models and guide to mineralization. A short course presented to the University of Western Australia in 1982 by R.S.J. Sparks, Cambridge Universty.

Sparks, R.S.J., Self, S. and Walker, G.P.L. 1973, Products of ignimbrite eruption. Geology 1, pp. 115 - 118.

Sparks, R.S.J. and Walker, G.P.L. 1973, The ground surge deposit: a third type of pyroclastic rock. Nature and Physical Science 241, pp. 62 - 64.

Sparks, R.S.J. and Wilson, L. 1976, A model for the formation of ignimbrite by gravitational column collapse. Journal Geological Society of London 132, pp. 441-451.

Sparks, R.S.J., Wilson, L. and Hulme, G. 1978, Theoretical modeling of the generation, movement and emplacement of pyroclastic flows by column collapse. Journal of Geophyscal Research 83, pp.1727-1739.

Sparks, R.S.J., and Wright, J.V. 1979, Welded air - fall tuffs. Geological Society of America Special Paper 180, pp. 155-166.

Srodon, J. 1980, Precise identification of illite/smectite interstratifications by X-ray powder diffraction. Clays and Clay Minerals, 28 pp. 401-411.

Srodon, J. 1981, X-ray identification of randomly interstratified illite-smectite in mixtures with discrete illite. Clay Minerals 16, pp. 297-304.

Srodon, J 1984, X-Ray powder diffraction identification of illitic clay minerals. Clays and Clay Minerals 32, pp. 337-349.

Stelck, C.R., Wall, J.H., Bahan, W.G. and Martin, L.J., 1956, Middle Albian Foraminifera from Athabasca and Peace River drainage areas of western Canada. Research Council of Alberta Report 75, 60p.

Stelck, C.R. 1975, The upper Albian *Milliamina manitobensis* zone in northwestern British Columbia. Geological Association of Canada, Special Paper 13, pp. 253 - 275.

Stelck, C.R. 1958, Sratigraphic position of the Viking sand. Alberta Society of Petroleum Geologists Journal 6, pp.2-7.

Stott, D.F. 1963, The Cretaceous Alberta Group and equivalent rocks, Rocky Mountain foothils, Alberta. Geological Survey of Canada Memoir 317, pp. 22 - 292.

Stott, D.F. 1984, Cretaceous sequences of the foothills of the Canadian Rocky Mountains, *in:* The Mezozoic of Middle North America, D.F. Stott and D.J. Glass eds., Canadian Society of Petroleum Geologists, Memoir 9, pp.85 - 107.

Taylor, G.A. 1958, The 1951 eruption of Mount Lamington, Papau. Australian Bureau of Mineral Resources, Geology Geophysics Bulletin 38, pp. 1 - 11.

Thompson, R.L. and Axford, D.W.A. 1953, Notes on the Cretaceous of southwestern Alberta. Alberta Society of Petroleum Geologists, Third Annual Field Conference Guidbook, pp.32-59.

Tizzard, P.G. and Lerbekmo, J.F. 1975, Depositional history of the Viking Formation, Suffield Alberta, Canada. Bulletin of Canadian Petroleum Geology 23, pp.715-756.

Walker, G.P.L. 1972, Crystal concentration in ignimbrites. Contributions to Mineralogy and Petrology 36, pp.135 - 146.

Walker G.P.L. 1973, Explosive volcanic eruptions-a new classification scheme, Geol Rundsch. 62, pp, 431 - 446.

Walker, G.P.L., Wilson, C.J.N. and Froggat, P.C. 1981, An ignimbrite veneer deposit - The trail marker of a pyroclastic flow, Journal of Volcanology and Geothermal Research 9, 409-421.

Warren, P.S. 1933, Geological Section in Crowsnest Pass. Royal Canadian Institute, Transactions XIX, pt. 2, pp. 56-70.

Warren, P.S. and Stelck, C.R. 1958, Continental margin, western Canada Journal Alberta Society of Petoleum Geologists, 6 pp. 29-41.

Waters, A.C. and Fisher, R.V. 1971, Base surges and their deposits: Capelinhos and Taal volcanoes. Journal of Geophysical Research 766 , pp. 5596 - 5614.

Wedepohl, K.H. 1978, ed. Handbook of Geochemistry, Springer - Verlag, Berlin - Heidelberg - New York.

Williams G.D. and Stelck, C.R. 1975, Speculations on the Cretaceous paleogeography of North America. *in:* The Cretaceous System in the Western Interior of North America. W.G.E. Caldwell (ed). Geological Association of Canada, Special Paper **13**, pp. 1 - 20.

Williams, H. and McBirney, A. 1979, Volcanology. Freeman, Cooper and Co., San Francisco, 391p.

Wilson, C.J.N. and Walker, G.P.L. 1982, Ignimbrite depositional facies: the anatomy of a pyroclastic flow. Journal Geological Society of London **139**, pp.581 - 592.

Winchester, J.A. and Floyd, P.A. 1977, Geochemical discrimination of different magama series and their differentiation products using immobile elements. Chemical Geology **20**, 1977, pp. 235-343.

Wohletz, K.H. and Sheridan, M.F. 1979, A model of pyroclastic surge. Geological Society of America, Special Paper **180**, pp. 177 - 194.

Wooley, A.R. and Symes, R.F.,1976, The analcime porphyritic phonolites blairmorites and associated kenytes of Lupata Gorge, Mozambique. Lithos, **9**, pp. 9-1.

Workman, L.E. 1959, The Blairmore Group in the subsurface of Alberta. Alberta Society of Petoleum Geologists, Guidebook, 9th Annual Field Conference, pp.122-129.

Wright, J.V. and Walker, G.P.L. 1977, The ignimbrite source problem, significance of a co-ignimbrite lag fall deposit. Geology **5**, 729 - 732.

IX. APPENDIX A

A. PROPOSED TYPE SECTION STRATIGRAPHIC COLUMN

General Characteristics

Exposures at the proposed type section exhibit the following features which are common throughout the sequence:

1. All deposits are parallel-bedded except where noted otherwise. Some may show pinch and swell features.
2. The strike is between 0 and 15° north and the dip is between 45 and 55° west.
3. With some exceptions, all beds contain matrix, phenocryst and rock fragment phases unless noted.

Stratigraphic Descriptions (see Foldout A)

Unit I

O "O" - marker at most eastern exposure of Crowsnest volcanics.

O - 2.75 m. Recessive outcrop. The zone consisted of a very poorly sorted deposits containing coarse cognate (rounded) fragments and occasional purple shale lenses or clasts. The matrix is clay-rich and contains abundant garnet, sanidine and other crystal components. Minor malachite (Cu) stain Bedding is very poorly defined. (WCH-1 (matrix), WCH-2 (matrix)).

2.75 - 4.99 m. Continuation of the deposit from below, with increasing abundance of garnets in the clay-rich matrix. Again, bedding contacts, if any, are poorly defined. (WCH-3, (matrix), WCH-4 (matrix), WCH-5 (cognate clast)).

4.99 - 9.36 m. Continuation of the lower deposit. Matrix is becoming light green and may contain garnet and/or sanidine-rich horizons. The deposit remains very poorly sorted (WCH-6 (cognate clast), WCH-7 (matrix)).

9.36 - 10.36 m. As below, red shale lenses and clasts becoming slightly more abundant and may define a faint bedding plane (WCH-8, matrix).

10.36 - 10.43 m. Purple, crystal tuff containing fine crystals, <2mm, and small lithic fragments (WCH-9).

10.43 - 12.43 m. Poorly sorted bed similar to those below the purple tuff. Contains cognate fragments, accidental shale lenses/fragments (red & brown) supported by a dark green, clay-rich matrix containing abundant crystals (garnets and sanidines). The upper bedding plane is vague and is defined by an apparent broken shale horizon (WCH-10, matrix).

12.43 - 14.93 m. As below, poorly sorted bed with slightly increased abundances of shale lenses. Occasional garnet/sanidine-rich horizons in the matrix. Upper contact is defined by a discontinuous red shale horizon. A white clay rim is noted on many cognate fragments (WCH-11, shale clast; WCH-12, matrix).

Unit II

14.93 - 19.93 m. This interval consists of two deposit types: The lower is dominated by thinly-bedded, purple, crystal tuffs; pink, crystal tuffs and lapilli tuffs and light green, crystal ashes/tuffs many of which are calcareous (wch-14). The pink beds are

generally more resistant and contain sanidine and garnet as major constituents. Internally, some beds show reverse and/or normal grading, however, it is generally poorly defined. Bedding generally does not exceed 20 cm. Contacts may be sharp or gradational. The upper contact of these deposits is abrupt and unconformable, showing 1.5-2 meters of relief, marked by a thin (.5cm) green clay horizon. The thin beds are deformed at the contact and dip slightly into the channel.

Infilling the channel is a massive, coarse, pink/brown agglomerate consisting of large, round to subrounded cognate clasts which exhibit trachytic textures, baked rims, and slight plastic deformation. The matrix consists of euhedral, broken sanidines and garnet crystals averaging around 2 mm and less. Occasionally, a faint trachytic texture is observed in matrix. The bed is clast supported and ranges from 2 meters to 5 meters (channel) in thickness. The clasts fine slightly towards the upper contact which is sharply gradational into cross-bedded surge deposits. (WCH-13, coarse agglomerate)(WCH-14, (Plate 2.7a) calcareous, lower pink crystal tuff), (see Plates 5.1b. 5.3d).

19.93 - 26.53 m. Cyclic, sequences: fine pink agglomerate - lapilli tuff-surge. (Plate 5.3d) Agglomerates (coarse-medium lithic lapilli tuffs) are fine-grained (ave. 3cm) containing cognate clasts. Basal contacts are generally well defined. Basal agglomerates fine into massive, pink crystal lapilli tuff which may grade vertically and laterally into cross-bedded/laminated deposits. Occasionally large round cognate clasts may occur in the finer deposits. Some are draped by surges (defined by density stratified horizons)(WCH-15, WCH-16).
The upper bed is marked by a 1 m agglomerate. The top of which shows an abrupt contact with more recessive overlying beds.

Unit III

26.53 - 26.88 m.
+ 15 cm: Thin, well bedded green crystal ash (4 cm) + crystal lithic tuff (purple).
+10 cm: Reverse graded, lithic tuff with increasing size of lithic fragments to the top.
+ 7 cm: pink crystal lapilli tuff.
+12 cm: 3-4 green crystal ash beds. of approx. 4 cm each. Some may normally grade into thin brown clay horizons (bentonite).

26.88 - 27.48 m. Purple, coarse tuff - lapilli tuff, lithic and crystal-rich, poorly consolidated and poorly sorted, clasts up to 2 cm. Base of the first trilogy (WCH-18).

27.48 - 27.53 m. Green crystal (garnet and sanidine) coarse ash, very poorly consolidated with a green clay matrix. Contains abundant Fe-calcite (replacement) in the matrix. No depositional features were observed (WCH-19).

27.53 - 27.60 m. Purple, coarse-medium crystal/lithic tuff similar to WCH-18 poorly consolidated with moderate sorting. Larger sanidines may occur (WCH-20).

27.60 - 27.84 m. Massive, purple, coarse tuff with small garnet, sanidine and analcime crystals (euhedral) supported in a fine, well consolidated, purple tuff matrix. Becomes poorly consolidated towards the top where pea-sized lithic fragments occur (Reverse grading?). WCH-21 and 22.

27.84 - 28.2 m. Brown-green, poorly lithified, coarse, crystal tuff/ash with green crystal tuff lenses carrying euhedral, broken sanidines. Gradational upper and lower bedding contacts. Moderately recessive.

28.2 - 28.48 m. Purple-brown, coarse crystal tuff wth large euhedral sanidine crystals up to 1.5 cm and slightly smaller euhedral garnets supported by a fine tuff matrix. Slight reverse grading is noted with respect to sanidine crystals. Slightly gradational bedding contacts, recessive.

28.48 - 28.52 m. Green, coarse, crystal ash (sanidine + garnets) with green clay matrix, very poorly consolidated. Bed seems to pinch and swell slightly possibly representing mantle bedding. Recessive

28.52 - 28.64 m. Pink, fine-grained, well lithified, lapilli tuff showing fine bedding and or laminations up to 5 cm. Distinct density-stratification of garnets with small sanidine-rich lenses. Normal size grading of sanidines through the bed. Sharp bedding contacts, moderately resistant.

28.64 - 28.79 m. Light pink-brown, fine, crystal-lapilli tuffs, three beds. Slight normal grading with large euhedral sanidine assemblage, recessive (WCH-24).

28.79 - 28.85 m. Massive, pink, coarse crystal (sanidine) tuff, moderately sorted with minor garnets. The bed grades into a 2 cm green crystal ash bed at its top. Slightly resistant.

28.85 - 29.41 m. Purple, pink, fine to coarse, crystal tuff carrying 1 cm euhedral sanidine crystals (many broken) some show excellent twinning. Larger crystals are slightly concentrated at the top of the bed, reverse grading (WCH-25). Gradational bedding contacts, moderately recessive.

29.41 - 30.1 m. Agglomerate with overlying cross-bedded surged deposit. Variable thickness with rounded cognate clasts (3-7 cm) supported by a matrix-rich in sanidine and garnet phenocrysts. The unit normally grades into a thin 10-20 cm surge deposit showing parallel and cross lamination and pronounced density-stratification. The base of the unit is marked by a thin green-grey clay zone. Resistant.

30.1 - 30.4 m. Purple-brown, fairly massive, coarse, crystal tuff; garnet-rich with subordinate sanidine and cognate rock fragments. Moderately resistant (WCH-26).

30.4 - 30.67 m. Pink, fine-medium crystal lapilli tuff. Abundant sanidine crystals (5-1 cm). Marked normal grading, moderately resistant (WCH-27).

30.67- 30.7m. Coarse, green, crystal ash with green clay matrix. Abundant garnet and sanidine phenocrysts, recessive.

30.7 - 30.8 m. Purple, coarse, crystal tuff, small garnet, sanidine and analcime phenocrysts (.75 cm) in fine purple tuff matrix, moderate sorting (WCH-28).

30.8 - 30.85 m. Green, crystal ash, recessive.

30.8 - 30.85 m. Purple, coarse, crystal tuff, garnet-rich, with multiple reverse size and density grading. Moderately resistant (WCH-29).

31.25 - 31.39 m. Purple, fine, crystal (sanidine and garnet) lapilli tuff. Sanidine phenocrysts up

to 2 cm in fine purple tuff matrix (normal crystal size grading), slight normal density grading (garnets).

31.39 - 31.46 m. Fine, well sorted, light, purple/pink, crystal tuff (sanidine and garnets up to .3 cm). Moderately resistant with gradational upper and lower contacts (WCH-30).

31.46 - 31.56 m. Fine, purple, crystal (sanidine and garnet), lapilli tuff/coarse tuff. Garnets and sanidine, upto 4 mm and 1 cm respectively, in a fine tuff matrix. Moderately resistant (WCH-31).

31.56 - 31.77 m. Green, coarse, crystal ash. Garnets, sanidine and rock fragments up to 4 mm, 1 cm and .5 cm respectively in an abundant green clay matrix. Parallel bedded, recessive. Faint normal density and size grading. Slightly gradational upper and lower contacts (WCH-32), (Plate 6.1a).

31.77 - 31.98 m. Purple-pink, crystal, lapilli tuff showing marked normal size and density grading (sanidine and garnets). Slightly gradational lower contact, gradational upper contact. Welded, resistant (WCH-33b, m, t), (Plates 2.7d, 5.6a).

31.98 - 32.28 m. Broken, poorly consolidated, crystal tuff with coarse, well consolidated, pink, crystal tuff lenses. Contacts are slightly gradational. The bed pinches and swells over its length. Slightly resistant.

32.28 - 32.78 m. Well lithified, crystal, lapilli tuff. Feldspar crystals up to 1 cm. Occasional thin green ash horizons/lenses. The bed(s) show occasional symmetrical reverse to normal grading.

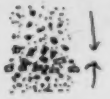

The exposure is moderately resistant and is slightly faulted (WCH-34).

32.78 - 33.78 m. Thin (10 cm), green, crystal ash and purple tuff beds. Parallel-bedded.
1. Tuff: purple, grainsize < 2 mm (coarse tuff), no apparent grading, well consolidated, moderately recessive.
2. Ash: Poorly consolidated, recessive small garnet and sanidine crystals (WCH-35).

33.78 - 34.18 m. Massive, welded pink crystal lapilli tuff showing marked reverse grading and thin laminations at the base. Relatively sharp contact. For the most part, resistant, however, becomes less consolidated towards the top (WCH-36).

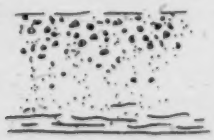

34.18 - 34.48 m. Purple, fine, crystal, lapilli tuff/coarse tuff with green crystal ash partings up to 3 cm thick, moderately recessive.

34.48 - 35.23 m. Massive, pink, crystal/lithic, lapilli tuff, well consolidated, moderately welded. Grades slightly towards the top where it becomes a finer, purple tuff, moderately

sorted, resistant (WCH-37).

35.23 - 35.67 m. Pink/green, crystal/lithic, lapilli tuff, graded as shown, with green, crystal ash lenses (1.5 cm sanidines). Relatively sharp contacts, resistant. (WCH-37).

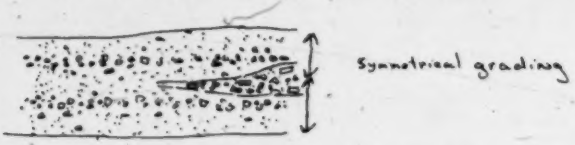

35.67 - 35.92 m. Purple, fine, crystal/lithic, lapilli tuff, poorly consolidated at base and top, more competent towards the middle.

35.92 - 36.22 m. Massive, pink, coarse, crystal/lithic tuff to fine, lapilli tuff, well consolidated (welded) showing marked cross-stratification up to 40°, normal grading and sharp uneven lower contact.

36.22 - 36.78 m. Massive, fine, pink, crystal/lithic tuff showing laminations and cross-stratification (density-stratification)(<30°), lenses of fine-medium, crystal tuff show best cross-stratification (25°). The bed shows normal grading and is resistant (WCH-38).

36.78 - 37.5 m. Green and purple, sanidine, crystal tuffs and lapilli tuffs, poorly consolidated, purple tuff lenses, in green, lapilli tuff.

37.5 - 38.0 m. Massive, pink, ungraded, coarse, crystal/lithic, lapilli tuff, resistant (welded), faint cross-lamination (5-10°) (marked by density-stratification) (WCH-39).

Unit IV

38.0 - 38.65 m. Pink, massive, crystal/lithic, ungraded, fine-medium, lapilli tuff (calcareous), showing a large, 1-3 meter erosional dune form and poorly developed cross-stratification (WCH-40).

38.65 - 38.95 m. Purple, medium, crystal tuff with green, coarse, sanidine, crystal tuff lenses and partings. The upper contact is uneven, apparently due to scour. Moderately resistant (WCH-41).

38.95 - 39.35 m (Variable). Basal zone of overlying, crystal/lithic tuff. Normal grading and cross- stratification (<30°). The bed pinches and swells, especially on the lower contact. Resistant (WCH-42 and 43(calcareous)).

39.35 - 46.85 m. Massive, resistant, pink, crystal/lithic, lapilli tuff, no apparent grading, poor-moderately sorted, the base is marked by a fine, reversely graded basal zone (6 cm). Green, crystal ash lenses develop towards top where the bed fines slightly. (base = WCH-44, WCH-45, WCH-46, WCH-47, WCH-48 = top), (Plate 6.1a).

46.85 - 47.60 m. Fine-coarse, crystal, tuff/lapilli tuff. Symmetrical, reverse to normal grading. Moderately resistant (WCH-49).

47.60 - 49.00 m. Massive, resistant, pink, medium-fine, crystal/lithic, lapilli tuff, non graded, rubbly base, apparent bombs or clasts at the top are draped by subsequent bed (WCH-50 - 51 top).

49.00 - 49.85 m (Variable). Green, (dark), coarse, crystal tuff with 5 cm light green crystal (sanidine) ash/tuff lenses/horizons. Interbedded green-black purple crystal tuffs. Basal beds drape the bombs/clasts of lower bed, moderately recessive (WCH-52, 53).

49.85 - 53.30 m. Massive, pink, medium (ave. clast size 1-3 cm), crystal/lithic, lapilli tuff (highly calcareous), with faint normal grading, crystal mainly resistant, welded. (WCH-54 base, 55 top).

53.30 - 54.0m. Moderately recessive beds:
+15 cm (WCH-56)-green, coarse, crystal (sanidine) ash.
+20 cm (WCH-57) Purple, medium, crystal/lithic tuff, showing normal grading.
+20 cm (WCH-58) Green, lithic/crystal ash:
+15 cm (WCH-59) Purple, crystal tuff.

54.0 - 54.91 m. Massive, purple/pink, coarse, crystal/lithic, lapilli tuff with thin trains/lenses of fine, pink, crystal tuffs. Resistant (WCH-60).

54.91 - 55.35 m. Moderately recessive beds:
+5 cm (WCH-61)- pink/brown, coarse crystal ash showing strongly defined normal grading (Plate 5.6b).
+15 cm - Purple, coarse crystal tuff showing normal grading of sanidine crystals.
+3 cm (WCH-62)- fine, brown clay horizon (bentonite).
+6 cm (WCH-63)- green, crystal ash.
+10 cm - Purple, crystal tuff showing faint normal grding of sanidine crystals.
+5 cm (WCH-64)- green crystal ash and fine brown clay (bentonite) bed, symmetrical normal to reverse grading, uneven upper contact.

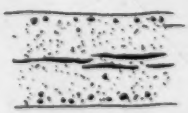

55.35 - 56.05 m. Purple, fine, crystal, lapilli tuff (calcareous) with slight normal grading, moderately resistant (WCH-65).

56.05 - 56.65 m. Massive, purple, fine-coarse, crystal tuff with abundant garnets. 6 cm clay (bentonite)/green ash at top, moderately resistant (WCH-66).

56.65 - 59.08 m. Recessive beds, green, crystal ashes to a maximum of 15 cm interbedded with fine-coarse, purple tuffs up to 20 cm. Some ash beds show symmetrical normal to reverse grading and both normal and reverse grading (WCH-67 (highly calcareous), 68, 69).

59.08 - 62.83 m. Massive, pink, crystal/lithic, lapilli tuff beds ranging up to fine agglomerates (round clasts). Lithic clasts up to 10 cm. Normal grading of clasts and slight reverse grading of crystals. Some beds show a faint, fine-grained, reversely graded basal zone. 4 and 5 cm green crystal ash beds occur towards the top. The sequence is resistant (WCH-70 base, 71, 72 top).

Unit V

62.83 - 62.98 m. Green/purple, crystal, ash/tuff with abundant garnets and brown, clay (bentonite) lenses, possibly symmetrically graded. Recessive (WCH-73).

62.98 - 63.05 m. Massive, purple, medium crystal tuff, moderately sorted, moderately resistant.

63.05 - 63.45 m. Five beds, two green, crystal (garnets) ashes and three purple, crystal tuffs (garnets), recessive.

63.45 - 64.15 m. Massive, purple, medium, crystal tuffs with abundant garnets and sanidines in a finer matrix. Moderately resistant.

64.15 - 64.52 m. Purple/green, medium, crystal, (sanidine/garnet) tuff with moderate sorting. Recessive.

64.52 - 64.59 m. Green, crystal ash and clay (bentonite) showing normal to reverse symmetrical grading, recessive.

64.59 - 64.99 m. Purple, coarse, garnet, crystal tuff, garnets up to 3 mm in fine purple tuff matrix, moderately resistant (WCH-74).

64.99 - 65.04 m. Yellow/green, garnet-rich, crystal ash (WCH-75).

65.04 - 65.34 m. Purple, coarse, garnet, crystal tuff.

65.34 - 65.41 m. Green, crystal ash, garnet-rich, with normal to reverse symmetrical grading. A fine, brown bentonite represents the finest fraction. The top surface is uneven and mantled by a thin brown clay (bentonite bed). Recessive.

65.41 - 65.61 m. Purple, fine to medium, non-calcareous, crystal tuff supporting 3-25 cm calcareous (Fe-calcite) bulbous, spheroidal and almond-shaped bombs. Moderately recessive (WCH-76).

65.61 - 65.68 m. Green, coarse, crystal (garnets and sanidine) ash, recessive.

65.68 - 65.88 m. Purple, fine, crystal tuff, recessive (WCH-77).

65.88 - 65.91 m. Green, coarse, crystal ash, with fine brown clay (bentonite) lenses.

65.91 - 66.01 m. Purple, fine, crystal tuff supporting 1-15 cm bulbous, spindle and almond-shaped bombs, moderately resistant.

66.01 - 66.11 m. Fine, green crystal ash, recessive.

66.11 - 66.91 m. Purple fine-grained, non- calcareous , crystal tuff supporting 5. to 25 cm calcareous, almond, bulbous and spheroidal bombs, moderately recessive (WCH-78, Cb, B_1 and 101), (Plates 2.6d,e,f, 5.6c) Occasional green crystal ash lenses.

66.91 - 66.98 m. Green/purple, fine grained, crystal tuff, recessive.

66.91 - 67.03 m. Green, coarse, crystal/lithic ash, recessive.

67.03 - 67.05 m. Green, fine, crystal ash with fine, light brown clay (bentonite) lenses/partings, recessive.

67.05 - 67.85 m. Purple, fine, non-calcareous, crystal tuff supporting large, calcareous, bulbous, spheroidal, almond and spindle-shaped bomb. Moderately recessive.

67.85 - 67.88 m. Green, fine, crystal ash, recessive.

67.88 - 68.68 m. Purple, fine, non- calcareous, crystal tuff supporting large 10-25 cm, calcareous bulbous, almond, spheroidal and spindle bombs. Bombs are normally graded.

68.68 - 68.75 m. Normal to reverse graded, green, crystal ash and purple, crystal tuff, recessive.

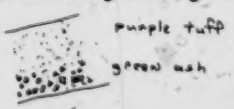

68.75 - 68.80 m. Purple, fine-grained, crystal tuff, recessive.

68.80 - 68.85 m. Green, crystal ash bed with pinch and swell bedding, abundant clay lenses or partings, recessive.

68.85 - 68.95 m. Purple, fine, crystal tuff, recessive. Exposure becomes poor.

68.95 - 69.68 m. Purple, fine, crystal tuff with coarse, green crystal (sanidine) ash lenses. Moderately resistant.

69.68 - 69.78 m. Green, coarse, crystal ash, recessive.

69.78 - 70.45 m. Purple, fine-grained, garnet, crystal tuff, recessive.

70.45 - 70.52 m. Green/brown, coarse crystal ash, recessive.

70.52 - 70.72 m. Coarse, green, garnet-rich, crystal ash, recessive.

70.72 - 71.12 m. Green-brown, garnet-rich, crystal tuff, garnets show marked normal density grading, recessive.

71.12 - 72.05 m. Covered, purple, crystal tuff in float.

72.13 - 72.80 m. Green-grey, coarse, lithic, lapilli tuff/fine agglomerate (rounded fragments), reverse grading of lithic fragments with garnets and sanidines in matrix. Poorly consolidated, moderately recessive.

72.80 - 74.30 m. Purple, fine-grained, non- calcareous tuff, few visable crystals, supporting 6-20 cm bulbous, spindle and almond-shaped, calcareous bombs, recessive.

74.30 - 74.50 m. Purple/green, medium, crystal tuff, recessive.

74.50 - 74.61 m. Green, crystal (garnets and sanidine) tuff, recessive.

Unit VI

74.61 - 76.17 m. Massive, moderately resistant, crystal/lithic, lapilli tuff beds up to 15 cm. They show marked density, cross and planar stratification and a marked fining upwards (normal grading) within single beds. Moderately resistant (Plates 5.2a,b,c).

76.17- 77.20 m. Coarse, lithic, lapilli tuff/fine agglomerate (round cognate clasts), welded, clasts show baked margins. Matrix consists of sanidine and garnets, slight fining upwards. Moderately resistant.

77.20 - 77.36m. Fine, crystal, lapilli tuff showing marked density, cross and parallel stratification. Moderately resistant.

77.36 - 77.40 m. Red, fine-grained tuff, recessive.

77.40 - 78.10 m. Covered, purple, crystal tuff in float.

78.10 - 78.21 m. Purple, fine, crystal tuff in float.

78.21 - 79.10 m. Covered.

79.10 - 79.41 m. Massive, welded, lithic/crystal, lapilli tuff, average clast size: 5-1 cm Moderately resistant.

79.41 - 82.01 m. Coarse, crystal tuff, showing density, cross and parallel stratification, recessive, rubbly.

82.01 - 85.5 m. Covered, massive, pink, lithic/crystal, lapilli tuff and fine, purple, crystal tuff in float.

85.5 - 86.03 m. Subcrop, (3-6 in cover) massive, lithic/crystal, lapilli tuff, apparently welded (baked rims), sanidine and garnets in matrix (WCH-110).

86.03 - 88.81 m. Covered.

88.81 - 89.09 m. Broken exposure. Massive, fine, pink, coarse, lithic lapilli tuff with cognate clasts showing baked margins. Matrix is composed of garnets, sanidines and smaller rock fragments in Fe-calcite matrix. Recessive (WCH-111).

89.09 - 89.60 m. Covered.

89.60 - 89.80 m. Subcrop (3 in of cover). Purple, fine-grained crystal tuff.

89.80 - 90.31 m. Covered.

90.31 - 90.66 m. Subcrop (4 in cover). Massive, pink, coarse, lithic lapilli tuff with cognate clasts up to 7 cm Clast show slightly baked margins (WCH-112).

90.31 - 97.1 m. Covered, coarse, pink, lithic, lapilli tuff and fine, purple tuff in float and subcrop.

97.1 - 97.5 m. Subcrop (3-5 in cover). Dense, purple, lithic, lapilli tuff with cognate clasts. (WCH-112).

97.5 - 105.5 m. Mostly covered, purple, fine to medium, crystal tuff exposed by digging (6-8 in cover) at 100-103 m. Fine purple tuffs in float. Beds indestinguishable in excavations (WCH-113).

105.5 - 106.11 m. Subcrop (3-6 in cover). Purple fine, crystal tuff showing density cross stratification.

106.11 - 108.41 m. Covered.

108.41 - 110.4 m. Subcrop (1-3 in cover). Massive, green, garnet-rich, medium, crystal/lithic, lapilli tuff. Average grain size = .5-3 cm Matrix is especially garnet-rich, massive.

110.4 - 112.03 m. Outcrop, massive, dark purple, feldspar porphyry (crystal-rich matrix), clasts showing baked margins up to 1 cm (WCH-114).

112.03 - 119.0 m. Small outcrop, dark green, coarse, lithic, lapilli tuff.

119.0 - 123.5 m. Covered, purple, pink, fine agglomerate in float. Cognate clasts supported by crystal-rich matrix.

TOP LOWER MEMBER

BASE UPPER MEMBER

Unit VII

123.5 - 124.8 m. 1st continuous outcrop of the upper member. Massive, purple, welded, agglomerate/pyroclastic breccia with subrounded cognate clasts (7-10 cm). Red hematite staining zones occur throughout, fine matrix with few large crystals.

124.8 - 130.4 m. Massive, purple agglomerate with cognate and possibly juvenile clasts up to 10 cm Baked rims are very common. Matrix is composed of finer fragments and crystals, some sanidines show flow imbrication. Very poorly sorted. Moderately resistant.

130.4 - 143.0 m. Massive, light green to pink, welded agglomerate/pyroclastic breccia (subrounded clasts) .5-25 cm, cognate and juvenile, marked baked margins and plastic deformation. Matrix consists of crystals, crystal fragments and small rock fragments, faint imbrication of sanidine phenocrysts. Resistant. (WCH-115), (Plate 2.7f).

143.0 - 153.7 m. Massive, dark green to pink, welded agglomerate/pyroclastic breccia (subrounded cognate clasts), poorly sorted, clast range in size from 4-15 cm Matrix is composed of crystals and small rock fragments. Moderately resistant.

153.7 - 161.8 m. Medium-dark green, coarse, lithic, lapilli tuff, welded, clasts (cognate and juvenile) 5-7cm, normal size grading over the whole bed. Matrix is garnet and sanidine-rich showing slight imbrication, 65% clasts, resistant. (Paleomagnetic drill hole 160 m) (WCH-87).

161.8 - 165.4 m. Very light green, coarse, welded, lithic/crystal tuff. Cognate clasts, .5-3 cm, baked rims and plastic deformation supported by a fine crystal/lithic matrix, moderately resistant.

165.4 - 166.8 m. Light green, poorly consolidated, crystal/lithic tuff, rock fragments up to 1 cm, reversely graded, moderately recessive.

166.8 - 167.1 m. Green, lithic, lapilli tuff, cognate clasts up to 6 cm, moderately resistant.

167.1 - 170.9 m. Medium, green, fine, welded agglomerate (rounded clasts), cognate clasts, plastic deformation and baked margins, matrix supported, sanidine, garnet and sanidine phenocrysts. Sanidines show faint imbrication. Moderately resistant.

170.9 - 171.9 m. Garnet-rich, crystal, lapilli tuff, marked density and cross-stratification (5-25°). Moderately resistant (WCH-116).

171.9 - 175.8 m. Purple, massive welded, coarse lapilli tuff/fine agglomerate (round clasts). Cognate clasts, 5-7 cm, poorly sorted, faint crystal, trains in matrix, imbricated sanidines. Resistant.

175.8 - 176.1 m. Black, crystal ash/lapilli tuff showing density and cross-stratification, moderately resistant (WCH-80).

Unit VIII

176.1 - 250.9 m.

Massive, green/grey, coarse, pyroclastic breccia, 60% (1-30 cm) clasts at base to 70% at top. Clast are angular to sub rounded showing baked/resorbed margins and plastic deformation. The clasts are supported by a fine, very dense, dark green matrix not resembling that of the lower member. Some clasts resemble cored bombs with strongly resorbed margins.

Net increase in apparently juvenile clasts (dark green, very fine-grained and intensely deformed blairmorite). Very faint flow imbrication (trachytic texture?) of sanidine crystals in matrix and some clasts.

Marked decrease in the number of free crystal phenocrysts. Continuous bed, no marked color changes or abrupt changes in grain or clast size. The bed is however marked by a net fining (normal grading) of rock fragments over its whole thickness. Very resistant (Paleomagnetic drill hole 189.82 m, 223 m). (WCH-88).

250.9 - 272.8 m. Dark green coarse pyroclastic breccia. Lower bedding contact marked by abrupt change in clast size (ave. 6 cm below contact to ave. 15 cm above contact) and color change from green grey to dark grey (Plate 6.1a). Cognate juvenile and accidental clasts from 0.01-3.5 m in size. Strongly baked/resorbed margins and plastic deformation. Normal grading of clasts towards the top. 50-70% clasts supported by a dense, massive fine crystalline matrix. Upper contact is intruded by a melanocratic finely-crystalline dyke/sill carrying small 1-3 cm clasts (up to 20%) showing strong resorbed/baked margins and few phenocrysts. The intrusive shows a 1-3 cm chilled margin and brecciates some rock into which it intrudes (WCH-83, 85, 94). The breccia contains abundant calcite. The dyke strongly resembles the matrix of the massive beds of the upper member at this section.

272.8 - 294.78 m. Contact marked by abrupt clast size change and color change from green to tan (see Plate 6.1). Yellow/green, pyroclastic breccia; cognate, juvenile and occasional accidental clasts, 0.5-10 cm, 20-50% fragments supported in a dense, massive, finely crystalline matrix (WCH-95) (Paleomagnetic drill hole 273.4 m).

294.78 - 338.1 m. Dark green, massive, pyroclastic breccia, 20-40% cognate, juvenile clasts, supported by massive, finely crystalline matrix, as above, slight normal grading of clasts, upper contact is not well defined (WCH-96).

338.1 - 392.1 m. Dark green, pyroclastic breccia, 20-35% clasts (cognate juvenile and accessory) up to 9 cm, no distinguishable grading. Clasts are supported by a dense, massive, finely crystalline matrix as below (slightly calcareous). Charred wood occurs towards the top of this bed at the "roadside turnabout". Resistant (WCH-97 bottom, WCH-98 top).

392.1 - 393.2 m. Dark green, angular breccia. Clasts are dark green, very finely crystalline, in a matrix of calcite and similar green material (chlorite). Bed is discontinuous (WCH-99).

393.2 - 396.1 (approx.)m. Dark green pyroclastic breccia, containing cognate and juvenile clasts showing baked/resorbed margins, 20 to 50% clasts supported by a dense mafic matrix. Charred wood again occurs.

396.1 - 397.1 m. Light tan very fine crystalline welded tuff. Very dense, conchoidal fracture. The bed is 1 m thick and is visable on the "roadside turnabout".

397.1 - 404.4 m. Dark green, pyroclastic breccia, 20-40% clasts, as below. Charred wood.
404.4 meters = Total Crowsnest Section,
(1326.4 ft)

404.4 - 411.1 (approx.)m. Grey/brown shales of the Blackstone Formation. Watinoceras found at 200 ft above Crowsnest contact by Dr. C.R. Stelck.

X. Appendix B

A. Analytical Methods

Outcrop and Hand Specimen Descriptions

The newly exposed section through the Crowsnest Formation along Highway No. 3 west of Coleman, Alberta was logged on a detailed scale of 1 cm = 1 m (Appendix A). All beds greater than 1 cm are represented. 125 samples were taken, eighty-five from the lower member and forty-five from the upper member. All types deposits are represented in the samples taken. Of these samples, one-hundred and twenty were cut for thin section work, thirty-five were crushed for geochemical analysis and some thirty were cut and polished for detailed descriptions.

Support sections were mapped at the Pipeline section (1.2 km south) and the Willoughby Ridge section (NE 10 km south). Both of these sections exposed part of the lower member and most of the upper member. The Willoughby Ridge section exposes the critical contact between the Blairmore Formation and the Crowsnest Formation. Fifteen samples were collected from this section, while ten were collected from the Pipeline section.

At all three sections, critical structures were sketched and photographed.

Thin Section Descriptions

All one-hundred and twenty thin sectioned samples from the proposed type section were described in detail to determine the mineralogy and textural features. Sections were stained with alizarin red for carbonate identification and with sodium cobaltinitrite for potassium feldspar identification. The percentage of primary components (phenocrysts, rock fragments and aphanitic material), and diagenetic components (alteration assemblages) were determined by point counting.

Polished sections (probe mounts) were used to identify the opaque minerals.

Scanning Electron Microscopy

Chip samples approximately 0.5-0.75 cm in width were taken from various samples from both the lower and upper member. The chips were mounted on SEM stubs with a conductive silver paint. Proper conduction was ensured by coating the samples with approximately 20 nm of gold/silver. A Cambridge Stereoscan S250 was used for all samples with a fixed accelerating voltage of 25 K.V. A Kevex 7000 was coupled with the SEM and provided qualitative chemical analysis.

X-Ray Diffraction

Bulk Sample

Twenty four samples were crushed to an average size of less than 0.1 mm and mounted in a "back pack" to determine whole rock mineralogy

Clay Fraction
Size Fraction Separation:

Sample preparation and analytical procedures are described in detail by Ignasiak *et al.* (1983) and Foscolos *et al.* (1982).

Using the settling velocity, the $<2\mu m$, 2 - 5 μm and the 5 - 2μm size fractions were separated. After being shaken, the sample is allowed to settle a given time according to the temperature. The $<2\mu m$ is separated first followed by the latter two size fractions. For each fraction, 900 ml of the 1000 ml in the cylinder is removed by syphoning after the given time for that size range. This procedure is repeated three times for each size fraction. After the three sizes are separated they are placed in a hot water bath for one day. Bleach is added before the bath to floculate the clays. The water bath destroys any organics present in the sample.

Washing:

After the water bath, each of the three size fractions are cleaned to remove bleach. This is done by centrifuging the sample, pouring off the excess water and remixing with distilled

water. This procedure is repeated until all the bleach is removed from the three sizes. $AgNO_3$ can be used to test the excess water for bleach.

Calcium and Potassium Saturation:

The <2μm was divided into three lots, while the other size fractions were left alone. KCl was added to one (K^+ saturation), $CaCl_2$ was added to the second (Ca^{2+} saturation) and the third was left "as is". After being left for three hours, the washing procedure above is repeated. The samples were then freeze dried in preparation for the next step.

Discs Preparation:

After freeze drying, about 40 milligrams of a given sample are mixed with 10 ml of distilled water and poured onto a ceramic disc which is mounted in suction equipment. The procedure is repeated for each sample. The discs are removed from the suction equipment after 45 minutes and are left to dry. When finished this step, a <2μm, K^+ saturated disc, a <2μm Ca^{2+} saturated disc, a 2-5μm "as is" disc, and a 5 - 20μm "as is" disc were produced. All discs were oriented as a result of the suction process.

X-Ray Diffraction Procedures:

X-ray diffraction analysis was carried out on all discs using CoKα radiation. In brief, the discs were prepared as follows:

1. Less than 2μm K^+ saturated at zero humidity. The disc was kept in an oven at 100°C for 24 hours before being run with nitrogen in the XRD chamber.
2. Less than 2μm K^+ saturated at 54% humidity. The disc in "a" was placed in a 54% humidity chamber for 24 hours before being run in a humidity control chamber of the XRD.
3. Less than 2μm K^+ saturated at 300°C. The K^+ saturated disc was heated to 300°C for 3 hours before being run in the presence of nitrogen.
4. Less than 2μm K^+ saturated at 550°C. The sample was heated to 550°C for 2 hours before being run in the presence of nitrogen.
5. Less than 2μm Ca saturated at 54% humidity. The disc was placed at 54% humidity chamber for 24 hours before being run under humidity controlled conditions.
6. Less than 2μm Ca glycolated. The calcium sample was placed in a glycol chamber and heated to 100°C for 24 hours.
7. 2 - 5μm "as is" at 54% humidity.
8. 5 - 20μm "as is" at 54% humidity. Nitrogen was used to simulate anhydrous conditions in the XRD chamber.

The following X-ray diffractograms were obtained for the <2μm size fraction:

1. K-disc at 0% relative humidity;
2. K-disc at 54% relative humidity;
3. K-disc at 300°C;
4. K-disc at 500°C;
5. Ca-disc at 54% relative humidity;
6. Ca-glycolated disc.

The relative percentage of clay minerals in each size-fraction was determined by measuring peak heights on specific diffractograms. For the <0.2μm and <2μm sizes, the (*001*) X-ray diffraction peaks were measured for illite and kaolinite group minerals using the Ca-saturated, ethylene-glycol diffractograms. The $(001)_{17}/(001)_{10}$ X-ray diffraction at about 13Å was used for mixed-layer clays. For chlorite, the height of the (*001*) X-ray diffraction from the K-saturated, heat-treated (550°C) sample was used. The following form factors were used to account for the variation in crystallinity between clay mineral species:

1. Illite (10Å) = 1.000;
2. Mixed-layer clay (13Å) = height of 13Å peak/2 x height of 10Åpeak;
3. Chlorite (14Å) = height of 14Å peak/3 x height of 10Å peak;
4. Kaolinite (7Å) = height of 7Å peak/2.5 x height of 10Å peak.

Relative percentages of each species was calculated from the sum of the above factors. As the diffractions for kaolinite (*001*) and chlorite (*002*) overlap, the relative percentage of chlorite is subtracted from kaolinite.

TABLE B-1 MAJOR DIFFRACTIONS FOR CROWSNEST ILLITE/SMECTITES (Ca - GLYCOLATED)

WCH	$(001)_{10}/(001)_{17}$	$(001)_{10}/(002)_{17}$	$(002)_{10}/(003)_{17}$	$(003)_{10}/(005)_{17}$
WCH-1	12.4	9.5	5.1	3.3
WCH-9	12.8	9.1	5.2	3.3
WCH-14	12.6-13.2	9.3	5.2	3.3
WCH-17	12.8	9.3	5.2	3.3
WCH-18	12.8	9.4	5.3	3.3
WCH-19	12.9	9.3	5.3	3.3
WCH-31	13.2	9.5	5.2	3.3
WCH-32	13.2	9.4	5.3	3.3
WCH-33	13.1	9.5	5.3	3.4
WCH-40	12.8	9.5	5.2	3.3
WCH-52	13.7	9.6	5.3	3.3
WCH-59	12.8	9.7	5.2	3.3
WCH-62	12.9	9.3	5.2	3.3
WCH-75	13.2	9.4	5.3	3.3

1
OF/DE

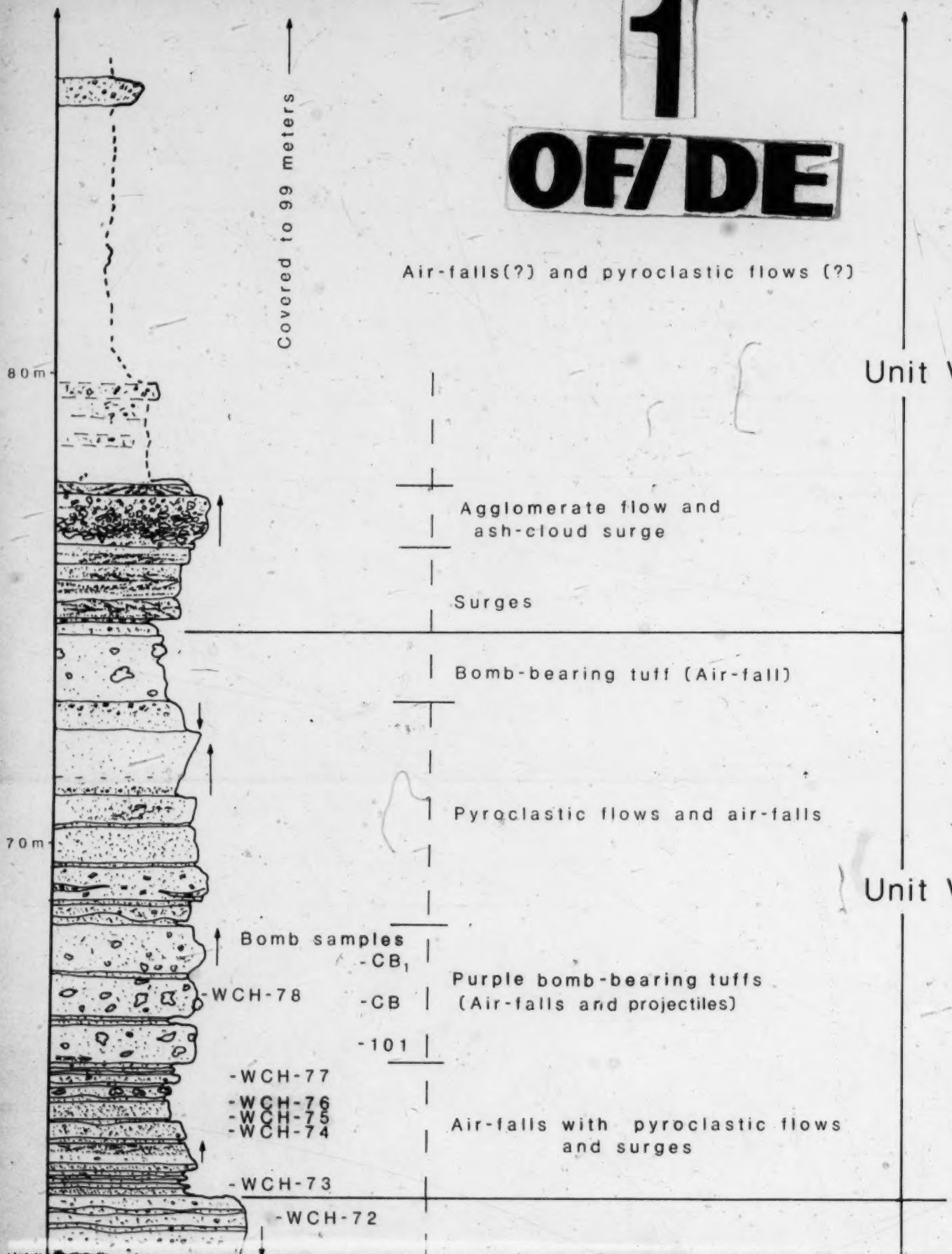
Covered to 99 meters
Air-falls(?) and pyroclastic flows (?)
Unit VI
80m
Agglomerate flow and
ash-cloud surge
Surges
Bomb-bearing tuff (Air-fall)
Pyroclastic flows and air-falls
70m
Unit V
Bomb samples
-CB1
-WCH-78
-CB
Purple bomb-bearing tuffs
(Air-falls and projectiles)
-101
-WCH-77
-WCH-76
-WCH-75
-WCH-74
Air-falls with pyroclastic flows
and surges
-WCH-73
-WCH-72

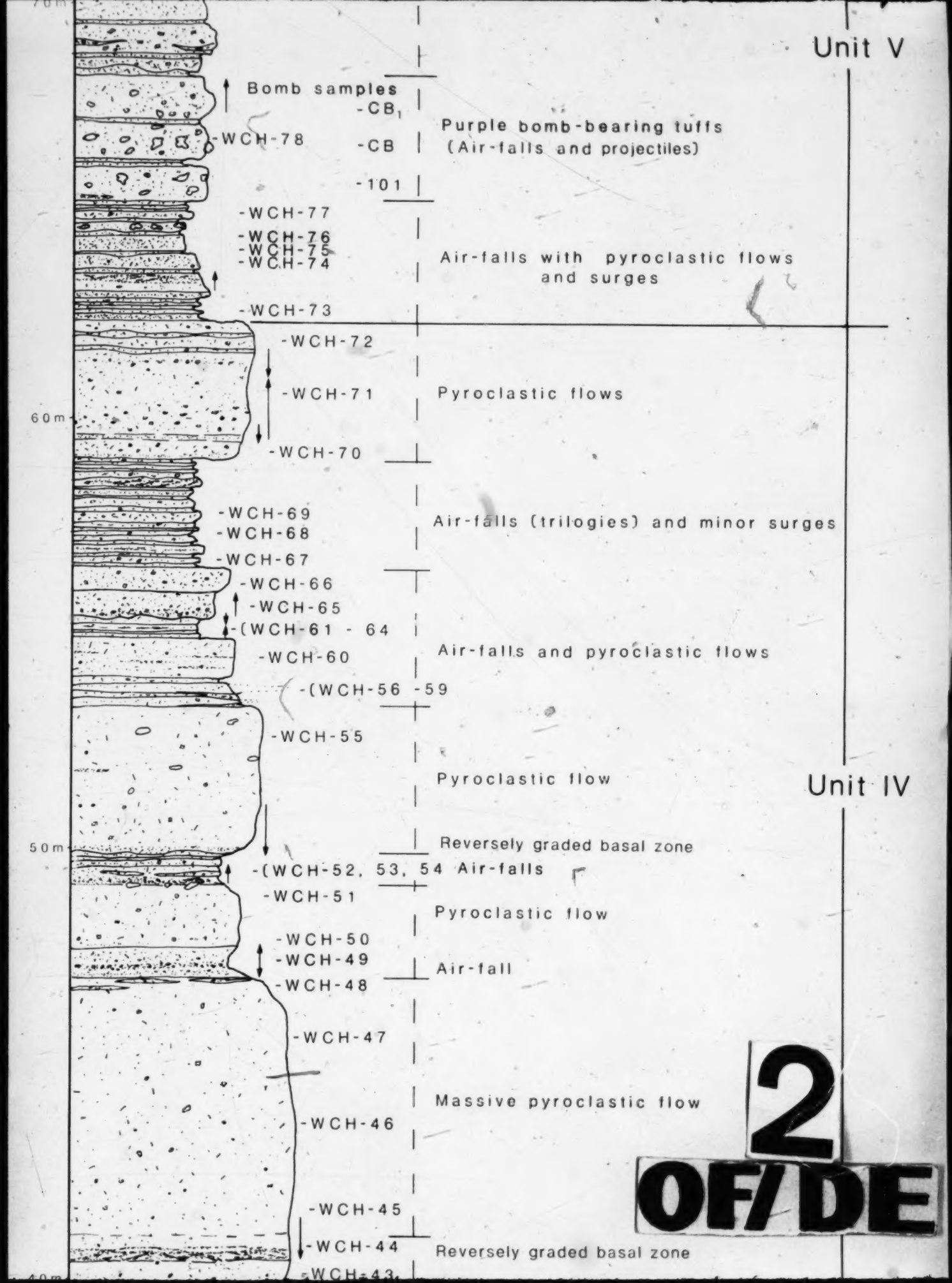
Unit V
Bomb samples
-CB1
-WCH-78
-CB
Purple bomb-bearing tuffs
(Air-falls and projectiles)
-101
-WCH-77
-WCH-76
-WCH-75
-WCH-74
Air-falls with pyroclastic flows
and surges
-WCH-73
-WCH-72
-WCH-71
Pyroclastic flows
60m
-WCH-70
-WCH-69
-WCH-68
Air-falls (trilogies) and minor surges
-WCH-67
-WCH-66
-WCH-65
-(WCH-61 - 64
-WCH-60
Air-falls and pyroclastic flows
-(WCH-56 -59
-WCH-55
Pyroclastic flow
Unit IV
Reversely graded basal zone
50m
-(WCH-52, 53, 54 Air-falls
-WCH-51
Pyroclastic flow
-WCH-50
-WCH-49
Air-fall
-WCH-48
-WCH-47
Massive pyroclastic flow
-WCH-46
-WCH-45
-WCH-44
Reversely graded basal zone
-WCH-43
40m

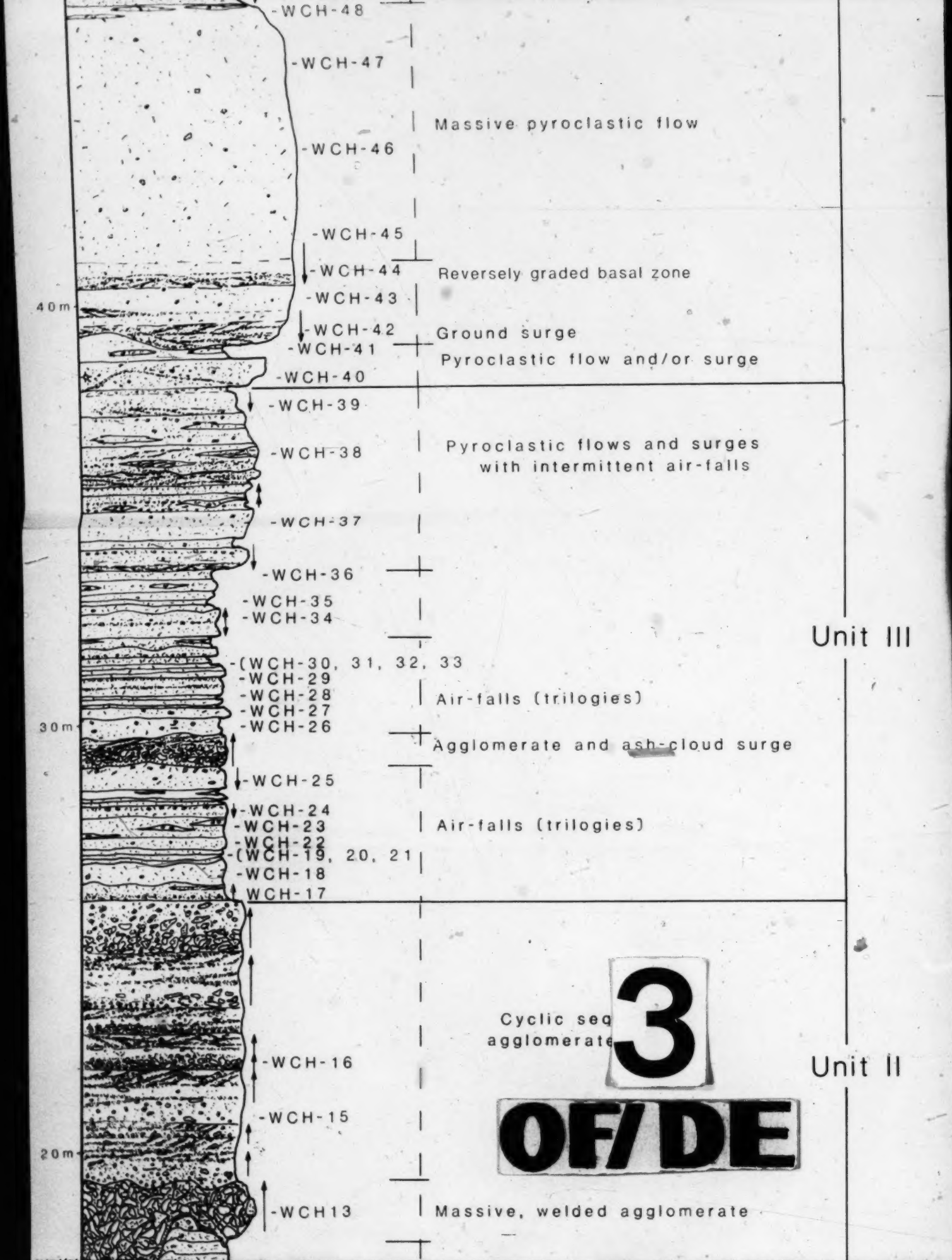
-WCH-48
-WCH-47
Massive pyroclastic flow
-WCH-46
-WCH-45
-WCH-44
Reversely graded basal zone
40m
-WCH-43
-WCH-42
Ground surge
-WCH-41
Pyroclastic flow and/or surge
-WCH-40
-WCH-39
-WCH-38
Pyroclastic flows and surges
with intermittent air-falls
-WCH-37
-WCH-36
-WCH-35
-WCH-34
Unit III
-(WCH-30, 31, 32, 33
-WCH-29
-WCH-28
Air-falls (trilogies)
-WCH-27
30m
-WCH-26
Agglomerate and ash-cloud surge
-WCH-25
-WCH-24
-WCH-23
Air-falls (trilogies)
-WCH-22
-(WCH-19, 20, 21
-WCH-18
WCH-17
Cyclic seq
agglomerate
3
-WCH-16
Unit II
-WCH-15
20m
-WCH13
Massive, welded agglomerate

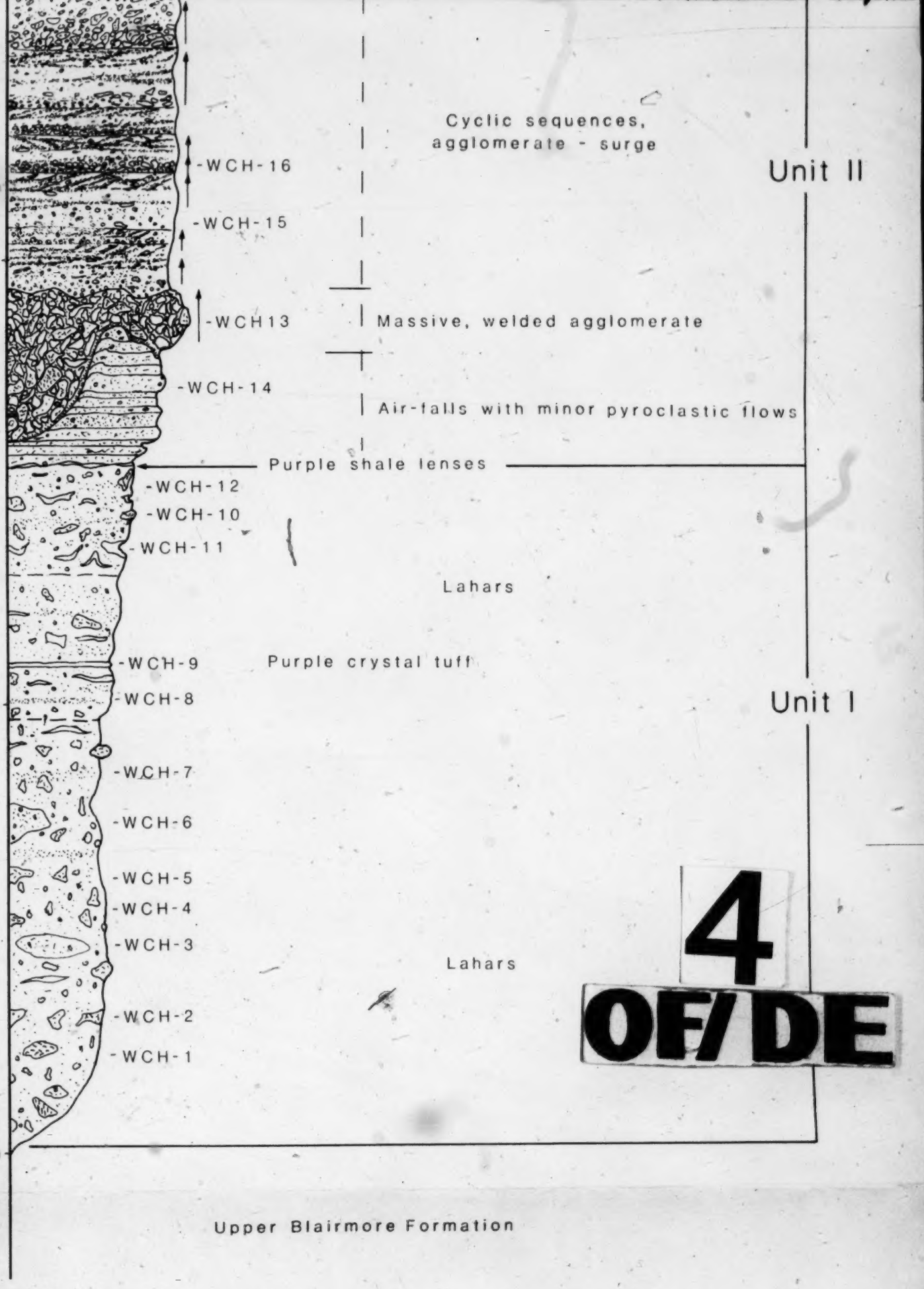
Cyclic sequences,
agglomerate - surge
Unit II
-WCH-16
-WCH-15
20m
-WCH13
Massive, welded agglomerate
-WCH-14
Air-falls with minor pyroclastic flows
Purple shale lenses
-WCH-12
-WCH-10
-WCH-11
Lahars
-WCH-9
Purple crystal tuff
10m
-WCH-8
Unit I
-WCH-7
-WCH-6
-WCH-5
-WCH-4
-WCH-3
Lahars
-WCH-2
-WCH-1
0m
Upper Blairmore Formation
Legend:

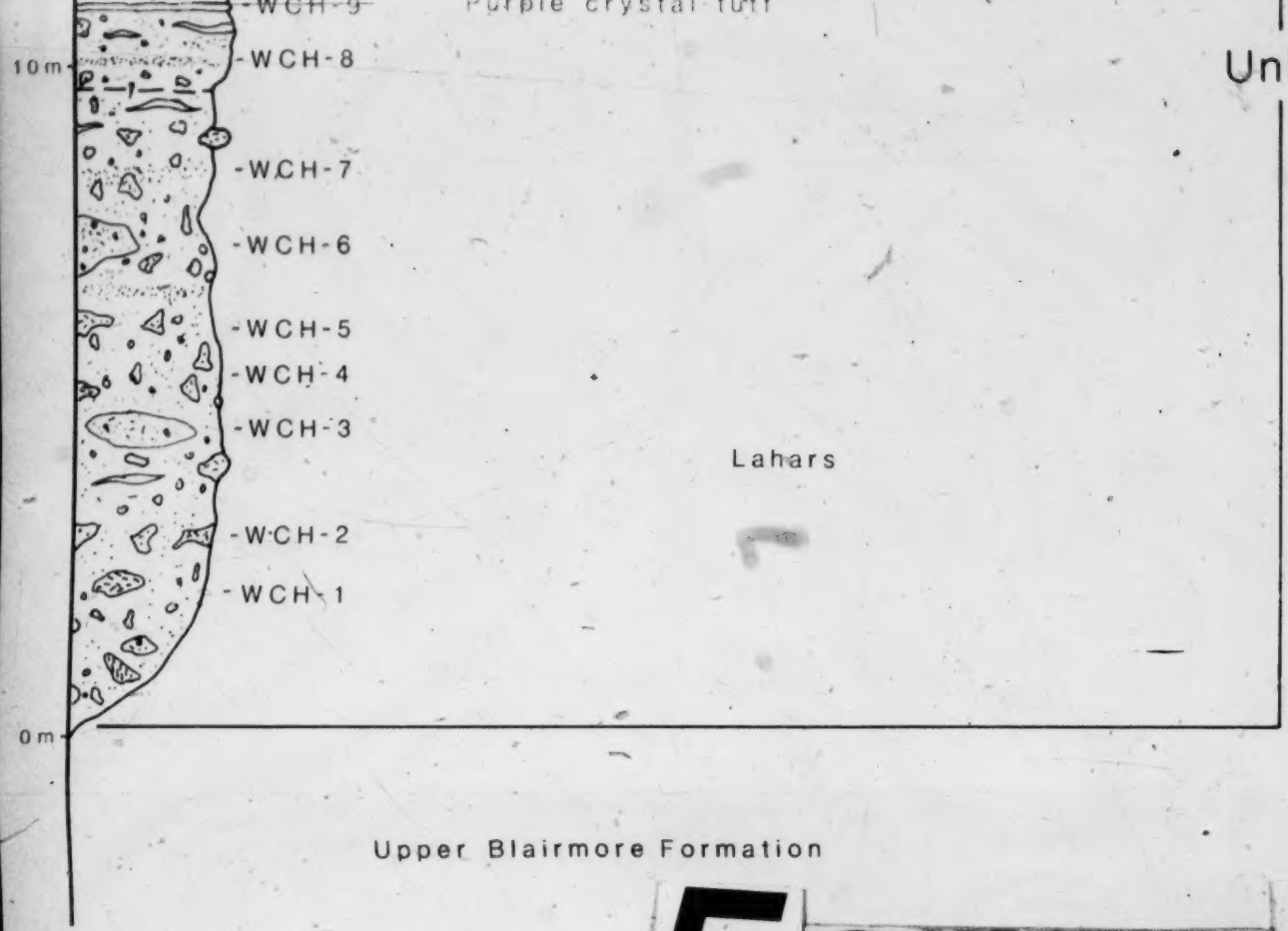

5 OF/ DE 5

Legend:

WCH-X Sample No.

- Shale lenses (Lahars)
- Cognate clasts
- Crystal-rich ash lenses
- Bombs
- Garnet crystals
- Feldspar crystals (Sanidine)
- Clay horizon
- Density cross stratification

- Normal grading
- Reverse grading
- Multiple grading
- Symmetrical normal to reverse grading
- Symmetrical reverse to normal grading

- Well defined contact
- Poorly defined contact
- Pinchout

Foldout A:

Detailed Lithologic Section of the Lower Crowsnest Formation at its proposed Type Section

1OF/DE

20 km

Willoughby Ridge Section

2 OF/ DE

20 km

Blackstone Formation

1.2 km

Proposed T
(Highway No.

Pipeline Section

?

4000

3000

Crowsnest Formation

3 OF/ DE

1.2 km

Proposed Type Section
(Highway No. 3, West of Coleman, Alberta)

km

Blackstone Formation

Pipeline Section

?

400 m

300 m

Watinoceras and Inoceramus labiatus

Unit VIII

Crowsnest Formation

4 OF/ DE

5 OF/ DE

Crowsnest Formation

Upper Member

Lower Member

Crowsnest Formation

300m

200m

100m

Crowsnest Formation

?

Upper Member

Lower Member

Crowsnest Formation

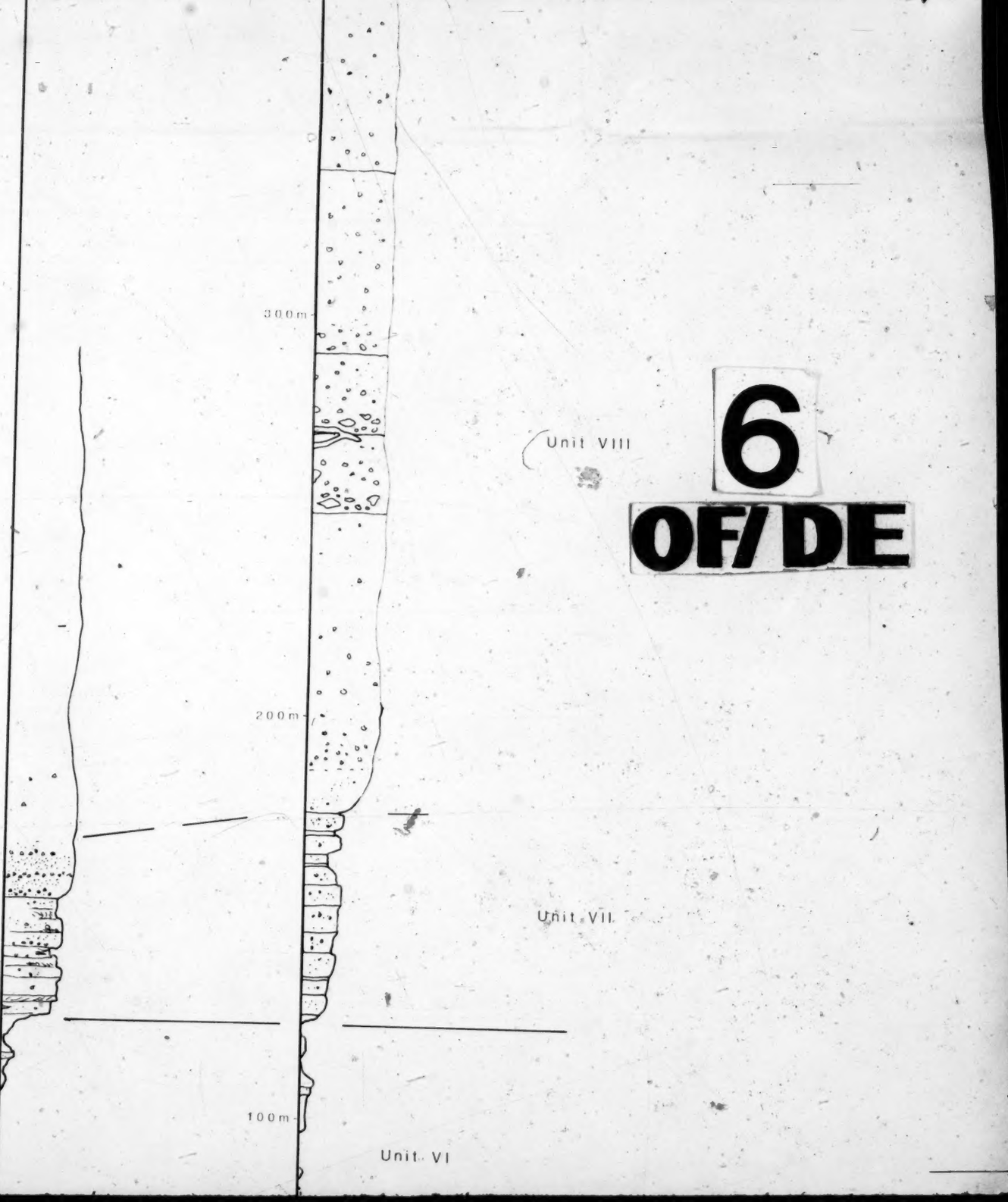

6

OF/DE

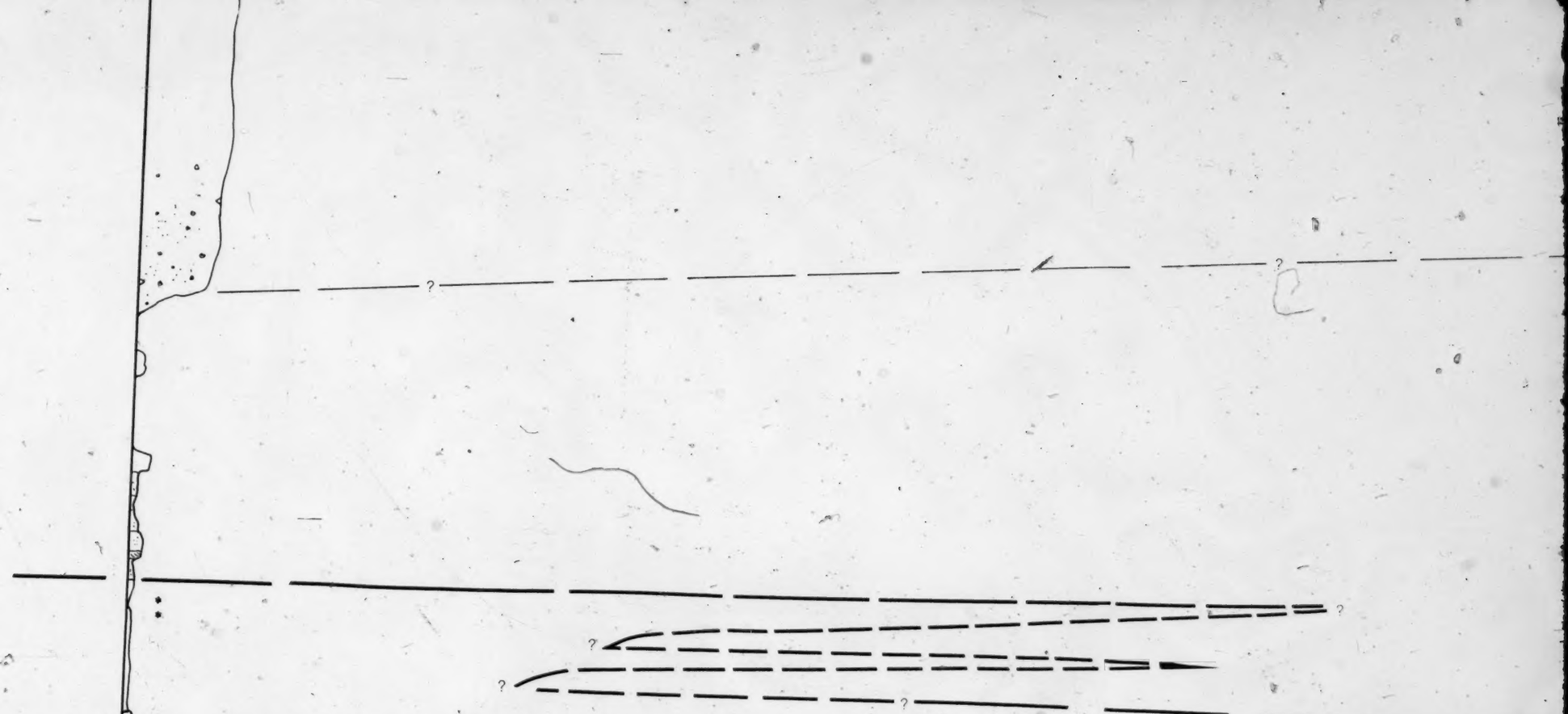

• Blairmore sediments carrying minerals derived from the Crowsnest Formation.

7 OF/ DE

Upper Member

Lower Member

Crowsnest Formation

rrying minerals
nest Formation

Blairmore Formation

Foldout B :
Local Stratigraphic Cro
Through the Propo
Type Section of
Crowsnest Format

8 OF/ DE

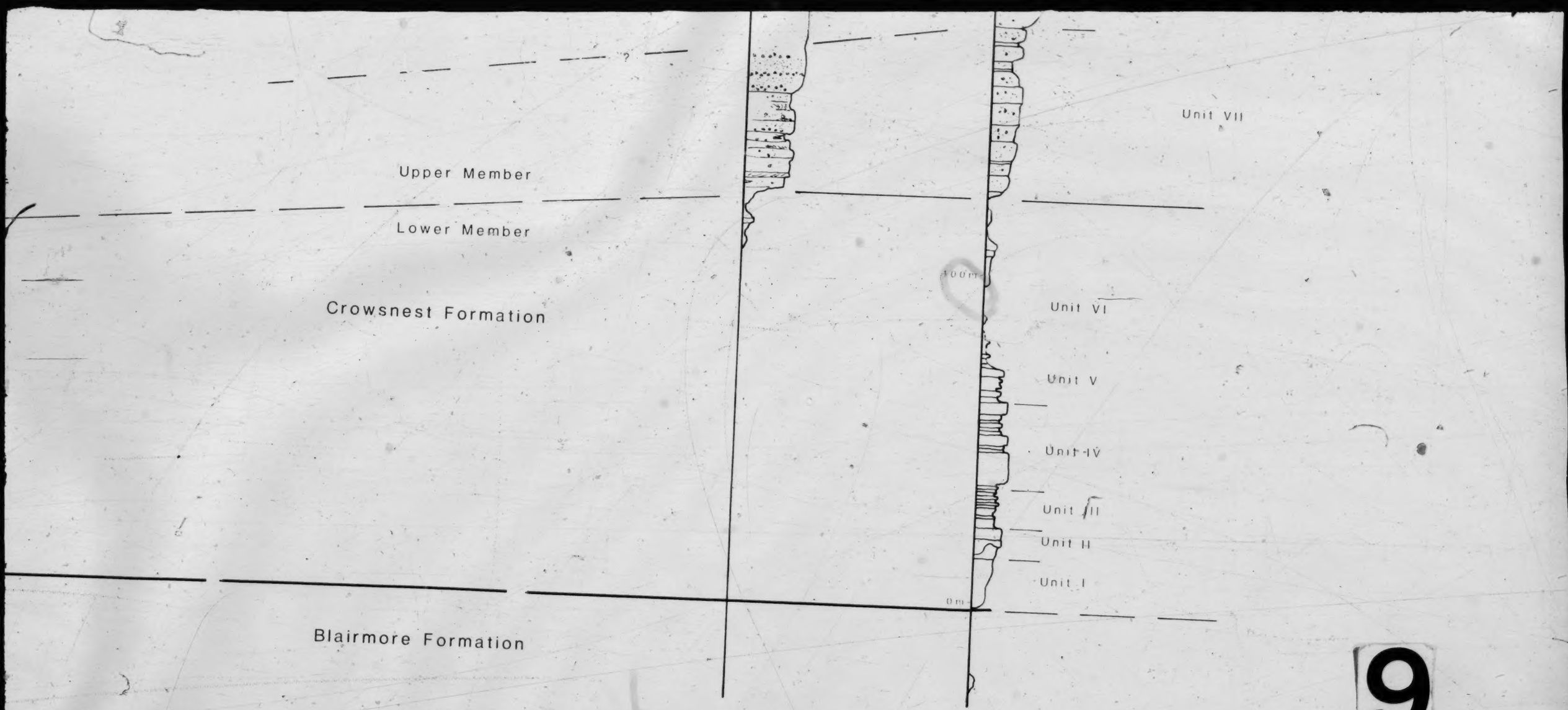

Foldout B :
Local Stratigraphic Cross Section Through the Proposed Type Section of the Crowsnest Formation

9
OF/DE
9